Volume C – Physical Baseline

RIO TINTO SIMFER S.A.

Social and Environmental Baseline Study

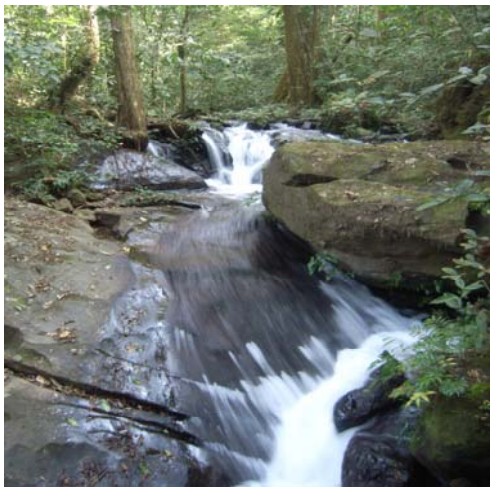
Simandou Project – Mine Component

FINAL REPORT



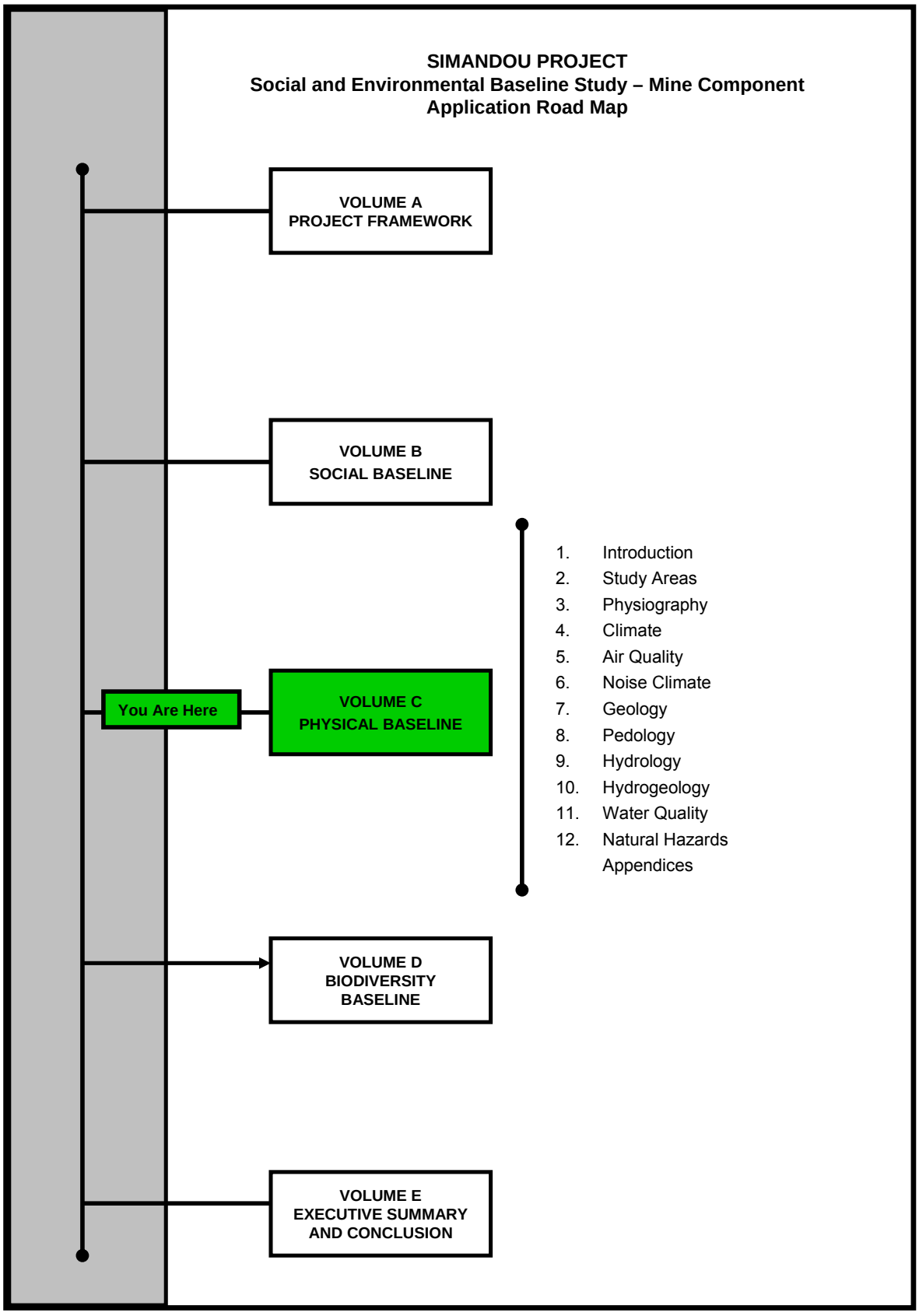
Project No.: 604917

August 2010



SNC·LAVALIN Environment

REPORT ROAD MAP



NOTICE TO READER

This document contains the expression of the professional opinion of SNC-Lavalin Inc, Environment Division (SLE) as to the matters set out herein, using its professional judgment and reasonable care. It is to be read in the context of the Contract date October 11, 2006 (the "Contract") between SLE and Simfer S.A. (the "Client") and the methodology, procedures and techniques used, SLE's assumptions and the circumstances and constraints under which its mandate was performed. This document is written solely for the purpose stated in the Contract, and for the sole and exclusive benefit of the Client. The Client may disclose the document to third parties at its absolute discretion. This document is meant to be read as a whole, and sections or parts thereof should not be read or relied upon out of context.

To the extent permitted by law, SLE disclaims any liability to third parties with respect to the publication, reference, quoting or distribution of this document or any of its contents to and reliance thereon by any third party.

TABLE OF CONTENTS

NOTICE iii

1. INTRODUCTION **1.1**
1.1 CONTEXT 1.1
1.2 METHODOLOGY 1.1
1.3 STRUCTURE AND ORGANIZATION OF THE VOLUME 1.2

2. STUDY AREAS **2.1**

3. PHYSIOGRAPHY **3.1**
3.1 INTRODUCTION 3.1
3.2 METHODS 3.1
3.3 RESULTS 3.1
3.3.1 Physiographical Regions 3.1
3.3.2 Geomorphological Units 3.3
3.3.3 Topography 3.3

4. CLIMATE **4.1**
4.1 INTRODUCTION 4.1
4.2 METHODOLOGY 4.1
4.2.1 National Direction of Meteorology Data 4.1
4.2.2 Rio Tinto Meteorological Network 4.1
4.2.3 Climatological Study Approach 4.5
4.3 RESULTS 4.5
4.3.1 Regional Climatic Context 4.5
4.3.2 Results in the Local Study Area 4.6
4.3.2.1 Atmospheric Pressure 4.9
4.3.2.2 Solar Radiation 4.10
4.3.2.3 Temperature 4.11
4.3.2.4 Wind 4.12
4.3.2.5 Humidity 4.15
4.3.2.6 Evaporation 4.15
4.3.2.7 Precipitation 4.17
4.3.3 Climate Change in Guinea 4.24

5. AIR QUALITY **5.1**
5.1 INTRODUCTION 5.1
5.2 METHODS 5.1
5.2.1 Measured Parameters 5.2
5.2.1.1 NO_2, SO_2 and O_2 ..... 5.2
5.2.1.2 Particulate Matter 5.2
5.2.2 Operation of the Stations 5.2
5.3 RESULTS 5.5

5.3.1 NO_2, SO_2 and O_3 Results 5.5
5.3.2 Particulate Matter Results 5.5
5.3.2.1 Mean Annual Concentrations 5.6
5.3.2.2 Mean 24-hour Concentrations 5.7
5.4 SUMMARY 5.8

6 NOISE CLIMATE 6.1

6.1 INTRODUCTION 6.1
6.2 METHODS 6.1
6.2.1 Field measurements 6.2
6.2.2 Data Analysis 6.2
6.3 RESULTS 6.5

7. GEOLOGY 7.1

7.1 INTRODUCTION 7.1
7.2 METHODS 7.1
7.2.1 Mineral Exploration Drilling and Sampling 7.1
7.2.2 Geochemical and Environmental Testing 7.2
7.3 RESULTS 7.2
7.3.1 Regional Geology and Structure 7.2
7.3.2 Local Geology in Pic de Fon and Ouéléba Deposits 7.5
7.3.3 Iron Ore Deposits 7.9
7.3.4 Acid Rock Drainage 7.10

8. PEDOLOGY 8.1

8.1 INTRODUCTION 8.1
8.2 METHODS 8.1
8.2.1 Soil Sampling 8.1
8.2.2 Sampling Protocol 8.1
8.2.3 Laboratory Analysis 8.1
8.3 RESULTS 8.2
8.3.1 Types of Soil and Agricultural Value 8.2
8.3.2 Chemical Characteristics of Soils 8.5

9. HYDROLOGY 9.1

9.1 INTRODUCTION 9.1
9.2 METHODS 9.1
9.2.1 Regional River Gauging Stations 9.1
9.2.2 Local Hydrometric Network 9.2
9.2.3 Springs Surveys 9.3
9.3 RESULTS 9.3
9.3.1 Regional Hydrology 9.3
9.3.2 Main Hydrological Features in the Local Study Area 9.5
9.3.3 Hydrological Regime 9.6
9.3.3.1 Base Flow and Storm Flow 9.15
9.3.3.2 Watersheds Draining the Mountains 9.15

9.3.3.3 Watersheds Draining to the Villages 9.18
9.3.4 Water Balance 9.20
9.3.5 Spatial Patterns of Flow 9.23
9.3.5.1 Spring Flow 9.23
9.3.5.2 Stream Flow 9.24

10. HYDROGEOLOGY 10.1

10.1 INTRODUCTION 10.1
10.2 METHODS 10.1
10.2.1 Groundwater Elevation Data 10.2
10.2.1.1 Standpipe Piezometers 10.2
10.2.1.2 Vibrating Wire Piezometers 10.3
10.2.2 Hydrogeological Properties 10.3
10.2.3 Groundwater Discharge 10.4
10.2.4 Groundwater Discharge 10.7
10.3 RESULTS 10.7
10.3.1 Hydrostratigraphy 10.7
10.3.1.1 Weathered Carapace 10.7
10.3.1.2 Hematite 10.8
10.3.1.3 Itabirite 10.8
10.3.1.4 Phyllite 10.10
10.3.1.5 Basement 10.10
10.3.2 Hydraulic Properties 10.10
10.3.2.1 Particle Size Distributions 10.11
10.3.2.2 Porosity and Permeability 10.12
10.3.3 Groundwater Levels 10.14
10.3.3.1 Spatial Variations in Groundwater Levels 10.14
10.3.3.2 Temporal Variations in Groundwater Levels 10.15
10.3.4 Groundwater Flow Systems in the Local Study Area 10.21
10.3.4.1 Conceptual Model Framework 10.21
10.3.4.2 Groundwater Recharge Mechanisms 10.21
10.3.4.3 Groundwater Flow Mechanisms 10.22
10.3.4.4 Groundwater Discharge 10.23
10.3.4.5 Conceptual Groundwater Flow Model 10.26

11. WATER QUALITY 11.1

11.1 INTRODUCTION 11.1
11.2 METHODS 11.1
11.2.1 Surface Water Sampling Campaigns 11.1
11.2.2 Groundwater Sampling Campaigns 11.2
11.2.3 Water Sampling and Analytical Methods 11.2
11.3 RESULTS 11.10
11.3.1 Surface Water Quality 11.10
11.3.1.1 Springs 11.10
11.3.1.2 Streams 11.12

11.3.1.3 Temporal Variations in Surface Water Chemistry.....11.12
11.3.1.4 Spatial Variations in Surface Water Chemistry.....11.17
11.3.2 Groundwater Quality.....11.18
11.3.3 Village Wells and Boreholes Water Quality 11.20

12. NATURAL HAZARDS.....12.1

12.1 INTRODUCTION 12.1
12.2 METHODS.....12.1
12.3 RESULTS.....12.1
12.3.1 Terrain Hazards.....12.1
12.3.2 Regional Seismicity 12.3
12.3.3 Floodable Areas 12.3

GLOSSARY

ACRONYMS AND ABBREVIATIONS

REFERENCES

APPENDICES

LIST OF TABLES

Table 4.1 Annual means rainfall in relation with altitude in the local study area.....4.20
Table 4.2 Maximum short-term rainfall depths and intensities in the local study area.....4.23
Table 5.1 Characteristics of the ambient air quality stations.....5.1
Table 5.2 NO_2, SO_2 and O_3 results ($\mu g/m^3$).....5.5
Table 5.3 24 h of particulate matter results ($\mu g/m^3$).....5.6
Table 5.4 WHO Air Quality Guidelines for particulate matter ($\mu g/m^3$).....5.6
Table 6.1 Characteristics of the noise measurement locations.....6.1
Table 6.2 Noise level instrumentation.....6.2
Table 6.3 Hourly and daily noise levels measured at villages and camp.....6.6
Table 7.1 Characteristics of the main lithological units encountered in Pic de Fon and Ouéléba deposits.....7.9
Table 7.2 Main types of iron ore mineralisation at Pic de Fon and Ouéléba deposits.....7.10
Table 8.1 Summary statistics for soil samples in the local study area.....8.6
Table 9.1 River gauging stations located downstream of the local study area.....9.2
Table 9.2 Characteristics of Whisky 1, 2 and 5 watersheds.....9.6
Table 9.3 Summary of monthly stream flow data at Whisky 1, 2 and 5.....9.14
Table 9.4 Results of base flow and storm flow separation on Whisky 1 and 2 (2007).....9.15
Table 9.5 Summary of monthly stream flow data at village gauging stations.....9.19
Table 9.6 Annual summary water balance for Whisky 1 and 2 (2004-2008).....9.23
Table 9.7 Spring flow in Pic de Fon and Ouéléba.....9.24
Table 9.8 Spring flow as a proportion of rainfall.....9.24
Table 10.1 Summary results of particle size distribution analyses.....10.11
Table 10.2 Relationship between lithology and porosity.....10.12
Table 10.3 Summary of laboratory analysis of competent core samples.....10.13
Table 10.4 Results of variable-head tests undertaken in some piezometers in the Ouéléba ore body.....10.13
Table 10.5 Groundwater flow mechanisms identified in the local study area.....10.22
Table 10.6 Summary of stream flows at boundary measurement sites.....10.24
Table 11.1 Parameters analysed in water samples.....11.9
Table 11.2 Summary statistics of spring water chemistry.....11.11
Table 11.3 Summary statistics of stream water chemistry.....11.13
Table 11.4 Summary of water quality parameters at Whisky 1.....11.14
Table 11.5 Summary of water quality parameters at Whisky 2.....11.15
Table 11.6 Summary statistics for groundwater chemistry.....11.19
Table 11.7 Summary statistics for village well and borehole water chemistry.....11.22

LIST OF FIGURES

Figure 1.1 Physical baseline studies road map 1.3
Figure 3.1 Main physiographical regions in southeastern Guinea 3.2
Figure 4.1 Monthly mean atmospheric pressure in the local study area 4.9
Figure 4.2 Monthly mean solar radiation in the local study area 4.10
Figure 4.3 Monthly mean ambient temperature in the local study area 4.11
Figure 4.4 Monthly mean relative humidity in the local study area 4.15
Figure 4.5 Monthly mean evapotranspiration (ETo) in the local study area 4.16
Figure 4.6 Monthly mean evaporation (E_o) in the local study area 4.17
Figure 4.7 Monthly mean rainfall in the local study area 4.19
Figure 5.1 Mean annual concentrations of $PM_{2.5}$ and PM_{10} compared to WHO guidelines 5.7
Figure 5.2 Maximum daily average concentrations* of $PM_{2.5}$ and PM_{10} compared to WHO guidelines 5.8
Figure 9.1 Regional watersheds and national hydrometric network context 9.4
Figure 9.2 Annual stream flow measured in the Niger, Dion and Milo gauging stations and total flow in the Milo as proportion of annual total flow in the Niger 9.9
Figure 9.3 Annual stream flow measured at Bac River gauging station on the Diani River 9.10
Figure 9.4 Seasonal hydrographs in the Niger, Milo, Diani and Dion rivers (1975-1979) 9.12
Figure 9.5 Whisky 1 and 2 daily instantaneous flow measurements and rainfall (2003-2008) 9.13
Figure 9.6 Separation of the storm flow and base flow components in the Whisky 1 hydrograph (2007) 9.17
Figure 9.7 Monthly mean base flow hydrographs 9.20
Figure 9.8 Conceptual hydrological model of Whisky 1 and 2 watersheds 9.22
Figure 10.1 Schematic cross-section of the hydrogeological setting in the Pic de Fon deposit 10.9
Figure 10.2 Piezometer hydrographs in Pic de Fon compared with rainfall data 10.17
Figure 10.3 Short-term groundwater level fluctuations in piezometers located in the Pic de Fon deposit 10.19
Figure 10.4 Short-term groundwater level fluctuations in piezometers located in the Ouéléba deposit 10.20
Figure 11.1 Turbidity and flow during storm flow events measured at Whisky 1 weir 11.16
Figure 11.2 Total suspended solids and flow measured at Whisky 5 weir 11.17

LIST OF PHOTOS

Photo 3.1 Typical landscape of the Simandou Range 3.4
Photo 3.2 Typical hillslopes in the Pic de Fon area 3.4
Photo 4.1 Automatic weather station 4.2
Photo 4.2 Hill fog on the western side of Pic de Fon 4.24
Photo 5.1 Cloudy haze typical of the dry season 5.1
Photo 5.2 Slash and burn activities 5.1
Photo 5.3 Ambient air quality monitoring station in Mandou 5.2
Photo 8.1 Typical soil texture and surficial deposits exposed near a drilling pad located on Pic de Fon 8.5
Photo 9.1 Typical weir part of the local hydrometric monitoring network 9.3
Photo 10.1 Typical exploration hole collar (left) and completed piezometer (right) 10.3
Photo 10.2 Rock samples collected during mineral exploration drilling 10.4
Photo 11.1 Portable winch used for groundwater sampling in piezometers 11.9
Photo 11.2 Typical dug well and hand pump borehole in the local study area 11.21
Photo 12.1 Examples of landslides resulting from natural causes on Pic de Fon 12.2

LIST OF MAPS

Map 2.1 Physical baseline study areas 2.3
Map 3.1 Geomorphological units in the regional study area 3.5
Map 3.2 Topography in the local study area 3.7
Map 4.1 Rio Tinto meteorological network in the local study area 4.3
Map 4.2 Regional climate context 4.7
Map 4.3 Wind roses in the local study area 4.13
Map 4.4 Rainfall contour in the local study area 4.21
Map 5.1 Ambient air measurement stations in the local study area 5.3
Map 6.1 Ambient noise measurement stations in the local study area 6.3
Map 7.1 Geological formations in the regional study area 7.3
Map 7.2 Lithology and structural features in the local study area 7.7
Map 8.1 Pedology in the local study area 8.3
Map 9.1 Local watersheds and hydrometric network in the local study area 9.7
Map 9.2 Spring locations and stream flow isocontours in the local study area 9.25
Map 10.1 Sampling stations for groundwater characterisation and piezometric contours in the local study area 10.5
Map 10.2 Results of the flow accretion survey in the local study area 10.29
Map 10.3 Hydrogeological conceptual model in the local study area 10.31
Map 11.1 Surface water quality monitoring network in the local study area 11.3
Map 11.2 Groundwater quality monitoring network in the local study area 11.5
Map 11.3 Water quality monitoring network of village wells and boreholes in the local study area 11.7

LIST OF APPENDICES

Appendix A: Characteristics of the Rio Tinto automatic weather stations, rain gauges and manual rain gauges
Appendix B: Temperature and rainfall statistics at DNM stations in Southeast Guinea
Appendix C: Summary data on atmospheric pressure
Appendix D: Summary data on solar radiation
Appendix E: Summary data on temperature
Appendix F: Summary data on compass roses
Appendix G: Summary data on relative humidity
Appendix H: Summary data on evapotranspiration and evaporation
Appendix I: Summary data on rainfall
Appendix J: Air quality technical form
Appendix K: Average concentrations of $PM_{2.5}$ and PM_{10}
Appendix L: Noise curves
Appendix M: Results of geochemical testing
Appendix N: Soil sampling logs
Appendix O: Soil chemical analysis certificates
Appendix P: Characteristics of Rio Tinto stream gauging stations
Appendix Q: Details of piezometers
Appendix R: Flow accretion survey data
Appendix S: Water quality data

CHAPTER 1

Introduction

1. INTRODUCTION

The Physical Baseline Volume constitutes a baseline inventory and analysis of the physical conditions present in the Simandou region. The purpose of the physical baseline study is to characterise the initial conditions of the physical components against which to monitor and assess the project progress and effectiveness during the implementation and operation phases.

1.1 CONTEXT

The Pic de Fon Classified Forest (PdF CF) presents unique physical characters in terms of geology, topography and climatic conditions that are important as they relate to hydrology and hydrogeology, land use capability and livelihoods in adjoining villages. Also, the physical characters conditioned the biological features which explain the presence of evergreen forest and the biodiversity richness of PdF CF.

Indeed, from the earliest stages of the exploration programme, the sensitivity of the Simandou region's physical environment was recognised. The Simandou mountain range, by its north-south orientation and altitude, has an influence on the regional climate. The range is also at the headwaters of a number of important watersheds and is a major underground recharge area. Moreover, surface water and groundwater (wells and boreholes) are used for different purposes by the neighbouring communities.

The potential impacts associated with the development of the Simandou Project on the physical environment are potential changes in local microclimate by altering rainfall patterns that will affect hydrology; changes in groundwater levels and groundwater flow systems will also affect hydrology; and changes in water quality downstream from the project site.

For these reasons extensive surveys were performed in order to understand the climate, hydrological and hydrogeological regimes prevailing in the Simandou region.

1.2 METHODOLOGY

Contrary to Volume B (Social baseline) and Volume D (Biodiversity baseline) where general methodology is applicable, there is a specific methodology for each physical baseline component. Consequently, the description of the methodology applicable to each component appears in its respective chapter.

Over the last decade, a series of physical studies have been conducted within the PdF CF and within the general framework of the Simandou Project. These studies were performed by Water Management Consultants (WMC) and include preliminary climate data analysis and site visit reports on hydrology and hydrogeology (Figure 1.1). In general, these studies were provisional and provide basic knowledge on the physical context of the PdF CF.

The second box in Figure 1.1 identifies the comprehensive surveys, monitoring, and studies carried out during the baseline study. Apart from the surveys performed by

SNC-Lavalin Environment, UK Met Office (UKMO) has conducted a three-phase climatology study at the PdF CF, while Water Management Consultants (WMC) has conducted substantial surveys related to hydrology, hydrogeology and geochemistry.

Monitoring programmes continue at the existing climatological stations and sampling sites to pursue the existing baseline conditions of some components (hydrology, hydrogeology and climate).

The data collected during the physical baseline study and all spatially geo-referenced information was stored in a database. The data collected by Water Management Consultants (WMC) was stored in a different database to that managed by the Consultant.

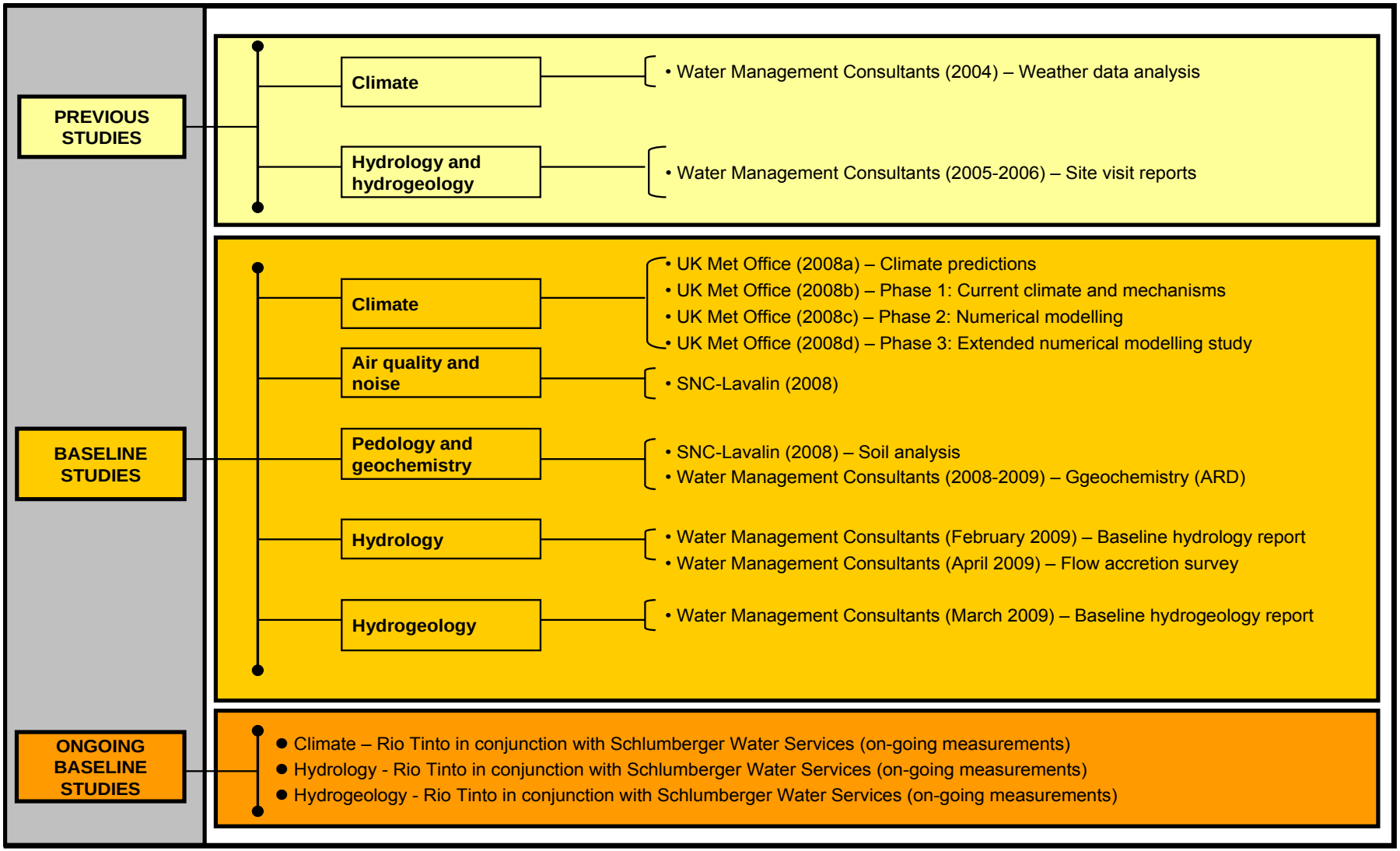
The study team involved in these surveys and studies are presented in Appendix A of Volume A.

1.3 STRUCTURE AND ORGANIZATION OF THE VOLUME

In addition to the present Introduction, the physical baseline volume includes eleven other chapters as follow:

- determination of the physical study areas (Chapter 2);
- description of the physiographical regions, geomorphological units and topography (Chapter 3);
- presentation of the regional climatic context and characterisation of local climate (Chapter 4);
- characterisation of existing ambient air quality (Chapter 5);
- characterisation of the existing noise background (Chapter 6);
- presentation of the regional and local geology (Chapter 7);
- description of soil types (pedology) and their agricultural value (Chapter 8);
- description of regional hydrology and main local hydrological features and regime (Chapter 9);
- description of the hydrogeological system, hydrostratigraphy and hydraulic properties, groundwater levels and groundwater flow systems (Chapter 10);
- characterisation of surface water and groundwater quality (Chapter 11);
- identification of the natural hazards (Chapter 12).

Figure 1.1 Physical baseline studies road map



CHAPTER 2

Study Areas

2. STUDY AREAS

Two project areas have been defined in order to characterise the physical components of the Simandou Project as shown on Map 2.1. A broader or regional study area (RSA) delimited to better understand the insertion context of the Simandou Project and a local study area (LSA) that focuses on specific physical features of the Pic de Fon Classified Forest (PdF CF).

The RSA covers a large portion of the Forest Guinea region which presents homogeneous physical characteristics in terms of regional rainfall, physiographic units, geological formations of the Simandou Range, and hydrological characteristics of the regional watersheds which drains the range.

All physical baseline information pertaining to the RSA comes from existing data that have been gathered from literature reviews and from national-level sources (e.g. hydrological and meteorological data from *Direction Nationale de l'Hydraulique* – DNH and *Direction Nationale de la Météorologie* – DNM).

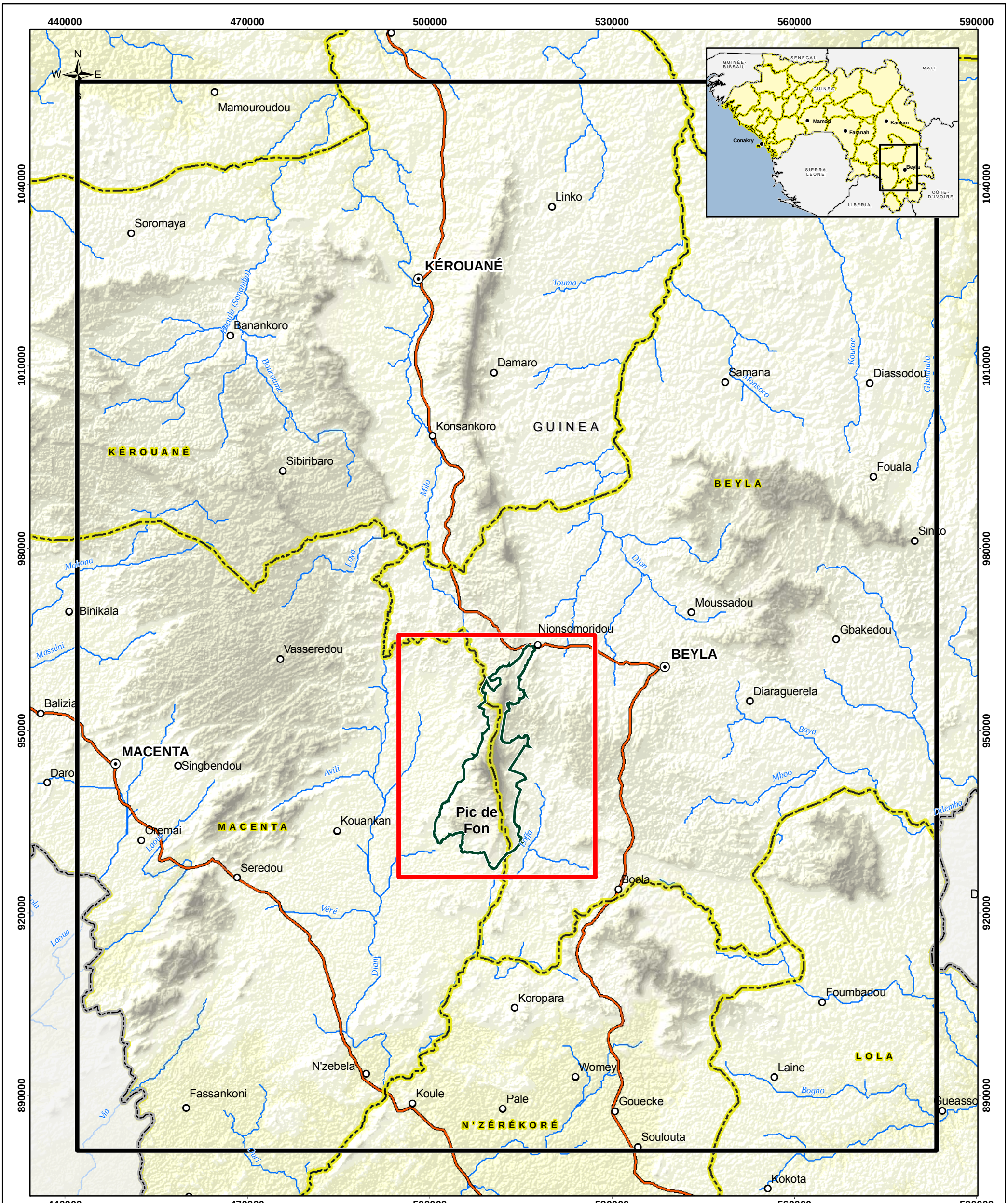
The LSA is based on the spatial extent of the project's footprint as well as on the potential effects of the project on the physical receiving environment. All baseline surveys and monitoring were performed within the LSA, mostly within the PdF CF boundary and surrounding villages.

The Simandou Range by its north-south orientation, altitude and scale has an influence on the local climate patterns (rainfall, fog, wind, etc.). As it is possible that mining may modify local climate patterns at the project site, the baseline study focused mainly on the LSA.

Anticipated emissions and discharge effluents from the project could potentially have downwind or downstream effects on sensitive receptors. Therefore, surveys and monitoring for noise background, air quality, and water quality focused on neighbouring villages of the PdF CF.

The baseline topography, geomorphology, and lithology associated with the Simandou iron ore deposit and its hydraulic properties were also characterised at a local scale as they are closely related to hydrology and hydrogeology.

Surface water and groundwater domains are complex and closely linked in the context of mountainous regions and therefore require examination in detail within the LSA. Given that groundwater recharge is local and influences the flow process of the PdF CF, the baseline surveys focused on the ridge and the slopes of the two mining areas and to a lesser extent the surrounding areas.



Repères géographiques / Geographical landmarks

Chef-lieu de préfecture	Prefecture centre
Chef-lieu de CRD et CU	CRD and CU centre
Frontière nationale	National border
Limite de préfecture	Prefecture boundary
Route principale	Main road
Hydrographie	Hydrography
Forêt classée du Pic de Fon	Pic de Fon Classified Forest

Zones d'étude / Study areas

Zone d'étude locale	Local study area
Zone d'étude régionale	Regional study area

Sources :
1- Landsat imagery mosaic 2002-2003;
2- Shuttle Radar Topography Mission (SRTM);
3- Carte topographique IGN 1:50 000/1:200 000;
4- Geographic Coordinate System: WGS84, UTM, Zone 29N.

Note : Les limites administratives proviennent de sources multiples et sont approximatives / Administrative boundaries are from multiple sources and are approximate.

Titre / Title

Zones d'étude du milieu physique / Physical baseline study areas

Échelle / Scale	Projet / Project	Volume C Carte/Map 2.1
0 3 6 12 Km 1:600,000	SIMANDOU	

Directeur de projet (client) Project manager (client)	Directeur de projet Project manager	No. pr./ P. number
Leon Payne	Richard Fontaine	604917

No.	aaaa/mm/jj yyyy/mm/dd	Description	Dessiné/Drawn	Vérifié/Verified
01	2010/06/15	Final	M. Dupré	M. Stapinsky
00	2009/12/16	Preliminary	M. Dupré	M. Stapinsky

CHAPTER 3

Physiography

3. PHYSIOGRAPHY

3.1 INTRODUCTION

The main physiographical features examined for the baseline study consist of geomorphological units and the topographical characteristics observed in the study area. An understanding of geomorphology and topography is essential for the baseline study, because it provides information on the processes responsible for the formation of soils and the characteristics of surface and groundwater flow systems. The analysis of physiographic regions and geomorphologic units provides the extent of the area where similar physical characteristics and associated ecosystems may be encountered, and consequently where similar human activities can occur.

3.2 METHODS

The physiographic features were examined both in the local and regional study areas as shown on Map 2.1.

A desktop study approach was used in order to characterise the physiographical features of the study areas. Most of the data were extracted from existing documentation, such as reports, maps, satellite imagery, aerial photographs, and were completed by field observations. More specifically, the information on geomorphology in the study areas has come from an exhaustive report entitled «*Carte morphopédologique, République de Guinée»,* published by the Institut de Recherches pour le Développement (IRD) (Boulvert 2003).

Ground surface elevations were taken during an aerial survey carried out by Rio Tinto in December 2006, and the results used for the preparation of a Digital Terrain Model (DTM) with a 2 m resolution and a vertical accuracy of 0.21 m.

3.3 RESULTS

3.3.1 Physiographical Regions

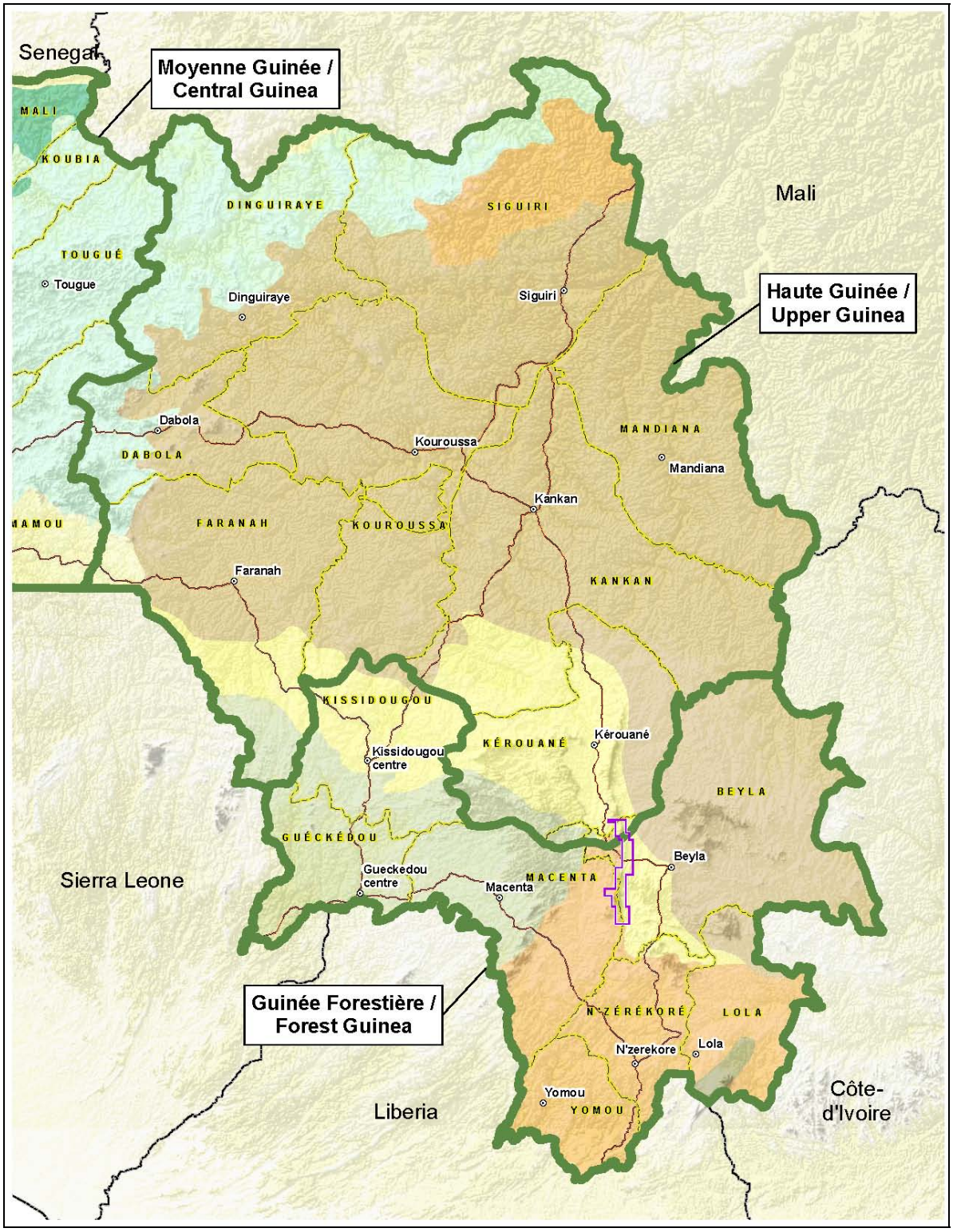
Physiographical regions are typically established according to physical characteristics of the environment, including climate, topography, landform and geology. Guinea is divided into four large physiographical regions with distinct physical characteristics:

- Upper Guinea
- Central Guinea
- Lower Guinea (also referred to as Maritime Guinea)
- Forest Guinea

The Simandou Project is situated in the Forest Guinea physiographical region, which is located in the southeastern part of the country (Figure 3.1). The Forest Guinea region is bordered by Sierra Leone, Liberia and Côte d'Ivoire, and is located between north latitudes 7°30' and 9°30', and west longitude 8° and 10°30'. The region covers an area

of approximately 49,500 km^2, which represent about 20% of the total land area of Guinea.

Figure 3.1 Main physiographical regions in southeastern Guinea



Source: Boulvert 2003

The Simandou Project is located within a vast area dominated by forest cover that forms distinct ecosystems specific to southeastern Guinea (see Chapter 4 of Volume D). The important forest cover and the topography also demonstrate the significance of the rainy conditions typical of southeastern Guinea, which will influence soils, and surface and groundwater flow systems.

3.3.2 Geomorphological Units

The Forest Guinea physiographic region is characterised by a few distinct geomorphological units, classified primarily on the basis of topography, nature of the soils and surface deposits, and geology. These units are closely associated with the West African Craton, one of the four large continental rock masses that merged together to form Africa in the late Precambrian and early Palaeozoic geological eras.

Four geomorphological units are encountered in the RSA (Map 3.1): the Senko Pediplain, the Macenta Granites, the Guinean Dorsal and the N'Zérékoré Notch. However, only the Guinean Dorsal and N'Zérékoré Notch are found in the LSA, and are located, respectively, to the east and west sides of the Simandou ridge.

The Guinean Dorsal (also called Loma-Man Dorsal) geomorphological unit is a group of disjointed high elevation mountain ranges, such as the Simandou Range, which run parallel to the Atlantic coast. It presents a shape in the relief displaying a large radius convexity, spanning some 800 km from the northwest to the southeast, and is characterised by a crystalline rock basement composed primarily of granitic igneous rocks, typical of the West African Craton. The Dorsal is also the water divide for the Niger and Senegal river watersheds, and other important coastal rivers.

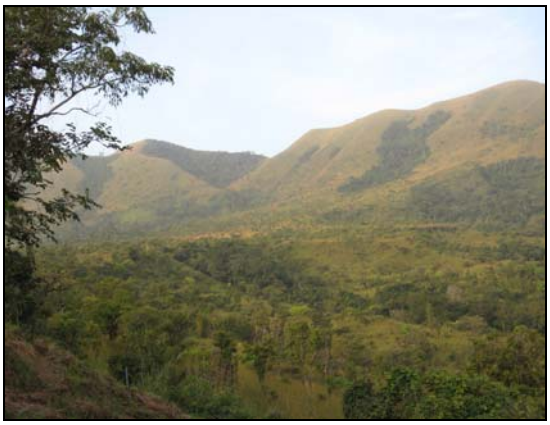
The N'Zérékoré Notch on the western side of the ridge, also part of the West African Craton, presents typically lower elevations than the Guinean Dorsal, although it is similar in nature. However, it is characterised by gneissic metamorphic rocks.

3.3.3 Topography

The general topography is mountainous along the Simandou Range and undulating in surrounding areas. The topography of the Simandou Range consists in steeply-sloped hills, separated by deep depressions (ravines), gradually changing into foothills in the piedmont area, and then into low-elevation plateaus. The ravines, of varying size, often contain small streams in dry inland valleys, known as *bas-fonds*; and alluvial plains along rivers and creeks (IRAG 2009). Photo 3.1 presents the typical landscape.

The Simandou Range presents a north-south axis, with an altitude exceeding 1,000 m over a distance of 25 km. It has an average ridge width varying between 1 and 2 km. The ridge is at its largest in the Pic de Fon Classified Forest (PdF CF), where the altitude is higher than 1,000 m and the width approximately 4 km. The average altitudes in Pic de Fon and Ouéléba areas are in the order of 1,500 and 1,200 m respectively.

Photo 3.1 Typical landscape of the Simandou Range




Source: SNC-Lavalin Environment 2008

Typically, the study area rises as a prominent ridgeline of approximately 600 to 700 m above the plateaus, reaching a maximum altitude of 1,656 m at Pic de Fon, 1,650 at Pic Dabatini, 1,132 m at Ouéléba and 1,165 m at Pic de Foko which is located in the southern part of the PdF CF (Map 3.2). The plateau located on the western side of the Simandou Range has a width of approximately 20 km and an altitude ranging from 550 to 650 m. The altitude of the plateau located on the eastern side of the ridge is higher, and exceeds 650 m, with some plateaus reaching altitudes in the order of 800 m.

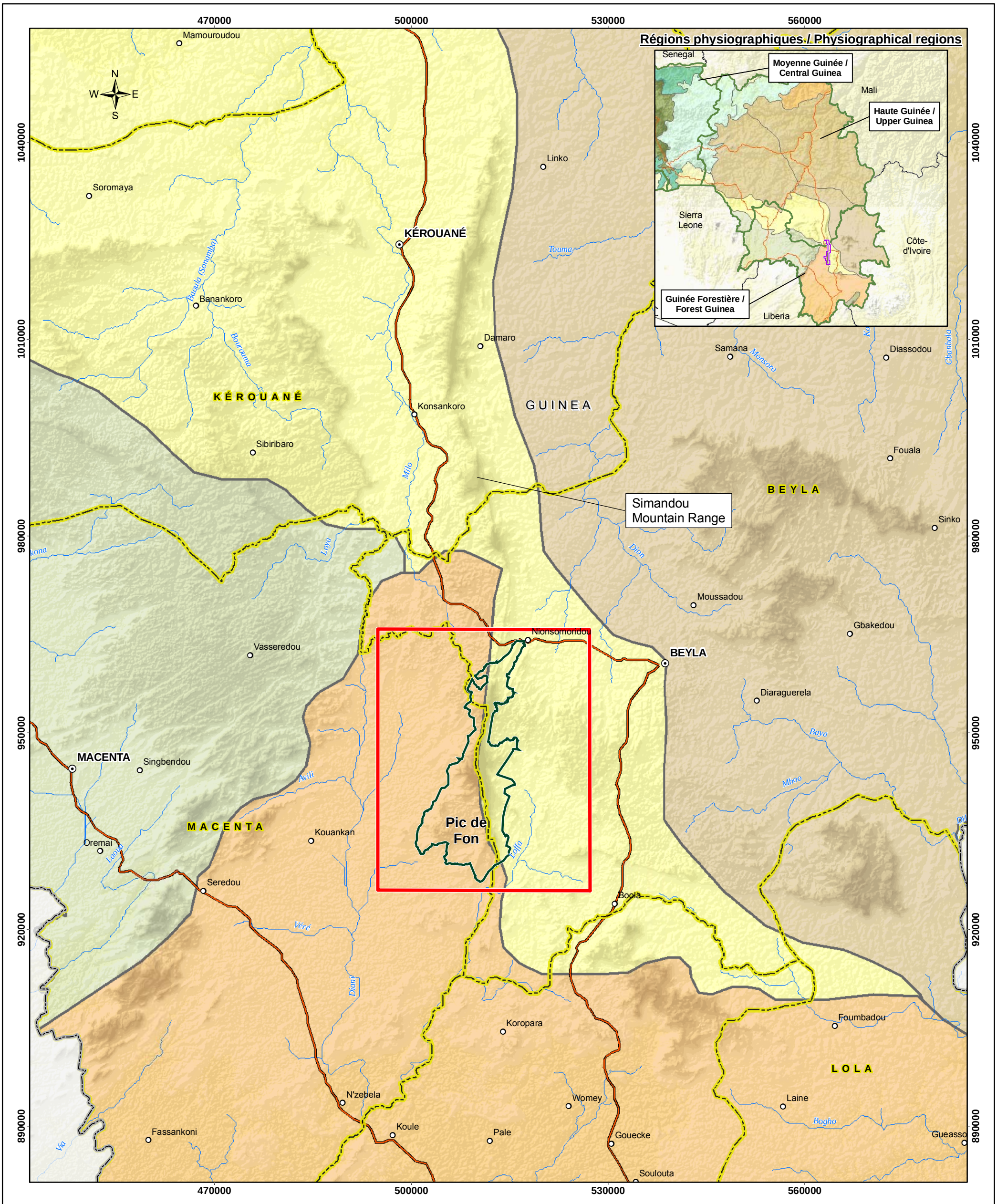
The steep topography of the Simandou Range can be observed in Photo 3.2, and the main typical morphological features are the following:

- Natural slopes varying from 25° to more than 40° on the flanks of the ridge. In Ouéléba, the slope angles are shallower than at Pic de Fon, although the western flank of Ouéléba is delineated by a prominent escarpment.
- The very steep slopes are generally encountered in the harden series of itabirite rocks, which are part of the mountain core, and are often found at mid-hillslope elevations.
- In Ouéléba, the phyllites series of rocks, typically encountered at the basis of the range, are deeply weathered and notched.

Photo 3.2 Typical hillslopes in the Pic de Fon area




Source: SNC-Lavalin Environment 2008



Régions physiographiques / Physiographical regions

Unités géomorphologiques / Geomorphological units

Dorsale guinéene	Guinean Dorsal
Entaille de N'Zérékoré	N'Zérékoré Notch
Massif granitique de Macenta	Macenta Granites
Pédiplaine de Senko	Senko Pediplain

Zone d'étude / Study area

Zone d'étude locale	Local study area

Sources :
1- Base map - 2006 0.5m ADS40 Aerial Photographs, 2006 Spot Imagery;
2- 2002-2003 Landsat Imagery;
3- Shuttle Radar Topography Mission (SRTM);
4- Carte topographique IGN 1:50 000/1:200 000;
5- IRD - Yves Boulvert (2004), Carte morphopédologique de Guinée, 1:200 000;
6- Geographic Coordinate System: WGS84, UTM, Zone 29N

Repères géographiques / Geographical landmarks

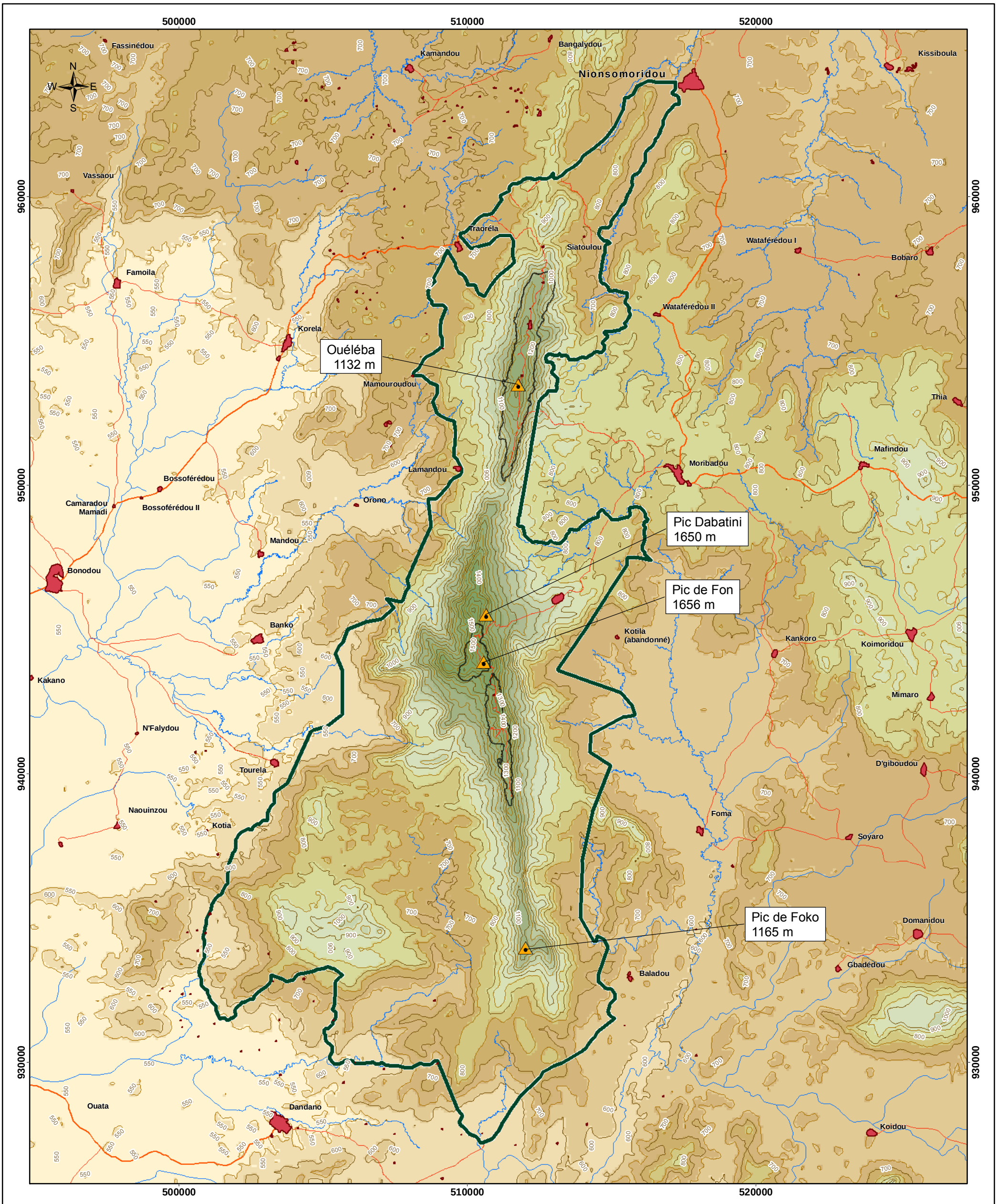
Chef-lieu de préfecture	Prefecture centre
Chef-lieu de CRD et CU	CRD and CU centre
Frontière nationale	National border
Limite de préfecture	Prefecture boundary
Route principale	Main road
Hydrographie	Hydrography
Forêt classée du Pic de Fon	Pic de Fon Classified Forest

Note : Les limites administratives proviennent de sources multiples et sont approximatives / Administrative boundaries are from multiple sources and are approximate.

Titre / Title

Unités géomorphologiques dans la zone d'étude régionale / Geomorphological units in the regional study area

Échelle / Scale: 0 2.75 5.5 11 Km — 1:550,000			Projet / Project: SIMANDOU	Volume C 3.1
Directeur de projet (client) / Project manager (client): Leon Payne		Directeur de projet / Project manager: Richard Fontaine		No. pr./ P. number: 604917
01	2010/06/15	Final	M. Dupré	M. Stapinsky
00	2010/01/04	Preliminary	M. Dupré	M. Stapinsky
No.	aaaa/mm/jj yyyy/mm/dd	Description	Dessiné/Drawn	Vérifié/Verified



Élévation / Elevation (m)

501 - 550	901 - 950
551 - 600	951 - 1000
601- 650	1001 - 1050
651 - 700	1051 - 1100
701 - 750	1101 - 1200
751 - 800	1201 - 1300
801 - 850	1301 - 1400
851 - 900	1401 et / and +

Courbe de niveau (équidistance : 50 m) — Contour Line (Interval : 50 m)

Sources :
1- Base map - 2006 0.5m ADS40 Aerial Photographs, 2006 Spot Imagery;
2- 2002-2003 Landsat Imagery;
3- Shuttle Radar Topography Mission (SRTM);
4- Carte topographique IGN 1:50 000/1:200 000;
5- Geographic Coordinate System: WGS84, UTM, Zone 29N

Repères géographiques / Geographical landmarks

Principal sommet	Main summit
Route secondaire	Secondary road
Piste	Track
Hydrographie	Hydrography
Forêt classée du Pic de Fon	Pic de Fon Classified Forest
Milieu bâti	Built area
Aire minière	Mining area

Titre / Title

Topographie dans la zone d'étude locale / Topography in the local study area

Échelle / Scale	Projet / Project	Volume C Carte/Map 3.2
0 0.625 1.25 2.5 Km — 1:125,000	SIMANDOU	

Directeur de projet (client) Project manager (client)	Directeur de projet Project manager	No. pr./ P. number
Leon Payne	Richard Fontaine	604917

No.	aaaa/mm/jj yyyy/mm/dd	Description	Dessiné/Drawn	Vérifié/Verified
01	2010/06/15	Final	M. Dupré	M. Stapinsky
00	2010/01/04	Preliminary	M. Dupré	M. Stapinsky

CHAPTER 4

Climate

4. CLIMATE

4.1 INTRODUCTION

This chapter presents the baseline regional and local climate including the meteorology aspects. Data from the synoptic and climatological stations of the *Direction Nationale de la Météorologie* (DNM) have been used to characterise the climate in the regional study area (RSA). For the local study area (LSA), the climate characterisation is based on the data extracted from the Rio Tinto meteorological network.

In addition to the regional and local climate characterisation, a specific study on rainfall conditions within the LSA in correlation with altitude and the ridge exposure (east versus west facing slopes) was undertaken by the UK Met Office (UKMO). The three-phase study relied on empirical measurements of rainfall and a numerical modelling study.

4.2 METHODOLOGY

4.2.1 National Direction of Meteorology Data

Daily data for several parameters, including temperature and rainfall, were provided by the DNM for the following weather stations: Beyla, N'Zérékoré, Kissidougou, Macenta and Kérouané (see locations on Map 3.2).

All five stations are located on a plateau, therefore at a relatively low altitude (UKMO 2008b). Beyla station is at the highest elevation (700 m), the other weather stations are at locations with altitudes ranging between 500 and 550 m. The similarity in altitude is useful in the evaluation of factors controlling their climatic differences (UKMO 2008b). All the stations have long term records of climatic data (from 40 to 90 years).

The DNM data were used mainly to characterise the RSA climate.

4.2.2 Rio Tinto Meteorological Network

Rio Tinto has established an extensive meteorological network in the LSA which, in 2008, included five automatic weather stations, 15 automatic rain gauges[1], ten manual rain gauges near villages, three fog gauges, and four fog cameras (WMC 2008) (Map 4.1).

[1] Automatic rain gauge located in Beyla town doesn't appear on Map 3.1.

Initially, a network of three automatic weather stations was installed in 2001. These stations were arranged in an east-west transect across the range: at the base of the Simandou Range on the east and west sides (at an altitude of 830 m at Mafindou and of 710 m at Mandou), and on the crest of the range at Dabatini (1,650 m altitude). Photo 4.1 shows the set up of an automatic weather station. The initial three automatic weather stations were supplemented in July 2007 by two additional weather stations which were installed on the Pic de Ouéléba (1,330 m) and at Foko West (810 m), the latter located in a clearing in the forest on the western slope of the range. Powered by solar panels, the stations recorded rainfall, temperature, humidity, wind speed and direction, solar radiation and barometric pressure at 30 minute intervals. Not all parameters were measured continuously at each station and there are some gaps in the records owing to equipment malfunction (WMC 2008). However, since July 2007, all stations have been recording all the parameters.

Photo 4.1 Automatic weather station



Source: WMC 2009

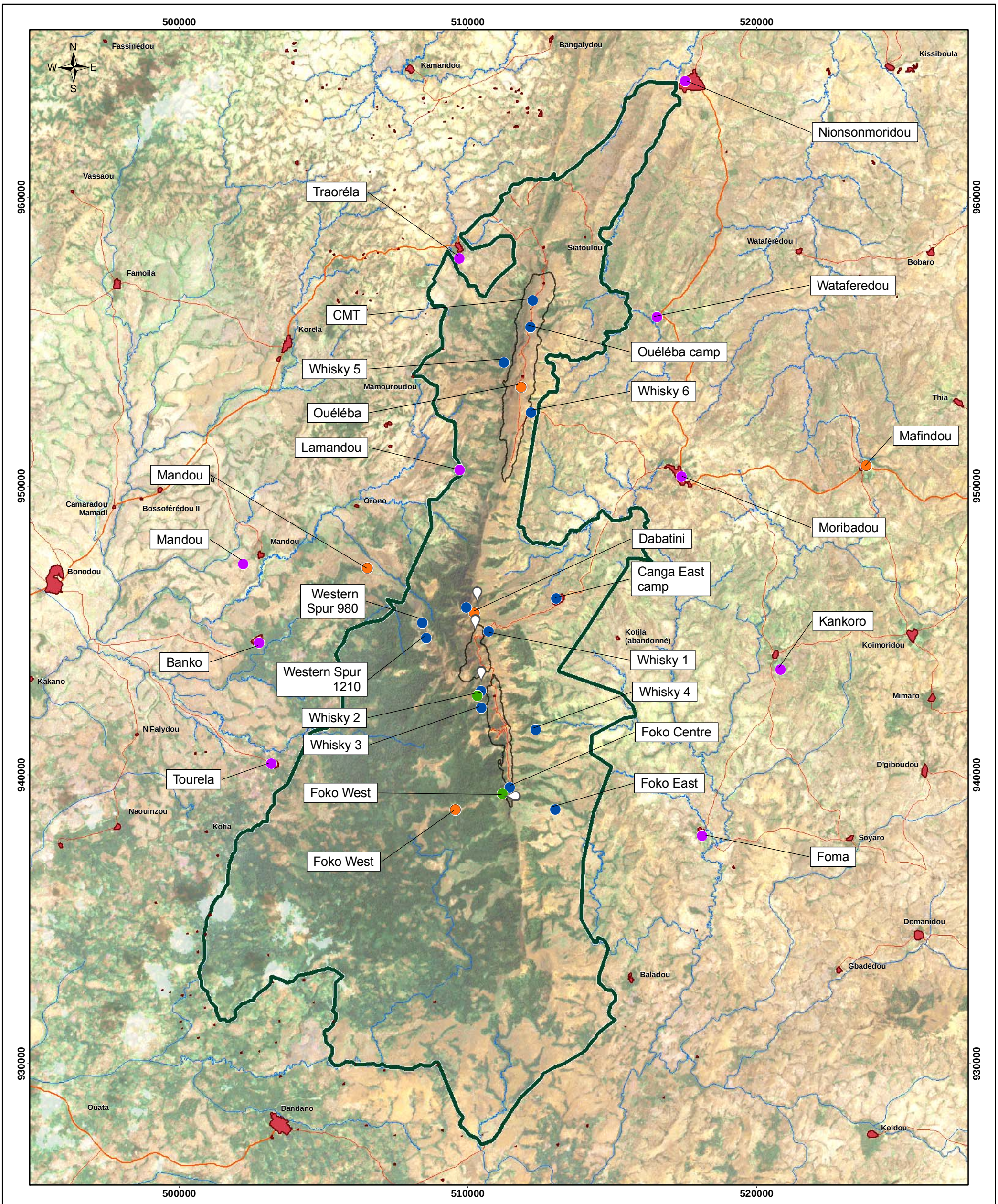
In addition to the automatic weather stations, 15 automatic rain gauges were installed in 2006-2007 to provide detailed information on rainfall in different locations of the LSA (Map 4.1). Their locations were chosen so as to form additional east-west transects across the Simandou Range to the north and south of the Mafindou-Dabatini-Mandou transect. Powered by batteries, the automatic rain gauges recorded rainfall depth at 30 minute intervals (the same as the automatic weather stations).

Also, during 2007, 10 manual rain gauges were installed in certain villages surrounding the Simandou Range to provide additional information on rainfall (Map 4.1).

A first fog gauge was installed in 2009 on the west side of the ridge at 1,030 m altitude. As no fog was recorded yet as of June 2009, it is possible that the gauge was installed below the fog zone. One other fog gauge was then installed at the end of 2009 at 1,350 m altitude near Whisky 2 along with four time lapse fog cameras (Map 4.1). Finally, village based observers recorded occurrence of rainfall and thunder storms.

The main characteristics of the weather stations, automatic rain gauges and manual rain gauges are presented in Appendix A.

For the purpose of the baseline study, the data was analysed up to December 2008.



Stations météorologiques de Rio Tinto / Rio Tinto meteorological stations

Station météorologique automatique	Automatic weather station
Station pluviomètrique automatique	Automatic rain gauge
Station pluviomètrique manuelle	Manual rain gauge
Jauge de brouillard	Fog gauge
Caméra et direction	Fog camera (with direction)

Repères géographiques / Geographical landmarks

Route secondaire	Secondary road
Piste	Track
Hydrographie	Hydrography
Forêt classée du Pic de Fon	Pic de Fon Classified Forest
Milieu bâti	Built area
Aire minière	Mining area

Sources :
1- 2002-2003 Landsat Imagery;
2- Geographic Coordinate System: WGS84;
3- Water Management Consultants, 2008

Titre / Title

Réseau météorologique de Rio Tinto dans la zone d'étude locale / Rio Tinto meteorological network in the local study area

Échelle / Scale		Projet / Project	Volume C Carte/Map 4.1
0 0.625 1.25 2.5 Km — 1:125,000		SIMANDOU	
Directeur de projet (client) / Project manager (client): Leon Payne		Directeur de projet / Project manager: Richard Fontaine	No. pr./ P. number: 604917
01	2010/06/15	Final	M. Dupré	R. Fontaine
00	2010/01/04	Preliminary	M. Dupré	M. Stapinsky
No.	aaaa/mm/jj yyyy/mm/dd	Description	Dessiné/Drawn	Vérifié/Verified

4.2.3 Climatological Study Approach

A three-phase climatological study was undertaken by UKMO (2008b) with the overall objective to assess the potential impact on local rainfall and humidity related to the lowering of the Simandou ridge during mining operations.

Phase 1 includes a climatological study to characterise local and regional climate; establish dominant rainfall producing mechanisms; and if possible assess the significance of orographic rainfall in the Simandou hills. Phases 2 and 3 involve detailed modelling of local climate with and without the proposed excavation during the mining operation phase.

The results on the rainfall mechanisms (phase 1) are presented in Section 4.3.2.7. Results of Phases 2 and 3 will be integrated in the SEIA assessment phase.

4.3 RESULTS

4.3.1 Regional Climatic Context

The climate of Guinea is dominated by phenomena that are driven by the interaction of: (a) the seasonal migration of the overhead sun and zone of maximum radiation, and heating northwards during January to July and southwards during August to December; (b) related seasonal changes in the distribution of subtropical high pressure systems over the Sahara Desert and the Atlantic Ocean to the south (WMC 2008). Large scale uplift of air is associated with the zone of maximum heating, creating a migrating latitudinal zone of low pressure into which converge dry surface winds from the northeast and moist surface winds from the southwest originating from the zones of high pressure over the Sahara Desert and Atlantic Ocean respectively. This zone is often called the Inter-Tropical Convergence Zone (ITCZ) and is characterised as a zone of instability and increased rainfall resulting from widespread uplift (convection) of moist air.

There is a substantial decrease, northwards across Guinea, in annual rainfall amounts (1,200 mm at Siguiri compared to 2,600 mm in Macenta) and in the duration of the wet season (UKMO 2008b). The wet season is longest in the south of the country (9-10 months in N'Zérékoré/Macenta) and shortest (5 months) in the north. There is also a decreasing rainfall gradient from the ocean inland.

A feature of the temperature is the limited annual variation in daily maxima and minima. In Guinea generally, the wet season is also the cooler season, with the lowest daytime maxima in August (27.5 ^{o}C). Highest daily maxima occur in March (32-34 ^{o}C). However, daily minima are highest in the latter part of the wet season, August to November, and lowest in December, but vary only between about 16 ^{o}C and 20 ^{o}C (UKMO 2008b).

The climate of southeast Guinea, which corresponds approximately to the RSA, is seasonal humid tropical and dominated by the West African monsoon. Map 4.2 shows the general distribution of mean annual rainfall and temperature in the RSA as recorded at the five DNM weather stations.

The mean annual precipitations are significantly higher in Macenta (> 2,800 mm) than at Kérouané and Beyla reflecting the west to east and south to north gradients generally observed in southeast Guinea. Because air to the south of the ITCZ is moist, rainfall over Guinea is seasonal and monsoonal. The wet season lasts approximately eight months, from March to October. At all stations, the wettest months are either August or September (Map 4.2). The dry season lasts from November to February. Approximately 90-95% of annual rainfall occurs in the wet season in southeast Guinea (WMC 2008).

The annual mean temperatures are, within tenths of a degree, identical at the five DNM weather stations (24 ^{o}C). The highest temperatures occur in the early part of the year with March being the hottest month all over southeast Guinea. In general, temperatures are lower in the middle of the year, corresponding to the peak of wet season and cloud cover, and also in December and January, corresponding to the dry season (Map 4.2).

In summary, there are two different seasons in the RSA, distinguished by the rainfall regime rather by the temperature (UKMO 2008b). This is a characteristic of a monsoon climate: a long wet season and a short dry season. The climate is characterised by high annual rainfall, typically at least 1,700 mm per year. It is warm throughout the year with small seasonal variations in temperature. The warmest period is at the end of the dry season.

Tables that detail the monthly mean, daily maximum and minimum temperatures and rainfall for the five DNM weather stations (1961-1991) are presented in Appendix B.

4.3.2 Results in the Local Study Area

The data extracted from Rio Tinto's meteorological network have been compiled, analysed and regrouped by parameter.

The climate characterisation in the local study area includes the following parameters: atmospheric pressure, solar radiation, temperature, wind, humidity, evaporation, and precipitation. Summary of all data collected are included in the following sections and detailed data are presented in appendices (see respective sections for appendix numbers).

320000 350000 380000 410000 440000 470000 500000 530000 560000 590000

1100000 1070000 1040000 1010000 980000 950000 920000 890000 860000 830000 800000 770000

N W E S

1600 1800 2000 2500 3000

Kissidougou Centre

Kérouané

Macenta

Beyla Centre

N'zérékore

KISSIDOUGOU CENTRE

KÉROUANÉ

SIMANDOU RANGE

MACENTA

BEYLA

N'ZÉRÉKORE

GUECKEDOU CENTRE

YOMOU

LOLA

Niandan Balé Milo Kouraé Dion Gbanhala Délé Quaou Meli Diani Leoua Oua Mani

CÔTE-D'IVOIRE

SIERRA LEONE

GUINEA

Senegal Mali Sierra Leone Liberia

1200 1400 1600 1800 2000 2200 2400 2600 2800 3000 3400

320000 350000 380000 410000 440000 470000 500000 530000 560000 590000

Stations météorologiques de la DNM / DNM meteorological stations

Courbe pluviométrique (mm) (1961-1991) — Rainfall contour (mm) (1961-1991)

Station climatologique — Climatological station

Station synoptique — Synoptic station

Sources :
1- 2002-2003 Landsat Imagery;
2- Geographic Coordinate System: WGS84;
3- Water Management Consultants, 2008

Précipitation moyenne annuelle / température / Mean annual rainfall / temperature



Précipitation (mm) — Rainfall (mm)

Température (C) — Temperature (C)

Repères géographiques / Geographical landmarks

Chef-lieu de préfecture — Prefecture centre

Frontière nationale — National border

Route principale — Main road

Hydrographie — Hydrography

Forêt classée du Pic de Fon — Pic de Fon Classified Forest

Titre / Title

Contexte climatique régional / Regional climatic context

Échelle / Scale	Projet / Project	Volume C Carte/Map 4.2
0 5.5 11 22 Km 1:1 100 000	SIMANDOU	

Directeur de projet (client) / Project manager (client)	Directeur de projet / Project manager	No. pr./ P. number
Leon Payne	Richard Fontaine	604917

No.	aaaa/mm/jj yyyy/mm/dd	Description	Dessiné/Drawn	Vérifié/Verified
01	2010/06/15	Final	M. Dupré	R. Fontaine
00	2010/01/28	Preliminary	M. Dupré	R. Auger

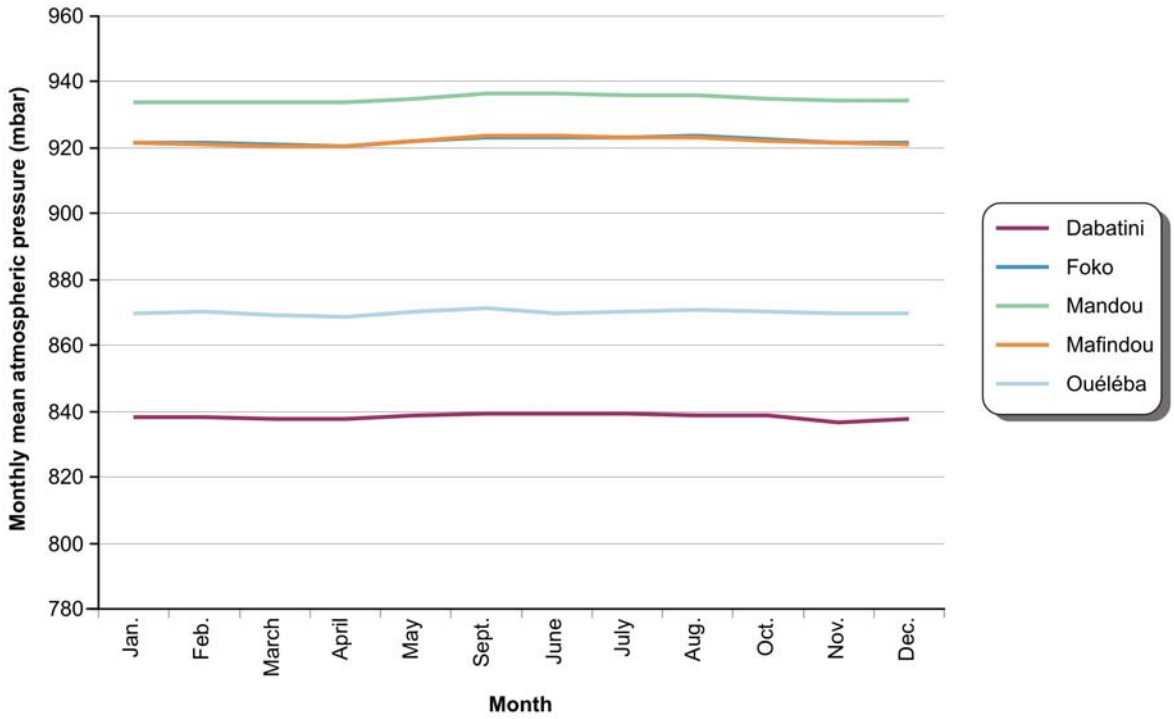
4.3.2.1 Atmospheric Pressure

The atmospheric pressure is the force exerted against a surface by the weight of the air above that surface. Therefore, as elevation increases, there is less overlying atmospheric mass resulting in a decrease in atmospheric pressure (WMC 2008).

As is typical of tropical regions there is only a small seasonal variation in atmospheric pressure which is related to low variation in temperature (Figure 4.1). Pressure varies from day to day throughout the year, but rarely by more than 3 mbar. The period of highest pressure (the wet season) coincides with the period of lowest temperature (which itself is related to cloud cover and high humidity), and the period of lowest pressure (the dry season) coincides with the period of highest temperature (WMC 2008).

The weather stations located at the base of the Simandou ridge at an altitude of around 700-800 m (Foko West, Mafindou and Mandou) registered average atmospheric pressures of 922-935 mbar while the stations located on the top of the ridge, above 1,300 m (Dabatini and Ouéléba), registered average atmospheric pressures of 838-870 mbar (Figure 4.1). If the average altitude of the Pic de Fon ridge is assumed to be 1,400 m the average pressure on the ridge top is 864 mbar. On Ouéléba the average pressure is 870 mbar (WMC 2008).

Figure 4.1 Monthly mean atmospheric pressure in the local study area



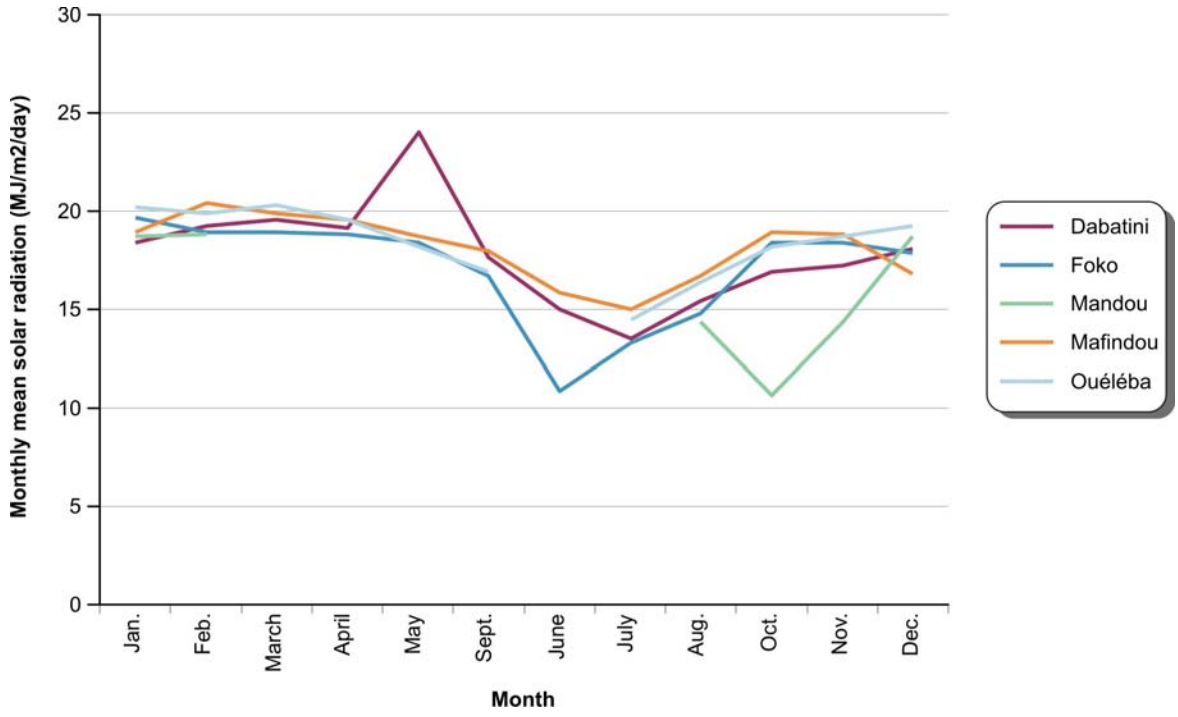
Note: Refer to Appendix C for detailed data and date of records.

4.3.2.2 Solar Radiation

The monthly mean solar radiations for the five different weather stations are illustrated in Figure 4.2. There is considerable day to day variation in radiation throughout the year depending on cloudiness, particularly at the start and end of the wet season (WMC 2008). During the wet season, cloud cover and fog significantly reduce solar radiation levels from those on a clear day. At all stations the monthly mean radiation is lowest during the wet season with values varying from 11 to 16 MJ/m^2/day, and increases towards the dry season to reach 19-20 MJ/m^2/day.

The weather stations located on the west side of the ridge (e.g. Mandou – mean solar radiation of 15.90 MJ/m^2/day) receive annually less solar radiation than the stations located on the east side of the ridge (e.g. Mafindou – mean solar radiation of 18.08 MJ/m^2/day), indicating greater cloud cover and fog on the west side than on the east. The same pattern applies for Dabatini and Foko West who receive the lowest radiation in the wet season. The Pic de Ouéléba is less prone to low cloud and fog, and receives more radiation than Dabatini during the dry season[2]. Mafindou on the east side of the ridge receives the most radiation in the wet season (mean of 15.83 MJ/m^2/day).

Figure 4.2 Monthly mean solar radiation in the local study area



Note: Refer to Appendix D for detailed data and date of records.

[2] Data gaps for the wet season

4.3.2.3 Temperature

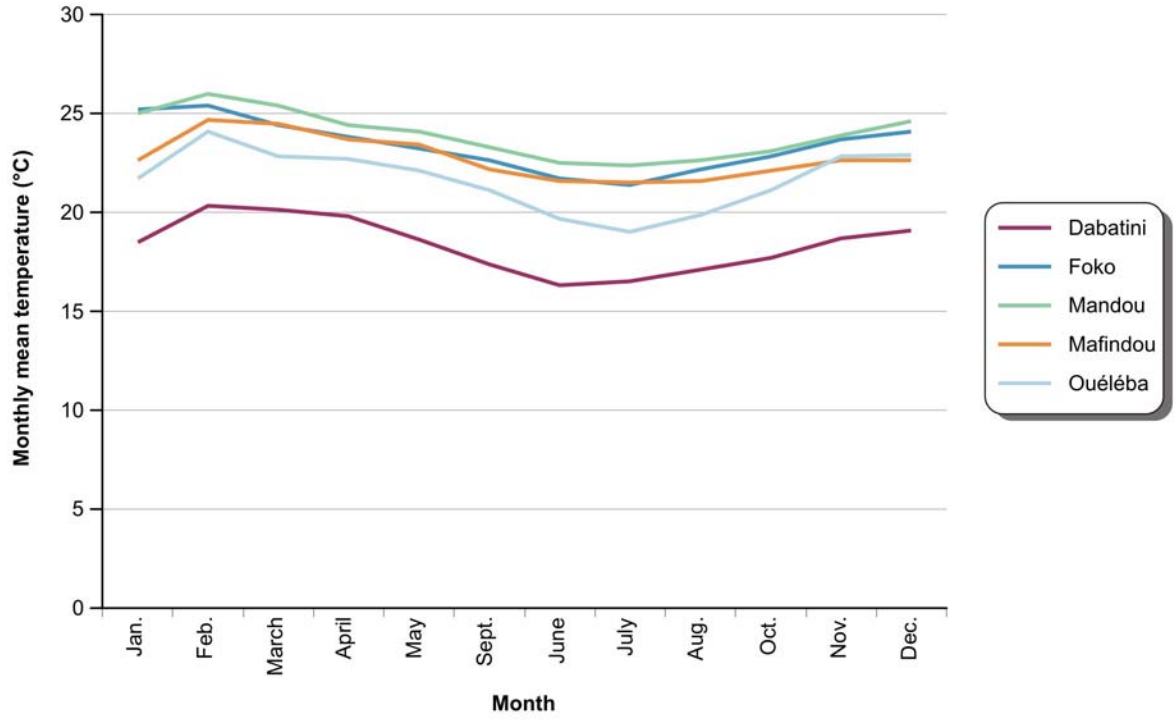
The ambient temperature variations within the LSA are mainly attributed to seasons (cloudiness and rain), and altitudes. As shown in Figure 4.3, the seasonal temperature trend is similar at all five weather stations.

The temperatures are the lowest (from 16 to 22.5 °C) during the wet season (July-August) and increase during the dry season to reach a maximum (varying from 20 to 26 °C) in February when the sky is clear and the solar radiation levels are the highest.

On Pic de Dabatini, the average wet season (July-August) temperature is approximately 16 °C compared to the dry season (February-March) temperature of about 20 °C. The monthly mean temperatures in Dabatini are significantly lower by approximately 5 °C (and up to 10 °C for the monthly maximums) compared to other stations located at the foot of the Simandou Range. The temperatures in Ouéléba are half way between those at Dabatini and the other stations during the wet season (Figure 4.3).

In addition to the seasonal trend, temperatures also vary with altitude. The annual mean temperatures decrease with altitude, being the coldest at Dabatini (annual mean of 18.3 °C – 1,650 m alt.) and the warmest at Mandou (annual mean of 23.9 °C – 710 m alt.).

Figure 4.3 Monthly mean ambient temperature in the local study area



Note: Refer to Appendix E for detailed data and date of record.

4.3.2.4 Wind

Within the LSA, wind speed and direction vary significantly over the course of the year depending on site and elevation. Map 4.3 illustrates seasonal (dry and wet seasons) wind roses for the 2004-2009 period[3] at the five weather stations (see Appendix F for data).

The wind speeds are higher on the more exposed ridges of Pic de Fon (Dabatini station) and Ouéléba than at the base of the mountains (Mafindou, Fokou and Mandou). The annual wind speeds equal 19.8 km/h and 14.4 km/h at Dabatini and Ouéléba stations but don't exceed 5.7 km/h at the other stations. As for the daily maximum wind speed, it reached 115.2 km/h at Dabatini, 89.6 km/h at Mandou and 67.7 m/s at the Mafindou station. Moreover, the top of the ridge receives a minimum wind speed of 7-11 km/h, which is not the case at the base of the mountain where wind speeds were recorded as low as 1.8 km/h.

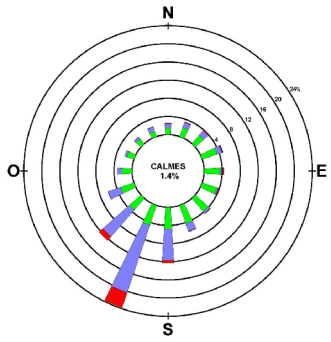
At high altitudes, the winds mostly come from the east and the west. At Ouéléba, the wind direction drastically veers from a westerly dominant wind in the wet season to an easterly dominant wind which is maintained throughout the dry season (Map 4.3). Dabatini, which is 320 m higher than Ouéléba, experiences strong dominant easterly winds which overlie the surface winds and blows all year round with some variation during the wet season. The depth of the monsoon wind layer is probably insufficient to reach the elevation of Dabatini, explaining why the dominant wind doesn't change during the wet season (WMC 2008).

The seasonal pattern is somewhat altered at the lowland stations on either side of the ridge by the north-south oriented orography which tends to enhance the northerly or southerly components of winds. This is well illustrated at Foko West with a strong proportion of low southerly winds during the wet season and northeast winds during the dry season. The main exception is at Mafindou on the eastern side of the range when the harmattan wind blows from the northeast in the dry season and is distributed from the south-southwest to the east during the wet season. Wind direction at Mandou is more variable, perhaps indicating the presence of wind rotors (WMC 2008).

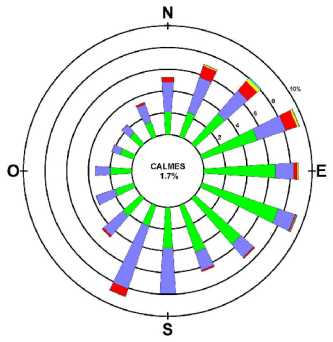
[3] Period varies depending of the station

MANDOU - Mai 2004 à avril 2005 / May 2004 to April 2005

Saison des pluies (mars à octobre) / Wet Season (March to October)



Saison sèche (novembre à février) / Dry Season (November to February)

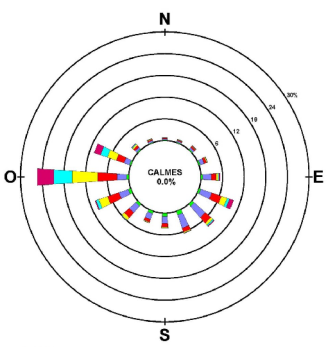


NOTE:
DIAGRAMME DE LA FRÉQUENCE DE PROVENANCE DU VENT
FREQUENCY DIAGRAM OF DIRECTION FROM WHICH THE WIND IS BLOWING

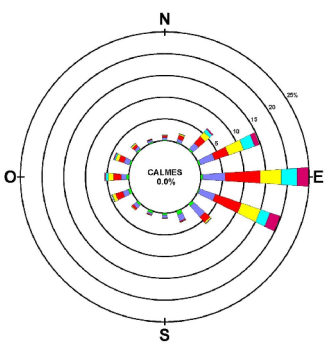
Alt: 710 m.

OUÉLÉBA - Novembre 2007 à octobre 2009 / November 2007 to October 2009

Saison des pluies (mars à octobre) / Wet Season (March to October)

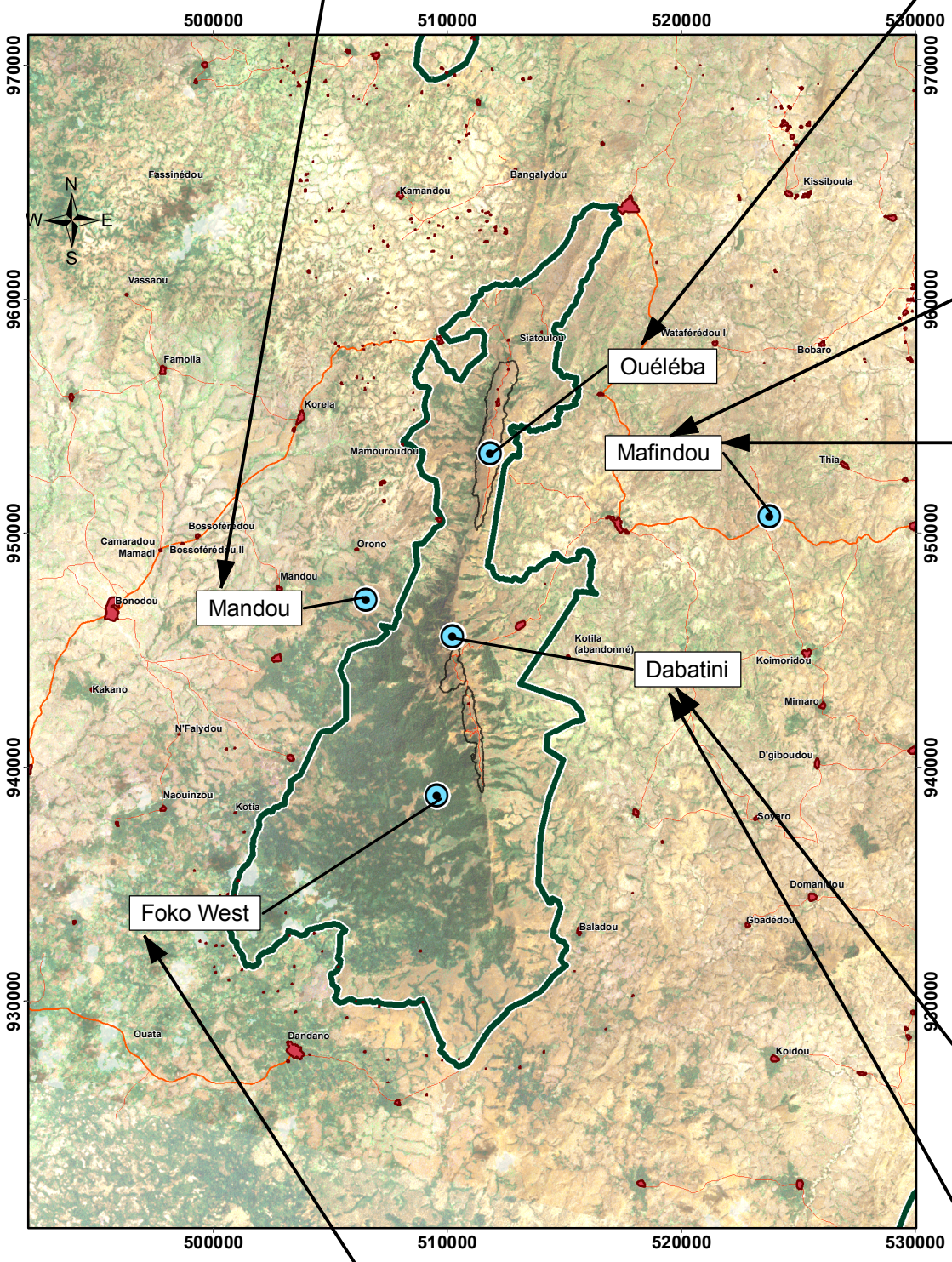


Saison sèche (novembre à février) / Dry Season (November to February)



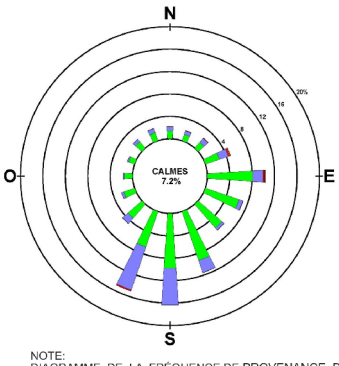
NOTE:
DIAGRAMME DE LA FRÉQUENCE DE PROVENANCE DU VENT
FREQUENCY DIAGRAM OF DIRECTION FROM WHICH THE WIND IS BLOWING

Alt: 1,330 m.

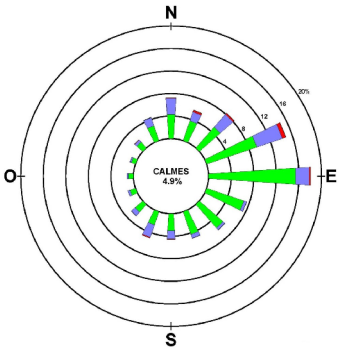


MAFINDOU - Mai 2004 à avril 2005 / May 2004 to April 2005

Saison des pluies (mars à octobre) / Wet Season (March to October)



Saison sèche (novembre à février) / Dry Season (November to February)

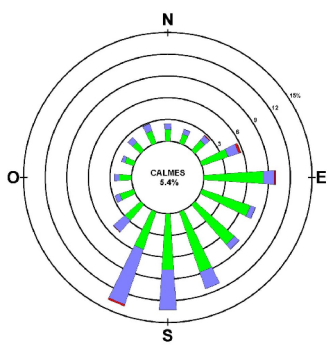


NOTE:
DIAGRAMME DE LA FRÉQUENCE DE PROVENANCE DU VENT
FREQUENCY DIAGRAM OF DIRECTION FROM WHICH THE WIND IS BLOWING

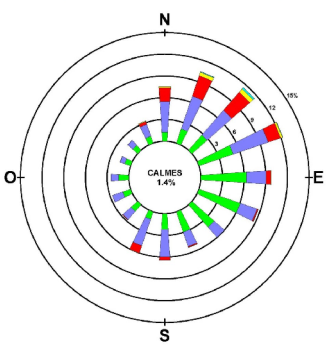
Alt: 830 m.

MAFINDOU - Novembre 2007 à octobre 2009 / November 2007 to October 2009

Saison des pluies (mars à octobre) / Wet Season (March to October)



Saison sèche (novembre à février) / Dry Season (November to February)

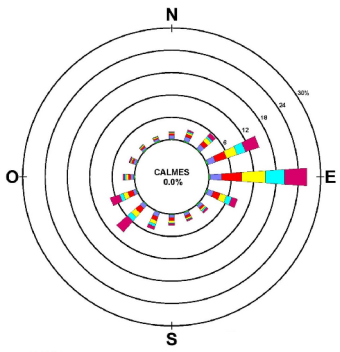


NOTE:
DIAGRAMME DE LA FRÉQUENCE DE PROVENANCE DU VENT
FREQUENCY DIAGRAM OF DIRECTION FROM WHICH THE WIND IS BLOWING

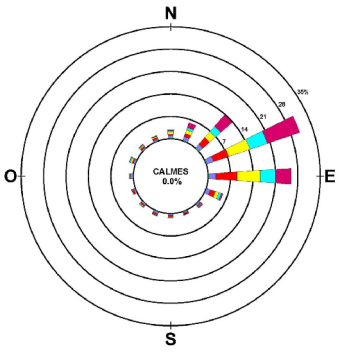
Alt: 830 m.

DABATINI - Juin 2004 à mai 2005 / June 2004 to may 2005

Saison des pluies (mars à octobre) / Wet Season (March to October)



Saison sèche (novembre à février) / Dry Season (November to February)

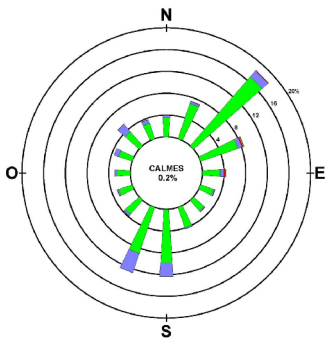


NOTE:
DIAGRAMME DE LA FRÉQUENCE DE PROVENANCE DU VENT
FREQUENCY DIAGRAM OF DIRECTION FROM WHICH THE WIND IS BLOWING

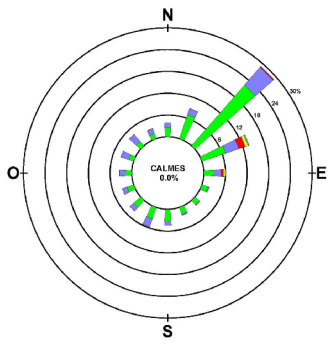
Alt: 1,650 m.

FOKO - Novembre 2007 à octobre 2009 / November 2007 to October 2009

Saison des pluies (mars à octobre) / Wet Season (March to October)



Saison sèche (novembre à février) / Dry Season (November to February)

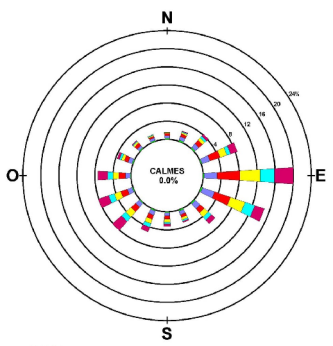


NOTE:
DIAGRAMME DE LA FRÉQUENCE DE PROVENANCE DU VENT
FREQUENCY DIAGRAM OF DIRECTION FROM WHICH THE WIND IS BLOWING

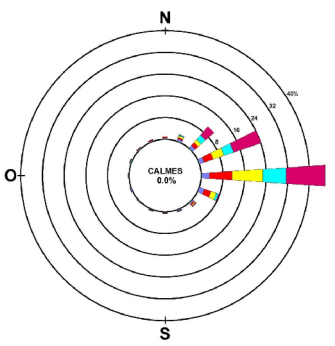
Alt: 810 m.

DABATINI - Novembre 2007 à octobre 2009 / November 2007 to October 2009

Saison des pluies (mars à octobre) / Wet Season (March to October)



Saison sèche (novembre à février) / Dry Season (November to February)



NOTE:
DIAGRAMME DE LA FRÉQUENCE DE PROVENANCE DU VENT
FREQUENCY DIAGRAM OF DIRECTION FROM WHICH THE WIND IS BLOWING

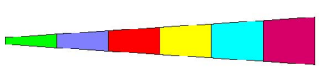
Alt: 1,650 m.

Stations météorologiques de Rio Tinto / Rio Tinto meteorological stations

Station météorologique automatique — Automatic weather station

CLASSES DE VITESSE DES VENTS (KM/H)
WIND SPEED CLASSES (KM/H)

0-5 5-10 10-15 15-20 20-25 >25



Repères géographiques / Geographical landmarks

Route secondaire	Secondary road
Piste	Track
Forêt classée du Pic de Fon	Pic de Fon Classified Forest
Milieu bâti	Built area
Aire minière	Mining area

Sources :
1- 2002-2003 Landsat Imagery;
2- Geographic Coordinate System: WGS84;
3- Water Management Consultants, 2008

Titre / Title

Rose des vents dans la zone d'étude locale / Wind Roses in the local study area

Échelle / Scale	Projet / Project	Volume C Carte/Map 4.3
0 1.375 2.75 5.5 Km — 1:275 000	SIMANDOU	

Directeur de projet (client) / Project manager (client)	Directeur de projet / Project manager	No. pr./ P. number
Leon Payne	Richard Fontaine	604917

No.	aaaa/mm/jj yyyy/mm/dd	Description	Dessiné/Drawn	Vérifié/Verified
01	2010/06/15	Final	M. Dupré	R. Fontaine
00	2010/01/04	Preliminary	M. Dupré	R. Auger

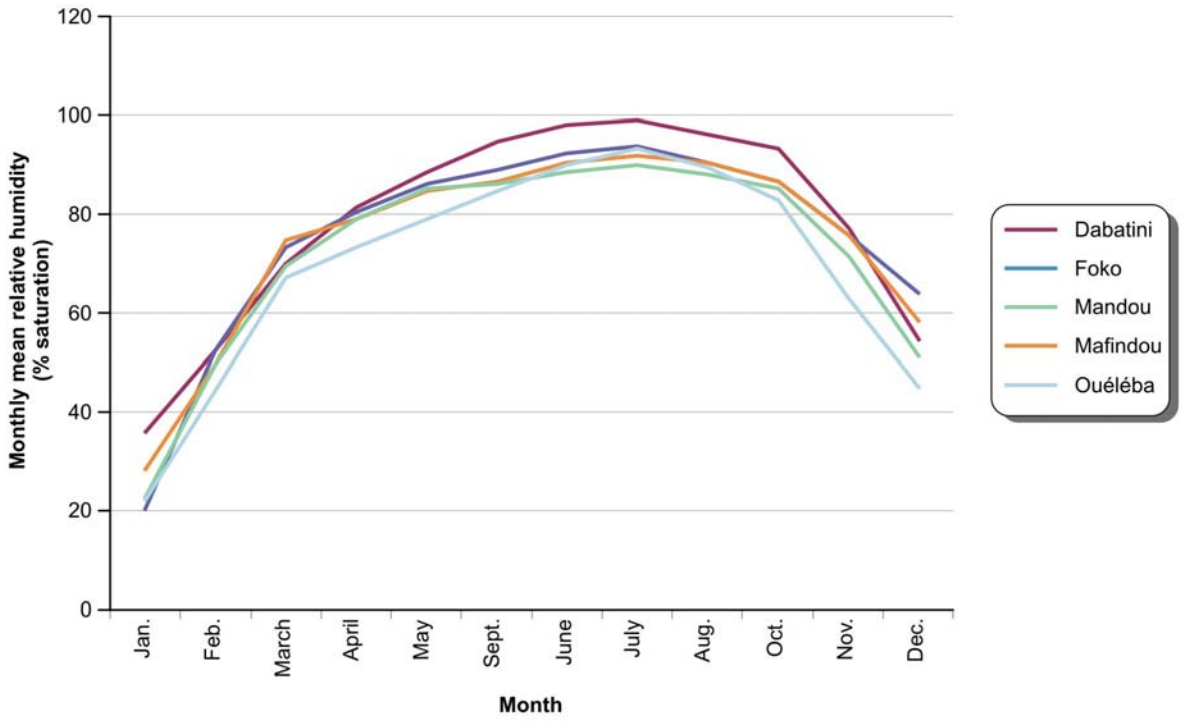
4.3.2.5 Humidity

The water vapour content of the air within the LSA, as measured by relative humidity, is strongly related to the provenance of the wind (WMC 2008). Northeasterly and easterly winds (harmattan) bring drier air while southerly and southwesterly winds (monsoon) bring air of higher humidity. Therefore, there is a strong seasonal variation in humidity (and rainfall) which is closely related to the seasonal variation in wind direction.

For much of the wet season, the air is close to saturation at all weather stations, with limited variability (Figure 4.4). With the onset of the dry season and the variability of wind direction and provenance, humidity becomes more variable. Daily mean relative humidity at the height of the dry season reaches lows of around 20% with the influence of the harmattan, but can reach maxima of 90-98% during incursions of moist air from the south.

As altitude increases, the temperature decreases which results in a higher percentage of humidity. Therefore, the air at Dabatini (annual mean of 78.4% – 1,650 m alt.) is more humid than the air at Mandou (annual mean of 72.2%) – 710 m alt.).

Figure 4.4 Monthly mean relative humidity in the local study area



Note: Refer to Appendix G for detailed data and date of records.

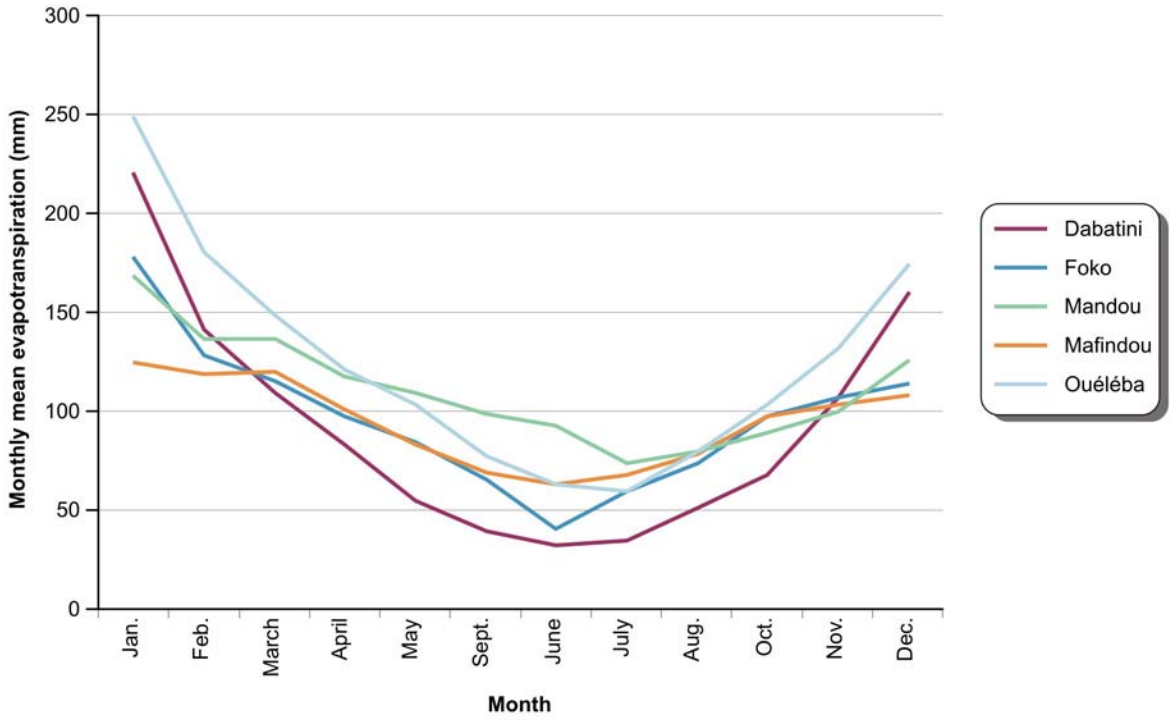
4.3.2.6 Evaporation

Evaporation occurs from open water surfaces, bare ground surfaces, and transpiration from the leaves of plants (called evapotranspiration). Evaporation may be measured

directly using an evaporation pan, or estimated indirectly by using existing meteorological data (WMC 2008). Direct measurements of evaporation have not been made at the project site. Instead, reliance has been placed on estimation of evaporation using meteorological data recorded by the automatic weather stations. Two indices of estimated evaporation were used: a) reference crop evapotranspiration (ET_o); and b) evaporation from an open water surface (E_o).

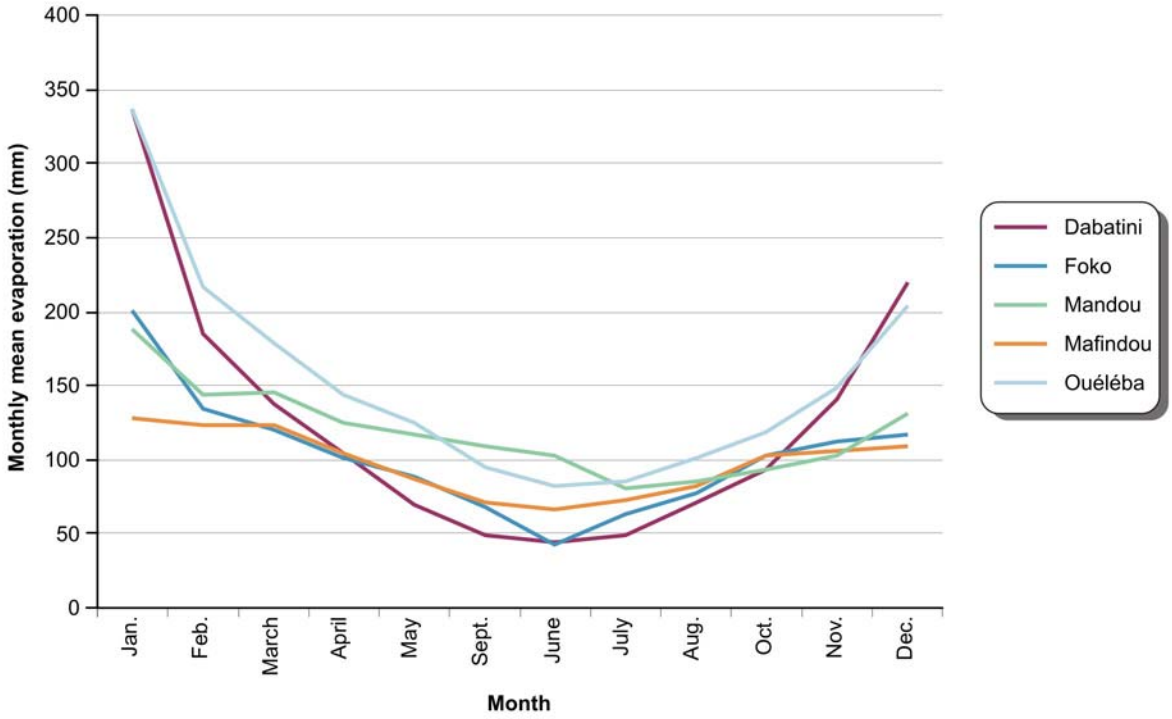
At all stations, monthly trends show the dry season as having the highest rates of ET_o and E_o whilst June to August records the lowest (Figure 4.5 and Figure 4.6). The maximum is reached at Ouéléba and Dabatini for the month of January with respective values of 248 mm for ET_o and 336 mm for E_o at Ouéléba, and 220 mm for ET_o and 336 mm for E_o at Dabatini. The high wind speeds recorded during this period at Ouéléba and Dabatini are responsible for this high evaporation rate (WMC 2008).

Figure 4.5 Monthly mean evapotranspiration (ETo) in the local study area



Note: Refers to Appendix H for detailed data and date of records.

Figure 4.6 Monthly mean evaporation (E_o) in the local study area



Note: Refer to Appendix H for detailed data and date of records. Precipitation

4.3.2.7 Precipitation

Precipitation at the LSA occurs as rainfall, fog and hail. Rainfall is the dominant form of precipitation in the LSA. Hail is a rare form of precipitation in the Simandou region.

This section characterise the rainfall mechanisms, the rainfall distribution and variability, and the rainfall intensity. Fog characterisation completes the rainfall pattern.

Rainfall Mechanisms

The rainfall over the Simandou Range is governed by the annual incursion northwards (during the northern hemisphere summer) and recession southwards (during the northern hemisphere winter) of the West African southwesterly monsoon. This monsoon generates heavy rainfall throughout the Simandou Range, irrespective of the topography. The fundamental mechanisms of that monsoon are energy from the sun, the annual cycle in the latitude of overhead sun path and the annual cycles of temperature and humidity differential that this generates between the Gulf of Guinea and the Sahara Desert. This should not be taken to imply that, topography is not a factor in modulating the rainfall, but it is not the primary mechanism for rainfall generation (UKMO 2008b).

The general rain mechanisms at the Simandou Range can be summarised as follows (UKMO 2008b):

- High moisture content air from the Gulf of Guinea;

- Large scale rising air motion in mid-troposphere (mid-wet season);
- Strong sun leading to intense convection (dominant in early and late wet season);
- Westward moving atmospheric disturbances intensifying the rainfall; and
- Modulation of the rainfall by topography (orographic enhancement).

Except where uplift mechanisms carry the moist monsoon air aloft, the moist monsoon air is confined to the lower troposphere and so could have its progress inland impeded by mountain barriers. While it is conceivable that an east-west or southeast-northwest aligned mountain barrier might delay the progress northwards of the monsoon, the narrow, north-south aligned profile of the Simandou Range should have little impact on its northward progress UKMO 2008b).

Towards the northern boundary of the monsoonal rain-prone band, convection is a major rainfall trigger. Although high ground may enhance convection, the convective storms develop widely, irrespective of topography, and are usually imported into Simandou from the east rather than developing in-situ (UKMO,2008b).

Rainfall records from PdF CF and adjacent plateaus show no clear proportionality between rainfall and altitude, but do show a relationship between rainfall and exposure. Sites on the western slopes and adjacent plateau receive more rain than sites on the eastern slopes and adjacent plateau.

There are two possible mechanisms for enhancement of rainfall by the Simandou ridge (UKMO 2008b):

- The moist surface winds in the wet season often have an upslope component on the western side of the Simandou ridge and so, are likely to constantly regenerate an orographically induced low cloud layer in the western approaches to the ridge. Because the moist monsoon layer is relatively shallow, this orographic cloud layer alone is seldom likely to be deep enough to generate more than drizzle or light rainfall. However it may, by a process of cloud droplet scavenging, increase the intensity of rain falling through it from convectively or dynamically induced clouds aloft.
- Any orographic convective enhancement of rainfall by the Simandou ridge is most likely to be triggered over the summit of the ridge, when mountain summits get warmer than the adjacent atmosphere at summit altitude, and then carried westwards by the easterly wind aloft. This situation occurs especially at the early or late wet season when more sun is present. This enhancement mechanism is the only one that can occur during the dry season.

Rainfall Distribution

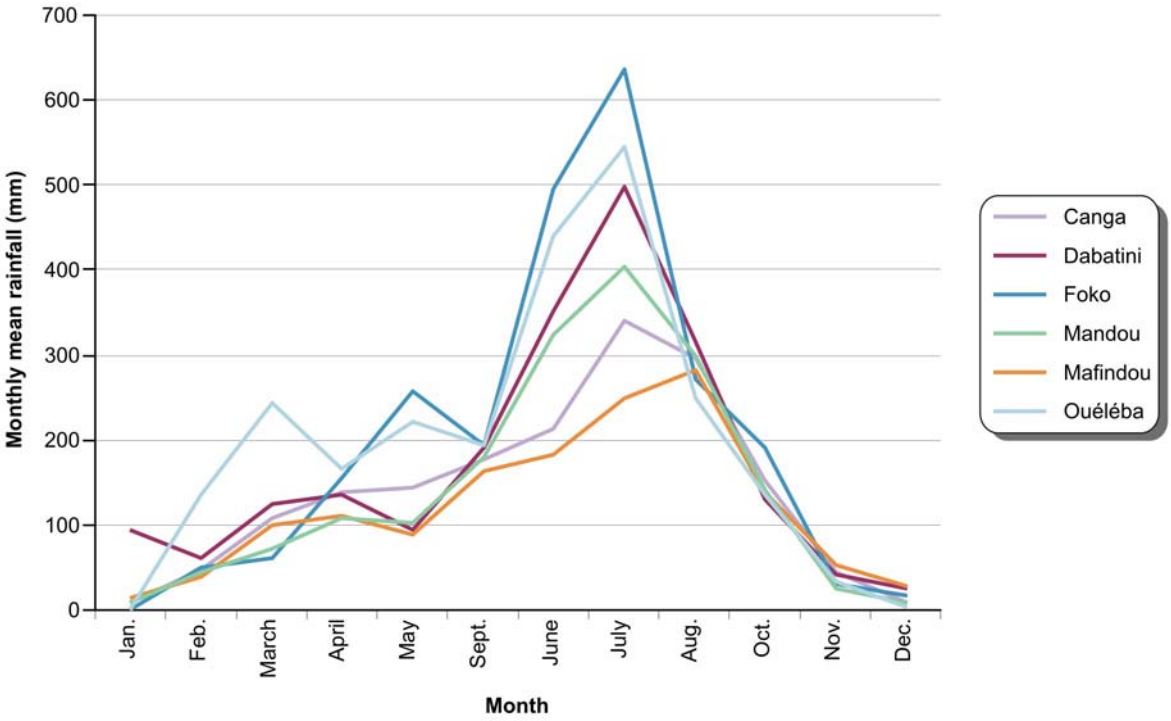
The spatial distribution of estimated mean annual rainfall for the 2002-2008 period is illustrated in Map 4.4. The map suggests that there is a zone of high rainfall (2,300 mm/yr) over the northern end of the Pic the Fon area, near Pic Dabatini. The rainfall contour is oriented north-south and is broadly centred over the ridge. The zone

of high rainfall is limited to the north and south by the lower rainfall estimates at Dabatini and Foko Centre/Foko West respectively.

A second zone of high rainfall (over 2000 mm/yr) is suggested in the southeast of the ridge at Foko East. This is possibly caused by the hills between the Foko East rain gauge and Foma village. The range of rainfall observed on the Pic de Ouéléba is between 1,700 and 1,800 mm. Rainfall over the lowlands is, overall, higher to the west of the ridge than to the east. Rainfall increases with altitude with no direct proportionality on both sides of the range.

As shown in Figure 4.7 there is a strong seasonality to the rainfall distribution. On average, around 90% of the annual rainfall within the LSA falls in the eight-month period from March to October. Rainfall follows a ‘’saw tooth’’ annual cycle, rising gradually from January to July, peaking in August, and falling quickly from September to November. While some months are sometimes completely rainless, peaks of rainfall are occasional, and often localised, during the dry season.

Figure 4.7 Monthly mean rainfall in the local study area



Note: Refer to Appendix I for detailed data and date of records.

Apart from seasonality, rainfall within the LSA appears to increase with altitude on both sides of the ridge (Table 4.1 and Map 4.4), Dabatini records an annual mean of 2,356 mm and Ouéléba 1,928 mm.

The fact that the Canga East and Mafindou stations (located on the east side of the ridge) receive less rain than Foko West and Mandou stations (located on the west

side) reinforces the suggestion that the west side of the ridge receives more rainfall than the east (Table 4.1).

Table 4.1 Annual means rainfall in relation with altitude in the local study area

Station	Altitude (m)	Rainfall (mm)
Canga East	965	1,675
Mafindou	830	1,452
Foko West	810	2,061
Mandou	710	1,717
Dabatini	1,650	2,356
Ouéléba	1,330	1,928 (1)

(1) Excludes rainfall from July which was not available.

Rainfall distribution in the study area can be summarised as follows:

- Rainfall is more related to exposure than elevation;
- The centre of mass of rainfall lies to the west of the range – rainfall is higher to the west than to east;
- Rainfall decreases from the south to the north;
- Rainfall rises with altitude on both sides of the range;
- During the dry season, the orography exerts little influence on rainfall.

Rainfall Diurnal Variability

In the wet season, maximum rainfall is in the afternoon and overnight and minimum rainfall in the morning, when the convective cycle is at its minimum. It takes time for the convective process initiated by daytime heating to die down overnight, as the radiant cooling of cloud tops after sunset increases instability and consequent uplift. In the Simandou region, the wet season rainfall is intermittent, in contrast to the coast of Guinea where, through July and August, it rains all day almost every day (WMC 2008).

Rainfall is variable diurnally in the LSA and has a strong convective (thundery) characteristic. Short and intense downpours are characteristic of early and late wet season. During mid-wet season, rainfall is more prolonged but not quite as intense. In the months associated with the dry season there are rainfall peaks between 9:00 and 10:30 and between 15:00 and 19:30 (WMC 2008).

The diurnal variation is very marked in the dry season with clear peaks in rainfall between 1:00 and 2:30 and between 15:00 and 18:00, related to the timing of convection.

510000 520000

960000 950000 940000

N W E S

Ouéléba
1332 m

Pic de Fon
1656 m

Pic Dabatini
1650 m

Foko Centre

Foko West

Foko East

Korela

Mamouroudou

Orono

Mandou

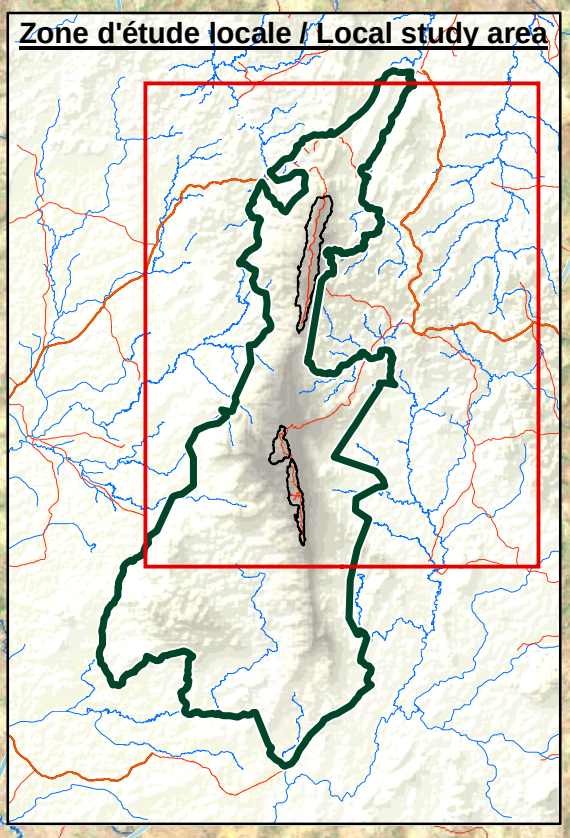
Siatoulou

Wataférédou I

Kotila
(abandonné)

1300 1400 1500 1600 1700 1800 1900 2000 2100 2300

Zone d'étude locale / Local study area



Courbe pluvimétique / Rainfall contour

(2002-2008) (mm)

1300 1400 1500 1600 1700 1800 1900 2000 2100 2300

Sources :
1- 2002-2003 Landsat Imagery;
2- Geographic Coordinate System: WGS84;
3- Water Management Consultants, 2008

Repères géographiques / Geographical landmarks

Principal sommet	Main summit
Route secondaire	Secondary road
Piste	Track
Hydrographie	Hydrography
Forêt classée du Pic de Fon	Pic de Fon Classified Forest
Milieu bâti	Built area
Aire minière	Mining area

Titre / Title

Courbe pluviométrique dans la zone d'étude locale / Rainfall contour in the local study area

Échelle / Scale	Projet / Project	Volume C Carte/Map 4.4
0 0.4 0.8 1.6 Km — 1:80,000	SIMANDOU	

Directeur de projet (client) Project manager (client)	Directeur de projet Project manager	No. pr./ P. number
Leon Payne	Richard Fontaine	604917

No.	aaaa/mm/jj yyyy/mm/dd	Description	Dessiné/Drawn	Vérifié/Verified
01	2010/06/15	Final	M. Dupré	R. Fontaine
00	2010/01/04	Preliminary	M. Dupré	M. Stapinsky

Rainfall Intensities

Rainfall can be intense, resulting from convective activity and thunderstorms. Daily rainfalls, as high as 179 mm, were recorded in the LSA.

Table 4.2 provides the maximum rainfall intensities on record for storms of 0.5, 1 and 1.5 hours duration. High rainfall intensities is maximum (60.3 mm) at Dabatini for the 1.5 hours period and minimum (32.6 mm) at Mafindou station.

Table 4.2 Maximum short-term rainfall depths and intensities in the local study area

Station (alt.)	Parameter	30 minutes	1 hour	1.5 hours
Dabatini (1,650 m)	Depth (mm)	38.8	68.2	90.5
	Intensity (mm/hr)	77.6	68.2	60.3
Mafindou (830 m)	Depth (mm)	33.3	43.7	48.9
	Intensity (mm/hr)	66.6	43.7	32.6
Mandou (710 m)	Depth (mm)	39.4	71.5	85.6
	Intensity (mm/hr)	78.8	71.5	57.1

Source: WMC 2008

Fog

Fog occurs where the dewpoint temperature is reached for any specific level of atmospheric humidity. At the dew point temperature the air is saturated with water vapour and any further drop in temperature causes water vapour to condense into fine water droplets. The high humidity of the southwesterly monsoon flow combined with uplift and cooling is responsible for the formation of (orographic) fog on the western side of the ridge. In the dry season, the warm dry harmattan wind from the northeast acts to inhibit the formation of fog (UKMO 2009).

Fog is a common phenomenon on the west side of the Pic de Fon ridge (Photo 4.2) and at Ouéléba on most mornings during the wet season. It tends to rise up the western slope during the mornings and spill over the ridge and flow down the eastern slope, dissipating as the air warms on its descent. The fog on the west side of the ridge usually dissipates by late morning unless cloud limits temperature increases, reforming by following morning.

Photo 4.2 Hill fog on the western side of Pic de Fon



Source: WMC 2008

Vertical depth of fog depends on season. At early and late wet season, dry east wind blowing across summits confines fog to western slopes. At mid-wet season, hill fog penetrates across summits, which are often in cloud at the same time.

In summary the hill fog mechanism in the LSA is based on the following (UKMO 2008b):

- Fog caused by monsoon air forced to rise up windward slopes, cooling as it does so;
- Above a certain altitude, the rising air cools to below its saturation points. From this altitude upward fog forms;
- Daytime temperature rises often evaporate the hill fog by late morning.

4.3.3 Climate Change in Guinea

The data collected at the five DNM stations (Beyla, Kérouané, Kissidougou, Macenta and N'Zérékoré) were analysed (from 1930 to present) by using moving means and linear regression with the objective to detect climate change on a decadal timescale and in the long term. In general, the records are too short to make valuable inference on climate change (WMC 2008). However, some observations can be made:

- The rainfall records at Kérouané date from 1956 and, despite missing records, suggest a long-term downward trend in rainfall. This is also suggested by the more complete records at Kissidougou and N'Zérékoré which show a long-term downward trend in rainfall from the 1930s to the present day. The trend is most marked at Kissidougou.
- The 10-year moving means applied to the rainfall records indicate that cyclic change takes place on a decadal timescale and that similarities exist between the stations. Periods of low rainfall and downward trends are succeeded by periods of increasing rainfall. These patterns were also found by Gauthier et al. (1998) and Balme et al. (2006) whose studies covered a wider area of West Africa. The first

five years of the 21st century appears to be a period of increasing rainfall in the Simandou area.

- The annual temperature record at Beyla and Kérouané are too incomplete to indicate trends (WMC 2008). Temperature records at N'Zérékoré and Kissidougou indicate that there is a gradual long-term upward trend in annual mean temperatures (mean maximum and minimum).

CHAPTER 5

Air Quality

5. AIR QUALITY

5.1 INTRODUCTION

An air quality baseline was required to identify current local sources contributing to the presence of contaminants in the atmosphere in order to eventually assess the project's impacts on air quality. Currently there is no industry within the study area. The major sources that can generate pollutants and dust are:

- The dry harmattan wind blowing from the northeast and the Sahara Desert, often loaded with suspended particulate matter (Photo 5.1);
- The slash and burn activities (Photo 5.2).

Photo 5.1 Cloudy haze typical of the dry season



Photo 5.2 Slash and burn activities



Source: SNC-Lavalin Environment 2008

5.2 METHODS

Two ambient air monitoring stations are currently in operation, one near Mandou village, and the other one in Moribadou village (Map 5.1). The air quality characterisation is based on the data collected at these two stations from mid-February 2008 to mid-March 2009.

The stations are located in the axis of prevailing winds blowing from the northeast during the dry season, downwind and upwind of the future mining areas (Table 5.1). The stations are located away from the villages and roads to avoid influences from human activities (such as dust, smoke from cooking, vehicles, etc.). The installations are fenced and guarded 24 h a day (Photo 5.3).

Table 5.1 Characteristics of the ambient air quality stations

Villages	Position	Location
Moribadou	Upwind (northeast)	Remote site in a field used for grazing without savanna and tree.
Mandou	Downwind (southwest)	Remote site surrounded by high grass savanna and a few trees.

5.2.1 Measured Parameters

Monthly determinations of gaseous contaminants (passive samplers) were conducted at both stations for nitrogen dioxide (NO_2), sulphur dioxide (SO_2), and ozone (O_3) as well as continuous monitoring of particulate matter (PM).

Photo 5.3 Ambient air quality monitoring station in Mandou



SNC-Lavalin Environment 2008

5.2.1.1 NO_2, SO_2 and O_2

Gas sampling (NO_2, SO_2 and O_3) was done with passive samplers. Their design is based on sampling by molecular diffusion of gaseous contaminants with a steady sampling flow. Gases are captured through a chemical reaction on a membrane precoated with a substance specific to each contaminant. Further analysis in a laboratory allows the determination of the quantity of contaminant captured. The passive samplers were exposed to ambient air for duration of approximately 30 days, before being sent to the Maxxam Analytics laboratory (Canada).

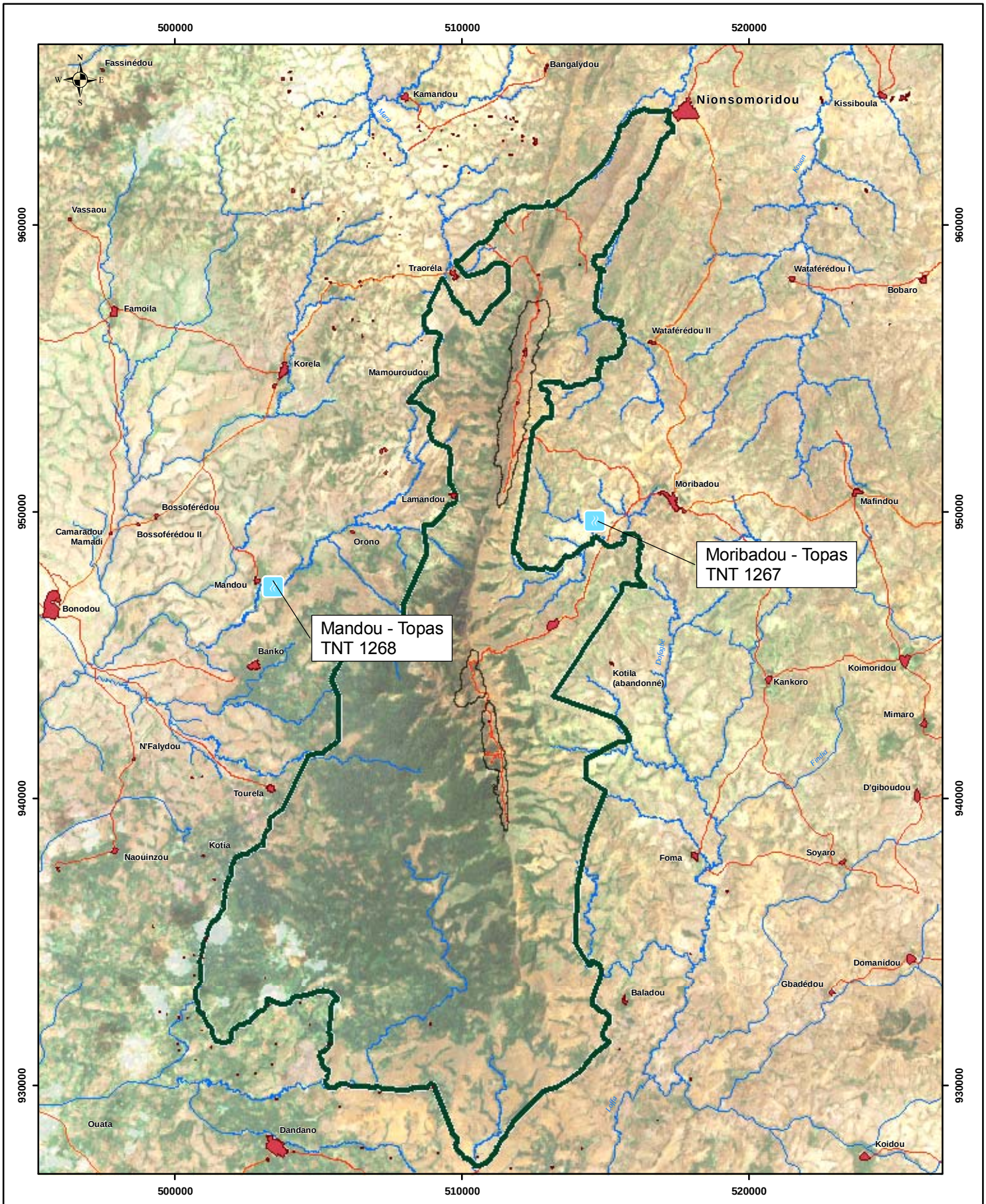
5.2.1.2 Particulate Matter

Particulate matter (PM) levels were measured with a continuous monitor (TOPAS from Turnkey Instruments) that utilises laser diffusion to count the number of particles drawn up into the air intake. The instrument classifies the particles in four categories, which are: PM_1 (particles ≤1 µm), $PM_{2,5}$ (particles ≤ 2,5 µm), PM_{10} (particles ≤ 10 µm) and finally Total Suspended Particulates (TSP). The instrument was also equipped with meteorological sensors measuring ambient air temperature, relative humidity, wind velocity, and direction. The instrument was set up to record 15-minutes averages for PM levels in ambient air and meteorological data.

5.2.2 Operation of the Stations

During sampling, the operator inspects the stations once a month to collect and replace the passive air samplers and download the data accumulated in the data acquisition system for the PM continuous monitors. Maintenance and verification of the systems were done at each inspection. The monthly technical sheet is presented in Appendix J.

During the sampling period, three gaps in the PM measurement record occurred at the Moribadou station. In March 2008, unusual low airflows were recorded at the station, introducing a bias in the data. In November 2008, the regulator was not operating correctly. The data recorded during these two periods were not considered in the analysis. Finally, a solar panel was stolen on 11 January 2009 and replaced on 7 February 2009, no data was therefore recorded during this period.



Stations de mesure / Measurement stations

Station de mesure de la qualité de l'air — Air quality measurement station

Repères géographiques / Geographical landmarks

Route secondaire	Secondary road
Piste	Track
Hydrographie	Hydrography
Forêt classée du Pic de Fon	Pic de Fon Classified Forest
Milieu bâti	Built area
Aire minière	Mining area

Sources :
1- 2002-2003 Landsat Imagery;
2- Geographic Coordinate System: WGS84;
3- SLEI Inventory

Titre / Title: **Stations de mesure de la qualité de l'air dans la zone d'étude locale / Ambient air quality measurement stations in the local study area**

Échelle / Scale	Projet / Project	Volume C Carte/Map 5.1
0 750 1 500 3 000 m 1:175 000	SIMANDOU	

Directeur de projet (client) Project manager (client)	Directeur de projet Project manager	No. pr./ P. number
Leon Payne	Richard Fontaine	604917

No.	aaaa/mm/jj yyyy/mm/dd	Description	Dessiné/Drawn	Vérifié/Verified
01	2010/06/15	Final	M. Dupré	R. Fontaine
00	2010/01/28	Preliminary	M. Dupré	R. Auger

5.3 RESULTS

5.3.1 NO_2, SO_2 and O_3 Results

The monthly concentration of NO_2, SO_2, and O_3 are representative of low levels found in rural areas that are not significantly affected by sources of contaminants (Table 5.2).

Annual average at the two stations for NO_2 are very low (1.0 $\mu g/m^3$ for Mandou and 1.7 $\mu g/m^3$ for Moribadou), compared to the World Health Organization (WHO) Air Quality Guideline (AQG) of 40 $\mu g/m^3$. In fact, concentrations are less than 4% of that reference value.

There is no WHO annual guideline for SO_2. However, the annual average background SO_2 concentrations (0.4 $\mu g/m^3$ for Mandou and 0.7 $\mu g/m^3$ for Moribadou) are considered low and representative of levels found in rural areas.

Monthly ozone levels cannot be directly compared to short-term AQG, but levels found are similar to the ones found in other rural areas. The maximum monthly value in Moribadou (194 $\mu g/m^3$) is significantly higher than the level measured in Mandou (52 $\mu g/m^3$), reflecting the higher level of human activities in the Moribadou area.

Table 5.2 NO_2, SO_2 and O_3 results ($\mu g/m^3$)

	(NO_2)	(SO_2)	(O_3)
Mandou station			
Annual average	1.0	0.4	33
Maximum monthly value	2.8	1.3	52
Moribadou station			
Annual average	1.7	0.7	53
Maximum monthly value	10.3	3.7	194
Annual WHO guideline value (1)	40	-	-

(1) There is no WHO guideline value for annual SO_2 (only for short terms 1-h or 24h), and O_3 (only for short terms 1-h or 8-h).

5.3.2 Particulate Matter Results

According to the US Environmental Protection Agency, particulate matter is a mixture of extremely small particles and liquid droplets. The classification is based on the size (2 main types). Coarse particulate matter (PM_{10}) is less than 10 micrometers in diameter. It primarily comes from dust, river beds and industrial activities. The second type are fine particulate matter ($PM_{2.5}$), less then 2.5 micrometers in diameter. $PM_{2.5}$ is a product of combustion primarily caused by burning fuels. Sources include power plants, vehicles, wood burning stoves and bush fires. Total suspended particulate matter (TSP) are particles ranging in size from 0.1 micrometer to about 30 micrometers in diameter. TSP includes a broad range of particle size including fine, coarse and supercoarse particles.

Depending on their size and their concentration, PM can cause environmental and health impacts.

Table 5.3 presents the percentile distribution for the four classes of particulates (PM_1, $PM_{2.5}$, PM_{10} and TSP) measured at each station. For example, the levels of PM_{10} at the Moribadou station were lower than 504 $\mu g/m^3$ for 95% of the time. It is useful to compare the background results with the WHO Air Quality Guidelines for particulate matter (Table 5.4) since the background PM concentration combined with the project contribution to PM will later be compared to the WHO guideline values. A high background value is a relevant element to consider in the impact assessment phase.

Table 5.3 24 h of particulate matter results ($\mu g/m^3$)

Class of PM	Percentile distribution										
	Min.	P50	P70	P80	P90	P95	P98	P99	Max.	Annual mean	Nb.(1)
Mandou station (17/02/2008 to 5/03/2009)											
PM_1	0.2	2.2	3.6	4.9	7.6	11	22	30	55	3.9	351
$PM_{2.5}$	0.7	8.9	15	20	32	46	98	119	220	16	351
PM_{10}	7.0	58	97	142	217	301	1157	2167	4553	144	351
TSP (2)	14	102	176	251	388	607	1751	2590	4916	224	351
Moribadou station (15/02/2008 to 5/03/2009)											
PM_1	0.3	2.2	3.1	5.8	12	16	26	27	34	4.3	273
$PM_{2.5}$	0.5	9.8	14	30	55	79	138	150	179	21	273
PM_{10}	6.1	47	70	124	299	504	907	1699	2355	198	273
TSP(2)	12.8	80	111	209	467	865	1516	2449	3062	286	273

(1) Nb.: Number of days for which data are available.
(2) TSP: Total suspended particulates (between 0.5 and 20 microns).

Table 5.4 WHO Air Quality Guidelines for particulate matter ($\mu g/m^3$)

Class of PM	24-hour concentration		Annual concentration	
	AQG	Interim target-1	AQG	Interim target-1
$PM_{2.5}$	25	75	10	35
PM_{10}	50	150	20	70

AQG: Air Quality Guidelines
Source: WHO Ambient Air Quality Guidelines 2005

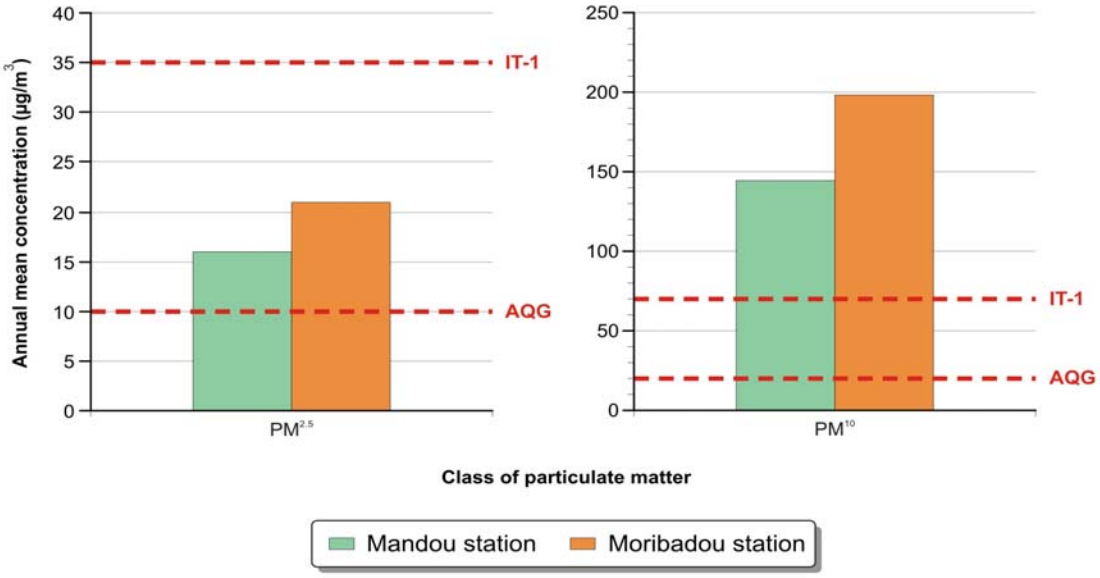
5.3.2.1 Mean Annual Concentrations

Figure 5.1 compares the annual particulate matter results with the WHO guidelines and interim target-1. This figure shows that the $PM_{2.5}$ and PM_{10} annual concentrations at the Mandou (16 and 144 $\mu g/m^3$) and Moribadou (21 and 198 $\mu g/m^3$) air quality

monitoring stations were higher than the WHO guidelines established at 10 and 20 μg/m^3 respectively.

Annual $PM_{2.5}$ concentrations at both the Mandou (16μg/m^3) and Moribadou (21 μg/m^3) stations were below the annual interim target-1 [1]of 35 μg/m^3. For PM_{10}, background results were higher than the annual interim target-1. The annual concentration being two to three times in excess of the WHO recommended concentrations.

Figure 5.1 Mean annual concentrations of $PM_{2.5}$ and PM_{10} compared to WHO guidelines



AQG: Air Quality Guidelines
IT-1: WHO interim target-1
Source: WHO Ambient Air Quality Guidelines 2005

5.3.2.2 Mean 24-hour Concentrations

Figure 5.2 compares the 24-hour particulate matter results with the WHO guidelines and interim target-1. As recommended by WHO, the 99th percentile (P99) of daily averages have been used for this comparison.

According to this figure, background $PM_{2.5}$ and PM_{10} levels are above the 24-hour WHO guidelines and interim target-1.

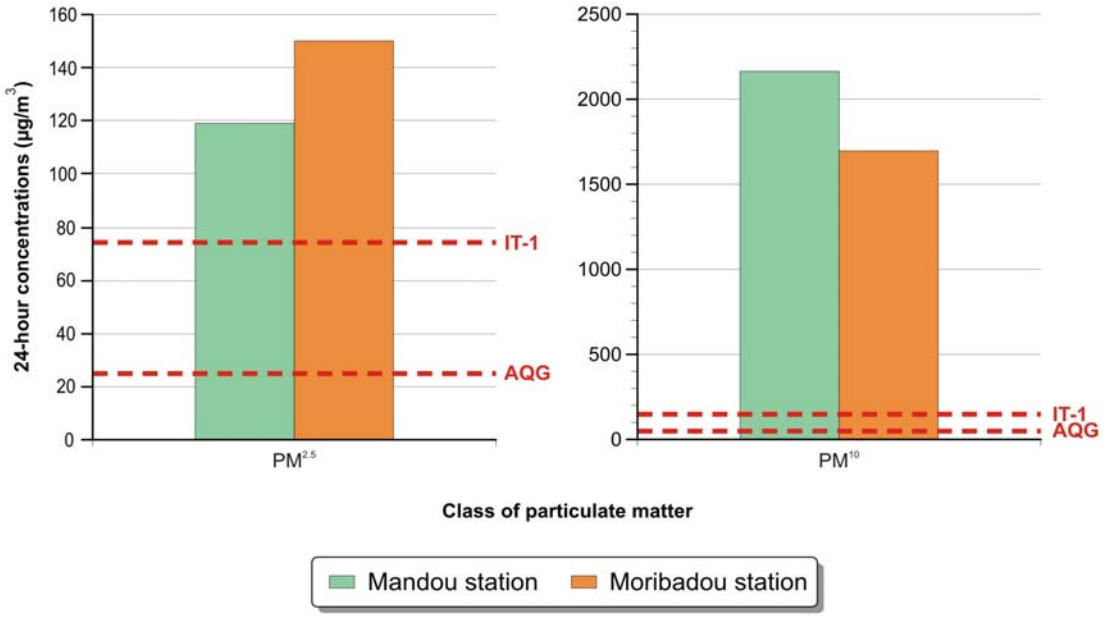
The $PM_{2.5}$ values recorded at the Mandou and Moribadou stations, are lower than the interim target-1 for respectively 97% and 94% of the time while WHO would require this target to be met 99% of the time.

The PM_{10} concentrations proved to be particularly high with P99 values of 2,167 and 1,699 μg/m^3 respectively at the Mandou and Moribadou stations. To meet the interim

[1] WHO promotes a shift from a concentration with acute, serious health consequence to a concentration that should result in significant reduction risks for acute and chronic effects.

target-1, the PM_{10} concentrations would have to be lower than the target value (150 μg/m^3) 99% of the time. This was not the case at both stations as the PM_{10} concentrations were below the targeted value only 82% of the time.

Figure 5.2 Maximum daily average concentrations* of $PM_{2.5}$ and PM_{10} compared to WHO guidelines



* using 99th percentile value
AQG: Air Quality Guidelines
IT-1: WHO interim target-1
Source: WHO Ambient Air Quality Guidelines 2005

The dry season, characterised by elevated ambient air temperature and low precipitation, is prone to the development of poor air quality. At both stations, the highest levels of particulate matter occurred in the three dryer months of the year (December, January and February), corresponding with the occurrence of the dry harmattan winds which bring dust and can create a cloudy haze. The wet season, on the other hand, brings rain, which wash the atmosphere and improve ambient air quality from March to November.

Moreover, data analysis led to the conclusion that the occurrence of several bushfires also contributed significantly to the increase of PM concentrations, especially at the Moribadou station as bushfires are frequent in this area. Combined with the harmattan, bushfires are a major cause of the poor air quality observed during the dry season.

5.4 SUMMARY

The monthly concentrations of NO_2, SO_2, and O_3 are low and in line with the the usual concentrations present in rural areas with no industrial activities.

The PM results indicate that the air quality of the study area is poor in the dry season but is generally good the rest of the year when the majority of the annual rainfall occurs. The high concentration of PM_{10} is typical of an area under the influence of the Harmattan.

Figures that detail the 24 h monthly average concentrations of $PM_{2.5}$ and PM_{10} for the Moribadou and Mandou stations are presented in Appendix K.

CHAPTER 6

Noise Climate

6 NOISE CLIMATE

6.1 INTRODUCTION

The objective of the baseline noise characterisation was to establish noise levels at sensitive locations within the LSA. The results of the characterisation will serve as the pre-project reference point against which future changes can be measured and compared with the WHO Guidelines for Community Noise.

A description of acoustical concepts and definitions used in this chapter are provided in the glossary and the list of acronyms at the back of this volume.

6.2 METHODS

The baseline noise environment was established using noise measurement data collected in eight villages surrounding the PdF CF and at Canga East camp (Map 6.1). It was assumed that the villages closest to the mining area are the receptors most likely to be affected during the operation of the mine (Table 6.1). The noise survey was undertaken from 13 to 23 February 2008.

Table 6.1 Characteristics of the noise measurement locations

Village (population)	Description	Distance from hut and road
Bangalydou (166)	Village in a wooded area, crossed by a road	Hut: 15 m; Road: 160 m
Traoréla (952)	Village in a wooded area	Hut: 30 m; Road: 180 m
Wataférédou II (279)	Village in expansion	Hut: 15 m; Road: 250 m
Moribadou (3,806)	Village in expansion, crossed by a road	Hut: 10 m; Road: 60 m
Kotila (n.a.)	Hamlet in a wooded area, not inhabited during the survey	n.a.
Foma (636)	Village in a wooded area	Hut: 10 m; Road: 160 m
Mandou (222)	Village in a wooded area	Hut: 10 m; Road: 100 m
Banko (558)	Village in a wooded area	Hut: 15 m; Road: n.a.
Canga East (n.a.)	Base Camp for the Simandou Project	Hut: 50 m; Road: 15 m

n.a.: not available

In order to measure the baseline noise without interference from human activities the data was collected at the outskirt of the village, at some distance from huts and roads.

6.2.1 Field measurements

An autonomous noise monitoring station was used to measure the ambient noise on a continuous basis over 24-hour periods (in 5 second intervals) at each sampling site. Noise measurements were taken with an integrating precision sound level meter of type 1 per IEC 651 standard (1979). The list of instruments used for the noise measurements is presented in Table 6.2. The calibration was done less than a year before the survey and was verified *in-situ* before and after each measurement with a portable noise calibrator. The microphones were protected with a shield against humidity and wind.

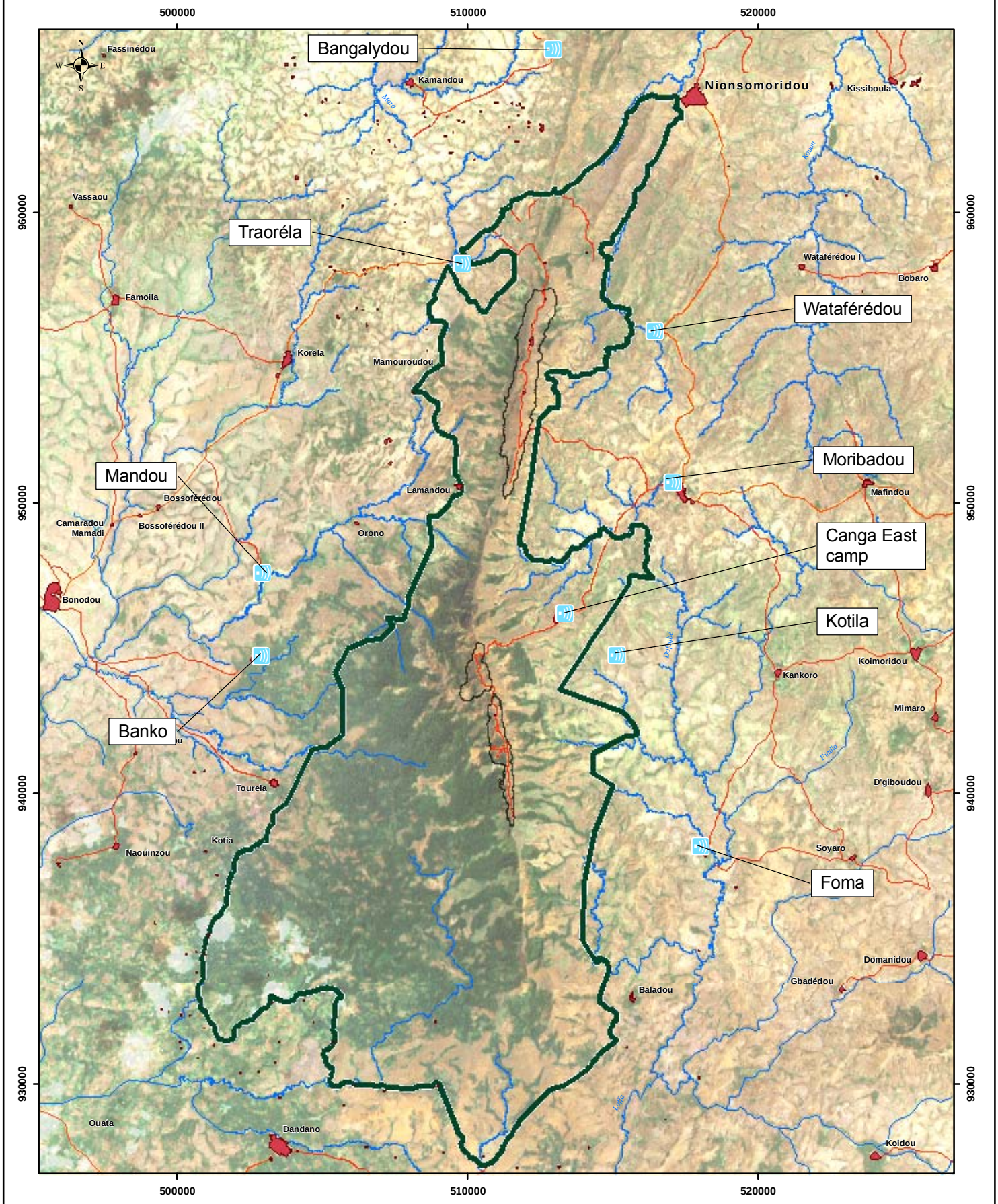
Table 6.2 Noise level instrumentation

Instrument	Brand	Model	Serial number
Integrating precision sound level meter	Larson-Davis	820	1380 and 1645
Microphone	Larson-Davis	2541	1490 and 8379
Pre-amplifier	Larson-Davis	828	2122 and 2575
Digital recorder	Olympus	DS-40	n.a.
Portable calibrator	Bruel and Kjaer	4231	2507134

The meteorological conditions observed during the noise survey were typical of the dry season, with a high ambient air temperature and low humidity in daytime and high at night. The wind did not have any significant effect on the measurements.

6.2.2 Data Analysis

Data was downloaded and analysed with a software programme (Environmental Noise Model) that calculates hourly L_{Aeq}, L_{A95} and $L_{dn,}$ which are the noise indicators used in this baseline study. The $L_{Aeq,T}$ represents the average noise level and the $L_{A95,T}$ represents the noise background. The daily noise level (L_{dn}) was calculated from the hourly records. It represents the average noise over 24 hours and it integrates a correction of +10 dBA for night-time between 22:00 and 7:00, considering that noise is more disturbing during this period.



Stations de mesure / Measurement stations

Station de mesure du bruit ambiant — Ambient noise measurement station

Repères géographiques / Geographical landmarks

Route secondaire	Secondary road
Piste	Track
Hydrographie	Hydrography
Forêt classée du Pic de Fon	Pic de Fon Classified Forest
Milieu bâti	Built area
Aire minière	Mining area

Sources :
1- 2002-2003 Landsat Imagery;
2- Geographic Coordinate System: WGS84;
3- SLEI Inventory

Titre / Title: **Stations de mesure du climat sonore dans la zone d'étude locale / Ambient noise measurement stations in the local study area**

Échelle / Scale	Projet / Project	Volume C Carte/Map 6.1
0 750 1 500 3 000 m — 1:175 000	SIMANDOU	

Directeur de projet (client) / Project manager (client)	Directeur de projet / Project manager	No. pr./ P. number
Leon Payne	Richard Fontaine	604917

No.	aaaa/mm/jj yyyy/mm/dd	Description	Dessiné/Drawn	Vérifié/Verified
01	2010/06/15	Final	M. Dupré	R. Fontaine
00	2010/01/28	Preliminary	M. Dupré	R. Auger

The noise period criteria used in the assessment are from 7:00 to 22:00 during daytime and 22:00 to 7:00 during night-time, as per IFC requirements.

6.3 RESULTS

The 24-hour ambient noise records collected for each of the nine monitoring stations are summarised in the figures of Appendix L. These figures illustrate the noise recorded every 5 seconds (fluctuating noise), the average hourly noise level $L_{Aeq,1h}$ and the hourly noise background which is exceeded 95% of the time $L_{A95,1h}$.

Ambient noise characteristics differ according to the villages. For example, insect sounds are the predominant source of noise in Traoréla. Insect noise is characterised by a narrow spectrum (range of 10 to 15 dBA) of fluctuating noise. Insect activity is so prominent in Traoréla that it is the only village for which the daily noise level (L_{dn}) is equal to that of the WHO guidelines of 55 dBA (WHO 1999).

During night-time, when insect sounds are not a significant source, typical noise levels in the LSA are, for the most part, slightly below 40 dBA, with a narrow band of 5 to 10 dBA of fluctuating noise (see figures in Appendix L).

Human activities in the LSA are reflected in the larger fluctuating noise level during daytime covering a typical range of 25 dBA, as in Foma or Mandou. The background noise $L_{A95,1h}$ in Foma remained at a level of approximately 30 dBA. In Mandou, the background noise $L_{A95,1h}$ during daytime was approximately 40 dBA, reflecting a higher level of human activity than in Foma at the day the measurement was taken.

The calm periods, when ambient noise is low, were selected for the analysis of the hourly noise levels. The hourly and daily baseline noise levels are presented in Table 6.3. In all the villages, in calm periods, the ambient levels in daytime are higher than the night-time levels, reflecting the usual human activities in the villages during daytime.

The measured noise levels are compatible with the noise guidelines recommended by IFC and WHO for a residential area ($L_{Aeq,1h}$: 55/45 dBA day/night and L_{dn}: 55 dBA). When the measured noise is higher than the guidelines during certain periods of the day/night, it comes from human activity at the villages or from insect sounds mostly during the evening. However, average hourly noise levels recorded during calm periods of day and night are lower than the WHO guidelines at all measurement points.

Table 6.3 Hourly and daily noise levels measured at villages and camp

Monitoring point	Date and hour of the measurement	Duration (h)	Hourly level in calm period				Daily level
			Day (7h00- 22h00)		Night (22h00-7h00)		
			$L_{Aeq, 1h}$ (dBA)	$L_{A95, 1h}$ (dBA)	$L_{Aeq, 1h}$ (dBA)	$L_{A95, 1h}$ (dBA)	L_{dn} (dBA)
Bangalydou	15 Feb. 2008 – 9:30	27	40	32	36	28	48
Traoréla	15 Feb. 2008 - 10:54	25	40	33	36	31	55
Wataférédou II	18 Feb. 2008 – 16:26	40	43	32	38	29	52
Moribadou	13 Feb. 2008 – 12:21	24	43	34	36	23	50
Kotila	17 Feb. 2008 - 8:13	26	38	26	28	24	46
Foma	13 Feb. 2008 - 9:17	25	39	30	34	22	47
Mandou	16 Feb. 2008 – 16:35	24	43	37	34	27	51
Banko	16 Feb. 2008 - 15:27	24	44	35	40	33	51
Canga East	19 Feb. 2008 – 18:43	12	n.a.	n.a.	41	39	n.a.

n.a.: not available
WHO guidelines for a residential area: $L_{Aeq,1h}$: 55/45 dBA day/night and L_{dn}: 55 dBA

CHAPTER 7

Geology

7. GEOLOGY

7.1 INTRODUCTION

Guinea is a country very rich in mineral resources, such as bauxite, gold, diamonds, copper, and iron. For this reason, the geology of Guinea was examined extensively over decades, notably by the French in the 1950's and Japanese in the 1970's. Major iron ore deposits have been identified in Mount Nimba, Pic de Fon and Ouéléba, all located within southeastern Guinea.

This section presents the main findings of the baseline geology. A good understanding of the geology is required in order to define the limits of the ore bodies and therefore the area that may be affected by mining activities; evaluate the geotechnical conditions, such as rock strength characteristics and water-bearing geological formations, as an aid to mine planning; explain the natural chemistry of water; and later assess the potential impacts of the tailings and waste rock disposal and management.

7.2 METHODS

Geological data from Pic de Fon and Ouéléba deposits has been collected by Rio Tinto since 1997 as part of the reconnaissance mineral exploration programme. This work has allowed the determination of the main lithologies of the geological formations encountered in the mining areas; the identification of the major structural features; and the delimitation of the iron ore deposits.

Some geological data was also collected, examined and interpreted by Water Management Consultants (WMC), during the studies performed for the Simandou Project water management system (WMC 2008 and 2009a). A summary of these findings is provided in the Results section (Section 7.3).

The work carried out specifically for the geological characterisation consisted in the following activities.

7.2.1 Mineral Exploration Drilling and Sampling

Rio Tinto has been conducting its exploration drilling programme in the Pic de Fon and Ouéléba deposits since 1997. Some 1,118 boreholes (555 in Pic de Fon; and 563 in Ouéléba) have been drilled in order to define the resource geometry, as well as the mineralogy, chemistry and physical properties of the deposits (Rio Tinto 2009).

Core samples were collected for laboratory analyses. Particle size distribution analyses, bulk density and porosity tests, and chemical analyses have been performed on samples in order to obtain information on rock type and texture, ore grade, and rock mechanical and hydraulic properties. The sample locations are shown on Map 7.2 in the Results section.

The data collected was compiled and interpreted in order to prepare several cross-sections which were used to construct a resource model of the geological setting.

7.2.2 Geochemical and Environmental Testing

A geochemical test work programme for the Simandou Project was initiated in March 2008 to characterise materials that will be mined, stored as waste, or exposed in the Pic de Fon and Ouéléba deposits with regard to their potential to generate Acid Rock Drainage (ARD) and metal leaching. This work has involved the use of static tests (paste pH, net acid, acid base accounting, bulk geochemical analysis, synthetic precipitation leaching protocol, and Rietveld x-ray diffraction) and kinetic test (humidity cell test) protocols.

Data from 154 rock samples (96 samples from Pic de Fon and 58 from Ouéléba) representing all major lithological units and ore/waste types has been analysed. Following the interpretation of preliminary results, 18 more samples were tested later in 2008, in order to complete the characterisation of sulphur-rich phyllite rocks.

7.3 RESULTS

7.3.1 Regional Geology and Structure

The RSA is characterised by the crystalline Precambrian rocks of the southwestern part of the West African Craton, which is mainly encountered in the eastern and southern regions of Guinea (i.e. in the Upper and Forest Guinea physiographical regions). The geological Precambrian age is divided into the Archean and the younger Proterozoic periods. Map 7.1 shows the main regional geological formations and the iron ore deposits along the Simandou Range.

The Craton contains some of the oldest rocks on earth, and consists in an Archean basement dominated by migmatites and/or gneisses of varying granitic composition with small lenses of amphibolites. The oldest rocks in the domain were estimated to approximately 3.5 billions years (Thiéblemont et al. 2001).

The Guinean Dorsal, also referred to as the Loma-Man Dorsal, characterises the geology of the Simandou Range. It forms a geological domain dominated by granitic rocks, and corresponds to a convexity of the crystalline Precambrian basement overlying the older Archean rocks. The geological domain also includes the N'Zérékoré Notch, which is dominated by gneiss rocks. Granitic plutonic rocks of the younger Eburnian and Liberain Orogenies are sparsely encountered within the domain, as well as older pre-liberian igneous rock intrusions (Boulvert 2003).

The Simandou Range is a younger meta-sedimentary rock sequence (Lower Proterozoic) composed of greenstone volcanic rocks with banded iron formations, which occur as linear belts and small relics throughout the Archean domain (Wright et al. 1985). It displays a northsouth sinusoidal strike length of approximately 110 km.

470000 500000 530000 560000

1040000 1010000 980000 950000 920000 890000

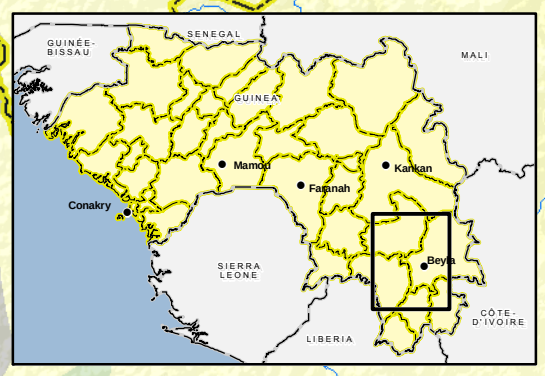
N W E S

Mamouroudou
Soromaya
Banankoro
Sibiribaro
Konsankoro
Linko
Damaro
Samana
Diassodou
Fouala
Sinko
Moussadou
Gbakedou
Nionsomoridou
Vasseredou
Diaraguerela
Singbendou
Oremai
Kouankan
Seredou
Boola
Koropara
Foumbadou
N'zebela
Womey
Laine
Fassankoni
Koule
Pale
Gouecke
Gueasso
Soulouta

KÉROUANÉ
KÉROUANÉ
GUINEA
BEYLA
BEYLA
MACENTA
MACENTA
LOLA

Pic de Fon

Boyuld (Somamba)
Bouroumo
Touma
Kourae
Monsoro
Gbanhala
Milo
Loya
Dion
Baya
Mboo
Avili
Laoud
Véré
Diani
Bogho
Via



Formations géologiques / Geological formations

Mésozoïque / Mesozoic

Dolérite, gabbro et diorite — Dolerite, gabbro and diorite

Protérozoïque inférieur / Lower Proterozoic

Granite et granodiorite — Granite and granodiorite

Archéen / Archean

- Gneiss à biotite — Biotite Gneiss
- Quartzite ferrugineuse — Ferruginous quartzite
- Gneiss quartzite — Quartzite gneiss
- Amphibolite — Amphibolite
- Formation ferrifère rubanée — Banded Ironstone

Sources :
1- Base map - 2006 0.5m ADS40 Aerial Photographs, 2006 Spot Imagery;
2- 2002-2003 Landsat Imagery;
3- Shuttle Radar Topography Mission (SRTM);
4- Carte topographique IGN 1:50 000/1:200 000;
5- Projet Allemano-Guinéen d'évaluation du potentiel minier de la Guinée 1995-1997, Ministère des Ressources Naturelles et de l'Énergie, Conakry et BGR, Hannover - Carte géologique et des minéralisations de la Guinée, 1:1 000 000, Conakry/Hannover 1998;
6- Geographic Coordinate System: WGS84, UTM, Zone 29N

Repères géographiques / Geographical landmarks

- Chef-lieu de préfecture — Prefecture centre
- Chef-lieu de CRD et CU — CRD and CU centre
- Frontière nationale — National border
- Limite de préfecture — Prefecture boundary
- Route principale — Main road
- Hydrographie — Hydrography
- Forêt classée du Pic de Fon — Pic de Fon Classified Forest

Note : Les limites administratives proviennent de sources multiples et sont approximatives / Administrative boundaries are from multiple sources and are approximate.

Titre / Title

Formations géologiques dans la zone d'étude régionale / Geological formations in the regional study area

Échelle / Scale	Projet / Project	Volume C Carte/Map 7.1
0 2.75 5.5 11 Km — 1:550,000	SIMANDOU	

Directeur de projet (client) / Project manager (client)	Directeur de projet / Project manager	No. pr./ P. number
Leon Payne	Richard Fontaine	604917

No.	aaaa/mm/jj yyyy/mm/dd	Description	Dessiné/Drawn	Vérifié/Verified
01	2010/06/15	Final	M. Dupré	M. Stapinsky
00	2010/01/04	Preliminary	M. Dupré	M. Stapinsky

There have been three main tectonic events of varying ages that have affected Precambrian basement rocks (Marten 2000 and 2004; Billa et al. 1999; Wright et al. 1985; and Rankin 2004). All of them contributed to the regional fabric of the rocks. Multiphase ductile deformation has created elongate tight synformal fold keels and sheared antiformal structures, with tectonic contacts between lithologies which typify the Simandou deposits. The oldest deformation observed in the Simandou Group rocks consists of tight-isoclinal eastwest striking folds, identified by intersection lineations and crenulation cleavages. A second phase of deformation defines the regional Simandou fabric with the development of a large-scale north-south sinistral shear system; this shear movement later transitioned into a more brittle regime creating northeast-southwest trending faults. The last deformations that occurred consist in kink folding, and east-west brittle faulting.

7.3.2 Local Geology in Pic de Fon and Ouéléba Deposits

In the study area, the Lower Proterozoic rocks are part of the Simandou Group that composed the ridge in the Pic de Fon and Ouéléba deposits. Map 7.2 illustrates these two deposits and shows where the geology has been investigated in detail.

At the base of the sequence, the lowest member of the Simandou Group which has been infolded into the basement in an overall synform and consists in a phyllite series of rock that unconformably overlies the Archean basement. Phyllite is a type of foliated metamorphic rock primarily composed of quartz, sericite mica, and chlorite; the rock represents a gradation in the degree of low metamorphism between slate and mica schist. Crystals of graphite, sericite, or chlorite impart a silky, sometimes golden sheen to the surfaces of cleavage (or schistosity). The phyllite varies from very weathered and goethitised at the surface, to fresh and pyritic at depth. Sandstones and quartzites are intercalated with phyllite in the vicinity of the deposits (Marten 2000). The series is generally encountered at the base of the Simandou Range.

An itabirite series conformably overlies the basal phyllite. Itabirite is a rock type that consists in a laminated, metamorphosed, oxide-facies iron formation in which the original chert mineral or jasper bands have been recrystallized into megascopically distinguished grains of quartz; and in which the iron is present as thin layers of hematite, magnetite, goethite, or martite. Subsequent deformation and enrichment of the itabirite impair the identification of any stratigraphy in the formation. The texture of the itabirite varies from friable to hard. Post-mineralisation thickness of the itabirite is estimated at 250 m (Van Oosterwijk 2004). The itabirite series is observed at higher elevations than the phyllite series on the slope of the Simandou Range.

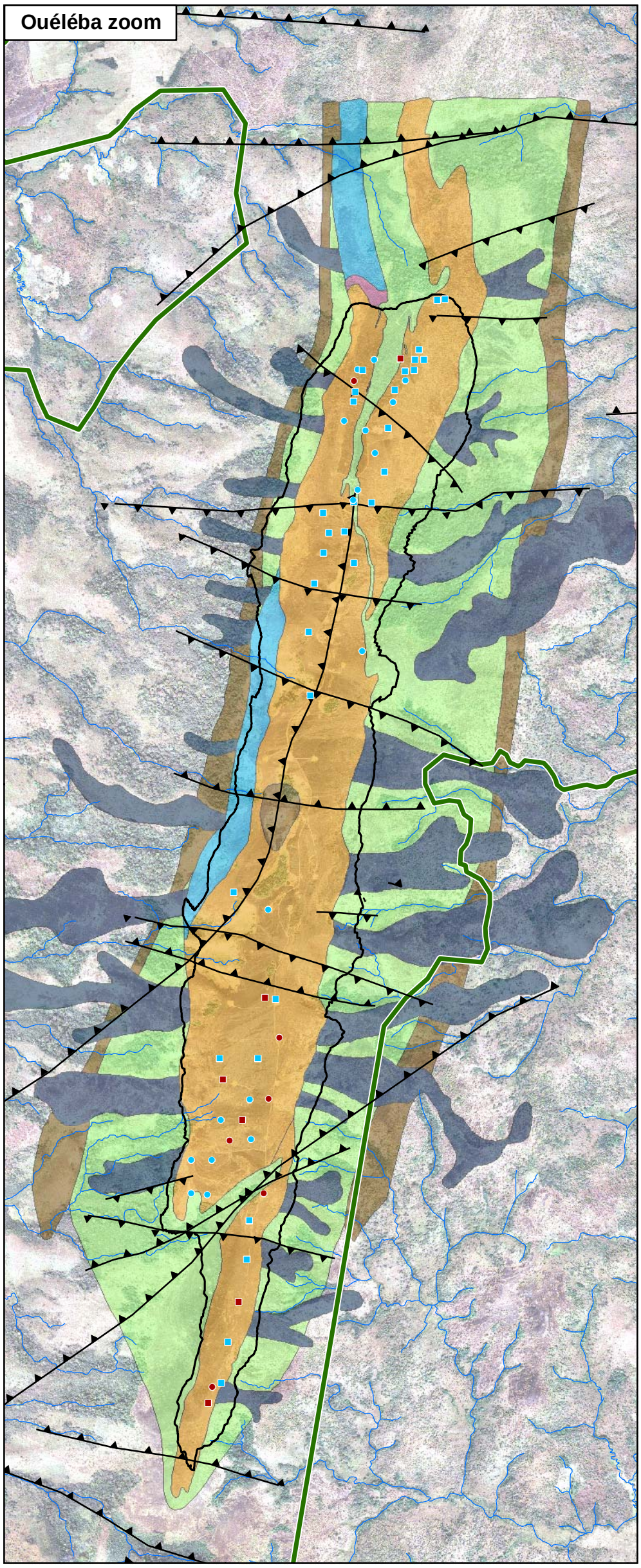
Iron ore mineralisation is generally located on the top of the ridge, overlying the itabirite series. At Pic de Fon, the mineralisation is particularly deep in the Western Spur area (Map 7.2). Mineralisation has been encountered to a depth of more than 300 m from the ground surface. The primary iron ore minerals consist of oxide-hydroxides minerals that have a composition that varies from hematite-martite (dominant at Pic de Fon) to hematite-martite-goethite mineralisation (dominant at Ouéléba). Hematite is a black to

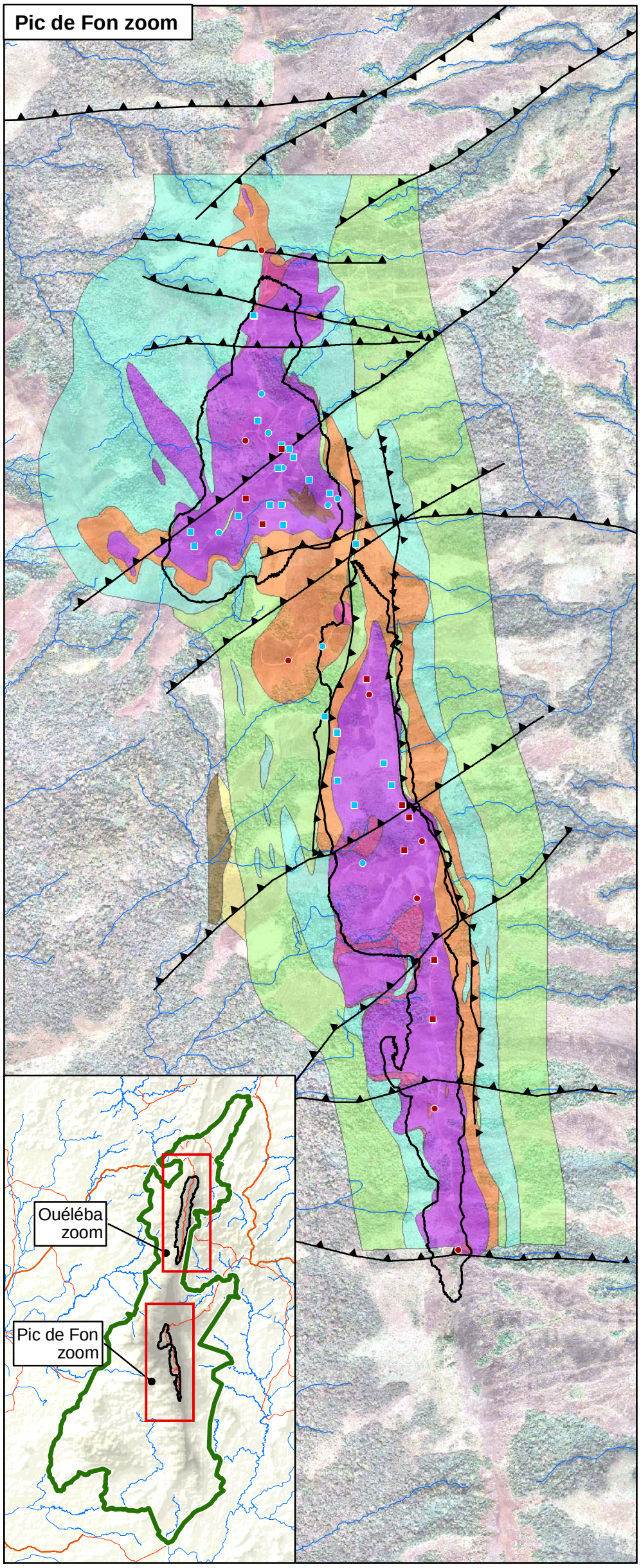
silver-gray, brown to reddish brown or red mineral. It is harder than pure iron, but much more brittle. Goethite is another iron oxide-hydroxides mineral along with limonite Typically, the texture observed in the martite/hematite type minerals is hard and dense, with the occurrence of plates in the hematite; varies in the martite/goethite type minerals from very soft to medium (also vitreous to limonite for goethite); and in the martite type minerals from very soft to hard.

Weathering and associated hydration have resulted in various degrees of hematite-goethite mineralisation forming a carapace, or a weathered crust, over iron formations at Pic de Fon and Ouéléba. More pervasive hydration at Ouéléba has resulted in a thicker goethite dominant hard crust that has been divided into two distinct units defined on the basis of texture, mineralogy and chemistry (carapace and transitional zone).

Finally, numerous debris flows have deposited iron rich detrital materials, referred to as cangas, which can be identified in Map 7.2 as linear geological deposits in perpendicular valleys to the range. The cangas unconformably overlie phyllite series and basement rock. They are polymict, poorly-sorted, clast to matrix supported breccias, with thicknesses ranging from a few metres up to 40 m (Van Oosterwijk 2004). Although the cangas are estimated to be mid-Tertiary to late Tertiary in age, they are characterised by periods of erosion within multi-phase deposition processes (Baynes 2007).

The main lithological units identified in Pic de Fon and Ouéléba geological formations are presented in Table 7.1 with their specific characteristics, as observed during drilling.





Lithologie / Lithology

Roche mère	Basement
Minéralisation de surface goethitique et gibbsite	Goethitique and gibbsite surface mineralisation
Canga	Canga
Hématite friable	Friable hematite
Hématite siliceuse	Siliceous hematite
Hématite dure	Hard hematite
Hématite goethitique	Geothitic hematite
Itabirite	Itabirite
Itabirite riche	Itabirite rich
Itabirite pauvre	Itabirite poor
Phyllite	Phyllite
Quartzite	Quartzite

Stations de forage / Borehole stations

Forage sec	Dry open borehole
Forage sec (relevé de résistivité)	Dry open borehole (resistivity survey)
Forage (relevé ponctuel)	Open borehole (spot measurement)
Forage (relevé de résistivité)	Open borehole (resistivity survey)

Caratéristiques structurales /Structural features

Faille — Fault

Repères géographiques / Geographical landmarks

Route secondaire	Secondary road
Hydrographie	Hydrography
Forêt classée du Pic de Fon	Pic de Fon Classified Forest
Aire minière	Mining area

Sources:
1- Base map - 2006 0.5m ADS40 Aerial Photographs, 2006 Spot Imagery;
2- Landsat imagery mosaic 2002-2003;
3- Shuttle Radar Topography Mission (SRTM);
4- Carte topographique IGN 1:50 000/1:200 000;
5- Water magagement consultant report;
7- Geographic Coordinate System: WGS84, UTM, Zone 29N.

Titre / Title

Lithologie et caratéristiques structurales dans la zone d'étude locale / Lithology and structural features in the local study area

Échelle / Scale		Projet / Project	Volume C Carte/Map 7.2
0 150 300 600 m	1:30,000	SIMANDOU	

Directeur de projet (client) Project manager (client)	Directeur de projet Project manager	No. pr./ P. number
Leon Payne	Richard Fontaine	604917

No.	aaaa/mm/jj yyyy/mm/dd	Description	Dessiné/Drawn	Vérifié/Verified
01	2010/06/15	Final	M. Dupré	M. Stapinsky
00	2009/12/16	Preliminary	M. Dupré	C. Roy

Table 7.1 Characteristics of the main lithological units encountered in Pic de Fon and Ouéléba deposits

Lithology	Characteristics
Surface	Weathered
	Weathered martite-goethite
	Weathered carapace
	Transitional zone
Mineralisation	Hard, medium-hard martite matrix with porosity
	Medium-hard martite matrix with porosity
	Soft martite matrix porous
	Very soft powderly martite
	Hard, medium-hard martite-matrix with goethite infill
	Medium-hard martite-goethite with goethite infill
	Soft martite-goethite with goethite infill
	Very soft martite-goethite
	Vitreous goethite
	Limonite goethite
	Very hard martite-hematite
	Micro-platy hematite, hard interlocking hematite plates
	Hard martite-hematite, dense fine grained
	Compact hematite
	Friable hematite
	Martite-goethite
	Enriched itabirite
Itabirite	Hard with goethite
	Friable with goethite
	Hard with hematite
	Friable with hematite
	Hard with magnetite
	Friable with magnetite

Source: Water Management Consultants 2009a

7.3.3 Iron Ore Deposits

The two main iron ore deposits that have been examined within the framework of the Simandou Project are the Pic de Fon and Ouéléba deposits located at the southern end of the Simandou Range. The ore bodies have reported inferred resources of more than two billion tons of high-grade iron ore. An additional 920 million tons approximately of high-grade and low-grade mineralisation may be converted to resources in the future. Further potential in low-grade itabirite resources at Pic de Fon and Ouéléba are also expected to be defined.

The Pic de Fon and Ouéléba deposits have approximately a 7 km strike length, and potential mineralisation to a depth of over 300 metres. Resources at Pic de Fon are predominantly dry, with only approximately 10% of the deposit below the water table, while approximately 50% of the Ouéléba deposit is below the water table. The mineralisation generally grades downwards into partially-enriched itabirite, and then into depleted (unenriched) itabirite. The mineralisation at Ouéléba is often directly in contact with phyllite indicating complete enrichment of the itabirite series (WMC 2009a and 2009c).

The ore quality is exceptional and these deposits would be some of the largest untapped high-quality iron ore resource in the world with an average grade between 66 and 67% Fe; a low content of SiO_2 (between 1 and 2%); and very low phosphorus (0.03-0.07%).

The main types of mineralisation at Pic de Fon and Ouéléba ore bodies are briefly described in Table 7.2.

Table 7.2 Main types of iron ore mineralisation at Pic de Fon and Ouéléba deposits

Material type	Geochemical characteristics
Hard hematite	≥ 60% Fe, < 6% SiO2
Friable medium hematite	≥ 60% Fe, < 6% SiO2
Goethitic hematite	≥ 60% Fe, < 6%SiO2
Itabirite rich	≥ 50% Fe, ≥ 6% SiO2

Source: Water Management Consultants 2009c

The iron ore bodies and underlying units present a bulk geochemistry and mineralogy controlled by iron oxides, silica and minor aluminous material. Intense leaching and the mobilisation of bases during the formation of the iron ore body and subsequent supergene processes has left in the mineralisation very small concentrations of trace metals. The processes which lead to the formation of the high-grade hematite mineralisation from itabirite at Simandou involved oxidation of magnetite to hematite, hypogene pre-conditioning, and subsequent supergene leaching of silica from the formation.

7.3.4 Acid Rock Drainage

A Rio Tinto Mineral Waste Optimisation Programme was conducted in the course of the Simandou Project. As expressed earlier, a series of static and kinetic tests were carried out by WMC (2008 and 2009a) on 172 samples in order to evaluate potential for Acid Rock Drainage (ARD) and propensity for leaching of metals. The results of these tests are included in Appendix M and are summarised as follows:

- Typical pH analysis results between 5.1 and 8.7 indicate no significant potential for the generation of acid contact waters associated with stored mineral acidity.
- Net acid generation test results indicate pH values in the range of 4.2 to 8.8 suggesting low acidity generated by spontaneous oxidation of sulphides.

- Total sulphur content of samples is typically low (< 0.02%); higher values are associated with phyllite lithological units, especially fresh phyllite (up to 4.5%).
- All lithological units tested to date exhibit very low acid generation potential indices (few kg $CaCO_3$/T), and also generally very low neutralization potential indices (-1.6 to 21.8 kg $CaCO_3$/T).
- Net neutralization potential values are in the range between -20 and 20 kg $CaCO_3$/T.
- Synthetic precipitation leaching protocol test results and preliminary humidity cell test results suggest a very low propensity for mobilisation of deleterious elements from all lithological units. Total dissolved solids content is smaller than 15 mg/l; and sporadic enrichment in Fe, Al and Mn is observed, which could be mobilised in water in contact with mine facilities.

These results suggest that geochemical hazard from mining activities will be low on the basis of the geochemistry (i.e. low sulfur and trace metal contents) of most of the rocks that will be exposed as pit wall, or stored in the waste facilities. Water in contact with these rocks should be neutral or weakly acidic, with extremely low concentrations in sulphates and dissolved metals (WMC 2009a). Consequently, the vast majority of the waste rock and ore produced by the project will essentially be geochemically inert. However, phyllite seems to be the exception.

Indeed, the analysis of fresh phyllite samples indicates that a low ARD or metal leaching risk (As, Sb, Cu, Ni, Zn) exists with this specific lithological unit. Geochemical data of these fresh phyllite samples exhibit pH values between 3.5 and 8.2; net acid generation pH values between 2.0 and 2.7 with net acid generation acidity values between 13.3 and 91 kg H_2SO_4; total sulphur content up to 4.5% with low neutralising potential values (average of 1.1 kg $CaCO_3$/T) and large acid generation potential values (average of 43 kg $CaCO_3$/T); and net neutralising potential values between -14.8 to -143 kg $CaCO_3$/T (classified as predominantly acid forming). These results indicate that fresh phyllite is definitely geochemically reactive.

CHAPTER 8

Pedology

8. PEDOLOGY

8.1 INTRODUCTION

This section presents the soil characteristics of the LSA. Determination of the soil characteristics is essential in order to evaluate the potential of land, notably for agricultural use, that will possibly be affected by the project and the selection of specific sites for industrial activities (waste disposal, gasoline and diesel storage, etc.). It is therefore important to assess the physical characteristics and initial quality of the soils prior to the start of the project.

8.2 METHODS

Existing information, such as data on soil types, and characteristics of the surface cover, has been compiled from an exhaustive document untitled *Carte morphopédologique, République de Guinée,* published by the Institut de Recherches pour le Développement (Boulvert 2003).

In the course of the baseline study, a soil characterisation programme was conducted in the Pic de Fon and Ouéléba areas with the objective of establishing soil characteristics and soil quality prior to the construction works and mine development. The sampling sites and sampling protocols followed during the campaign and the parameters analysed are described hereafter. Soil sampling logs and laboratory analytical result certificates are presented in Appendices N and O.

8.2.1 Soil Sampling

Twenty-four soil samples were collected between 13 and 18 February 2008, at representative sites. Twelve samples were taken in the Pic de Fon area (series MC) and twelve more samples were taken from the Ouéléba area (series MO). Sampling sites were selected on both sides of the Simandou ridge and outside of the perimeter planned for mining extraction. The location of the sampling sites is shown in Map 8.1.

8.2.2 Sampling Protocol

The 24 soil samples have been collected near the ground surface; at maximum depths of 15 cm. Sampling has been performed with a stainless-steel trowel after loosing up the soil crust at the surface with a pick. The samples collected were placed in glass containers provided by the laboratory performing the chemical analyses. The samples were kept at a cool temperature and protected from sunlight until their arrival at the laboratory.

8.2.3 Laboratory Analysis

The samples were sent to Maxxam Analytics laboratory in Canada to be analysed for the following parameters:

- Metals (arsenic, beryllium, cadmium, chromium, cobalt, copper, iron, manganese, mercury, nickel, lead and zinc)

- Sulphur
- Total cyanides
- Petroleum hydrocarbons (C_{10}-C_{50})

8.3 RESULTS

8.3.1 Types of Soil and Agricultural Value

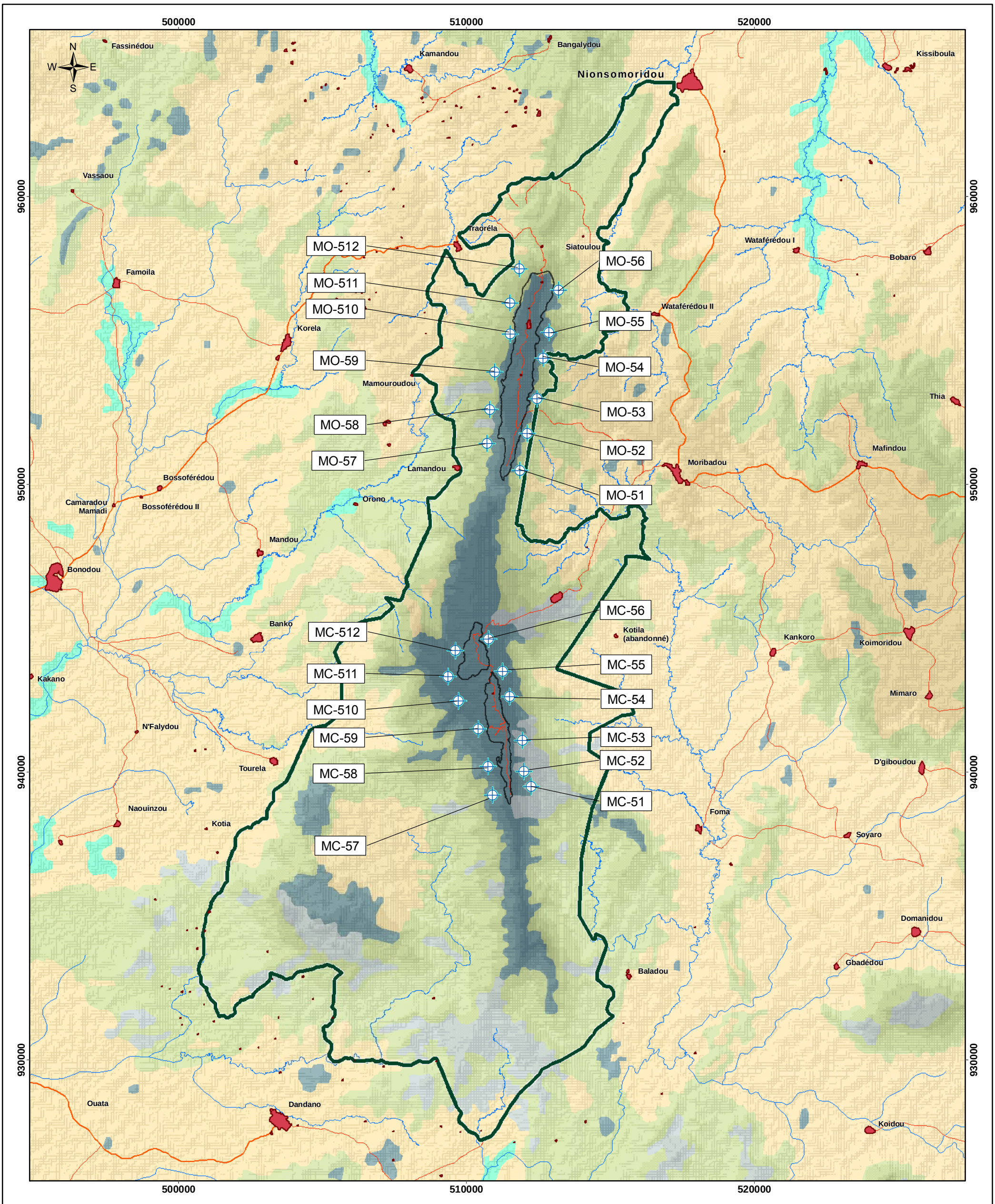
Typical soil types encountered as defined according to Boulvert (2003) and their spatial distribution are illustrated on Map 8.1.

As shown on this map, ferralitic soils dominate the study area. The soils on the plateaus surrounding the Simandou ridge vary mainly from loose ferralitic to indurate ferralitic soils. Ferralitic soils are extremely weathered soils, typically encountered under humid or very humid tropical climate. They are thick and show generally yellowish or reddish colours. Ferralitic soils are rated as having low agricultural value.

Typically, the soil profile encountered along the Simandou ridge consists in lithic soils developed over the carapace and bedrock. These soils are usually thin and display a lack of horizon resulting from a steep slope environment, or from the occurrence of parent materials without any permanent weatherable minerals. Lithic soils are known for offering no significant value for agricultural uses.

In some areas, bedrock erosion has exposed young materials that have accumulated in the piedmont areas. These soils, which have been rejuvenated by erosion, contain laterite soils and rock particles in various proportions. Some of them also include clay material. They are assumed to represent a moderate value for agricultural uses.

Finally, hydromorphic soils are locally encountered in the valleys of small intermittent streams and along several perennial streams. These types of soils generally developed under conditions of poor drainage. Hydromorphic soils typically exhibit medium to good value for agricultural uses, and can sustain various types of crops, such as cereals, vegetables and fruits. These soils are primarily encountered near the streams and *bas-fonds* (lowlands) that are potentially subject to occasional flooding.



Principaux types de sol / Main soil types

Cuirasse ou carapace	Duricust or crust
Lithosol sur roches diverses	Lithosol on various rocks
Sol rajeuni par l'érosion	Soil rejuvenated by erosion
Sol ferralitique	Ferrallitic soil
Sol hydromorphe	Hydromorphic soil

Stations d'échantillonnage / Sampling stations

Station d'échantillonnage de la qualité du sol	Soil quality sampling station

Repères géographiques / Geographical landmarks

Route secondaire	Secondary road
Piste	Track
Hydrographie	Hydrography
Forêt classée du Pic de Fon	Pic de Fon Classified Forest
Milieu bâti	Built area
Aire minière	Mining area

Sources:
1- Base map - 2006 0.5m ADS40 Aerial Photographs, 2006 Spot Imagery;
2- Landsat imagery mosaic 2002-2003;
3- Shuttle Radar Topography Mission (SRTM);
4- Carte topographique IGN 1:50 000/1:200 000;
5- IRD - Yves Boulvert (2004), Carte morphopédologique de Guinée, 1:200 000;
6- Station de mesure de la qualité du sol installé par SNC-Lavalin (SLEI) (L. Boisseau);
7- Geographic Coordinate System: WGS84, UTM, Zone 29N.

Titre / Title

Pédologie dans la zone d'étude locale / Pedology in the local study area

Échelle / Scale	Projet / Project	Volume C Carte/Map 8.1
0 0.625 1.25 2.5 Km 1:125,000	SIMANDOU	

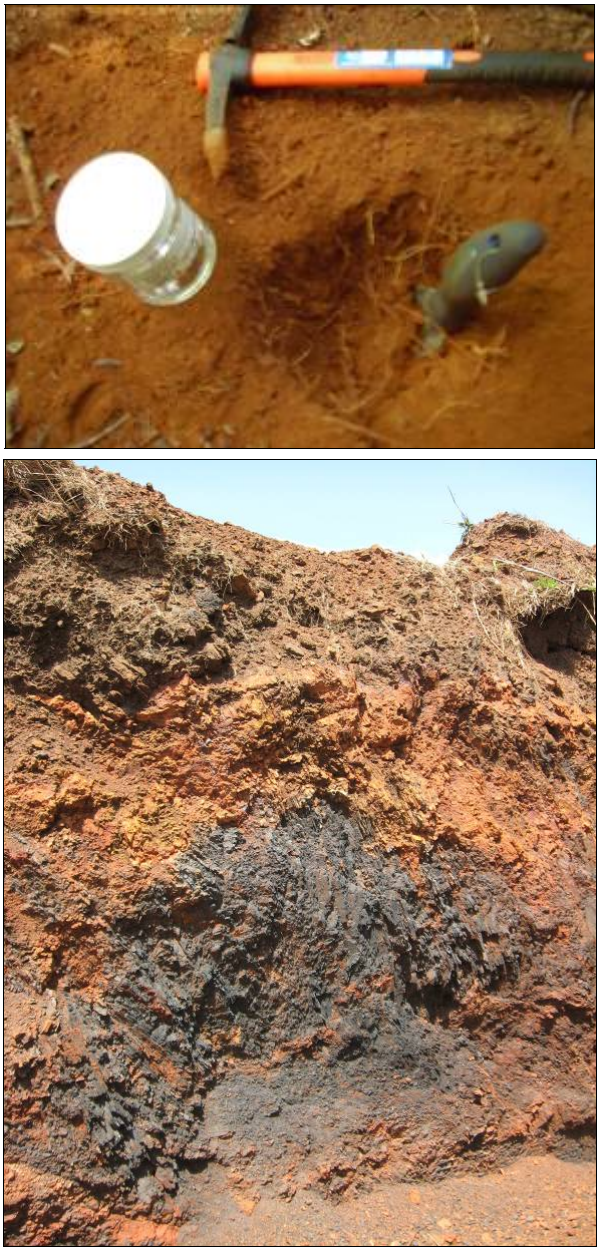
Directeur de projet (client) Project manager (client)	Directeur de projet Project manager	No. pr./ P. number
Leon Payne	Richard Fontaine	604917

No.	aaaa/mm/jj yyyy/mm/dd	Description	Dessiné/Drawn	Vérifié/Verified
01	2010/06/15	Final	M. Dupré	M. Stapinsky
00	2010/01/04	Preliminary	M. Dupré	M. Stapinsky

The texture of the soils exposed in the course of the sampling is generally sandy. The surface soils in the Pic de Fon area, more specifically near the canga material, consist in brown to dark reddish brown silty and gravely fine sand. The surface soils in the Ouéléba area are composed of either a) silty brown fine sand with gravel or trace of gravel, or b) silt with some or traces of sand and gravel. In both cases, roots have been observed in the soils.

A typical soil texture and profile is presented in Photo 8.1. The photo shows the reddish-brown sandy matrix soil developed over the bedrock.

Photo 8.1 Typical soil texture and surficial deposits exposed near a drilling pad located on Pic de Fon



Source: SNC-Lavalin Environment 2008

8.3.2 Chemical Characteristics of Soils

The soil sampling carried out for the current baseline study was performed in order to describe the initial soil chemistry.

The interpretation of the analytical results is based on the assumptions that the soils have not been affected by any mining activities.

Table 8.1 provides the summary statistics for the soil chemical analyses results. For the purpose of calculating summary statistics, values beneath the detection limit have been reset to half of the detection limit (bold).

The soil chemical analysis results generally vary within the same range of concentrations for a given element. Sulphur is a common non-metallic element typically present in soils and it is present in all soil samples collected. Most of the soil samples show total cyanides concentrations below the detection limit or slightly above. Beryllium, cadmium, cobalt and lead also indicate concentrations below detection limit or slightly above in all samples. Iron and manganese are the most abundant metal elements. Copper, mercury, nickel and zinc concentrations are also above the detection limit, with a few exceptions. Chromium concentrations are slightly higher in

comparison to the rest of the metals analysed, whereas arsenic concentrations remain constantly below the detection limit. All petroleum hydrocarbon concentrations are below the detection limit, or slightly above. As expected, the results indicate typically low background concentrations for all the parameters measured in the soil samples.

Table 8.1 Summary statistics for soil samples in the local study area

Parameter	Unit	Method detection limit	Minimum	Maximum	Median	Average
Sulphur	%	0.01	0.03	0.19	0.07	0.08
Total Cyanides	mg/kg	0.5	**0.25**	4	**0.25**	0.7
As	mg/kg	6	**3**	**3**	**3**	**3**
Be	mg/kg	0.5	**0.25**	**0.25**	**0.25**	**0.25**
Cd	mg/kg	0.5	**0.25**	1	**0.25**	0.28
Cr	mg/kg	2	8	130	37	43
Co	mg/kg	1	**0.5**	7	1	1.3
Cu	mg/kg	2	**1**	13	7	7
Fe	mg/kg	100	23,000	110,000	74,500	70,792
Mn	mg/kg	1	46	1,300	420	449
Hg	mg/kg	0.02	**0.01**	0.19	0.07	0.08
Ni	mg/kg	1	**0.5**	13	6	6
Pb	mg/kg	5	**2.5**	8	2.5	2.7
Zn	mg/kg	10	**5**	38	14	15
% Humidity	%	-	3	25	11.4	12.3
Petroleum hydrocarbons (C10-C50)	mg/kg	100	**50**	180	**50**	**50**

Note: Values in bold are values less than the detection limit that have been reset to half of the detection limit for purposes of calculating summary statistics.

CHAPTER 9

Hydrology

9. HYDROLOGY

9.1 INTRODUCTION

The Simandou Range is the headwaters of several major river systems in Western Africa, some of which are transboundary rivers, such as the Niger River which drains through Mali. Many people in the local study area (LSA), and downstream, depend on these surface waters for various purposes, such as drinking, bathing, washing, farming, etc.

Hydrological processes in mountainous regions are complex and require detailed examination. They are characterised by a large variability resulting from rainfall patterns, topography, soil and geology. Surface water and groundwater domains are also closely linked in mountainous regions. Groundwater discharge from the hillside supports perennial base flows in streams originating from the range.

For these reasons, and given that the potential impacts of mining operations on the flow and quality of surface waters is an important issue for the Simandou Project, an exhaustive hydrological monitoring programme has been implemented. The programme aims to collect hydrological data for the characterisation of the stream flow regime of the main tributaries that may be affected by the Simandou Project.

9.2 METHODS

The regional river gauging data that have been collected for major watersheds by national authorities (*Direction Nationale de l'Hydraulique* - DNH) for several decades were used to define the hydrological regional context of the Simandou Project.

Hydrological studies were initiated in early 2003 with the installation of the first weirs. An exhaustive hydrological monitoring programme was then implemented in 2006. Fieldwork and data interpretation for the baseline study were carried out by Water Management Consultants (WMC 2009b), now Schlumberger Water Services (SWS), with the assistance of Rio Tinto local personnel. Although this programme is ongoing, the results up to December 2008 from WMC are presented and discussed hereafter.

The methodology described in this section comprises three components: the regional river gauging network, the local hydrometric network and the spring surveys.

9.2.1 Regional River Gauging Stations

Early in the project, government-operated river gauging data provided by the DNH for stations downstream of the Simandou Project were used to examine the hydrological characteristics of the regional watersheds in which the project is located. Table 9.1 lists key details of the DNH stations examined in the current study, which are located downstream of the study area. Figure 9.1 (which can be found in the Results section) shows the location of the stations that are part of the national hydrometric monitoring network.

Table 9.1 River gauging stations located downstream of the local study area

Water course	Station	Station number	Drainage area (km^2)	Latitude	Longitude	Availability of data	Status
Niger River basin							
Niger	Dialakoro	-	68,330	11°27'00N	8°54'01"W	1954-date	Open
Niger	Tiguibery	-	67,600	11°22'02"N	9°10'01"W	1952-1979	Open
Milo	Kankan	1171501705	9,900	10°23'00"N	9°18'00"W	1952-2006	Open
Milo	Kérouané	1171501707	1,695	9°16'00"N	9°02'00"W	1970-1980	Open
Milo	Konsankoro	17151710	990	9°01'06"N	9°00'00"W	1955-1980	Closed
Sankarani	Mandiana	1171502005	21,900	10°37'05"N	8°41'01"W	1954-date	Open
Dion	Baranama	1171503506	6,590	10°07'30N	8°45'30"W	1971-2006	Open
Dion	Diamaradou	-	-	-	-	-	Closed
Diani River basin							
Diani	Bac	1173700105	4,095	8°03'20"N	9°43'00"W	1975-2006	Open

Source: Water Management Consultants 2009b

9.2.2 Local Hydrometric Network

The local hydrometric network specifically set up for stream flow monitoring consists of six concrete weirs and 20 rated cross sections. Map 9.1 (found in the Results section) shows the hydrometric monitoring network in regard to the local watersheds. Data was collected as early as 2003 at some monitoring sites. Appendix P contains details of the monitoring stations (GPS coordinates, elevation, drainage area and status).

The weirs installed in Pic de Fon (Whisky 1, Whisky 2 and Whisky 4) and in Ouéléba (Whisky 5, Whisky 6 and Ouéléba 1) have been constructed on small streams draining the steeper slopes of the mountains downstream of the proposed mining areas (see Map 9.1). One of the weirs which form part of the local hydrometric monitoring network is presented in Photo 9.1. The weirs are equipped with automatic digital logging equipment to monitor flow and water quality (temperature, electrical conductivity, pH, dissolved oxygen and turbidity).

Although six monitoring sites have been equipped to monitor stream flow, only three stations (Whisky 1, 2 and 5) recorded sufficient data for interpretation at the time of completing the baseline study report.

The hydrometric network has been completed with a total of 20 manual stream flow monitoring stations (Map 9.1). The stations have been installed at sites where local people collect or use water, typically located close to villages. The stations consist of rated cross sections, where stage boards have been installed. Twice a day, local observers record level, turbidity and colour of the water. Flow measurements have been performed at each site, by Rio Tinto personnel with the assistance of WMC, with a current meter in order to construct stage-discharge rating curves for conversion of the water level records to flows.

Photo 9.1 Typical weir part of the local hydrometric monitoring network



Source: SNC-Lavalin Environment 2008

9.2.3 Springs Surveys

In addition to stream flow monitoring, two spring surveys have been carried out on the flanks of Pic de Fon and Ouéléba. The first survey was carried out in the wet season of 2006, and the following survey was performed during the 2008 dry season. The objective of the surveys was to improve the understanding of the closely related hydrological and hydrogeological systems.

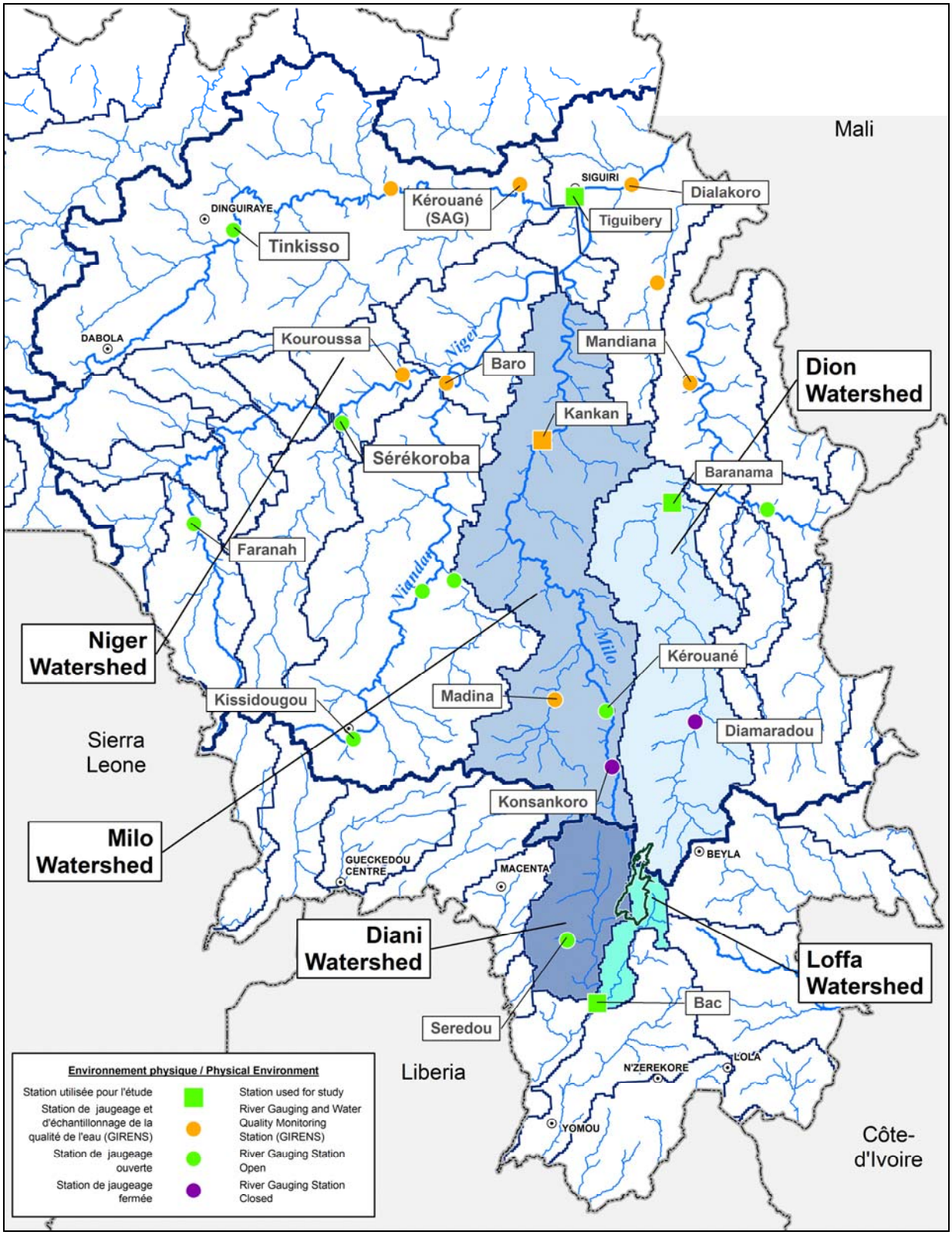
During the survey the exact location of each spring identified was recorded with a GPS instrument (Map 9.2 shown in the Results section), physico-chemical parameters were measured on-site and samples were collected for more detailed laboratory analyses. The flow at each spring site was also estimated.

9.3 RESULTS

9.3.1 Regional Hydrology

Because the Simandou Range is the headwaters of four major regional rivers, it is essential to firstly examine hydrological characteristics at the regional scale. The limits of the main regional watersheds draining the Simandou Range are presented in Figure 9.1.

Figure 9.1 Regional watersheds and national hydrometric network context



Source: Water Management Consultants 2009b

The watersheds drain in four directions:

- to the northeast in the Dion River, thence to the Sankarani River, which drains in the Niger River into Mali;
- to the northwest in the Milo River, a tributary of the Niger River;
- to the southeast in the Loffa River, a tributary of the Diani River; and
- to the southwest in the Diani River, an international transboundary river that flows into Liberia.

The Simandou Range is the southwestern headwaters of the Dion/Sankarani River watershed, and the southeastern headwaters of the Milo River watershed. The stream flow at Baranama, located on the Dion River, and at Konsankoro and Kérouané, located on the Milo River, consists primarily of water draining from the Simandou Range. The Niger River also receives flow from tributaries of the Milo and Dion Rivers which do not originate from the Simandou Range.

The contribution of the Milo and Dion rivers to the flow of the Niger River, at Tiguibery the confluence, has been estimated respectively at 18-20% (Milo at Kankan) and at 7-11% (Dion at Baranama) (WMC 2009b). The higher flows measured in the Milo River is associated with its location, i.e. on the western side of the Simandou Range, which typically experiences more rainfall than the eastern side.

The average flow in the watershed draining the Simandou Range into the Diani River is twice the flow of the Milo River, and is presumably associated to its southwesterly position and higher rainfall rate (WMC 2009b).

9.3.2 Main Hydrological Features in the Local Study Area

Detailed analysis of hydrological features has also been carried out at the local scale in the vicinity of the Pic de Fon Classified Forest (PdF CF). Emphasis has been placed on the baseline conditions of the major streams originating from the Pic de Fon and Ouéléba deposits, as well as the points of use, in terms of water quality and utilisation. Map 9.1 presents the limits of the local watersheds and sub-watersheds of the numerous streams draining PdF CF, which have been monitored in the course of the baseline study.

The Simandou ridge forms a north-south divide between the eastern and western watersheds. As previously observed in Figure 9.1, the Niger River watershed's southern limit runs east-west across Ouéléba, dividing the drainage between that flowing north and that flowing south.

From north to south, the main streams draining PdF CF include (see Map 9.1):

- the Mala and Kinyeko rivers, which drain the northwestern flank of Ouéléba and flow towards the Milo River;
- the Miya River, which drains the eastern flank of Ouéléba and flows towards the Dion River;

- the Loffa River, which drains the southeastern side of Ouéléba and the eastern flank of Pic de Fon, and is a tributary of the Diani River;
- the Woron River, which drains the southwestern flanks of Ouéléba and the northern and western flanks of Pic de Fon towards the Diani River; and
- the Foko West River, which drains the southwestern flank of Pic de Fon, flowing through the forest on the southwestern side of the range towards the Diani River.

The characterisation of the hydrological regime in local watersheds is based primarily on data collected at the weirs installed at Whisky 1, 2 and 5 monitoring stations. The streams monitored at these stations are draining towards the Loffa, Diani and Woron rivers, respectively for Whisky 1, 2 and 5. Some characteristics of the area covered by these monitoring stations are presented in Table 9.2.

Table 9.2 Characteristics of Whisky 1, 2 and 5 watersheds

Characteristic	Pic de Fon		Ouéléba
	Whisky 1	Whisky 2	Whisky 5
Watershed area	0.494 km^2	0.410 km^2	0.400 km^2
Proportion of area covered by grassland	60%	80%	43%
Proportion of area covered by forest	40%	20%	57%
Description	Canga East camp water supply abstraction upstream of weir	Assumed natural but presence of drill pads and tracks since 2007	Natural

Source: Water Management Consultants 2009b

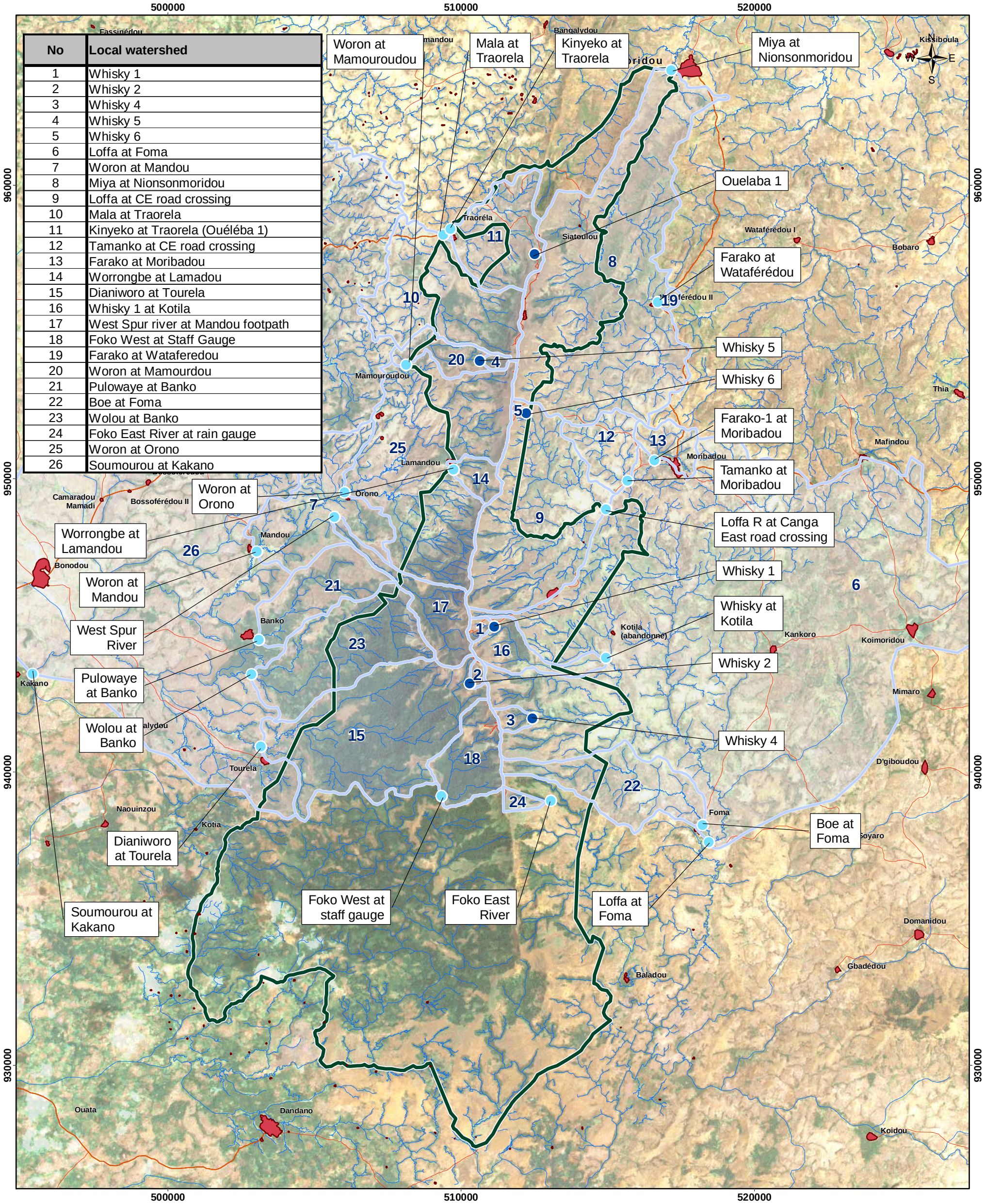
9.3.3 Hydrological Regime

Some of the government-operated river gauging stations located downstream of the study area have provided stream flow data as far as the early 1950's. However, there are several gaps observed over the years in the data series. Despite these gaps, the data clearly demonstrate annual fluctuations in stream flow, but long-term trends are difficult to interpret (WMC 2009b).

Figure 9.2 and Figure 9.3 show the time series for stream flow measured at Tiguibery, Baranama, Kankan and Bac rivers gauging stations, which are representative locations respectively for the Niger, Dion, Milo and Diani rivers.

The data series recorded at Tiguibery on the Niger River displayed a strong annual variability, and suggests an overall long-term decline in flow. Stream flow data recorded at Kankan on the Milo River also suggests a similar long-term decline. Conversely, data recorded at Bac on the Diani River seems to exhibit a long-term increase in flow.

No	Local watershed
1	Whisky 1
2	Whisky 2
3	Whisky 4
4	Whisky 5
5	Whisky 6
6	Loffa at Foma
7	Woron at Mandou
8	Miya at Nionsonmoridou
9	Loffa at CE road crossing
10	Mala at Traorela
11	Kinyeko at Traorela (Ouéléba 1)
12	Tamanko at CE road crossing
13	Farako at Moribadou
14	Worrongbe at Lamadou
15	Dianiworo at Tourela
16	Whisky 1 at Kotila
17	West Spur river at Mandou footpath
18	Foko West at Staff Gauge
19	Farako at Wataferedou
20	Woron at Mamourdou
21	Pulowaye at Banko
22	Boe at Foma
23	Wolou at Banko
24	Foko East River at rain gauge
25	Woron at Orono
26	Soumourou at Kakano



Réseau hydrométrique / Hydrométric network

Site de mesure du débit d'eau	Streamflow monitoring site
Déversoir	Weir
Hydrographie	Hydrography
Bassin versant local	Local watershed

Repères géographiques / Geographical landmarks

Route secondaire	Secondary road
Piste	Track
Forêt classée du Pic de Fon	Pic de Fon Classified Forest
Milieu bâti	Built area

Sources:
1- Base map - 2006 0.5m ADS40 Aerial Photographs, 2006 Spot Imagery;
2- Landsat imagery mosaic 2002-2003;
3- Shuttle Radar Topography Mission (SRTM);
4- Carte topographique IGN 1:50 000/1:200 000;
5- Water magagement consultant report;
7- Geographic Coordinate System: WGS84, UTM, Zone 29N.

Titre / Title

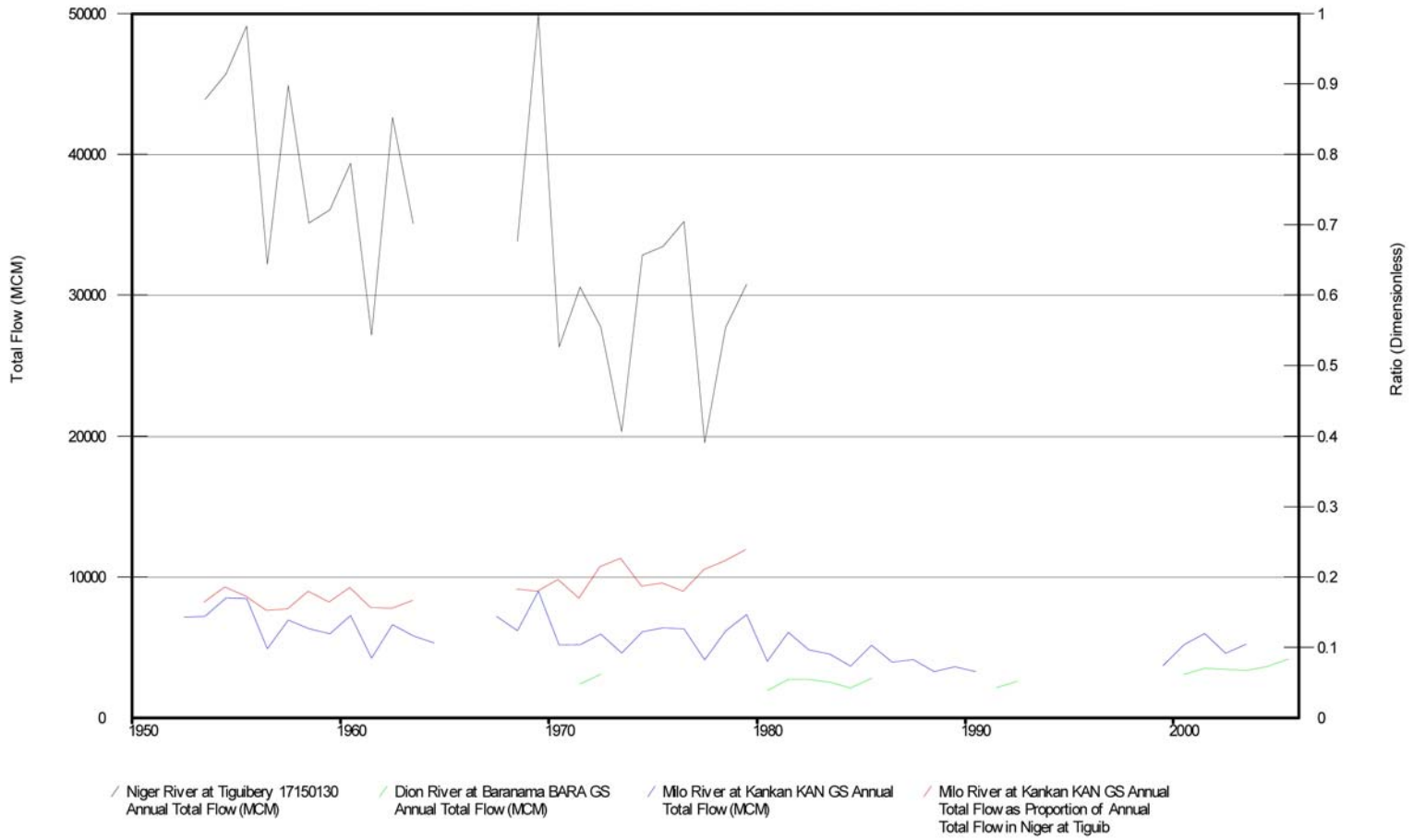
Bassins versants locaux et réseau hydrométrique dans la zone d'étude locale / Local watersheds and hydrometric network in the local study area

Échelle / Scale	Projet / Project	Volume C Carte/Map 9.1
0 0.625 1.25 2.5 Km 1:125,000	SIMANDOU	

Directeur de projet (client) Project manager (client)	Directeur de projet Project manager	No. pr./ P. number
Leon Payne	Richard Fontaine	604917

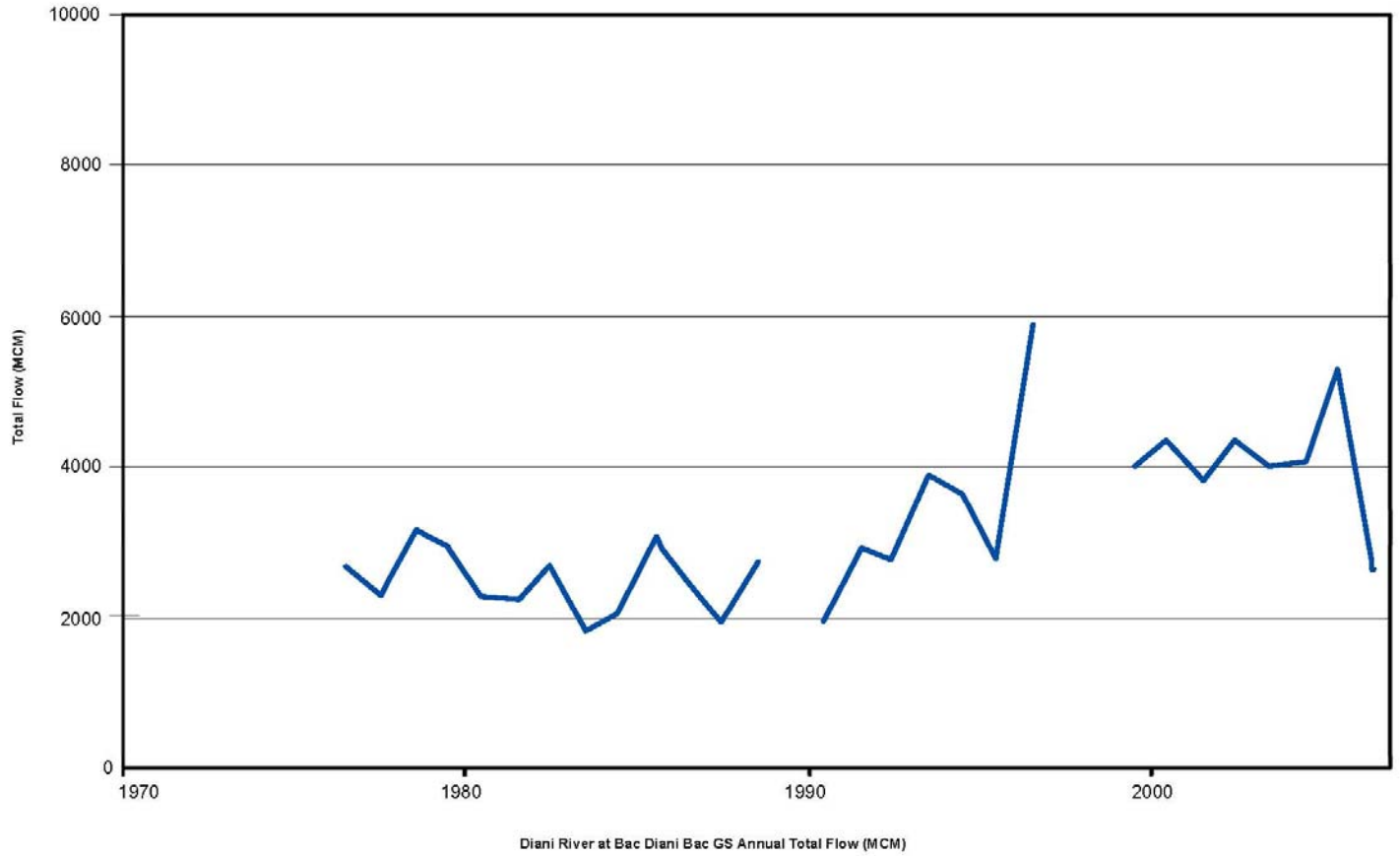
No.	aaaa/mm/jj yyyy/mm/dd	Description	Dessiné/Drawn	Vérifié/Verified
01	2010/06/15	Final	M. Dupré	M. Stapinsky
00	2010/01/04	Preliminary	M. Dupré	M. Stapinsky

Figure 9.2 Annual stream flow measured in the Niger, Dion and Milo gauging stations and total flow in the Milo as proportion of annual total flow in the Niger



Source: Water Management Consultants 2009b

Figure 9.3 Annual stream flow measured at Bac River gauging station on the Diani River



Source: Water Management Consultants 2009b

Figure 9.4 has been prepared in order to demonstrate the characteristics of the flow regime in the Niger, Milo, Diani and Dion rivers. The mean daily flow recorded at six gauging stations located on these rivers is presented for the 1975 to 1979 period, which is the only period of records common to each station. The figure shows the magnitude and timing of the seasonal hydrographs. The flow in each river is very low between February and May during the dry season; but it can increase significantly during the wet season, reaching its highest values in September and October.

The weirs installed at Whisky 1, 2 and 5 monitoring stations have allowed the detail analysis of the hydrological regimes of typical local watersheds and provided essential information on short-term hydrological processes.

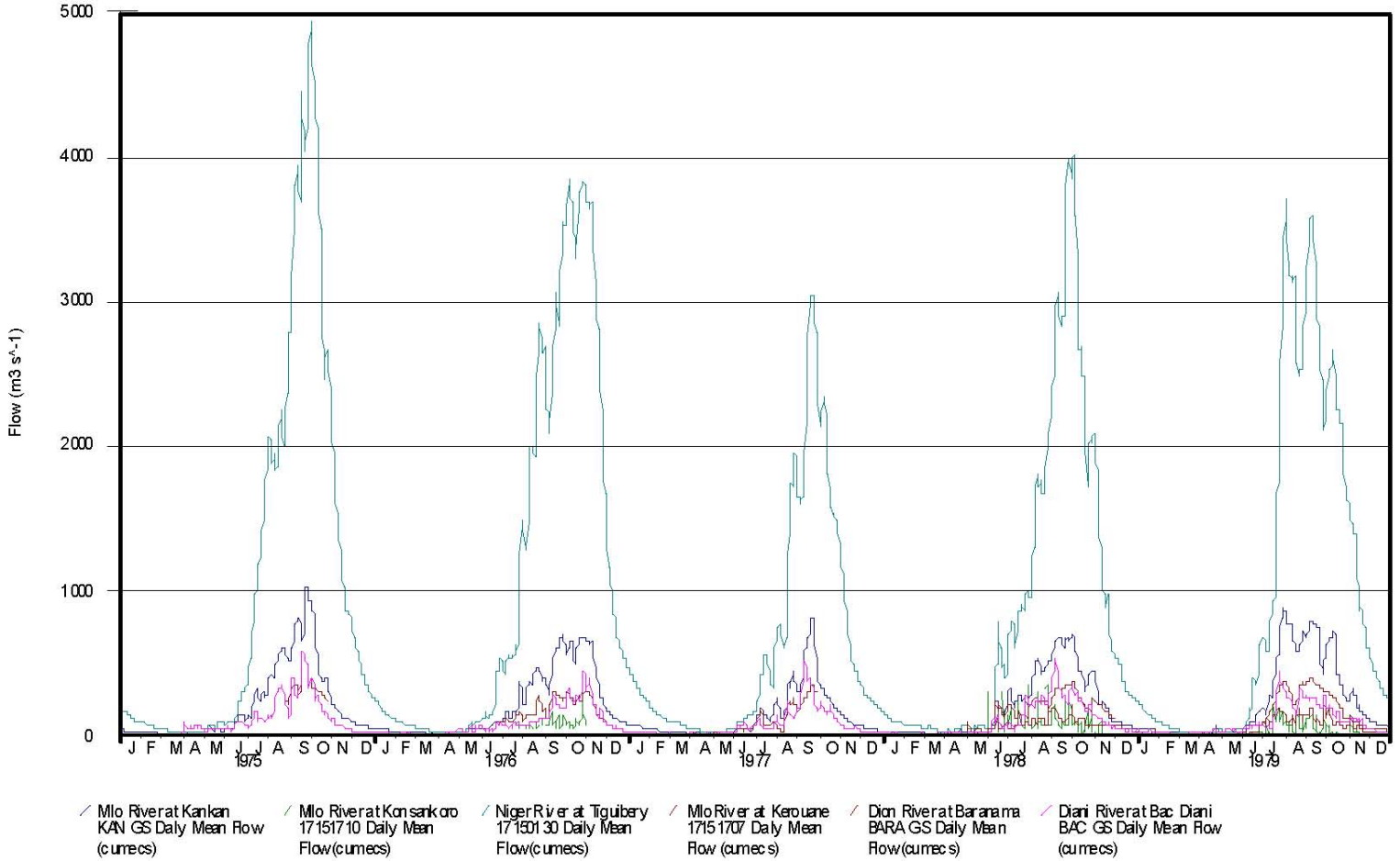
Figure 9.5 presents daily instantaneous flow measurements and rainfall recorded at Whisky 1 and 2, between July 2003 and December 2008. The data series from Whisky 5 was too short for any meaningful interpretation.

Analysis of the daily instantaneous flows at Whisky 1 and Whisky 2 compared with daily rainfall records from the Canga East rain gauge station displays a clear seasonal distribution of flow in response to the wet season. Typically stream flow begins to increase only in early July, although the wet season starts earlier in March. WMC (WMC 2009b) suggested that the delay in the stream flow response results from the discharge of a subsurface water reservoir in the hill slopes of the adjacent cangas that has been filling up since the beginning of the wet season. Seasonal flow remains high, as long as rainfall continues. As rainfall declines in September/October, the flow begins to decrease. The flow recession continues through the dry season, fed primarily by the groundwater flow system. The hydrological regime of Whisky 1 and Whisky 2 local watersheds is therefore perennial and dominated by groundwater discharge, but with a significant storm flow component superimposed on the perennial flow.

Other watersheds originating from Pic de Fon and Ouéléba are more or less similar to the Whisky 1, 2 and 5 watersheds on the basis of physical characteristics (slope, vegetation, soil and geology). Therefore, it is assumed that similar conclusions can be drawn from these observations. The main factor distinguishing watersheds is the proportions of their areas under forest and grassland.

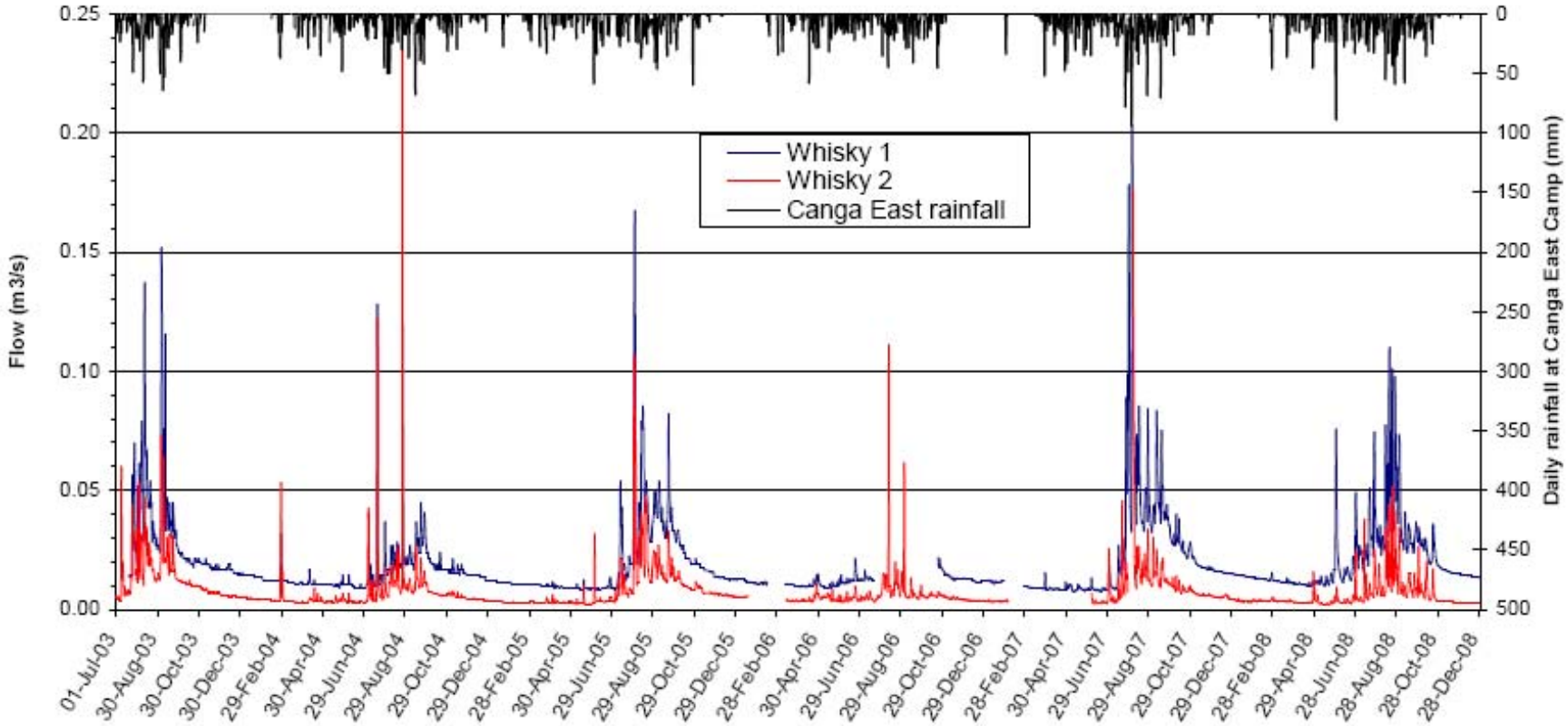
Table 9.3 presents the monthly mean flows, the mean normalised flows – according to the area drained ($L/s/km^2$), and the instantaneous maximum and the minimum flows in each month of record, since continuous monitoring started in December 2005 at Whisky 1 and 2. Monitoring at Whisky 5 was only initiated in August 2008.

Figure 9.4 Seasonal hydrographs in the Niger, Milo, Diani and Dion rivers (1975-1979)



Source: Water Management Consultants 2009b

Figure 9.5 Whisky 1 and 2 daily instantaneous flow measurements and rainfall (2003-2008)



Source: Water Management Consultants 2009b

Table 9.3 Summary of monthly stream flow data at Whisky 1, 2 and 5

	Jan.	Feb.	Mar.	Apr.	May	June	July	Aug.	Sep.	Oct.	Nov.	Dec.	Ann.
Whisky 1 (Dec. 2005-Dec. 2008)													
Monthly mean	12.4	11.3	10.3	10.0	10.5	13.7	23.7	47.5	33.5	22.6	16.0	13.7	18.8
Mean L/s/km^2	25.1	22.9	20.9	20.2	21.3	27.7	48.0	96.2	67.8	45.7	32.4	27.7	38.1
Instant. max.	22.5	23.2	24.0	154.8	147.8	90.9	268.5	2,195.6	965.0	334.8	41.2	41.5	2,195.6
Instant. Min.	9.1	8.4	7.3	7.0	6.7	7.3	7.8	29.6	28.4	15.4	10.7	10.6	6.7
Whisky 2 (Dec. 2005-Dec. 2008)													
Monthly mean	3.9	3.7	3.1	3.7	4.8	4.6	9.4	19.4	10.5	7.6	4.7	4.3	6.6
Mean L/s/km^2	9.5	9.0	7.6	9.0	11.7	11.2	22.9	47.3	25.6	18.5	11.5	10.5	16.1
Instant. max.	5.8	47.2	11.2	128.3	69.0	95.6	494.0	516.6	217.9	298.6	23.2	31.1	516.6
Instant. min.	2.3	2.7	2.7	2.4	1.7	2.2	2.7	4.7	4.2	4.5	3.5	2.9	2.2
Whisky 5 (Aug.-Dec. 2008)													
Monthly mean	-	-	-	-	-	-	-	27.8	21.8	12.9	7.7	6.2	-
Mean L/s/km^2	-	-	-	-	-	-	-	69.5	54.5	32.3	19.3	15.5	-
Instant. max.	-	-	-	-	-	-	-	142.0	77.9	59.3	1.3	7.8	-
Instant. min.	-	-	-	-	-	-	-	16.6	14.1	12.1	5.5	5.2	-

Source: Water Management Consultants 2009b

Despite differences in flow rates, the monthly flow regimes at Whisky 1 and 2 watersheds vary similarly through the year. The stream flow monthly mean is typically two to four times higher in Whisky 1 compared to Whisky 2. Also, for the same surface area, normalised flows in Whisky 2 are approximately half of the flows in Whisky 1. As observed in Table 9.3, maximum instantaneous values are significantly larger than the recorded monthly mean. The larger instantaneous values are potentially associated with rainfall events and not with normal stream flow fed by groundwaters.

As expressed earlier, the difference in flows could be attributed to the land cover in each watershed. Grassland and impermeable laterite cover a larger part of the Whisky 2 watershed than the Whisky 1 watershed (Table 9.2). Consequently, these conditions would increase runoff in the Whisky 2 watershed, and result in a smaller groundwater recharge feeding the stream flow.

9.3.3.1 Base Flow and Storm Flow

As observed in Figure 9.5, flood events in streams occur typically in response to heavy rainfall events. This hydrological process can be characterised in stream flow hydrographs as the combination of a storm flow component superimposed on a base flow component.

Base flow is the part of the flow that originates from the discharge of subsurface water, i.e. either or both groundwater and soil water. Storm flow is usually the result of overland flow, either as runoff from saturated zones close to stream channels, or as runoff from slopes as the result of exceeding soil infiltration capacities by heavy rainfall. Some storm flow may originate from subsurface flow in the soil zone.

The Base Flow Index (BFI) is a measure of the proportion of base flow within the total flow. The BFI is characterised by specific stream hydrological regimes, as it indicates the impact of soils and geology on stream flow. Separation of base flow from storm flow hydrographs has been performed routinely in hydrological studies of mountain and lowland watersheds in order to estimate characteristic BFI. Figure 9.6 illustrates an example of the separation of base flow and storm flow components at Whisky 1 for the period of May to December 2007, as provided by WMC. No such hydrograph was produced for Whisky 2.

9.3.3.2 Watersheds Draining the Mountains

As typical watersheds of the Simandou Range, Whisky 1 and 2 had their base flow hydrographs separated for 2007, and the results are summarised in Table 9.4 (WMC 2009b). The wet season hydrographs have been divided into periods (three periods for Whisky 1; and five periods for Whisky 2) within which each period seems to demonstrate similar responses to rainfall events. Base flows in corresponding time periods (July-September; September-November) displayed in Whisky 1 and 2 a percentage of the total flow within the same order of magnitude (similar BFI).However, this is not observed in the data prior to July.

Table 9.4 Results of base flow and storm flow separation on Whisky 1 and 2 (2007)

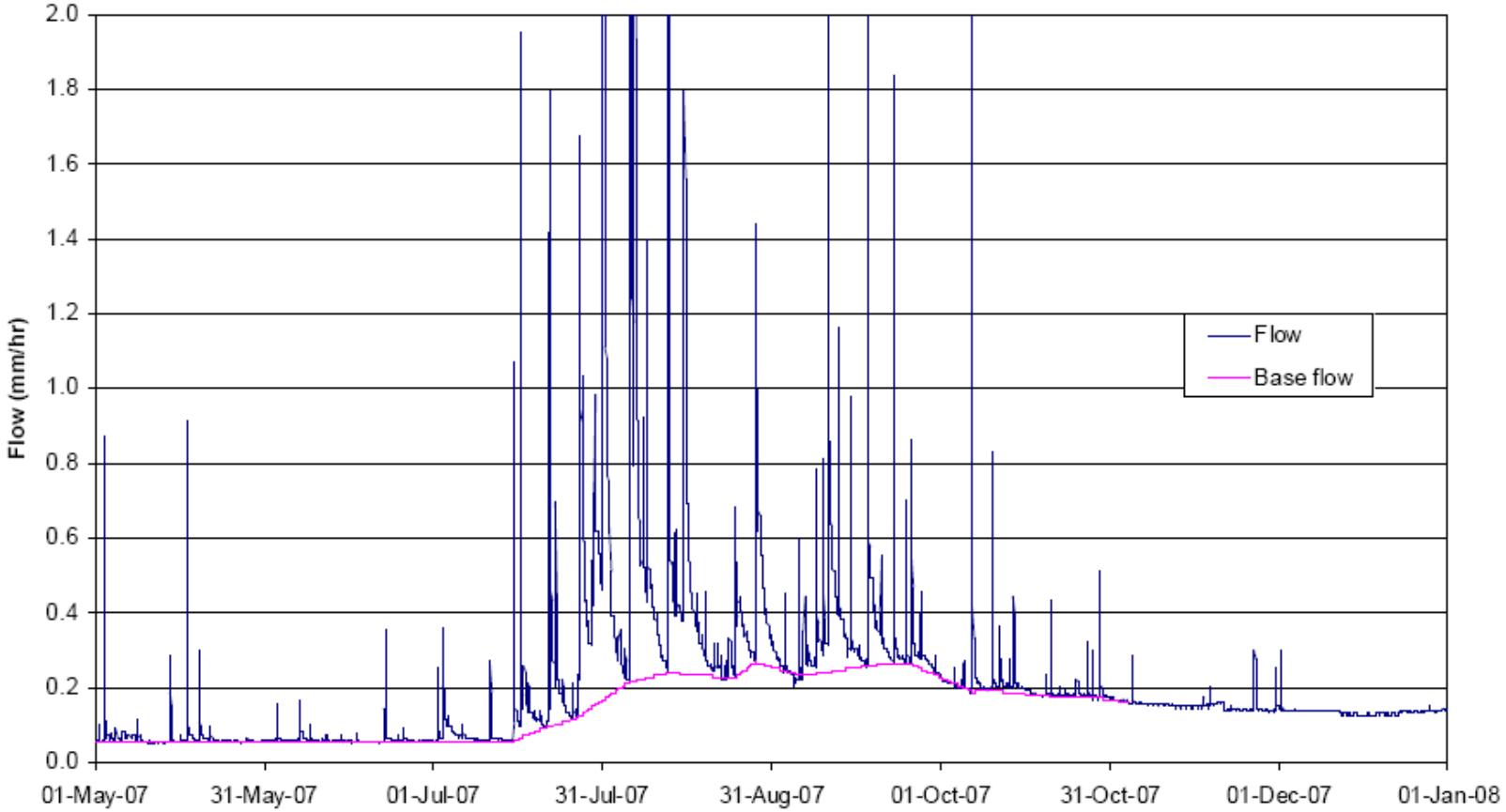
Start date (2007)	End date (2007)	Rainfall	Flow	Base flow	Storm flow	Flow / rainfall	Base flow / rainfall	Storm flow / rainfall %	Base flow index
		(mm)							
Whisky 1									
May 2	July 15	547.4	115.8	101.2	14.6	21.2	18.5	2.7	0.87
July 15	Sept. 22	1736.8	661.0	339.9	321.2	38.1	19.6	18.5	0.51
Sept. 22	Nov. 4	290.3	223.3	203.8	19.3	76.9	70.2	6.7	0.91
Whisky 2									
June 6	June 21	89.4	14.3	9.5	5.0	16.0	10.6	5.6	0.66
June 21	July 21	329.0	49.4	21.9	27.4	15.0	6.7	8.3	0.44
July 21	Sept. 20	1137.3	235.8	114.0	121.9	20.7	10.0	10.7	0.48

Start date (2007)	End date (2007)	Rainfall	Flow	Base flow	Storm flow	Flow / rainfall	Base flow / rainfall	Storm flow / rainfall %	Base flow index
		(mm)							
Sept. 20	Nov. 2	340.0	108.0	90.3	17.9	31.8	26.6	5.3	0.84
Nov. 2	Dec. 16	97.3	64.6	56.6	8.1	66.4	58.2	8.3	0.88

Source: Water Management Consultants 2009b

For Whisky 1, the flow during the first part of the wet season (2 May to 15 July) most likely represents a larger groundwater flow from the springs and from the valley sides into the stream channel in comparison to Whisky 2 where, as previously discussed, a smaller groundwater recharge is assumed (also see Figure 9.6). This flow is assumed to be affected negligibly by early wet season rainfall. The storm flow component shows very rapid increases in flow rates followed by equally rapid decreases with virtually no recession curves.

Figure 9.6 Separation of the storm flow and base flow components in the Whisky 1 hydrograph (2007)



Source: Water Management Consultants 2009b

The following period of the wet season (15 July to 22 September) is characterised by an increase in base flow, but also a substantial increase in storm flow. The stream flow during this period is dominated by the storm flow component, which is confirmed by the decrease observed in the BFI.

During the third period (22 September to 4 November), the base flow component decreases, so does the storm flow component. The storm flow component returns to a similar pattern as the one observed prior to 15 July, with no long lasting recessions. Base flow dominates again with rapid increases and decreases in storm flow in response to rainfall events. This can also be observed, to a lesser extent, for the October-December period in the example presented in Figure 9.6

Whisky 2 also presented a similar series of data, although five distinct periods could be identified during the wet season. Indeed, the hydrological sequence (base flow – storm flow – base flow dominant components) is the same, but the storm flow component in Whisky 2 dominates during a longer period (21 June to 20 September).

As previously discussed, the difference between the Whisky 2 and Whisky 1 results could be attributed to the fact the Whisky 2 watershed has 80% of its area covered by grassland overlying impermeable laterite, as opposed to 60% for Whisky 1 (Table 9.2). Both watersheds received similar inputs of rainfall, but since the Whisky 2 watershed is slightly smaller than the Whisky 1 watershed and the land cover less permeable (smaller groundwater recharge), it is expected that the BFI will be lower and that the storm flow percentage will be higher in Whisky 2.

These results suggest that in the first period of the wet season, the runoff is generated by rainfall falling primarily along the stream channels with limited or no contribution from elsewhere in the watershed. During the middle part of the wet season a different mechanism appears to be producing the storm flow runoff, with recession curves that last for considerable periods. At this stage, water is assumed to be discharged by storage that has been filled in the surficial deposits and the unsaturated zones during the wet season.

It is expected that other watersheds in the Pic de Fon and Ouéléba areas, as well as along the Simandou Range, will have hydrological regimes similar to Whisky 1 and Whisky 2. These observations tend to confirm that the key factor controlling the stream flow regime is assumed to be land cover (as expressed by the proportion of forest/grassland area). The occurrence of laterite (under grassland) will also limit infiltration and recharge of the groundwater system. Lastly, as discussed further in Chapter 11, the important storm flow component observed in the data collected temporally affects the quality of stream water as it is responsible for soil erosion and sediment transport following storm events.

9.3.3.3 Watersheds Draining to the Villages

Base flow, as measured at locations near villages, provides the baseline against which potential future impacts on water resource may be predicted and monitored. Table 9.5

shows monthly mean flows and normalised flows (in L/s/km^2), as evaluated at each village for the period of record (see Map 9.1 for location of stations).

As seen in Table 9.5, the seasonal variability is also observed in the monthly mean stream flow data. Typically, storm flow begins to increase in May and June, and reaches a maximum in September. The comparison between the data from Whisky 1 and Whisky 2 (Table 9.3) with data from the village gauging stations (Table 9.5) suggests that base flow in the mountain watersheds is higher (per unit area) than base flow from downstream larger watersheds. This can be observed in Figure 9.7 where monthly mean base flow is expressed in mm of runoff over the watershed area. These results suggest that most base flow at the villages originates from the mountain groundwater system and not from basement rocks in the plateaus, since mean normalised flows are typically smaller than at Whisky 1 and 2.

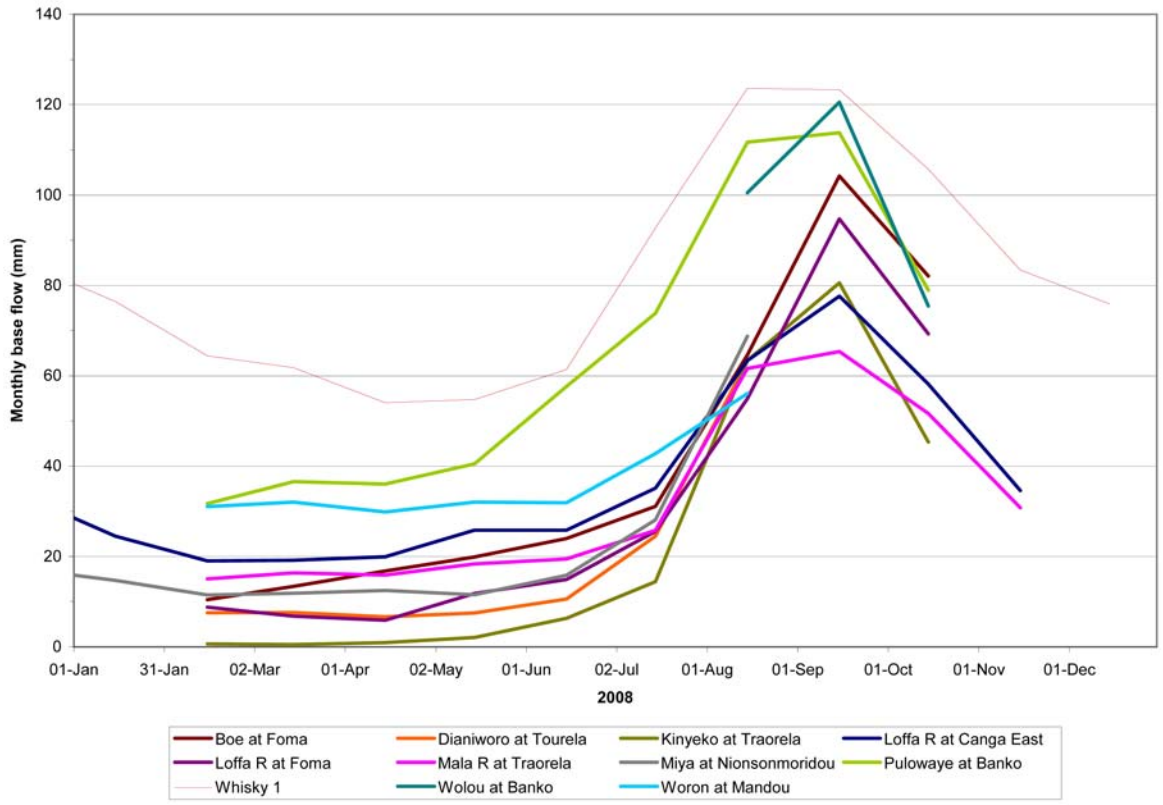
Table 9.5 Summary of monthly stream flow data at village gauging stations

	Jan.	Feb.	Mar.	Apr.	May	June	July	Aug.	Sep.	Oct.	Nov.	Dec.	Ann.
Boe River at Foma (Feb. 2008-Oct. 2008). Watershed area: 10.1 km^2													
Monthly mean	-	42	50	66	75	93	117	244	406	310	-	-	-
Mean L/s/km^2	-	4.2	5.0	6.5	7.4	9.2	11.6	24.2	40.2	30.7	-	-	-
Dianiworo River at Tourela (Feb. 2008-Aug. 2008). Watershed area: 23.9 km2													
Monthly mean	-	72	68	61	67	98	219	565	-	-	-	-	-
Mean L/s/km^2	-	3.0	2.8	2.6	2.8	4.1	9.2	23.6	-	-	-	-	-
Kinyeko River at Traorela (Jan. 2008-Nov. 2008). Watershed area: 8.86 km^2													
Monthly mean	-	2	2	3	7	22	48	210	275	150	-	-	-
Mean L/s/km^2		0.2	0.2	0.3	0.8	2.5	5.4	23.7	31.0	16.9	-	-	-
Loffa River near Canga East (May 2008-Nov. 2008). Watershed area: 22.1 km^2													
Monthly mean	202	168	158	170	213	220	290	523	662	480	296	-	
Mean L/s/km^2	9.1	7.6	7.1	7.7	9.6	10.0	13.1	23.7	30.0	21.7	13.4	-	
Loffa River at Foma (Feb. 2008-Oct. 2008). Watershed area: 187 km^2													
Monthly mean	-	656	473	424	827	1,077	1,784	3,835	6,833	4,836	-	-	
Mean L/s/km^2	-	3.5	2.5	2.3	4.4	5.8	9.5	20.5	36.5	25.9	-	-	
Mala River at Traorela (Jan. 2008-Nov. 2008). Watershed area: 15.0 km^2													
Monthly mean	89	90	92	92	103	113	146	345	378	289	178	-	-
Mean L/s/km^2	5.9	6.0	6.1	6.1	6.9	7.5	9.7	23.0	25.2	19.3	11.9	-	-
Miya River at Nionsomoridou (Aug. 2007-Aug. 2008). Watershed area: 46.3 km^2													
Monthly Mean	255	212	205	223	199	284	486	969	682	558	417	299	399
Mean L/s/km^2	5.5	4.6	4.4	4.8	4.3	6.1	10.5	20.9	14.7	12.1	9.0	6.5	8.6
Pulowaye River at Banko (Feb. 2008-Oct. 2008). Watershed area: 7.50 km^2													
Monthly mean	-	95	102	104	113	167	207	313	329	221	-	-	-

	Jan.	Feb.	Mar.	Apr.	May	June	July	Aug.	Sep.	Oct.	Nov.	Dec.	Ann.
Mean L/s/km^2	-	12.7	13.6	13.9	15.1	22.3	27.6	41.7	43.9	29.5	-	-	-
Wolou River at Banko (Aug. 2008-Oct. 2008). Watershed area: 14.3 km^2													
Monthly mean	-	-	-	-	-	-	-	537	665	403	-	-	-
Mean L/s/km^2	-	-	-	-	-	-	-	37.6	46.5	28.2	-	-	-
Woron River at Mandou (Feb. 2008-Aug. 2008). Watershed area: 51.7 km^2													
Monthly Mean	-	641	619	596	618	636	826	1,082	-	-	-	-	-
Mean L/s/km^2	-	12.4	12.0	11.5	12.0	12.3	16.0	20.9	-	-	-	-	-

Source: Water Management Consultants 2009b

Figure 9.7 Monthly mean base flow hydrographs



Source: Water Management Consultants 2009b

9.3.4 Water Balance

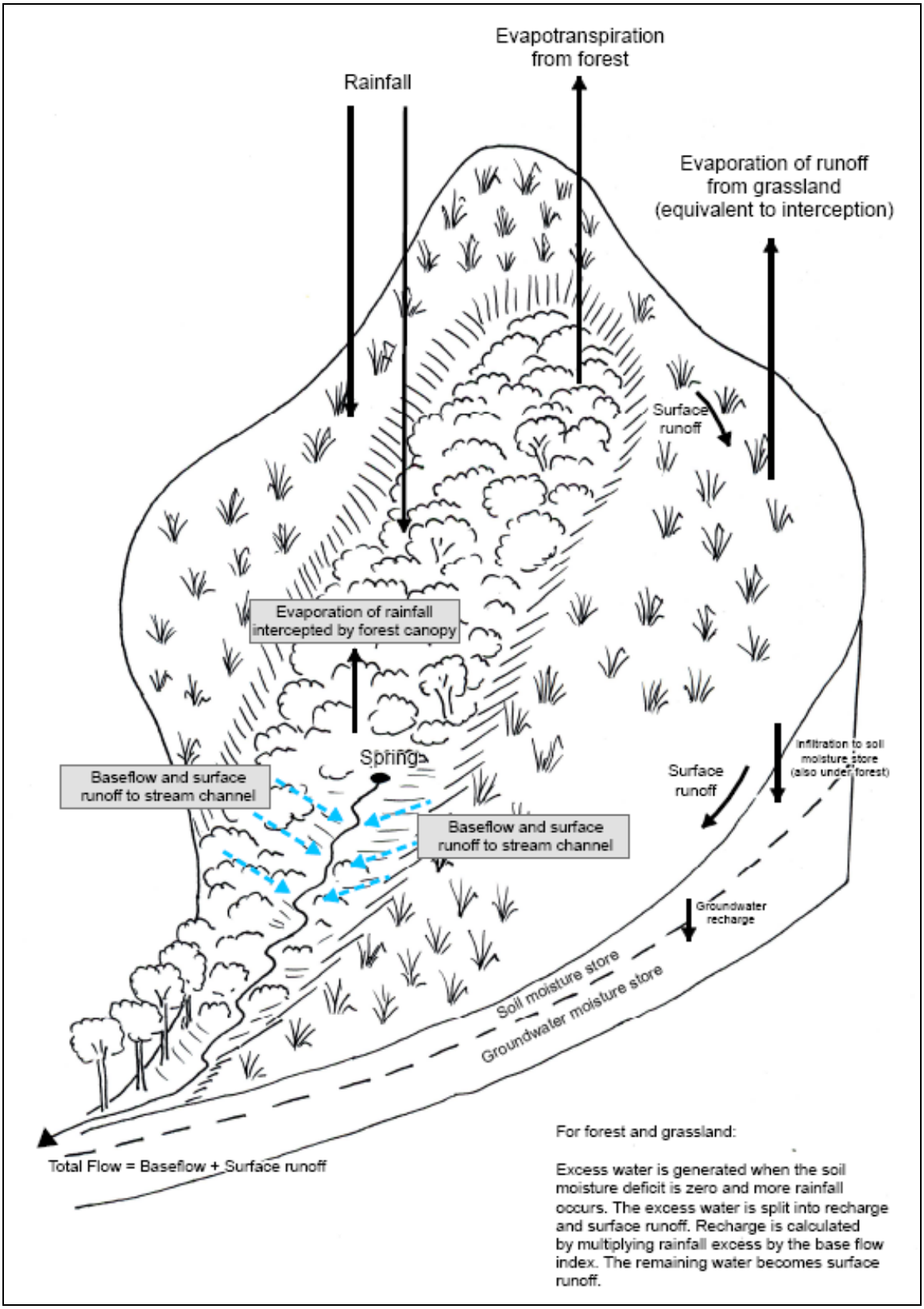
A simplified conceptual hydrological model, representative of Whisky 1 and 2 watersheds, was prepared by WMC (WMC 2009b). The key components of the model are illustrated in a schematic form in Figure 9.8. The conceptual model displays the physical hydrological system and the typical land cover in the watershed. Hydrological processes such as rainfall, evaporation and evapotranspiration, runoff and base flow, and groundwater recharge and storage that are involved in the watershed.

The components of the conceptual model were used to elaborate a water balance for Whisky 1 and Whisky 2 watersheds over the period of July 2003 to March 2008 using a simple soil moisture accounting model developed by WMC (WMC 2009b). The water balance is intended to assist in the evaluation of the relative importance of the various components of the hydrological and hydrogeological systems.

Input data in the water balance included rainfall, reference crop evapotranspiration (ET_o) and flow measured at the weirs. Canga East daily rainfall data was used to extend the daily rainfall record at the automatic rain gauges back to July 2003. Daily ET_o was calculated using data from the Dabatini weather station for 2007, and repeated for other years. Daily instantaneous flow recorded from July 2003 to November 2005 were assumed to represent daily mean flows and were added to the record of daily mean flows from November 2005 to March 2008. The model was fitted to the observed flow record by modifying model parameters until an acceptable visual match between the observed flow record and the predicted flows was obtained. Table 9.6 presents the annual summary water balance estimated for the two watersheds.

The results presented in Table 9.6 suggest that annual storm runoff for both watersheds are in the order of 8 to 9% of rainfall. Approximately 22% of rainfall recharges the groundwater system in Whisky 1, as opposed to only 13% in Whisky 2. Interception losses in Whisky 2 watershed are about 61% of rainfall, but only 49% in Whisky 1. These numbers agree with previous results presented in Section 9.3.3.1. They are assumed to result from the greater proportion of grassland and underlying laterite in the Whisky 2 watershed that limits infiltration, and also suggest variability in water balance components between the various mountain watersheds.

Figure 9.8 Conceptual hydrological model of Whisky 1 and 2 watersheds



Source: Water Management Consultants 2009b

Table 9.6 Annual summary water balance for Whisky 1 and 2 (2004-2008)

Year	Rainfall	ET_o (1)	Eta (2)	Interception (3)	Soil moisture change	Storm runoff	Recharge	Storm flow	Base flow	Total flow
	(mm)							(m^3/s)		
Whisky 1										
2004	2,250	1,033	503	1,083	11	190	462	0.003	0.013	0.016
2005	2,116	1,032	501	1,014	-10	169	442	0.003	0.012	0.014
2006	1,847	1,032	398	1,079	-3	75	298	0.001	0.010	0.011
2007	2,920	1,032	415	1,300	10	407	789	0.006	0.013	0.019
2008	2,325	1,061	403	1,182	-14	222	532	0.003	0.015	0.019
Average	2,292	1,038	444	1,132	-1	213	505	0.003	0.013	0.016
% of rainfall	100%	45%	19%	49%	0%	9%	22%	-	-	-
% of total flow		-	-	-	-	-	-	19%	81%	100%
Whisky 2										
2004	2,137	1,033	453	1,284	7	143	250	0.002	0.004	0.005
2005	2,022	1,032	460	1,225	-6	114	228	0.001	0.003	0.004
2006	1,805	1,032	330	1,294	-1	36	145	0.000	0.002	0.003
2007	2,921	1,032	396	1,607	5	393	520	0.004	0.005	0.009
2008	2,338	1,061	370	1,434	-9	208	336	0.002	0.005	0.007
Average	2,245	1,038	402	1,369	-1	179	296	0.002	0.004	0.006
% of rainfall	100%	46%	18%	61%	0%	8%	13%	-	-	-
% of total flow		-	-	-	-	-	-	33%	67%	100%

(1) ET_o = Penman-Monteith reference crop evapotranspiration (Allen et al. 1998) calculated using meteorological data from Dabatini automatic weather station for 2007.
(2) ET_a = estimated actual evapotranspiration.
(3) Canopy interception is interception by forest plus evaporation of part of the runoff from grassland.
Source: Water Management Consultants 2009b

9.3.5 Spatial Patterns of Flow

9.3.5.1 Spring Flow

Springs surveys at Pic de Fon and Ouéléba were carried out in the wet season (August-October) of 2006 and the dry season (January-February) of 2008. As they are taken at the stream's source the spring flow measurements are more representative of base flow rather than storm flow. Table 9.7 presents the total flow and the average flow per spring in the dry and wet seasons at Pic de Fon and Ouéléba. However, only the locations of the springs identified in the dry season survey are shown in Map 9.2, because this survey is considered more reliable[1] and is more representative of base flow (limited storm flow component).

[1] A total of 149 springs were identified in the wet season survey, and 278 springs in the dry season survey. Approximately twice as many springs were found on both mountains in the dry season as in the wet season due to the use in the dry season of a more sensitive GPS able to determine more efficiently coordinates underneath the tree canopy. Consequently, more springs were identified in the dry season (WMC 2009b).

Table 9.7 Spring flow in Pic de Fon and Ouéléba

	Dry season (January-February 2008)						Wet season (August-October 2006)					
	Pic de Fon			Ouéléba			Pic de Fon			Ouéléba		
	East	West	All	East	West	All	East	West	All	East	West	All
Flow per spring (L/s)	0.16	0.77	0.40	0.13	0.25	0.21	0.51	0.26	0.42	0.52	0.56	0.54
Total flow (L/s)	16.5	54.3	70.6	4.4	16.5	20.9	26.0	6.57	33.0	10.9	16.3	27.2
Number of springs (1)	105	71	176	35	67	102	60	31	91	29	29	58

(1) The total number of springs = 278 for the dry season survey and 149 for the wet season survey.
Source: Water Management Consultants 2009b

If wet season spring flow data are multiplied by the ratio of wet season springs to dry season springs, the result suggests that there is little seasonal variation in spring flow in Pic de Fon. However, wet season discharge in Ouéléba is approximately twice the discharge in the dry season (WMC 2009b).

The most distinctive pattern in the data collected concerns spring density between the east and west sides of the range. During the dry season, there are between three to four times as much spring flow drained to the west as flow drained to the east on both Pic de Fon and Ouéléba areas. This pattern is not observed in the wet season dataset, primarily because of the underestimation of the number of springs.

Finally, under the assumption that dry season spring flow is representative of annual spring flow, Table 9.8 indicates that spring flow is approximately 5% of estimated mean annual rainfall in Pic de Fon and 3% in Ouéléba.

Table 9.8 Spring flow as a proportion of rainfall

	Area within springs (km^2)	Mean annual rainfall within spring area (mm)	Total flow from springs (L/s)	Spring flow as a % of mean annual rainfall
Pic de Fon	23.2	1941	70.6	5
Ouéléba	13.7	1597	20.9	3

Source: Water Management Consultants 2009b

9.3.5.2 Stream Flow

Periodical flow measurements were performed along streams draining Pic de Fon and Ouéléba areas. The measurements were carried out during the wet season (May-July 2007) and the dry season (January-February of 2008 and 2009) in order to improve the understanding of stream flow spatial patterns. Map 9.2 illustrates the isocontours of flow measured for the 2008 survey.

505000 510000 515000 520000

955000 950000 945000 940000

N W E S

Traoréla
Siatoulou
Wataférédou II
Mamouroudou
Lamandou
Orono
Moribadou
Kotila (abandonné)
Foma

Western Spur Valley

Foko Valley

Zone d'étude locale / Local study area

Hydrologie / Hydrology

Source d'eau inventoriée en saison sèche	Spring locations (dry season survey)
Isocontour de débit (l/s)	Flow isocontour (l/s)
Isocontour projeté	Projected isocontour
Hydrographie	Hydrography

Repères géographiques / Geographical landmarks

Route secondaire	Secondary road
Piste	Track
Forêt classée du Pic de Fon	Pic de Fon Classified Forest
Milieu bâti	Built area
Aire minière	Mining area

Sources:
1- Base map - 2006 0.5m ADS40 Aerial Photographs, 2006 Spot Imagery;
2- Landsat imagery mosaic 2002-2003;
3- Shuttle Radar Topography Mission (SRTM);
4- Carte topographique IGN 1:50 000/1:200 000;
5- Water magagement consultant report;
7- Geographic Coordinate System: WGS84, UTM, Zone 29N.

Titre / Title

Sources d'eau et isocontours dans la zone d'étude locale / Spring locations and stream flow isocontours in the local study area

Échelle / Scale		Projet / Project	Volume C Carte/Map 9.2
0 325 650 1,300 m	1:65,000	SIMANDOU	

Directeur de projet (client) Project manager (client)		Directeur de projet Project manager		No. pr./ P. number
Leon Payne		Richard Fontaine		604917
01	2010/06/15	Final	M. Dupré	M. Stapinsky
00	2010/01/04	Preliminary	M. Dupré	M. Stapinsky
No.	aaaa/mm/jj yyyy/mm/dd	Description	Dessiné/Drawn	Vérifié/Verified

As expected, stream flow increases with the distance from the springs towards the first villages downstream. The rate of increase in stream flow appears to be relatively uniform to the east and west of the Ouéléba deposit. Conversely, there are significant differences in increases between the east and west sides of the Pic de Fon deposit. For instance, flow rates increase uniformly on the east side, but there are specific areas along the west side where flows increase very rapidly (narrower space between lines of equal flow). This suggests a substantial groundwater discharge from base flow within these stream sections, notably the Western Spur Valley to the northwest and the Foko Valley to the southwest of the Pic de Fon deposit (Map 9.2).

Similar patterns were observed in Pic de Fon and Ouéléba in 2009, including the Kinyeko and Siatouro rivers located at the northern end of Ouéléba, and some streams draining from the southwestern end of Ouéléba (see Map 9.1 for locations). Groundwater discharge will be examined in greater details in the next chapter (Hydrogeology) with the results of flow accretion surveys.

CHAPTER 10

Hydrogeology

10. HYDROGEOLOGY

10.1 INTRODUCTION

The groundwater system of the Simandou Range plays a major role in the regional surface water system as groundwater discharging from the hillside supports perennial flows in streams originating from the mountain.

Mining activities, such as excavation, dewatering, tailings and mineral waste disposal, can potentially influence the dynamics of groundwater flow systems, causing changes to groundwater levels, chemistry, flow and discharge. One of the main potential sources of social and environmental issues for the Simandou Project are changes in stream flow due to fluctuations in groundwater discharge caused by project activities. Therefore, it has been essential for the baseline hydrogeology programme to identify water-bearing geological formations, examine the hydraulic properties of the rocks encountered in the local study area, determine groundwater flow patterns, identify the main groundwater recharge and discharge zones, and assess the importance of groundwater in supporting the natural surface water regimes in the surrounding areas.

The hydrogeology baseline data was collected specifically for the characterisation of the hydrogeological system in the study area.

10.2 METHODS

Groundwater resources and flow processes that could potentially be influenced by the Simandou Project have been assessed in the study area. The baseline hydrogeological assessment has however, focused on an area that is located primarily on the ridge and slopes of the Pic de Fon and Ouéléba deposits, where the majority of exploration drilling activities have been carried out.

Characterisation of the groundwater system was performed by Water Management Consultants (WMC), now Schlumberger Water Services (SWS), and involved data collection alongside the resource drilling program, drilling within lowland plain bedrock, spring and stream flow accretion surveys, and well surveys in surrounding villages.

Groundwater level data collection and measurement of *in-situ* hydraulic properties for the various lithologies was limited during the current study due to the weak formations and the propensity for existing borehole walls to collapse (WMC 2009c).

Standpipe piezometers have been installed within boreholes drilled as part of the resource drilling programmes, which are concentrated around the Pic de Fon and Ouéléba ore bodies. In areas where it has not been possible to install piezometers due to the weak formation, the groundwater level dataset has been supplemented with information gathered from other sources (see section 10.2.1).

Groundwater level data has been used in the development of a conceptual groundwater level surface, from which groundwater flow directions can be derived. Incorporating data collected in spring and stream flow surveys (to identify groundwater seepage and major groundwater discharge areas), has enabled a complete conceptual

model to be developed for the groundwater flow system. The groundwater level surface is presented in Map 10.1.

Although the groundwater level monitoring and hydraulic testing programme is still ongoing, the currently available results are presented and discussed hereafter.

10.2.1 Groundwater Elevation Data

Groundwater level data has been collected since 2007 when WMC were commissioned to carry out the baseline groundwater study.

The lack of piezometric data in some critical areas has required that other data sources be used for the purpose of the project. Additional information on groundwater levels and the occurrence of perched water tables was obtained from open mineral exploration boreholes, downhole geophysics (resistivity), sample moisture content recorded during drilling, and spring elevations. The identification of dry exploration boreholes has also provided information on the thickness of the unsaturated zone (WMC 2009c) and helped to verify the presence of perched groundwater levels.

These data sources have supplemented the data collected from piezometers specifically installed for the groundwater baseline study. The location of the piezometers, boreholes, resistivity survey (geophysical logging in boreholes) and springs is presented in Map 10.1. Characteristics and details of piezometer construction can be found in Appendix Q.

10.2.1.1 Standpipe Piezometers

Standpipe piezometers consist of 2.5” PVC installed inside exploration boreholes, within which groundwater levels can easily be measured. In all 20 piezometers have been installed in the Pic de Fon area, and 53 piezometers in the Ouéléba area. Additional piezometers were installed outside of the resource areas to monitor groundwater levels in canga and bedrock; 5 canga piezometers are located in the Canga East camp area; and 3 bedrock piezometers are positioned along the Moribadou - Ouéléba access road, which measure groundwater levels in basement rock. Further drilling is planned with dedicated drilling for piezometer installation in locations further away from the ridge crest, and around the planned mineral waste disposal areas.

Groundwater levels have been measured manually using an electric water-level meter. Automatic logging pressure transducers (Divers) have also been installed in selected piezometers, providing continuous water level data. An exploration hole collar (open hole) and completed PVC piezometer are shown in Photo 10.1.

Photo 10.1 Typical exploration hole collar (left) and completed piezometer (right)





Source: SNC-Lavalin Environment 2008

10.2.1.2 Vibrating Wire Piezometers

Vibrating Wire Piezometers (VWPs) have been installed primarily to measure pore pressures in the phyllite and itabirite geological units at positions behind the planned pit base/walls. When completely grouted within the borehole, VWPs allow the measurement of pore water pressures in the geological formation directly adjacent to the piezometer. Grouting several VWPs into the same borehole allows the measurements of groundwater levels at different depths, which also allows the estimation of vertical hydraulic gradients (WMC 2009c).

Eleven VWPs had been installed at the time of writing this report; and several standpipe piezometers are awaiting VWP installation. Installation of VWPs in the phyllite unit of the planned pit walls is a priority in future works (WMC 2009c).

Signals from VWPs are read using a digital readout unit and these values are converted into water levels using sensor-specific equations, calibrated individually for each sensor prior to installation.

10.2.2 Hydrogeological Properties

As discussed earlier, the preliminary hydrogeological data for the determination of the hydraulic properties of the various lithologies has been obtained from exploration drilling conducted by Rio Tinto. Competent rock samples recovered as core during drilling have been submitted to a laboratory to undergo tests in order to determine texture, porosity and permeability of the lithologies. Rock samples typically recovered during diamond bit coring, and similar to that submitted for testing, are shown in Photo 10.2

Photo 10.2 Rock samples collected during mineral exploration drilling



Source: SNC-Lavalin Environment 2008

The opportunity to collect *in-situ* data on the hydraulic properties of the various geological units was limited during the current study. Therefore, hydraulic data are limited to the results of laboratory testing and a number of basic field permeability tests, such as variable-head hydraulic testing.

Normally, it is possible to conduct *in-situ* hydraulic tests, such as packer tests in open boreholes. This has not been possible due to the weak formations and the propensity for boreholes to collapse.

Variable-head hydraulic tests were performed in some boreholes equipped as piezometers. For each piezometer tested, about 500 to 600 litres of water were injected inside the piezometer from a tank, and the water level response was recorded by a Diver. The interpretation of the results of this type of test provides estimates of the bulk permeability (known as hydraulic conductivity) of the lithologies intersected by the piezometer screen (WMC 2009c).

10.2.3 Groundwater Discharge

The study of groundwater discharge areas has provided a valuable insight into the identification of groundwater watershed areas, and has also assisted in the development of a conceptual groundwater flow model.

As discussed in the hydrology section, spring surveys were carried out along the hill slopes of the Pic de Fon and Ouéléba areas in order to complete the groundwater level dataset collected to characterise the flow regime components. The surveys have provided additional information on the elevation of the water table at the spring locations, and spring flow at the source of many streams. Data from these surveys have been used in the analysis and interpretation of groundwater level data and in the development of the hydrogeological conceptual model.

Variable-head hydraulic tests were performed in some boreholes equipped as piezometers. For each piezometer tested, about 500 to 600 litres of water were injected inside the piezometer from a tank, and the water level response was recorded by a Diver. The interpretation of the results of this type of test provides estimates of the bulk permeability (known as hydraulic conductivity) of the lithologies intersected by the piezometer screen (WMC 2009c).

Ouéléba zoom

Pic de Fon zoom

Camp de Canga Est / Canga East camp

Canga East camp

Ouéléba zoom

Pic de Fon zoom

Canga East camp

Lithologie / Lithology

Roche mère	Basement
Minéralisation de surface goethitique et gibbsite	Goethitique and gibbsite surface mineralisation
Canga	Canga
Hématite friable	Friable hematite
Hématite siliceuse	Siliceous hematite
Hématite dure	Hard hematite
Hématite goethitique	Geothitic hematite
Itabirite	Itabirite
Itabirite riche	Itabirite rich
Itabirite pauvre	Itabirite poor
Phyllite	Phyllite
Quartzite	Quartzite

Stations d'échantillonnage / Sampling stations

Forage	Borehole
Piézomètre	Piezometer
Piézomètre à fil vibrant	Vibrating wire piezometer
Relevé de résistivité	Resistivity survey
Source	Spring

Hydrogéologie / Hydrogeology

Courbe isopièze (m)	Isopiezometric contour (m)

Repères géographiques / Geographical landmarks

Route secondaire	Secondary road
Hydrographie	Hydrography
Forêt classée du Pic de Fon	Pic de Fon Classified Forest
Aire minière	Mining area

Sources:
1- Base map - 2006 0.5m ADS40 Aerial Photographs, 2006 Spot Imagery;
2- Landsat imagery mosaic 2002-2003;
3- Shuttle Radar Topography Mission (SRTM);
4- Carte topographique IGN 1:50 000/1:200 000;
5- Water magagement consultant report;
7- Geographic Coordinate System: WGS84, UTM, Zone 29N.

Titre / Title

Stations d'échantillonnage pour la caractérisation de l'eau souterraine et courbes piezométriques de la zone d'étude locale / Sampling stations for groundwater characterisations and piezometric contours in the local study area

Échelle / Scale		Projet / Project	Volume C Carte/Map 10.1
0 150 300 600 m	1:30,000	SIMANDOU	

Directeur de projet (client) Project manager (client)	Directeur de projet Project manager	No. pr./ P. number
Leon Payne	Richard Fontaine	604917

No.	aaaa/mm/jj yyyy/mm/dd	Description	Dessiné/Drawn	Vérifié/Verified
01	2010/06/15	Final	M. Dupré	M. Stapinsky
00	2009/12/16	Preliminary	M. Dupré	C. Roy

10.2.4 Groundwater Discharge

The study of groundwater discharge areas has provided a valuable insight into the identification of groundwater watershed areas, and has also assisted in the development of a conceptual groundwater flow model.

As discussed in the hydrology section, spring surveys were carried out along the hill slopes of the Pic de Fon and Ouéléba areas in order to complete the groundwater level dataset collected to characterise the flow regime components. The surveys have provided additional information on the elevation of the water table at the spring locations, and spring flow at the source of many streams. Data from these surveys have been used in the analysis and interpretation of groundwater level data and in the development of the hydrogeological conceptual model.

Finally, flow accretion surveys were performed during the wet and dry seasons along selected streams. This type of survey involves measuring stream flow at numerous locations along the stream in order to evaluate the increase in baseflow within the channel, and therefore identify major zones of groundwater discharge. The most recent of these flow accretion surveys was completed by WMC in January-February 2009. Stream flow measurements have been performed in most of the streams flowing down from the Pic de Fon and Ouéléba deposits.

10.3 RESULTS

10.3.1 Hydrostratigraphy

A conceptual representation of the hydrogeological systems of the Pic de Fon and Ouéléba areas was prepared by WMC following interpretation of the geology, groundwater levels and hydraulic properties, spring and stream flow accretion surveys and the conceptual hydrological model presented in section 9.3.4.

The geology is represented in the hydrogeology conceptual model in terms of hydrostratigraphic units, defined on the basis of hydraulic properties (permeability, storage, etc.).

A schematic geological cross-section, prepared by WMC (2008) and illustrating the main hydrostratigraphic units in the Pic de Fon deposit is shown in Figure 10.1, as an introduction to the hydrogeological characteristics discussed in this chapter.

10.3.1.1 Weathered Carapace

At the ground surface, the weathered carapace and the transitional zone, as described in the Geology chapter of this report (Chapter 7), form a blanket over the iron ore formations of the Simandou ridge. The carapace is an extended surficial feature composed of clay, goethite and limonite, which fill fractures and voids into the parent iron ore formation located beneath. The hydraulic properties of this layer are typically poor, which consequently limits rainfall infiltration from the surface and increases the potential for surface runoff (WMC 2009c).

Typically, the carapace extends 5 to 20 m below ground surface. However, it is more extensive in the Ouéléba deposit with thicknesses reaching up to 150 m, more specifically in the Ouéléba central zone. It is understood that these conditions are the primary reason for the widespread occurrence of perched water in the central zone around the Ouéléba wetland, and in parts of the southern zone.

10.3.1.2 Hematite

Located below the carapace and transitional zone, the hematite ore unit occurs in distinct forms, each of which is characterised by different hydraulic properties that affect the ability of the rock to transmit groundwater. Three forms of hematite can be identified based on their permeability:

- Friable hematite with high to very high porosity and inter-granular permeability.
- Biscuit-like hematite, similar to friable, with moderate to high porosity.
- Hard hematite, competent rock with moderate porosity and low inter-granular permeability.

Friable and biscuit-like hematite forms the bulk of the ore bodies. Groundwater flow within these units occurs mainly via inter-granular flow mechanisms (i.e. matrix flow). The occurrence of zones with lower permeability within the hard hematite will however lead to compartmentalisation of the groundwater flow system, and the presence of local scale perched-water tables. As with the itabirite, the predominant flow mechanism in hard competent hematite will be fracture flow.

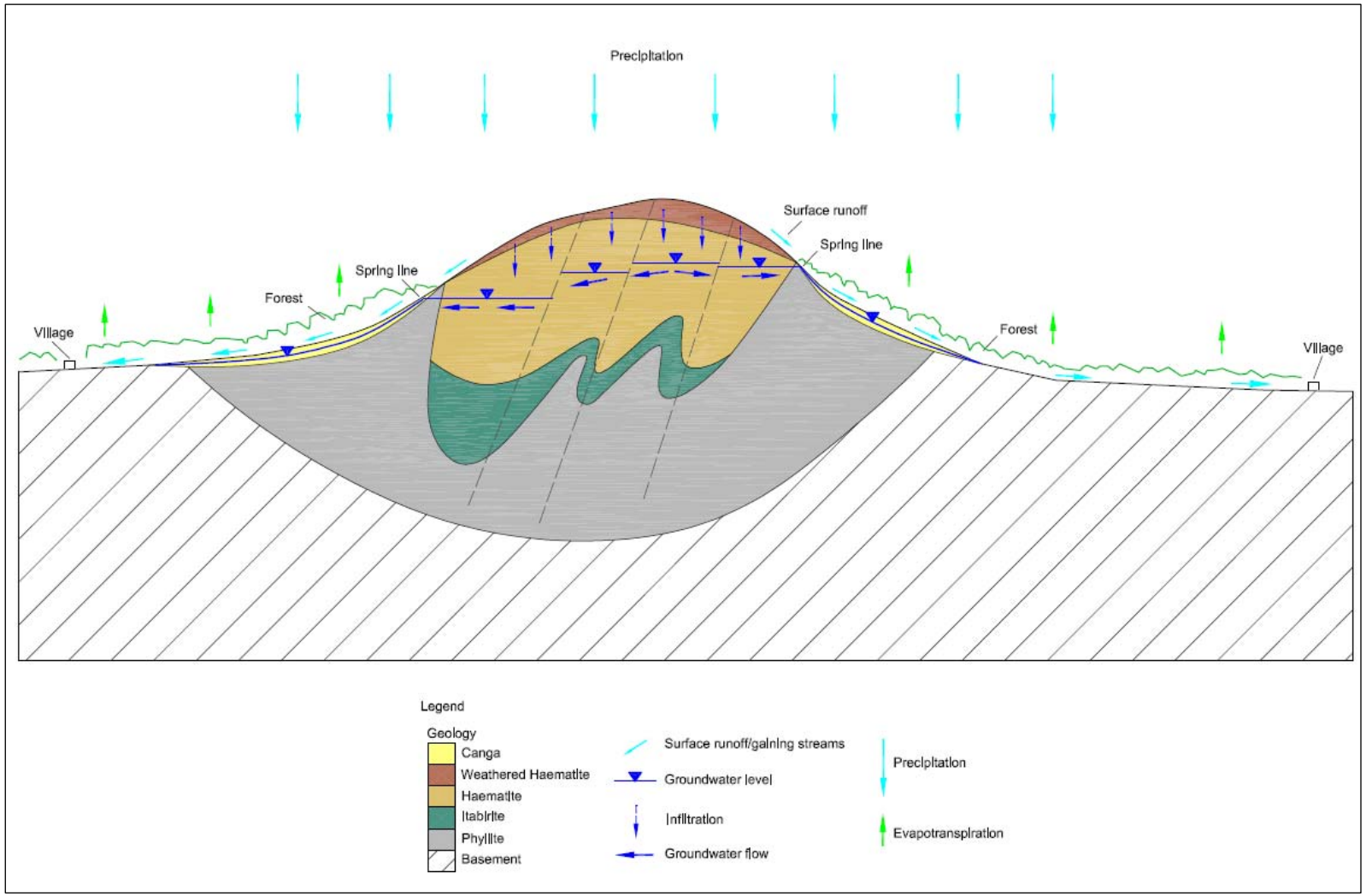
10.3.1.3 Itabirite

The contact between the underlying fresh itabirite and the hematite is typically gradational. In some areas, the itabirite is extremely friable and shows similar hydraulic properties to the friable hematite. The hydraulic properties of the friable itabirite contrast with those of the fresher compact itabirite, where permeability is either extremely low or controlled by fracture flow. Fracture density is generally very low where the itabirite is fresh and unweathered, such as on the western flanks of the Ouéléba deposit.

Weathered itabirite will however provide numerous fracture flow paths, whilst in some areas also forming a barrier to vertical drainage (WMC 2009c). The groundwater levels in the central zone of the Pic de Fon ore body are often measured at depths coinciding with the bottom of the hematite, overlying and perhaps supported by low permeability itabirite.

As the permeability of the itabirite is primarily related to the fracture network, deformation of the rock may have the effect of closing these flow paths. The structural control dividing high-groundwater levels beneath Pic de Fon from much lower-groundwater levels beneath the Western Spur Valley, located to the northwest of Pic de Fon, is within the itabirite, and could be associated with a low permeability barrier resulting from intense deformation in this area.

Figure 10.1 Schematic cross-section of the hydrogeological setting in the Pic de Fon deposit



Source: Water Management Consultants 2008

10.3.1.4 Phyllite

As described in the geology chapter, phyllite lithological units are encountered beneath the itabirite. In its weathered form, the phyllite exhibits a very wide range of characteristics. Geotechnical characterisation of the phyllite has been considered as a priority over mineralogical characterisation at the logging stage, specifically because the geotechnical properties of the phyllite will control to a large extent, the final design of the pit slopes. This objective led to the identification of four phyllite characteristic types that primarily describe variations in hardness that will also influence hydraulic properties: compact phyllite, weak phyllite, very weak phyllite and soil strength phyllite.

Fresh compact phyllite is predominantly found in the Pic de Fon area and is characterised by hard competent rock with low to very low porosity and permeability. The unit is generally massive, with some geological structure. Fresh phyllite will form an effective aquiclude to groundwater flow, i.e. a hydrostratigraphic unit characterised by low storage and very low permeability.

As phyllite is increasingly weathered, geochemical analyses conducted by Rio Tinto have shown an increase in the degree of alteration of mica minerals (that make up the fresh phyllite rock) to kaolinite. This process roughly leads to the softening of phyllite towards the soil strength phyllite material type. Observations suggest that the phyllite may allow some groundwater flow where it is weathered beyond compact phyllite.

10.3.1.5 Basement

The phyllite in the Pic de Fon and Ouéléba ore bodies is confined at depth by crystalline basement rocks. These rocks are typically unfractured with negligible matrix porosity. Therefore, they are generally considered as impermeable rocks.

Groundwater flow systems in basement rocks are typically localised, with the greatest groundwater storage and permeability within a shallow weathered regolith. Higher permeability areas are controlled by large geological structures, and deeper fracture zones are associated with a deeper weathering profile. These structures rarely contribute to regional groundwater flow systems.

Local village wells typically tap groundwater stored in the basement regolith for low yield supplies. These wells are completely isolated from the groundwater system contained within the resource areas on the ridgeline.

10.3.2 Hydraulic Properties

The various hydrostratigraphic units and their related lithologies have been investigated in order to evaluate their hydraulic properties. A series of laboratory tests were carried out on representative rock samples, and several *in-situ* hydraulic tests have also been performed in piezometers installed in distinct hydrostratigraphic units. The results are presented and discussed hereafter.

10.3.2.1 Particle Size Distributions

Laboratory test work has included particle size distribution analysis on soil and rock samples. The rock samples were dried and disaggregated before sieving. These tests are intended for rock classification and the description of the texture of the rock.

Table 10.1 summarises the results of the particle size distribution analyses carried out on rock samples from the Pic de Fon and Ouéléba deposits.

Table 10.1 Summary results of particle size distribution analyses

Lithology	% Gravel (2-60 mm)	% Sand (0.0625-2 mm)	% Silt (0.004-0.0625 mm)	% Clay (<0.004 mm)
Pic de Fon				
Transitional zone	66	21	12	1
Mineralisation:				
- *Friable hematite*	30-71 [44.6]	20-49 [38.5]	9-21 [15.8]	0-3 [1.0]
Itabirite:				
- *Friable*	25-67 [46.0]	19-36 [27.5]	13-40 [26.5]	1-2 [1.5]
- *Friable (other content)*	38-69 [53.5]	8-45 [26.5]	13-17 [15.0]	0 [0]
Phyllite:				
- *Soil strength*	10-78 [39.3]	25-42 [32.1]	7-47 [22.4]	3-13 [6.9]
- *Moderate to strong rock strength*	53-78 [42.3]	10-30 [17.0]	4-35 [11.5]	2 [2.0]
Ouéléba				
Mineralisation:				
- *Friable hematite*	4-73 [35.5]	10-61 [37.3]	12-70 [25.9]	0-5 [1.4]
Itabirite:				
- *Friable*	8-17 [12.5]	48-53 [50.5]	34-38 [36.0]	1 [1.0]
Phyllite:				
- *Soil strength*	0-66 [10.6]	4-68 [24.4]	9-86 [54.0]	1-28 [11.1]
- *Very weak rock strength*	0	9	83	8

Note: The range of sample percentages falling within each grain size group and average percentage [shown in brackets] are presented in the table.
Source: Water Management Consultants 2009c

The proportions of same size particles in all hematite, itabirite and phyllite material types are broadly similar, and typically dominated by gravel and sand size particles. Clay size particle content in all the material types is very low and is typically less than 2%. This is especially obvious in the Pic de Fon ore body samples, but the content in sand and silt sized particles in the Ouéléba ore body samples is higher.

The clay size particles content in all the phyllite material types is very low, as expressed by the very weak rock strength and moderate to strong rock strength samples. However, there is a greater component of clay size material in the soil

strength phyllite. The unique sample of weak phyllite shows silt as the majority grain size (83%). It is clear that the grain size characteristics are very variable in all phyllite material types. The typical coarser texture and the low clay content estimated in the samples suggest that some primary permeability may be present.

10.3.2.2 Porosity and Permeability

Rio Tinto and WMC have conducted laboratory tests on a large number of samples in order to determine bulk dry density and porosity of the ore and waste rocks. These parameters are an indication of the volume of voids within the rock matrix. The tests were performed using the core lock method (ASTM D 6752-03). General relationships could then be inferred between lithology, weathering, and porosity, as presented in Table 10.2.

Table 10.2 Relationship between lithology and porosity

Lithology	Porosity
Phyllite, fresh basal Itabirite, compact	Very low to low (~0 to 10%)
Mineralisation: hard martite-hematite, dense and fine grained Mineralisation: hard, medium-hard Martite matrix with porosity Mineralisation: hard, medium-hard Martite matrix with goethite infill	Moderate (~10 to 20%)
Mineralisation: medium-hard martite-goethite Mineralisation: medium-hard martite matrix with porosity Itabirite, friable	High (~20 to 30%)
Mineralisation: soft martite Mineralisation: highly weathered ore Phyllite, highly weathered	Very high (~30 to 50%)

Source: Water Management Consultants 2009c

As expected, the weathering process tends to significantly increase the porosity of the rock. Highly-weathered rocks can display porosity in excess of 30%. As opposed to compact rocks which typically present little porosity, from very tight matrix to 10% porosity.

Core samples have been collected by WMC and sent for laboratory analysis at the University of Reading in the United Kingdom. The samples are the same as those used by Rio Tinto in their core lock density analysis. The laboratory results are summarised in Table 10.3. It is important to appreciate that the values shown in this table represent sample values, and consequently may not be representative of bulk porosity and hydraulic conductivity in each geological formation.

Table 10.3 Summary of laboratory analysis of competent core samples

Lithology	Number of samples	Porosity (%)	Hydraulic conductivity (m/sec)
Weathered surface	5	19.5 – 25.4	2.13×10^{-06} – 1.60×10^{-09}
Mineralisation:			
- *Siliceous hematite*	5	17.9 – 26.8	6.14×10^{-07} – 6.23×10^{-08}
- *Hard ore*	5	9.6 – 25.0	7.40×10^{-07} – 3.79×10^{-08}
- *Friable ore*	4	32.8 – 42.7	2.32×10^{-02} – 1.81×10^{-03}
- *Goethite hard*	5	19.9 – 33.0	2.67×10^{-07} – 3.75×10^{-10}
Itabirite	5	1.6 – 11.9	1.15×10^{-07} – 9.66×10^{-10}
Phyllite	5	0.6 – 18.3	1.35×10^{-10} – 7.53×10^{-11}

Source: Water Management Consultants 2009c

The data obtained from laboratory testing demonstrate that there is a significant variation in hydraulic conductivity values within the various rock lithologies (Table 10.3). Furthermore, the review of geological logs from drill holes in the Pic de Fon and Ouéléba ore bodies shows that there is also a very high degree of variation in lithology with depth; i.e. that friable hematite being intercalated with hard and competent hematites, itabirites and phyllites and also with more weathered members of each lithology. These observations suggest that bulk-rock hydraulic conductivity could be high, due to the occurrence of permeable layers, and may also explain the formation of perched-water tables over impermeable lithologies.

Variable-head testing has been used to obtain estimates of *in-situ* hydraulic conductivity. Hydraulic testing has been performed in several Ouéléba boreholes in order to document bulk-rock hydraulic conductivity. All boreholes tested have been primarily drilled only into mineralisation, but in a few of the tests, piezometers also intersect small portions of phyllite and itabirite. The *in-situ* hydraulic conductivity estimates should therefore be more representative of the mineralisation due to its higher hydraulic conductivity. The results have been analysed with the Hvorslev (1951) method of slug test interpretation and are displayed in Table 10.4.

Table 10.4 Results of variable-head tests undertaken in some piezometers in the Ouéléba ore body

Lithology (dominant)	Borehole ID	Hydraulic conductivity (m/s)
Mineralisation:		
Hematite/goethite	RC08OUL308	1.66×10^{-6}
Hematite/goethite	RC08OUL323	4.54×10^{-7}
Hematite/goethite	RC08OUL330	6.85×10^{-7}
Hematite/goethite	RC08OUL347	1.30×10^{-7}
Hematite/goethite	RC08OUL382	3.0×10^{-7}
Hematite/goethite	RC08OUL468	1.55×10^{-6}

Lithology (dominant)	Borehole ID	Hydraulic conductivity (m/s)
Hematite/goethite	RD08OUL394	$2.15x10^{-8}$
Hematite/goethite	RC07OUL066	$7.47x10^{-8}$
Hematite/goethite	RC07OUL139	$2.72x10^{-8}$
Hematite/goethite	DD08OUL463	$7.62x10^{-7}$
Itabirite:		
Hematite/goethite - itabirite	RC08OUL318	$3.37x10^{-7}$
Hematite/goethite - itabirite	DD08OUL462	$8.37x10^{-9}$
Phyllite		
Hematite/goethite - phyllite	DD06OUL025	$5.54x10^{-8}$
Hematite - phyllite	DD08OUL464	$7.14x10^{-10}$
Phyllite	RC08OUL316	$9.86x10^{-9}$
Phyllite	RC08OUL363	$2.7x10^{-7}$
Carapace - phyllite	RC08OUL415	$5.86x10^{-7}$

Note: Due to access restrictions at Pic de Fon at the time of testing, only piezometers in Ouéléba area have been tested.

Source: Water Management Consultants 2009c

The estimates of *in-situ* hydraulic conductivity are in the same range as the laboratory estimates of hydraulic conductivity for compact and siliceous core samples (Table 10.3). *In-situ* hydraulic conductivity estimates however display slightly higher values than hydraulic conductivity estimates derived from core sample analysis. This is assumed to result from the occurrence of friable mineralisation, which in the laboratory tests exhibited much higher hydraulic conductivity (10^{-2} to 10^{-3} m/s), and the presence of secondary permeability in the fracture network which is included in the *in-situ* permeability testing.

Although not apparent in the results, hydraulic conductivity can also be underestimated during *in-situ* testing due to a residual mud cake within the borehole and uncertainties over the actual borehole diameter for use in the calculation.

10.3.3 Groundwater Levels

10.3.3.1 Spatial Variations in Groundwater Levels

Groundwater elevation data from all available sources have been compiled, and are displayed with extrapolated isopiezometric contours in Map 10.1 for the Pic de Fon and Ouéléba areas.

Groundwater elevations in the northern part of the Pic de Fon deposit vary from over 1,400 m (metres above reference level) beneath Pic de Fon itself, and decrease to about 1,230 m beneath the Western Spur Valley (Map 10.1). In the central and southern zones of the Pic de Fon deposit, groundwater levels are lower, and typically in the range of 1,050 to 1,200 m.

Groundwater levels in the northern and central part of the Ouéléba deposit are mainly in the range of 950 to 1,050 m, increasing in elevation from the lowest levels encountered at the edge of northern Ouéléba. For the southern part of Ouéléba, groundwater levels have been measured at elevations of around 1,150 m, and decrease to below 1,000 m in the southwestern part of the deposit.

In summary, the groundwater level depths at the Pic de Fon deposit are generally encountered 75 to 175 m below ground level. At the Ouéléba deposit, groundwater levels are generally 100 to 150 m below ground level.

Beneath the flanks in the deposit areas, groundwater elevations decline rapidly with falling topography, and as the geological sequence passes outward from the iron ore formation to phyllite and ultimately to basement rocks. These conditions (break in slope and impermeable lithology) explain in part the occurrence of the numerous springs observed outside the deposits (Map 9.2). At the base of the hill slope, the depth of groundwater in the basement rocks may vary from greater than 30 m between streams, to less than 5 m close to the beds of the main streams (WMC 2009c). At this stage, the depth below surface of the groundwater table has been approximated for the flank phyllite and basement rock. As the drilling program moves outward from the ridge to drill in flank positions, groundwater level data for these formations can be collected.

Vertical hydraulic gradients have been investigated using the data collected in the VWPs. VWPs are used to measure pore pressures at discrete positions within the stratigraphy, consequently showing the degree of hydraulic continuity between adjacent formations. The primary objective of the VWP's is thus to identify the degree of hydraulic continuity between the ore bodies and the adjacent formations that will form the wall rocks during mining. The water levels displayed in several of the VWP strings are similar, which suggests reasonable hydraulic continuity between the formations monitored.

10.3.3.2 Temporal Variations in Groundwater Levels

Monitoring of groundwater levels in piezometers has been done manually on a regular basis using a water level contact meter. Several logging pressure transducers (Divers) were also installed over the course of the baseline study by WMC in order to provide a continuous dataset from which to analyse temporal fluctuations in groundwater levels. The complete monitoring dataset is described with hydrographs in WMC's report (2009c). A summary of the findings is presented in this section.

Long-Term Monitoring

The longest period of groundwater level data were collected in the Pic de Fon area. The time series data consists of a five year record of manually measured groundwater levels since 2003. Figure 10.2 presents hydrographs for piezometers PDF163 and PDF081 located within the itabirite series of Pic de Fon in comparison with rainfall data from the Canga East rain gauge.

Long-term groundwater level monitoring at PDF163 and PDF081 clearly demonstrates the seasonal fluctuations, as a result of the wet season recharge. However, the recharge peak is delayed, and occurs in late December-early January. A smaller magnitude recharge peak occurs in PDF163, probably resulting from the occurrence of a thick unsaturated zone at this location that could diminish the recharge effect.

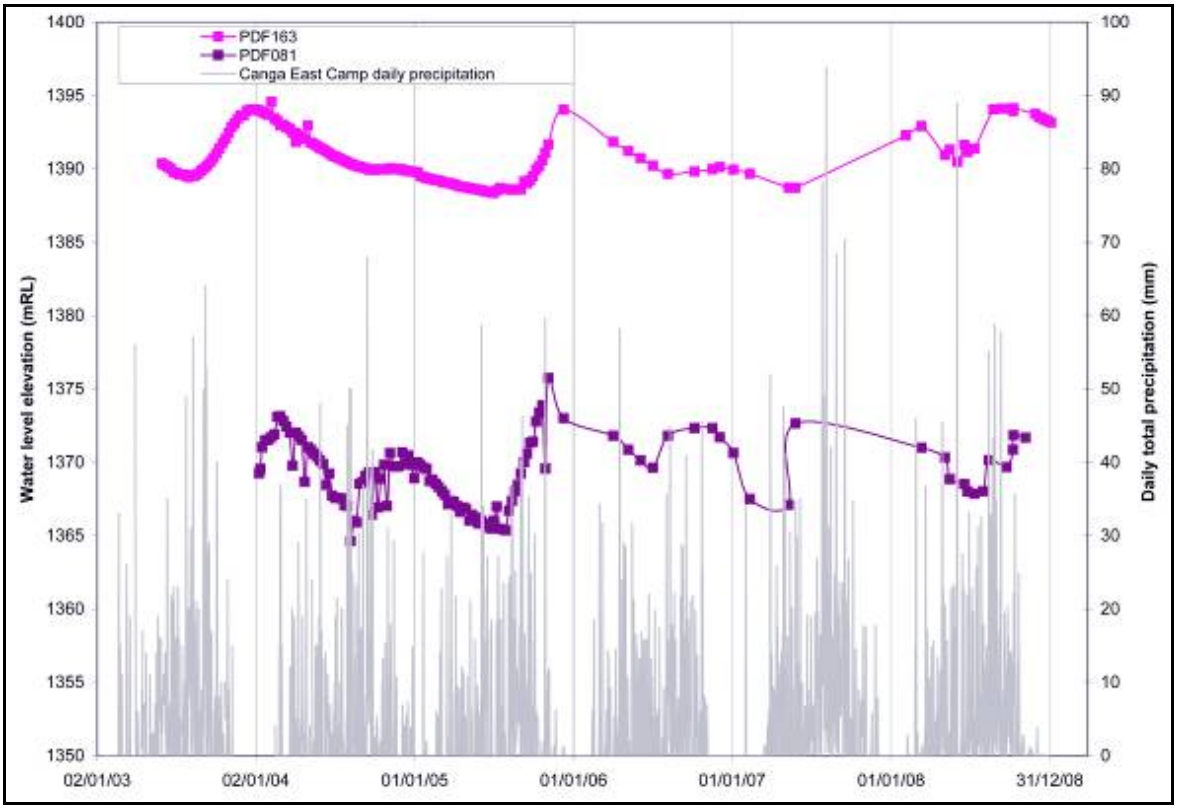
Short-Term Monitoring

The current continuous dataset available for many piezometers is unfortunately of short duration (1-2 months). Data has been mainly recorded over the dry season, and does not consequently display the recharge peaks observed in the long-term monitoring data described above. Some distinct groundwater level fluctuations have been observed according to the location of the piezometer.

Figure 10.3 and Figure 10.4 present short-term typical groundwater level fluctuations in piezometers located in the Pic de Fon and Ouéléba deposits.

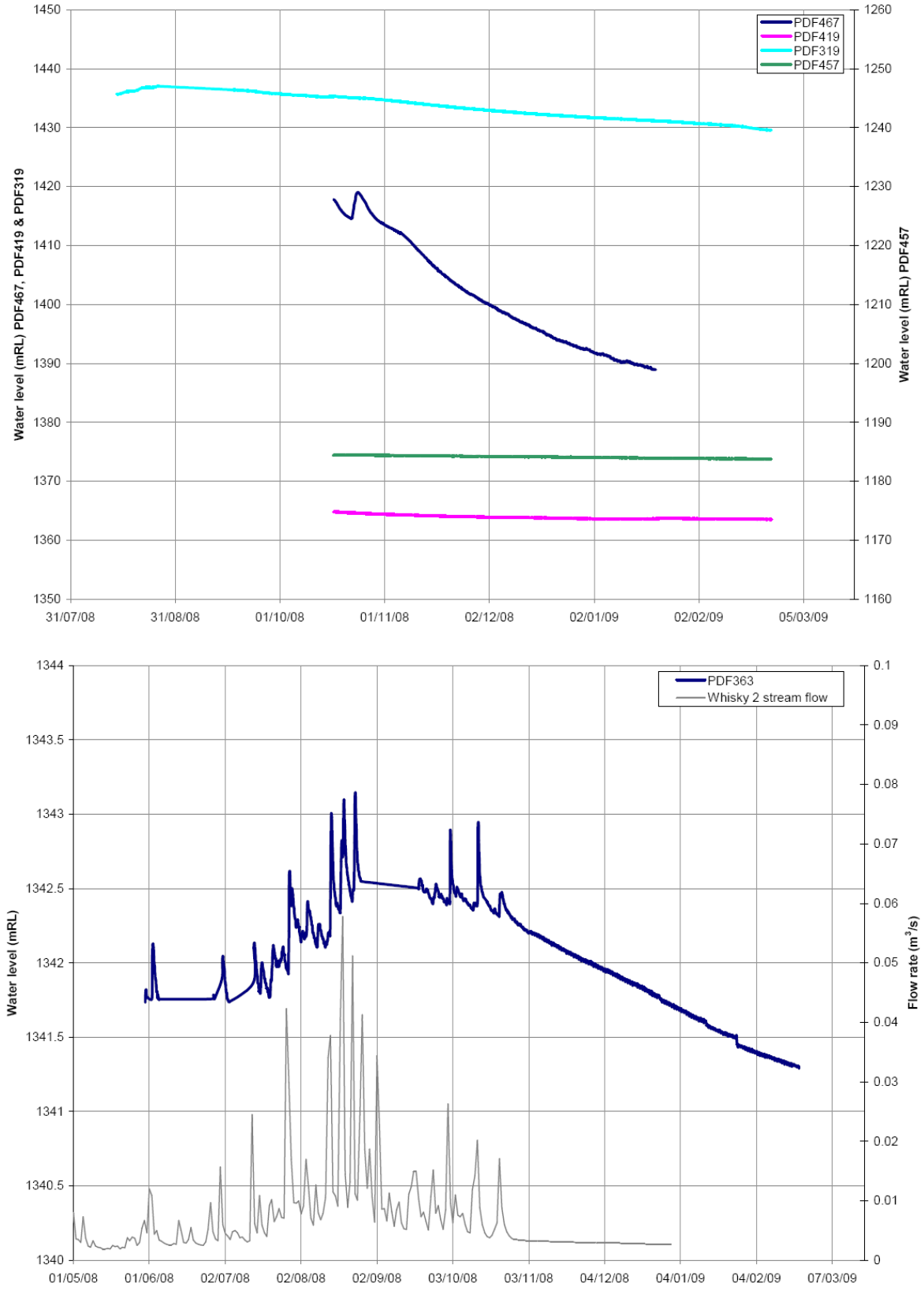
Divers installed in the Pic de Fon area piezometers (PDF319, PDF419, and PDF457) displayed slowly falling groundwater levels from July 2008 to May 2009. Groundwater variations are less than 5 m. However, piezometers monitoring perched groundwater, such as PDF467, exhibit rapid decreases in groundwater level by close to 30 m (between mid-October and mid-January), which agrees with the assumption that perched water tables in Pic de Fon are controlled by structure rather than low permeability geology. Storm flow fluctuations observed in the shallow groundwater systems in the PDF363 hydrograph, correlate well with flow rates measured in the nearby Whisky 2 weir. The Whisky 2 catchment is the discharge point for groundwater in the vicinity of PDF363. It is worth noting in this hydrograph, that the dry season decrease in groundwater storage (from groundwater discharge into Whisky 2) results in the relatively constant rate of dry season base flow in the stream.

Figure 10.2 Piezometer hydrographs in Pic de Fon compared with rainfall data



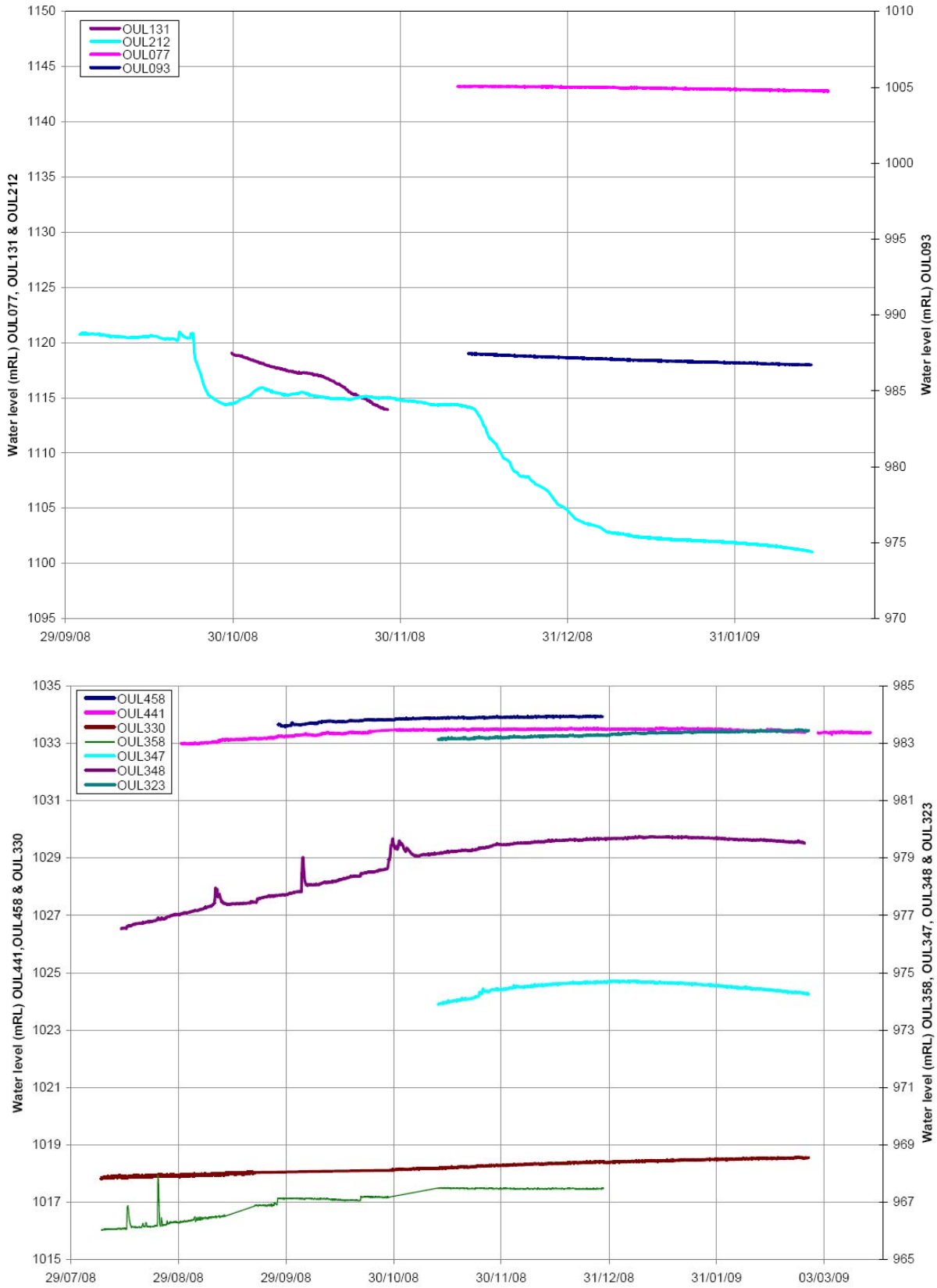
Source: Water Management Consultants 2009c

Figure 10.3 Short-term groundwater level fluctuations in piezometers located in the Pic de Fon deposit



Source: Water Management Consultants 2009c

Figure 10.4 Short-term groundwater level fluctuations in piezometers located in the Ouéléba deposit



Source: Water Management Consultants 2009c

Diver data recorded in piezometers located in northern Ouéléba deposit (OUL131, OUL212, OUL077, and OUL093) exhibited a similar decreasing trend as that observed in the Pic de Fon piezometer hydrographs for the same period of time. Other piezometers, such as OUL323, OUL330, OUL347, OUL348, OUL358, OUL441, and OUL458 show slow increases in groundwater levels over the same period, followed by a much later decrease in December. Diver data recorded in central and southern Ouéléba piezometers, included hydrographs from perched piezometers (OUL077 and OUL093), which displayed very slow dry season recession in the low permeability weathered carapace and transitional zone units.

The recharge peaks in the Ouéléba deposit is identified in early January in several piezometers indicating delayed recharge in comparison to the recharge peaks observed in August and September in several Pic de Fon piezometers.

10.3.4 Groundwater Flow Systems in the Local Study Area

10.3.4.1 Conceptual Model Framework

A conceptual groundwater flow model may be described as an idealised picture of a groundwater flow system. The conceptual groundwater flow model for Pic de Fon and Ouéléba was developed by WMC from interpretation of all available groundwater data, the hydrostratigraphy and geological structure, and the evidence for concentrated groundwater discharge areas identified in the various hydrological surveys. In a complex groundwater system such as this, the conceptual model unavoidably represents a simplification of the system. Such simplifications are however useful, in order that the key groundwater flow processes can be identified and categorised.

The conceptual model is used in the baseline to provide a summary of the current interpretation of the groundwater flow systems in the study area. The conceptual groundwater flow model will continue to be refined by WMC as additional data becomes available. It is, however, assumed that the data currently available is sufficient to allow an accurate representation of the groundwater flow systems. It is unlikely that this conceptual model will evolve significantly until pumping tests are carried out during the Feasibility Study in order to obtain large-scale estimates of hydraulic properties; evaluate hydraulic connection between groundwater and surface water; and assess the limits and geometry of the various water-bearing units.

10.3.4.2 Groundwater Recharge Mechanisms

As expressed earlier, hydrogeological properties in mountainous terrain can vary spatially according to the topography, rainfall patterns, soils, vegetation cover, underlying geology, etc. Significant local variations in recharge rates may therefore occur in the study area. Recharge at the regional scale is high within all watersheds in the Simandou Range, as a result of the typically high annual rainfall rates. The highest recharge has been estimated in the Pic de Fon area where it may exceed 600 mm/year, in comparison to the Ouéléba area where it has been estimated in the

range of 400 to 500 mm/year. Recharge rates further away from the range are substantially lower as a result of lower mean annual precipitation.

Most groundwater recharge occurs in the mid to late phases of the wet season, after the removal of the soil moisture deficit, which builds up throughout the dry season. On the hill slopes and on the basement plains, where unsaturated zones are thinner, rainfall infiltrates relatively rapidly to recharge the water table. Conversely, below the ridgeline, groundwater recharge is delayed significantly due to the very thick unsaturated zone (hundreds of metres in places) and the large number of perched water tables within that unsaturated zone. This is especially obvious in parts of the Ouéléba area where the groundwater level is deep, and recharge peaks are not observed in the groundwater level time series recorded in the deeper hydrostratigraphic units (WMC 2009c).

10.3.4.3 Groundwater Flow Mechanisms

Groundwater flow within the hydrostratigraphic units encountered in the study area occurs through a variety of flow mechanisms. Matrix flow or primary flow occurs where groundwater moves down-gradient within the primary porosity of the rock. Secondary flow is typically considered as the movement of groundwater within the fracture network of a hard and compact (non-porous) rock formation. Various combinations of both flow mechanisms are usually observed in complex geological environments such as this.

In addition to groundwater flow driven by hydraulic gradients, vertical drainage flows occur where groundwater overtops tight isoclinal fold structures at the hematite-itaberite boundary. The tight fold structures (i.e. between Pic de Fon and Western Spur) lead to the 'cascading' of groundwater between hydraulically isolated pockets of groundwater.

The characteristics of flow observed within the hydrostratigraphic units are summarised in Table 10.5.

Table 10.5 Groundwater flow mechanisms identified in the local study area

Hydrostratigraphic units	Flow mechanisms	Description
Weathered carapace and transition zone	Matrix (primary) and fracture (secondary)	Groundwater flow in perched groundwater systems. Lateral flow is highly localised, and most groundwater tends to infiltrate down into the underlying groundwater system through overtopping of the various perched water tables.
Highly porous and friable hematite (and in some cases itabirite)	Matrix (primary)	Observed in piezometers in the field as extensive flat water tables extending along the strike of the mountain, with water levels typically controlled by the elevation of discharge points.
Hematite and friable itabirite, underlain by low permeability phyllite and compact itabirite	Matrix(primary), underground "cascading" flow (secondary)	The occurrence of structures including high-permeability with low-permeability structures promotes underground "cascading" of groundwater flow above low-permeability units, from the shallower structures in the east to deeper structures on the west.

Hydrostratigraphic units	Flow mechanisms	Description
Compact itabirite	Fracture (secondary)	Secondary flow through the fracture network of compact itabirite.
Phyllite	Matrix (primary) and fracture (secondary)	Phyllite units vary from fresh rock to soil like, and can thus support both matrix and fracture groundwater flow.

Source: Water Management Consultants 2009c

10.3.4.4 Groundwater Discharge

Groundwater Discharge Mechanisms

Two primary flow mechanisms can be envisaged for discharge in the Pic de Fon and Ouéléba areas. Firstly, lateral discharge from springs (Map 9.2); and secondly, vertical drainage through the basal phyllite. The latter is likely to be negligible due to the large thickness of the unit, and its relatively low permeability (which is likely to significantly reduce under confining pressure at depth). Consequently, groundwater discharge from the mountain is primarily controlled by overspill of groundwater at the contact with underlying low-permeability compact itaberite or phyllite, or via permeable pathways presented by faulting or denser fracture networks in the geology surrounding the ore body.

Overspill type discharge areas are clearly observed in the Fokou West watershed in the Pic de Fon area, and are also likely to account for the major discharge areas in the north of the Ouéléba area. The Western Spur Valley is the only location where groundwater discharges through hematites and permeable itabirites in the absence of a low permeability underlying barrier to flow (phyllite series). As previously discussed, there are also numerous occurrences of springs and base flow discharging from shallow localised groundwater systems along the hill slopes of the Pic de Fon and Ouéléba deposits.

Quantifying Groundwater Discharge

Groundwater discharge has been examined from the results of a series of spring and flow accretion surveys. The spring surveys have been extremely useful in evaluating geological controls on groundwater flow and determining the elevation of groundwater on hill slopes in the Pic de Fon and Ouéléba areas (WMC 2009b). The results of the spring surveys have already been discussed in detail in section 9.3.5.

One of the major limitations of spring surveys is that the flow at the spring is rarely representative of the entire groundwater discharge within that area. Indeed, springs are often located in diffuse seepage zones and significant quantities of shallow subsurface flow may also occur in superficial deposits within these spring zones. Flow accretion surveys are considered as a more representative method of identifying groundwater discharge areas and quantifying discharge rates, as the majority of groundwater discharge does eventually find its way into the stream channels.

Flow measurement sites have been selected in each watershed assumed to represent the total groundwater discharge from the mountain. These measurement sites represent a boundary in each watershed, downstream of which the majority of flow accretion is due to groundwater discharge from lowland storage (such as the basement aquifer), rather than being due to groundwater discharge from the mountain. These boundary measurement sites have been selected through simple interpretation of topography (e.g. at the break in slope between the mountain and lowland plains), stream flow rates, and through interpretation of watershed normalised flow graphs (WMC 2009c).

The flow rates at each boundary measurement sites are summarised in Table 10.6. Appendix R presents stream flow data at boundary measurement points. Flow at each measurement site has been divided by its contributing watershed area in order to obtain normalised flow rate, which indicates the relative magnitude of base flow with respect to the size of the watershed. The mean flow rates from the Pic de Fon and Ouéléba deposits, and the central area between them (central ridge), have been used to evaluate projected groundwater watersheds. These groundwater watershed areas should only be considered as indicative rather than absolute, since they do not account for factors such as heterogeneity in groundwater recharge and geological formation hydraulic properties (WMC 2009c). The large differences estimated in the size of groundwater watershed areas suggest a system in which groundwater flow is concentrated towards a few key discharge areas.

Table 10.6 Summary of stream flows at boundary measurement sites

Local watershed	Boundary flow rate (l/s)	Surface water watershed area (km^2)	Watershed normalised flow rate ($l/s/km^2$)	Projected groundwater watershed area (km^2)	% of total discharge in area	% of total discharge from mountain
Ouéléba						
Kinyeko	56.1	1.05	**45.1**	**3.38**	14.3	3.9
Kinyeko trib 1	5.0	0.67	7.5	0.36	1.3	0.3
Kinyeko trib 2	23.0	1.86	12.4	1.64	5.9	1.6
Mala 1	26.5	3.49	7.6	1.89	6.8	1.8
Mala 2	15.7	1.64	9.6	1.12	4.0	1.1
Mala 3	21.5	2.85	7.5	1.52	5.5	1.5
Woron 1-N	44.6	3.99	13.1	3.73	11.4	3.1
Woron 1-S	35.5	1.82	19.5	2.53	9.1	2.5
Miya 1	74.8	1.38	**54.3**	**5.34**	19.1	5.2
Miya 2	22.5	2.34	9.6	1.60	5.7	1.6
Miya 2 trib	11.4	1.76	6.5	0.82	2.9	0.8
Miya 3	15.3	0.86	17.9	1.10	3.9	1.1
Miya 4	15.2	0.99	15.3	1.08	3.9	1.1
Whisky 6	24.9	3.25	7.7	1.78	6.4	1.7
Total	**392.0**	**27.95**	**-**	**27.89**	**-**	**-**
Central ridge (between Pic de Fon and Ouéléba)						
Woron 2-N	97.8	1.80	**54.4**	**4.78**	32.2	6.8

Local watershed	Boundary flow rate (l/s)	Surface water watershed area (km^2)	Watershed normalised flow rate ($l/s/km^2$)	Projected groundwater watershed area (km^2)	% of total discharge in area	% of total discharge from mountain
Woron 2-N trib	36.7	1.33	27.7	1.80	12.1	2.5
Woron 2	42.9	1.39	32.8	2.23	14.1	3.0
Loffa 1	17.5	2.11	8.3	0.86	5.8	1.2
Loffa 2	7.7	0.74	10.4	0.38	2.5	0.5
Loffa 3	58.9	2.74	21.5	2.88	19.4	4.1
Loffa 3 trib	16.2	1.54	10.5	0.79	5.3	1.1
Loffa 4	26.0	3.18	8.2	1.27	8.6	1.8
Total	**303.7**	**14.83**	**-**	**14.99**	**-**	**-**
Pic de Fon						
Western Spur	214.1	2.87	**74.5**	**10.70**	28.7	14.8
Pulowaye	64.2	2.80	23.0	3.22	8.6	4.5
Dianiworo 1	25.6	2.0	12.7	1.27	3.4	1.8
Dianiworo 2 (Wisky2)	53	7.78	6.8	2.65	7.1	3.7
Fokou West	146.3	1.24	**118.5**	**7.35**	19.6	10.1
Whisky 3	48.05	4.78	10.1	2.42	6.4	3.3
Whisky 1	45.5	3.13	14.6	2.29	6.1	3.2
Whisky 1-N	13.8	2.00	6.8	0.68	1.8	1.0
Whisky 1-N trib	11.0	1.24	8.9	0.55	1.5	0.8
Whisky 4-N	31.8	2.32	13.7	1.59	4.3	2.2
Whisky 4	30.5	2.22	13.7	1.52	4.1	2.1
Whisky 4 trib	19.2	1.26	15.2	0.96	2.6	1.3
Whisky 4-S	5.4	0.73	7.4	0.27	0.7	0.4
Boe	14.0	1.72	8.1	0.70	1.9	1.0
Foko East-N	8.3	0.53	17.4	0.46	1.1	0.6
Foko East	15.7	0.74	22.3	0.83	2.1	1.1
Total	**746.5**	**37.36**	**-**	**37.46**	**-**	**-**

Note: Character in bold indicate main groundwater discharge areas.
Source: Water Management Consultants 2009c

As seen in Table 10.6, total discharge from Ouéléba area, the central ridgeline and Pic de Fon area has been estimated as 392, 304 and 746 l/s, respectively, giving a total rate of groundwater discharge of 1,442 l/s for the entire study area. Main groundwater discharge areas are located in the Western Spur and Foko West streams draining the Pic de Fon area; in Woron stream draining the central ridgeline; and in the Miya and Kinyeko streams draining the northern tip of Ouéléba. Map 10.2 presents the results of the flow accretion surveys where the more important discharge areas can be easily identified from the size and the color of the symbol (see Map 9.1 for location of local watersheds).

When combined with observations from other data sources, such as the geological model and the groundwater level dataset, the projected groundwater watershed areas provide an effective means of delineating true groundwater watershed. They were used extensively to assist in the development of the conceptual groundwater flow model that will be described in the following section.

The data collected regionally in early 2009 were analysed by WMC (2009c) in order to assess the extent to which flows from the mountain range contributes to the regional hydrological network, as a provisional impact assessment for dry season stream flow impacts resulting from potential mining dewatering. Base flow contributions from the less permeable basement rocks is, as expected, considerably lower than base flow from the mountain range, as flow rates on several streams are seen to stabilise away from the mountain indicating that base flow is negligible in these areas.

The analysis of regional flow measurements suggest that the streams flowing away from the Simandou ridgeline provide a significant contribution to regional river flows (WMC 2009c). This contribution decreases moving downstream, as a greater part of flow is derived from off-hill watersheds. The relative magnitude of the contributions in downstream areas is, however, not clear. Some observations suggest that flow accreting in the on-hill streams is lost to varying degrees moving away from the range, due to stream bed seepage and subsequent evapotranspiration.

The assumption of total preservation of on-hill discharge in the regional river network is unrealistic. Normalised watershed flows are similar in measurements from regional *DNH* hydrometric stations and the downstream survey measurements in the Diani and Mala rivers, suggesting that the influence of the mountain on stream flow rates is low at these sites (WMC 2009c). A more dynamic system of continual flow accretion and flow loss may be occurring moving downstream, in which the influence of on-hill groundwater discharge gradually dissipates at greater distances from the Simandou Range.

10.3.4.5 Conceptual Groundwater Flow Model

The conceptual model of the groundwater flow system has been prepared for the Pic de Fon and Ouéléba areas (WMC 2009c) and is presented in Map 10.3. The dominant groundwater flow mechanisms (primary matrix flow; secondary fracture flow; cascading flow, etc.) in each area are indicated with different colour arrows. The size of the arrows is also indicative of the groundwater flow volumes.

The groundwater system is entirely local, which means that all water originates from rainfall, with the majority of groundwater leaving the study area as stream flow rather than groundwater flow. The local groundwater flow systems hence play a major role in the regional surface water system, maintaining perennial stream flows. The hematite is highly porous and has sufficient storage to contain the wet season rainfall-recharge events without resulting in very steep hydraulic gradients. In the dry season this storage is gradually released into streams as a relatively constant rate of baseflow. Some distinct characteristics of the groundwater flow systems in the Pic de Fon and Ouéléba areas are described hereafter.

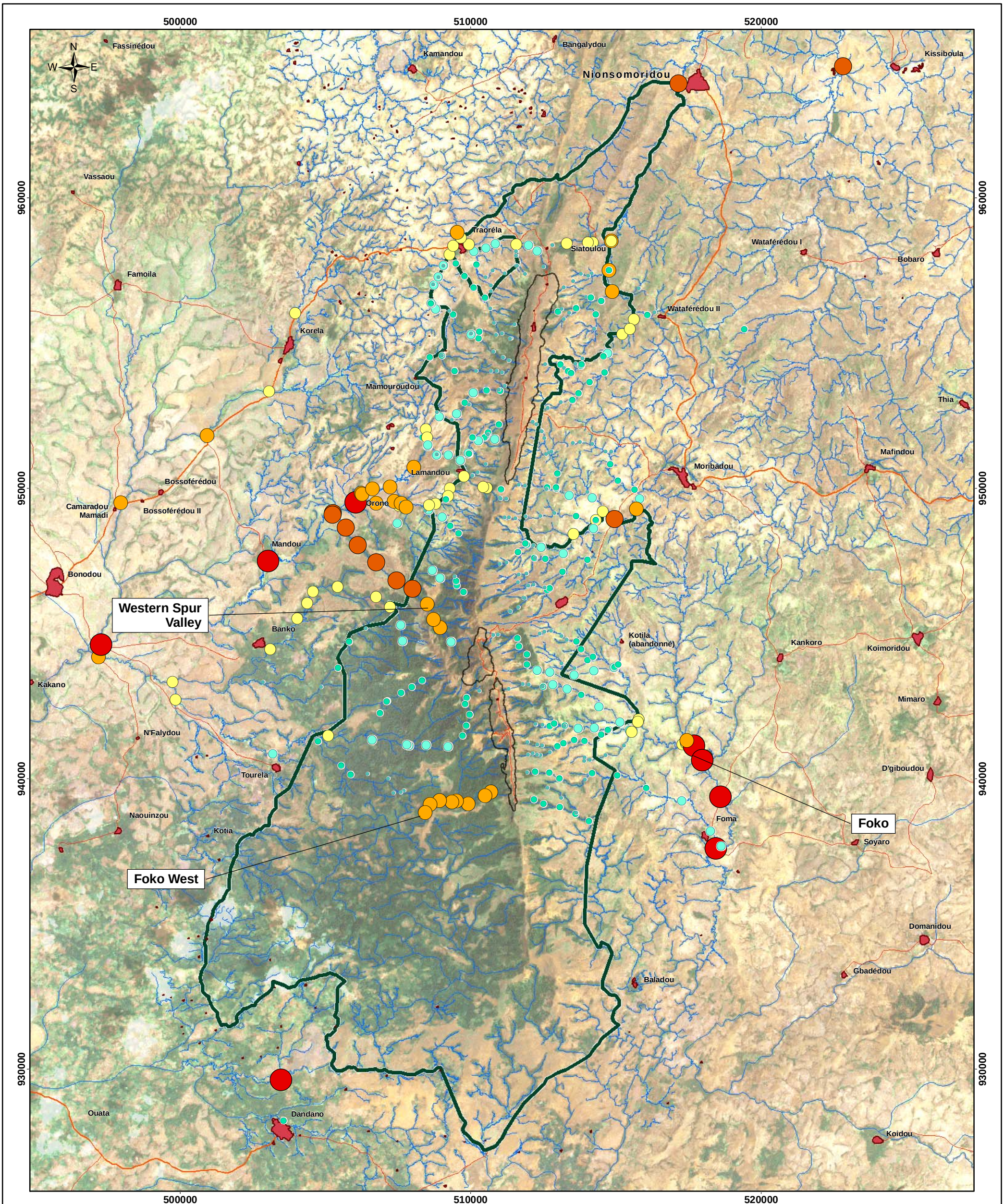
Two separate groundwater systems are present in the Pic de Fon area, the northern system dominated by groundwater flow from Pic de Fon towards Western Spur, and the central-southern system in which groundwater flows south within hematite and fractured itaberite towards Fokou West (Map 10.3). This can be clearly observed in the

results of the accretion surveys, which demonstrate the substantial volumes of groundwater discharged at these locations, as expressed by the proportional size of the symbols in Map 10.2. There are a series of smaller groundwater systems localised along the eastern hill slope, and also in the Whisky 2 and Whisky 3 watersheds to the west of the central and southern zones. These are fed from shallow localised groundwater bodies.

Groundwater levels and flow in the Pic de Fon area are controlled by the occurrence of the low permeability of phyllite, and the occurrence of large geological structures, more specifically the phyllite shear, which bisects the area and creates a boundary between the two groundwater systems. As a result, groundwater flow is mainly to the west via subsurface cascading over poorly permeable itabirites into deeper porous hematites in the Western Spur Valley area, where water levels are significantly lower. The Western Spur Valley is the final discharge area for most of the groundwater in the northern Pic de Fon groundwater system.

Groundwater flow in Ouéléba is limited to the east and west by the occurrence of low permeability phyllite. The primary groundwater discharge area in Ouéléba is located at the northern tip and flow towards this area is mainly directed into one of two north-south trending troughs of ore, which are separated by a phyllite shear (Map 10.3). The cross-cutting phyllite shear appears to isolate these two bodies of groundwater as the groundwater level data indicate a lower water table to the east of the shear. A structural control is present in the southern zone of Ouéléba which supports higher groundwater levels in this area, and separates it from the groundwater system to north. The majority of groundwater discharge in the southern area is towards the west into the Woron watersheds. All other watersheds along the eastern and western hill slopes drain localised groundwater systems with little or no discharge from the main Ouéléba groundwater system.

The central ridgeline is characterised by declining topography towards the north from the high elevation ground of Dabatini. From the Pic de Fon area, this sloping ridgeline is separated from Ouéleba by a low elevation saddle. This is the main groundwater discharge zone for the central ridgeline, with the majority of groundwater discharging west into the Woron stream. The projected groundwater watershed for groundwater discharging into the Woron stream area extends as far south as Dabatini. The current geological interpretation of this area is of a northern extension of a synformal trough of fractured, permeable itabirite. The saddle within the central ridgeline is caused by the presence of a major east-west trending fault structure. The itabirite here, is likely to have a high degree of fracture permeability (similar to that at Dabatini further south), and groundwater from Dabatini flows north along the ridgeline towards the saddle. The fault structure may act as a discharge pathway for groundwater flowing out of the itabirite trough. Groundwater flow into the remaining watershed areas in the central ridgeline is due to discharge from localised groundwater systems.



Débit / Flow (l/s)

0.00 - 10.00	
10.01 - 30.00	
30.01 - 60.00	
60.01 - 120.00	
120.01 - 250.00	
250.01 - 450.00	
450.01 - 668.00	

Repères géographiques / Geographical landmarks

Route secondaire	Secondary road
Piste	Track
Hydrographie	Hydrography
Forêt classée du Pic de Fon	Pic de Fon Classified Forest
Milieu bâti	Built area
Aire minière	Mining area

Sources:
1- Base map - 2006 0.5m ADS40 Aerial Photographs, 2006 Spot Imagery;
2- Landsat imagery mosaic 2002-2003;
3- Shuttle Radar Topography Mission (SRTM);
4- Carte topographique IGN 1:50 000/1:200 000;
5- IRD - Yves Boulvert (2004), Carte morphopédologique de Guinée, 1:200 000;
6- Station de mesure de la qualité du sol installé par SNC-Lavalin (SLEI) (L. Boisseau);
7- Geographic Coordinate System: WGS84, UTM, Zone 29N.

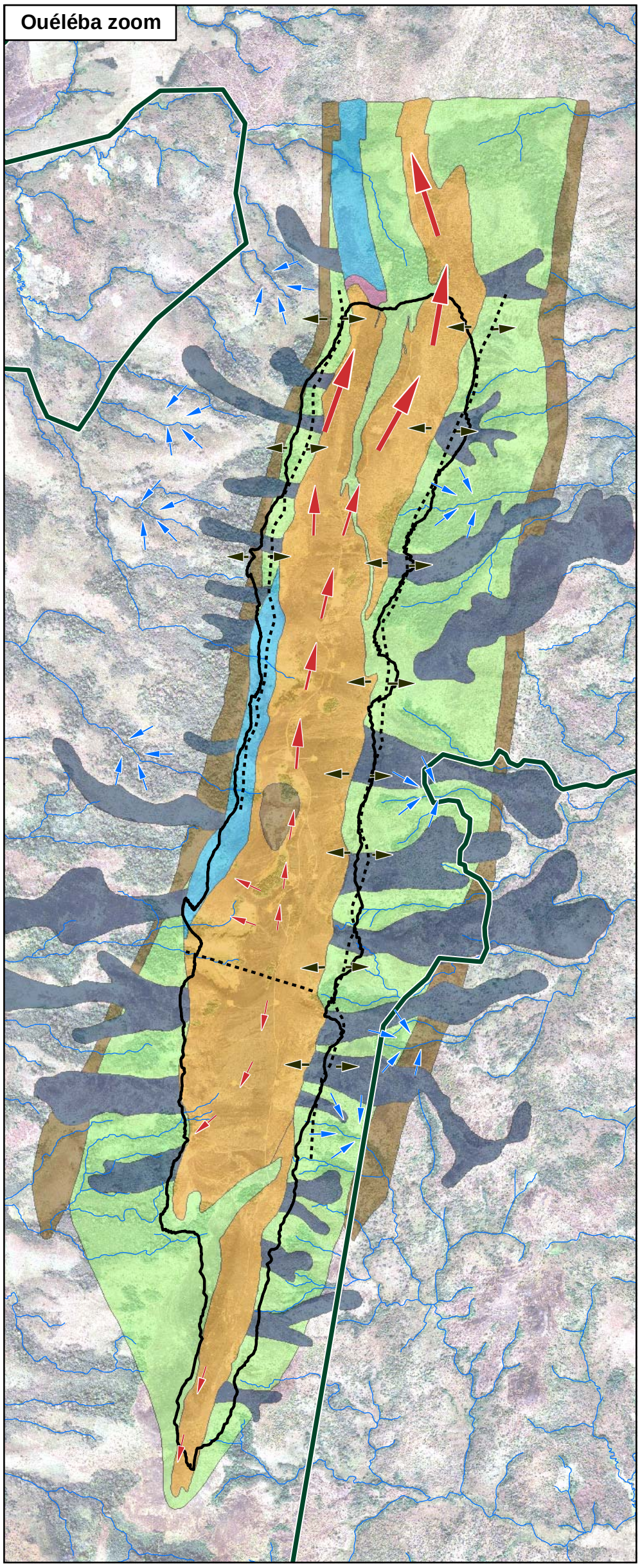
Titre / Title

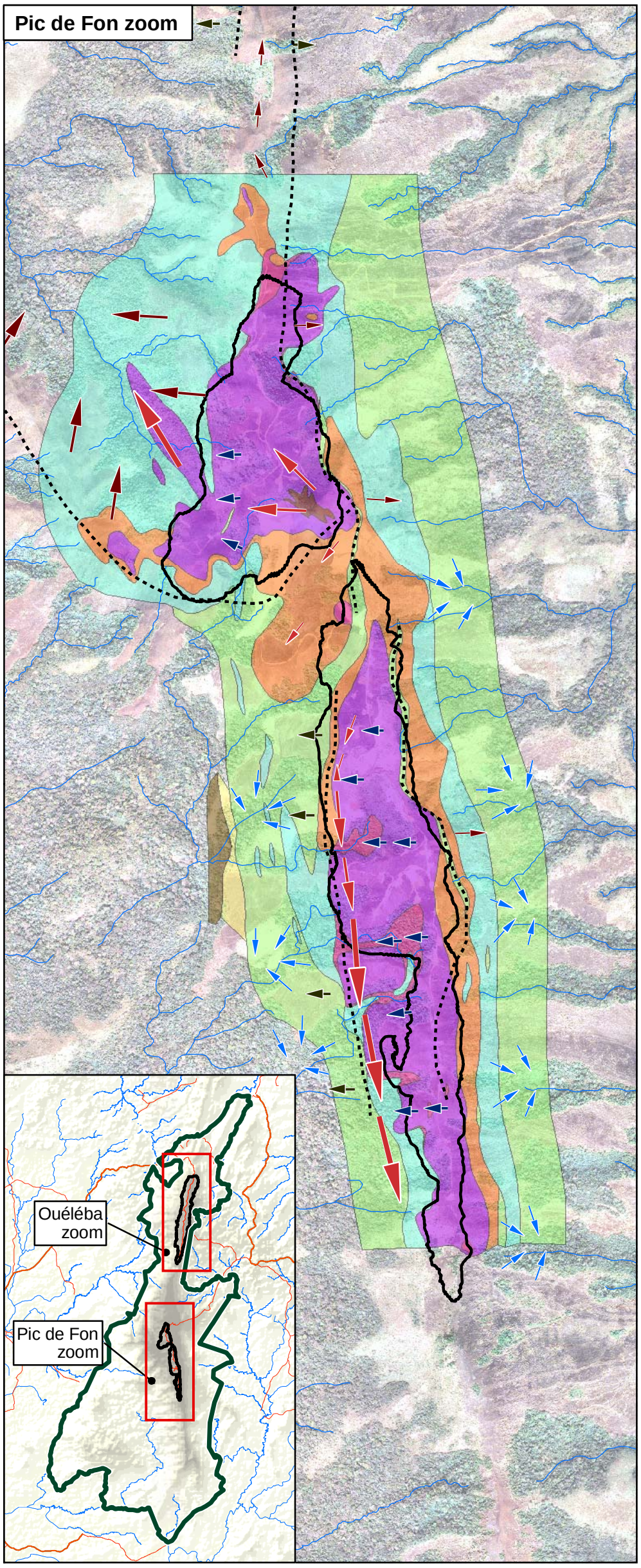
Accroissement des écoulements dans la zone d'étude locale / Flow accretion in the local study area

Échelle / Scale	Projet / Project	Volume C Carte/Map 10.2
0 0.625 1.25 2.5 Km — 1:125,000	SIMANDOU	

Directeur de projet (client) / Project manager (client)	Directeur de projet / Project manager	No. pr./ P. number
Leon Payne	Richard Fontaine	604917

No.	aaaa/mm/jj yyyy/mm/dd	Description	Dessiné/Drawn	Vérifié/Verified
01	2010/06/15	Final	M. Dupré	M. Stapinsky
00	2010/01/04	Preliminary	M. Dupré	M. Stapinsky





Lithologie / Lithology

Roche mère	Basement
Minéralisation de surface hematite goethitique et gibbsite	Goethitique hematite and gibbsite surface mineralisation
Canga	Canga
Hématite friable	Friable hematite
Hématite siliceuse	Siliceous hematite
Hématite dure	Hard hematite
Hématite goethitique	Geothitic hematite
Itabirite	Itabirite
Itabirite riche	Itabirite rich
Itabirite pauvre	Itabirite poor
Phyllite	Phyllite
Quartzite	Quartzite

Mécanismes d'écoulement / Flow mechanisms

Écoulement souterrain en cascade	Cascading subsurface flow
Écoulement dans la phyllite	Flow through phyllite
Écoulement localisé	Localised flow
Écoulement primaire (matix)	Primary flow (matix)
Écoulement secondaire (fracture)	Secondary flow (fracture)
Ligne de partage des eaux	Flow divide

Repères géographiques / Geographical landmarks

Route secondaire	Secondary road
Hydrographie	Hydrography
Forêt classée du Pic de Fon	Pic de Fon Classified forest
Aire minière	Mining area

Sources:
1- Base map - 2006 0.5m ADS40 Aerial Photographs, 2006 Spot Imagery;
2- Landsat imagery mosaic 2002-2003;
3- Shuttle Radar Topography Mission (SRTM);
4- Carte topographique IGN 1:50 000/1:200 000;
5- Water magagement consultant report;
7- Geographic Coordinate System: WGS84, UTM, Zone 29N.

Titre / Title

Modèle hydrogéologique conceptuel dans la zone d'étude locale / Hydrogeological conceptual model in the local study area

Échelle / Scale		Projet / Project	Volume C Carte/Map 10.3
0 150 300 600 m — 1:30,000		SIMANDOU	
Directeur de projet (client) / Project manager (client)	Leon Payne	Directeur de projet / Project manager	Richard Fontaine
			No. pr./ P. number 604917

No.	aaaa/mm/jj yyyy/mm/dd	Description	Dessiné/Drawn	Vérifié/Verified
01	2010/06/15	Final	M. Dupré	M. Stapinsky
00	2009/12/16	Preliminary	M. Dupré	C. Roy

CHAPTER 11

Water Quality

11. WATER QUALITY

11.1 INTRODUCTION

As previously mentioned in the Hydrology chapter (Chapter 9), the Simandou Range is known as the headwaters of major regional rivers, and lies partly in the transboundary Niger River watershed. Several villages in the LSA are located downstream of the proposed mining activities and related infrastructure, and depend on surface waters and groundwaters for various purposes, such as drinking, bathing, washing, irrigation, etc. Furthermore, groundwater discharge from the hill side supports perennial base flow in streams, where sensitive freshwater species and ecosystems are found (please refer to Volume D for information on these subjects).

As identified from the earliest stages of exploration programmes, changes to surface water and groundwater quality is a main concern with respect to the implementation of the Simandou Project. For these reasons, a water quality sampling programme was developed and implemented, as part of the hydrological and hydrogeological monitoring programme to characterise the baseline water quality. This baseline study is required in order to allow an appropriate assessment of the project's potential impacts on water quality.

This chapter examines the surface water quality of the numerous streams flowing down the Simandou ridge, but also groundwater quality in piezometers located in the vicinity of the proposed mining areas and in village wells.

11.2 METHODS

Fieldwork and data interpretation have been carried out by Water Management Consultants (WMC), now Schlumberger Water Services (SWS), with the assistance of local Rio Tinto personnel in the course of the baseline hydrological and hydrogeological studies (WMC 2009b, 2009c and 2009e).

Emphasis has been placed on surface water quality conditions in the vicinity of the Pic de Fon and Ouéléba mining areas and downstream at the points of use by local communities. Groundwater quality was also characterised within the mining areas as pre-mining baseline conditions. Although the monitoring programme is still ongoing, the results collected up to August 2008 are presented and discussed hereafter.

11.2.1 Surface Water Sampling Campaigns

Baseline surface water sampling was initiated in November 2006 with the objective of defining natural pre-mining surface water quality. Sampling campaigns have been performed by WMC (2009b), when possible on a quarterly basis. The current study includes the results of six sampling campaigns completed between November 2006 and August 2008. The results have been used to characterise the chemistry of surface water (springs and streams).

The surface water quality monitoring network consists in a total of 13 spring sampling stations located in the vicinity of the Pic the Fon and Ouéléba deposits, and 24 stream

sampling stations in the same areas and downstream (near villages). The monitoring network used for surface water sampling is illustrated on Map 11.1.

Twice daily records of flow, water colour and turbidity (using plastic turbidity tubes) were also initiated in early 2008 at 18 river gauging stations located near villages. The measurements were taken upstream and downstream of community water collection points. Lastly, continuous monitoring of turbidity, temperature, conductivity, dissolved oxygen and pH was conducted at a number of weirs (Whisky 1, 2, 4, 5 and 6) equipped with automatic systems. Detailed sampling of Total Suspended Solids (TSS) in natural stream waters was added to the programme in late 2008 (WMC 2009e). In addition, 140 spot samples of water have been collected from a number of streams during or shortly after storm events for turbidity and TSS analyses.

11.2.2 Groundwater Sampling Campaigns

Baseline groundwater quality sampling was also initiated in November 2006 in order to characterise natural pre-mining groundwater quality. Six sampling campaigns were completed by WMC (2009c) between November 2006 and July-August 2008), when possible on a quarterly basis. The groundwater quality sampling period has provided sufficient data for an initial characterisation of baseline groundwater quality.

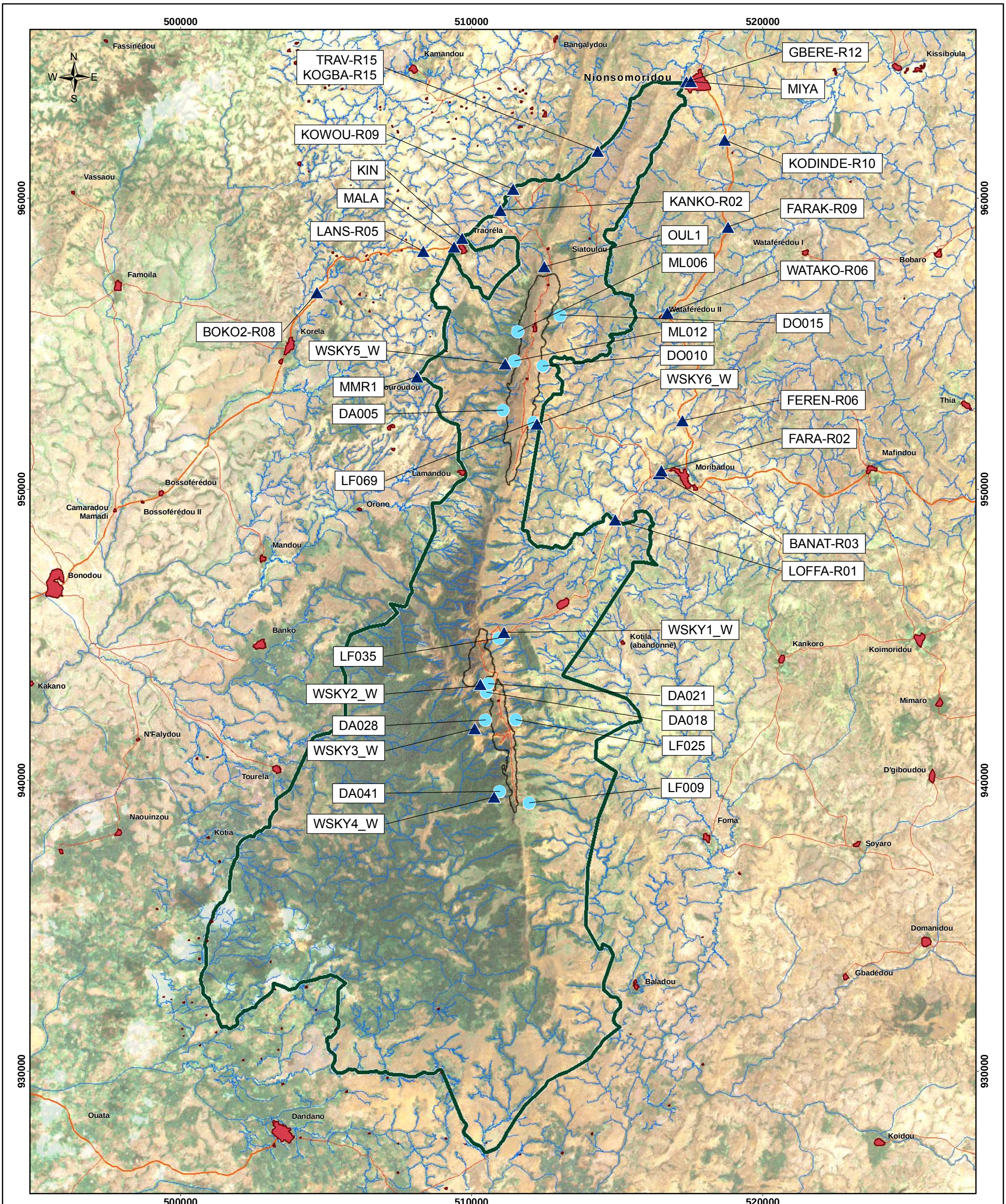
Groundwater was sampled from 25 piezometers located within the mining areas, including Pic de Fon (8 stations) and Ouéléba (8 stations); the basement rock along the Moribadou-Ouéléba access road (3 stations); and Canga East (6 stations). The groundwater quality monitoring network is illustrated on Map 11.2.

As part of the groundwater quality monitoring programme, water samples were also collected in some village wells and boreholes during a hydrocensus conducted by WMC (2009b). In all, 23 village wells and 10 boreholes were sampled, 16 of which are located in Moribadou. The location of the village wells and boreholes sampled is shown on Map 11.3.

11.2.3 Water Sampling and Analytical Methods

Water quality sampling of surface water was undertaken in conjunction with groundwater sampling. Details on the methodology/procedures followed for sampling, documentation, storage, field measurements and quality control are outlined in WMC's reports (2009b and 2009c). The methodology varied little for surface water and groundwater. All samples were filtered prior to analysis. Results are detailed in Appendix S.

Groundwater samples were collected with a plastic bailer lowered into the piezometer with a portable winch, as seen in Photo 11.1. Groundwater samples are assumed to be representative of the background concentrations despite the difficulty to find suitable piezometers for groundwater sampling in the area, due to borehole collapse, and the occurrence of a mud-cake into the boreholes which may have impaired the efficient purge of some of the piezometers (WMC 2009c). However, groundwater chemical content will be verified following the drilling and installation of additional piezometers specifically designed for groundwater sampling and water-level monitoring.



Stations d'échantillonnage / Sampling stations

Source	Spring
Eaux de surface	Stream

Repères géographiques / Geographical landmarks

Route secondaire	Secondary road
Piste	Track
Hydrographie	Hydrography
Forêt classée du Pic de Fon	Pic de Fon Classified Forest
Milieu bâti	Built area
Aire minière	Mining area

Sources:
1- Base map - 2006 0.5m ADS40 Aerial Photographs, 2006 Spot Imagery;
2- Landsat imagery mosaic 2002-2003;
3- Shuttle Radar Topography Mission (SRTM);
4- Carte topographique IGN 1:50 000/1:200 000;
5- Water magagement consultant report;
7- Geographic Coordinate System: WGS84, UTM, Zone 29N.

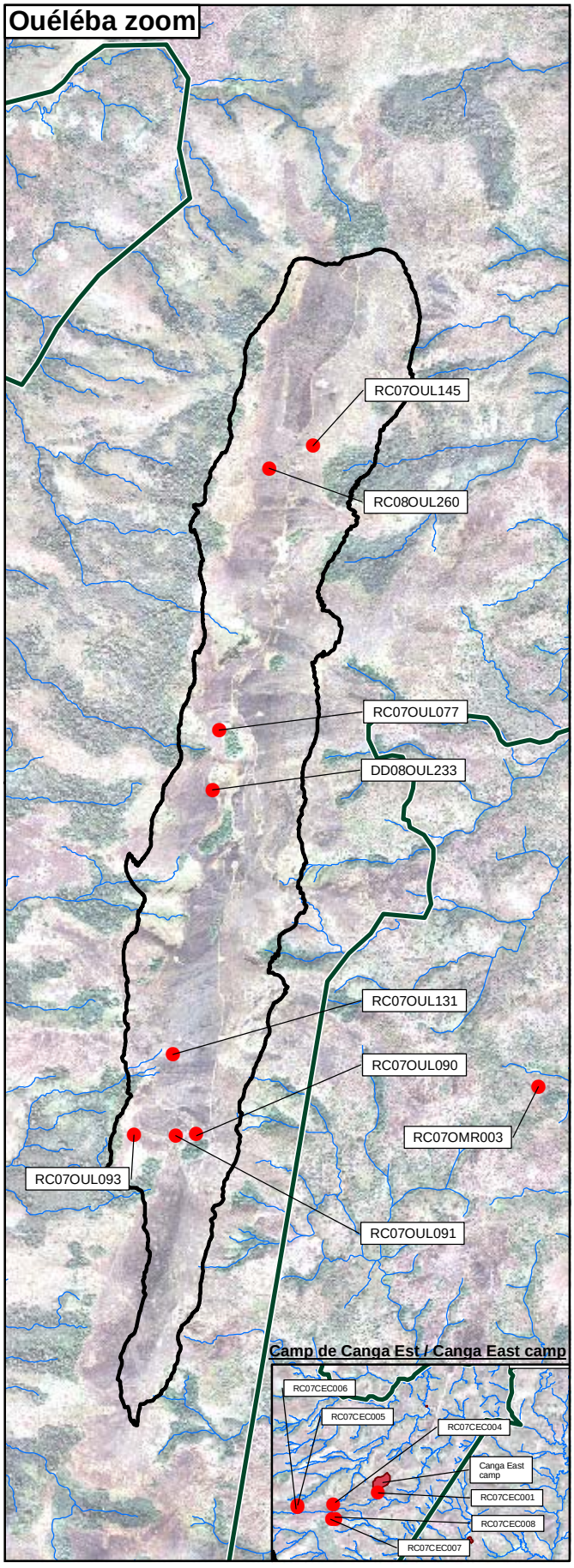
Titre / Title

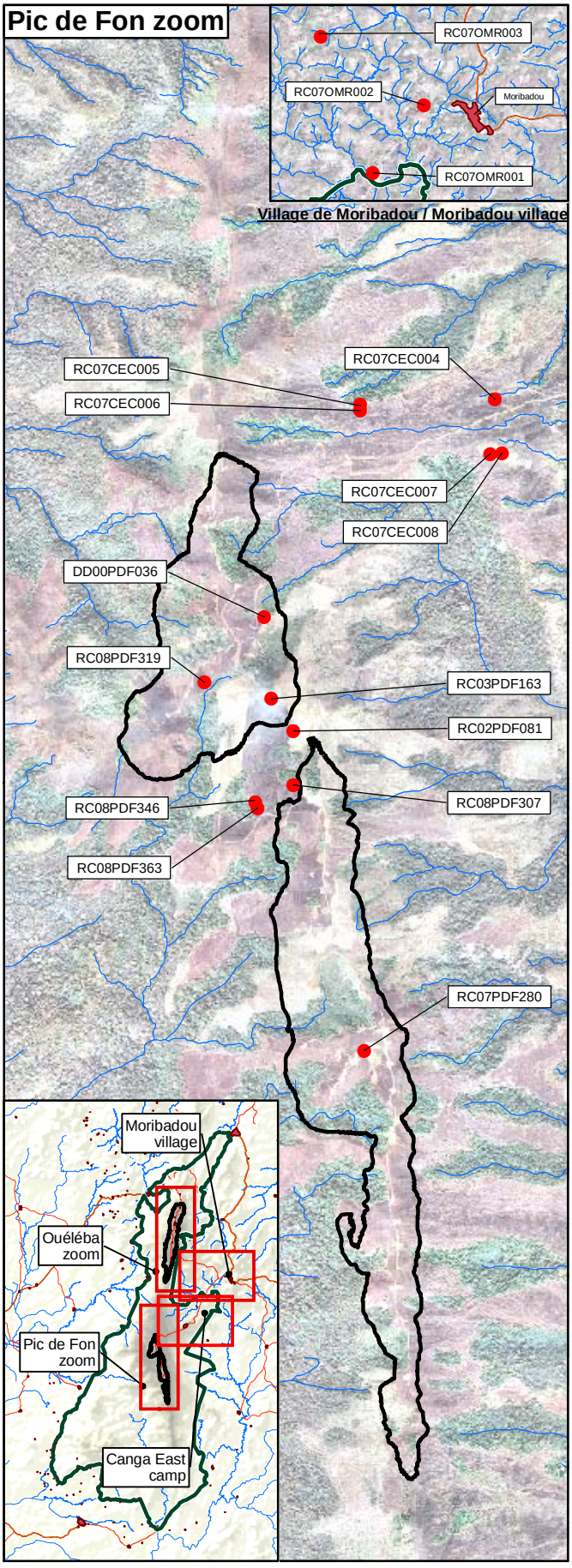
Réseau de suivi de la qualité de l'eau de surface dans la zone d'étude locale / Surface water quality monitoring network in the local study area

Échelle / Scale	Projet / Project	Volume C Carte/Map 11.1
0 0.625 1.25 2.5 Km — 1:125,000	SIMANDOU	

Directeur de projet (client) Project manager (client)	Directeur de projet Project manager	No. pr./ P. number
Leon Payne	Richard Fontaine	604917

No.	aaaa/mm/jj yyyy/mm/dd	Description	Dessiné/Drawn	Vérifié/Verified
01	2010/06/15	Final	M. Dupré	M. Stapinsky
00	2010/01/04	Preliminary	M. Dupré	M. Stapinsky





Stations d'échantillonnage / Sampling stations

Eau souterraine — Groundwater

Repères géographiques / Geographical landmarks

Route secondaire	Secondary road
Hydrographie	Hydrography
Forêt classée du Pic de Fon	Pic de Fon Classified Forest
Aire minière	Mining area

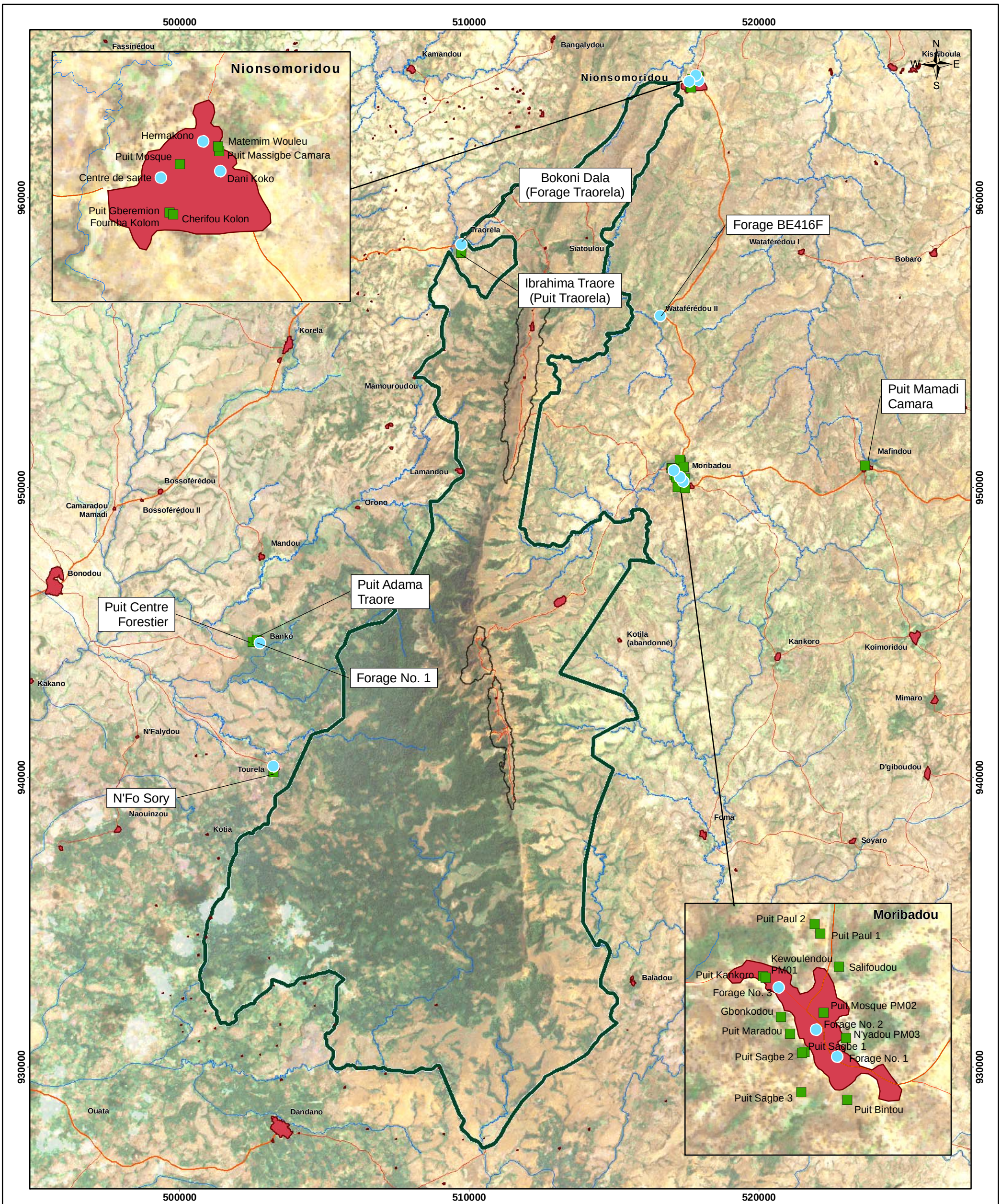
Sources:
1- Base map - 2006 0.5m ADS40 Aerial Photographs, 2006 Spot Imagery;
2- Landsat imagery mosaic 2002-2003;
3- Shuttle Radar Topography Mission (SRTM);
4- Carte topographique IGN 1:50 000/1:200 000;
5- Water magagement consultant report;
7- Geographic Coordinate System: WGS84, UTM, Zone 29N.

Titre / Title: **Réseau de suivi de la qualité de l'eau souterraine dans la zone d'étude locale / Groundwater quality monitoring network in the local study area**

Échelle / Scale	Projet / Project	Volume C Carte/Map 11.2
0 200 400 800 m 1:40,000	SIMANDOU	

Directeur de projet (client) Project Manager (Client)	Directeur de projet Project Manager	No. pr./ P. Number
Leon Payne	Richard Fontaine	604917

No.	aaaa/mm/jj yyyy/mm/dd	Description	Dessiné/Drawn	Vérifié/Verified
01	2010/06/15	Final	M. Dupré	M. Stapinsky
00	2009/04/15	Preliminary	M. Dupré	C. Roy



Stations d'échantiollonnage / Sampling stations

Puits	Well
Forage	Borehole

Repères géographiques / Geographical landmarks

Route secondaire	Secondary road
Piste	Track
Hydrographie	Hydrography
Forêt classée du Pic de Fon	Pic de Fon Classified Forest
Milieu bâti	Built area
Aire minière	Mining area

Sources:
1- Base map - 2006 0.5m ADS40 Aerial Photographs, 2006 Spot Imagery;
2- Landsat imagery mosaic 2002-2003;
3- Shuttle Radar Topography Mission (SRTM);
4- Carte topographique IGN 1:50 000/1:200 000;
5- Water magagement consultant report;
7- Geographic Coordinate System: WGS84, UTM, Zone 29N.

Titre / Title

Réseau de suivi de la qualité de l'eau des puits et forages dans les villages de la zone d'étude locale / Water quality monitoring network of village wells and boreholes in the local study area

Échelle / Scale	Projet / Project	Volume C Carte/Map 11.3
0 0.625 1.25 2.5 Km — 1:125,000	SIMANDOU	

Directeur de projet (client) Project manager (client)	Directeur de projet Project manager	No. pr./ P. number
Leon Payne	Richard Fontaine	604917

No.	aaaa/mm/jj yyyy/mm/dd	Description	Dessiné/Drawn	Vérifié/Verified
01	2010/06/15	Final	M. Dupré	M. Stapinsky
00	2010/01/04	Preliminary	M. Dupré	M. Stapinsky

Photo 11.1 Portable winch used for groundwater sampling in piezometers



Source: SNC-Lavalin Environment 2008

All water samples were analysed for the physico-chemical parameters indicated in Table 11.1. Temperature, pH, electrical conductivity, oxidation-reduction potential, and dissolved oxygen were also measured on-site with portable equipment.

Table 11.1 Parameters analysed in water samples

Category	Parameter (1)
Physico-chemical	pH, ORP, DO, EC, turbidity
Major ions	Ca, Na, K, Mg, Cl, F, SO_4, CO_3, HCO_3, NO_3, NO_2, PO_4
Metals	Ag, Al, As, Au, Ba, Be, Bi, Br, Cd, Ce, Co, Cr, Cs, Cu, Dy, Er, Eu, Fe, Ga, Gd, Ge, Hf, Hg, Ho, I, In, La, Li, Lu, Mn, Mo, Nb, Nd, Ni, Os, Pb, Pd, Pr, Pt, Rb, Re, Ru, Sb, Sc, Se, Si, Sm, Sn, Sr, Ta, Tb, Te, Th, Ti, Tl, Tm, U, V, W, Y, Yb, Zn, Zr
Others	Ammonia, total organic carbon (TOC)

(1) *In-situ* field measurements: electrical conductivity (EC), oxidation-reduction potential (ORP) and dissolved oxygen (DO).

In addition to sampling water for laboratory analyses, several samples taken during the hydrocensus were tested with a portable water quality meter for physico-chemical parameters and with an Oxfam del Agua system to measure the number of faecal coliforms.

11.3 RESULTS

11.3.1 Surface Water Quality

The surface water samples collected in the course of the sampling campaigns presented typically very low ionic concentrations. For this reason and the general lack of variability within the results, the main physico-chemical parameters analysis results have been compiled and presented as summary statistics of the springs and streams.

For the purposes of calculating summary statistics, values less than the detection limit have been reset to half of the detection limit. Since surface water may be used in the study area as drinking water, the World Health Organisation (WHO) *Guidelines for Drinking Water Quality* (2006) are also presented in the tables for reference.

11.3.1.1 Springs

According to Table 11.2, the spring water samples display the characteristics of water with very little mineralisation. Most of the parameters, including major anions and cations, and trace metals are below detection limit; or present at very low concentrations. Electrical conductivity is in the range of 2 to 22 µS/cm, which is somewhat in line with total dissolved solids values, ranging from 1.4 to 15.7 mg/l (applying a factor of 0.71 to electrical conductivity data).

The major cations and their median concentrations are: below 0.7 mg/l for calcium; 0.23 mg/l for sodium; 0.22 mg/l for potassium; and 0.20 mg/l for magnesium. Bicarbonate is the major anion present at a median concentration of 1.1 mg/l.

Dissolved silica, expressed as silicon, is reported in larger concentration than other major cations, with a median concentration of 3.1 mg/l. The occurrence of silica as a major solute in the surface waters is consistent with the weathering regime of a tropical banded ironstone formation (WMC 2009b). Dissolved iron is below the method detection limit of 10 µg/l in 36 of the 58 samples. Total organic carbon is very low in spring samples and present at a median concentration of 795 µg/l. Spring water turbidity is also typically very low with a median value at 0.9 NTU (Nephelometric Turbidity Units), indicating very clear water.

Field measurements of pH are typically low in spring water, and range between 1.2 and 9.6, with a median value of 4.0. WMC reported that the lowest pH readings may be unrepresentative, as there are evidences of instrument calibration error in measuring pH in such low conductivity water (WMC 2009b). They also suggested that carbonic acid generation can produce this pH effect. Limited data is available yet to explain high pH values. The dissolved oxygen content of the spring samples has a median value of 6.0 mg/l, indicating that the spring water is undersaturated in oxygen.

The concentrations for all parameters of the spring samples are below the WHO *Guidelines for Drinking Water Quality* (2006). The spring samples present the lowest solute concentrations among all water samples collected in the study area.

Table 11.2 Summary statistics of spring water chemistry

Parameter	Unit	Method detection limit	Minimum	Maximum	Median	WHO guideline
Temperature	°C	-	17.9	27	21.4	-
pH	pH unit	-	1.2	9.6	4	-
ORP	mV	-	-248	629	168	-
DO	mg/l	-	0.6	12.5	6	-
EC	µS/cm	-	2	22	8	-
Turbidity	NTU	0.1	0.1	22.8	0.9	-
Ca	mg/l	0.7	**0.35**	1.3	**0.35**	-
Na	mg/l	0.005	0.093	1.26	0.23	200
K	mg/l	0.03	0.04	0.96	0.215	-
Mg	mg/l	0.001	0.027	0.758	0.203	-
Cl	mg/l	0.03	**0.015**	1.35	0.135	-
SO_4	mg/l	0.03	**0.015**	0.55	0.055	500
CO_3	mg/l	-	0	0	0	-
HCO_3	mg/l	-	6.5	0.1	1.1	-
NO_3	mg/l	0.01	**0.005**	0.44	**0.005**	11.3
NO_2	mg/l	0.01	**0.005**	**0.005**	**0.005**	0.912
PO_4 (as P)	mg/l	0.02	**0.01**	1.46	**0.01**	-
Ammonia	mg/l	0.02	**0.01**	0.18	**0.01**	-
TOC	mg/l	0.01	0.1	4.27	0.795	-
Si	mg/l	0.2	0.5	4.3	3.05	-
F	µg/l	10	**5**	400	**5**	1500
Li	µg/l	1	**0.5**	1	**0.5**	-
Fe	µg/l	10	**5**	180	**5**	-
Mn	µg/l	0.1	**0.05**	11.9	1.95	400
Ni	µg/l	0.3	**0.15**	8.2	**0.15**	20
Ag	µg/l	0.2	**0.1**	**0.1**	**0.1**	-
Al	µg/l	2	**1**	77	12	-
As	µg/l	0.03	**0.015**	0.53	**0.015**	10
Hg	µg/l	0.2	**0.1**	**0.1**	**0.1**	-
Cr	µg/l	0.5	**0.25**	**0.25**	**0.25**	50
Ba	µg/l	0.1	2.1	38.7	4.15	700
Br	µg/l	3	**1.5**	14	**1.5**	-
Cd	µg/l	0.01	**0.005**	0.02	**0.005**	3
Cu	µg/l	0	0.1	1.4	0.1	2000
Pb	µg/l	0.01	**0.005**	1.38	0.03	10
Sr	µg/l	0.04	1.14	11.4	2.78	-
Zn	µg/l	0.5	**0.25**	29	0.8	-
U	µg/l	0.001	**0.0005**	0.029	**0.0005**	9
Be	µg/l	0.1	**0.05**	**0.05**	**0.05**	-
Se	µg/l	0.2	**0.1**	0.2	**0.1**	10
Sn	µg/l	0.1	**0.05**	0.2	**0.05**	-
Co	µg/l	0.005	**0.0025**	0.436	0.0665	-

Note: Values in bold are values less than the detection limit that have been reset to half of the detection limit for purposes of calculating summary statistics.

Source: Water Management Consultants 2009b

11.3.1.2 Streams

Stream water sample summary statistics are presented in Table 11.3. They exhibit slightly higher solute contents in comparison with upstream spring samples. Median electrical conductivity value of stream samples are 15 µS/cm with a total range between 3 and 140 µS/cm, which corresponds to total dissolved solids values between 2 and 100 mg/l, characteristic of essentially pure water.

The major cations median concentrations are: 0.9 mg/l for calcium, 0.98 mg/l for sodium, 0.64 mg/l for potassium and 0.67 mg/l for magnesium. Bicarbonate is again the most abundant anion at a median concentration of 5.5 mg/l and with lower concentrations.

Silicon is measured in the samples at relatively higher concentrations compared to other parameters, with a median concentration of 5.25 mg/l, which is similar to that of bicarbonate. Dissolved iron and manganese are also higher in the stream samples with median concentrations of 75 µg/l and 4 µg/l, respectively.

Total organic carbon in the stream samples has a median concentration of 1.5 mg/l, which is higher than the median value for the spring samples (630 µg/l).

Measured pH values for the stream samples are slightly less acidic than the very low values measured for the spring samples, with a median pH value of 5.7. These low pH values were also attributed to the pH effect of carbonic acid generation (WMC 2009b). The small increase in pH from spring samples to stream samples is expected, as a result from the small increase in buffer capacity likely occurring through dissolution of base components and the degassing of dissolved atmospheric CO_2 (WMC 2009b).

The major ion and trace element concentrations pattern for stream samples is similar to the spring samples pattern with values measured below detection limit, or present at very low concentrations. Median concentrations in stream samples are approximately twice the median levels measured in springs. The sample concentrations measured in the stream samples also fell below WHO *Guidelines for Drinking Water Quality* (2006) for all parameters.

11.3.1.3 Temporal Variations in Surface Water Chemistry

Temporal variability has been observed in surface water samples from Pic de Fon and Ouéléba deposits. Seasonal short-term variability in water quality has been observed down to individual storm events.

Table 11.4 and Table 11.5 provide monthly mean and instantaneous maximum and minimum values for the water quality parameters that have been continuously monitored at Whisky 1 and Whisky 2, respectively. Some conclusions on temporal variability can be drawn from these results.

Table 11.3 Summary statistics of stream water chemistry

Parameter	Unit	Method detection limit	Minimum	Maximum	Median	WHO guideline
Temperature	°C	-	15.8	25.6	20.55	-
pH	pH unit	-	2.1	9.1	5.65	-
ORP	mV	-	-267	680	76.6	-
DO	mg/l	-	0.6	72	6.6	-
EC	µS /cm	-	3	140	15	-
Turbidity	NTU	0.1	0.2	69.7	2.5	-
Ca	mg/l	0.7	0.35	11.6	0.9	-
Na	mg/l	0.005	0.12	8.98	1	200
K	mg/l	0.03	0.04	10.2	0.635	-
Mg	mg/l	0.001	0.14	4.86	0.7	-
Cl	mg/l	0.03	0.03	7.79	0.205	-
SO_4	mg/l	0.03	**0.015**	15.4	0.185	500
CO_3	mg/l	-	0	0	0	-
HCO_3	mg/l	-	80	1.6	5.5	-
NO_3	mg/l	0.01	**0.005**	262	**0.005**	11.3
NO_2	mg/l	0.01	**0.005**	0.07	**0.005**	0.9
PO_4 (as P)	mg/l	0.02	**0.01**	15.1	**0.01**	-
Ammonia	mg/l	0.02	**0.01**	0.2	**0.01**	-
TOC	mg/l	0.01	0.4	8.25	1.5	-
Si	mg/l	0.2	1.5	20.3	5.25	-
F	µg/l	10	**5**	230	**5**	1500
Li	µg/l	1	**0.5**	2	**0.5**	-
Fe	µg/l	10	**5**	2510	75	-
Mn	µg/l	0.1	**0.05**	1000	3.55	400
Ni	µg/l	0.3	**0.15**	0.7	**0.15**	20
Ag	µg/l	0.2	**0.1**	**0.1**	**0.1**	-
Al	µg/l	2	**1**	64	11	-
As	µg/l	0.03	**0.015**	0.21	0.06	10
Hg	µg/l	0.2	**0.1**	**0.1**	**0.1**	-
Cr	µg/l	0.5	**0.25**	**0.25**	**0.25**	50
Ba	µg/l	0.1	2	209	22.1	700
Br	µg/l	3	**1.5**	22	**1.5**	-
Cd	µg/l	0.01	**0.005**	0.03	**0.005**	3
Cu	µg/l	0.2	**0.1**	1.2	**0.1**	2000
Pb	µg/l	0.01	**0.005**	3.9	0.04	10
Sr	µg/l	0.04	2.25	118	10.95	-
Zn	µg/l	0.5	**0.25**	10.9	1.1	-
U	µg/l	0.001	**0.0005**	0.155	0.005	9
Be	µg/l	0.1	**0.05**	**0.05**	**0.05**	-
Se	µg/l	0.2	**0.1**	**0.1**	**0.1**	10
Sn	µg/l	0.1	**0.05**	**0.05**	**0.05**	-
Co	µg/l	0.005	**0.0025**	2.52	0.031	-

Note: Values in bold are values less than the detection limit that have been reset to half of the detection limit for purposes of calculating summary statistics.

Source: Water Management Consultants 2009b

Table 11.4 Summary of water quality parameters at Whisky 1

	Jan.	Feb.	Mar.	Apr.	May	June	July	Aug.	Sep.	Oct.	Nov.	Dec.
Water temperature (°C) (Dec. 2005-Dec. 2007)												
Monthly mean	18.4	19.5	19.9	20.7	20.7	20.2	20.2	20.2	20.4	19.8	18.9	20.0
Instant. max.	20.5	20.5	20.7	21.0	21.1	20.9	20.6	20.5	20.5	20.8	20.7	20.6
Instant. min.	17.3	18.1	19.1	20.0	20.0	20.0	19.7	19.8	19.9	19.9	18.5	18
Conductivity (µS/cm) (Dec. 2005-Dec. 2007)												
Monthly mean	7.0	7.3	7.3	7.5	7.9	7.0	7.1	9.2	6.7	6.5	6.4	6.8
Daily max.	9.4	16.2	11.7	9.3	9.3	10.1	9.3	17	8.0	7.2	8.4	9.0
Daily min.	5.8	5.8	6.7	6.8	7.0	6.9	5.7	5.9	6.0	6.0	6.0	5.4
pH (Dec. 2005-Dec. 2007)												
Monthly mean	6.2	5.9	5.9	6.2	6.1	6.0	5.8	5.8	5.9	6.5	6.4	6.3
Daily max.	6.7	6.2	6.4	6.5	6.6	6.2	6.3	6.3	6.7	6.8	6.6	7.3
Daily min.	5.73	5.8	5.4	5.9	5.9	5.5	5.2	5.0	5.2	6.1	5.8	5.5
Dissolved oxygen (% saturation) (Dec. 2005-Dec. 2007)												
Monthly mean	91.8	99.9	97.0	84.9	78.4	-	81.9	84.4	96.6	88.9	81.6	92.8
Daily max.	100.0	100.0	100.0	99.3	90.0	86.4	100.0	100.0	100.0	100.0	97.5	96.8
Daily min.	85.0	81.2	92.8	-	-	-	60.7	60.1	90.3	-	57.1	71.8
Dissolved oxygen (mg/l) (Dec. 2005-Dec. 2007)												
Monthly mean	7.8	8.1	7.8	6.7	-	-	6.5	7.6	7.6	7.3	8.3	7.6
Daily max.	8.9	8.3	8.2	7.8	7.2	6.9	8.8	8.8	8.1	8.1	8.5	8.6
Daily min.	6.8	6.4	7.3	0.4	0.1	0.2	4.8	4.7	7.2	2.6	4.6	5.7
Turbidity (NTU) (Dec. 2005-Dec. 2007)												
Monthly mean	52	26	56	47	67	61	162	485	420	149	54	94
Daily max.	201	184	284	154	202	240	514	5630	5880	1028	158	412
Daily min.	0	3	4	22	27	4	14	9	7	7	8	0

Source: Water Management Consultants 2009b

Table 11.5 Summary of water quality parameters at Whisky 2

	Jan.	Feb.	Mar.	Apr.	May	June	July	Aug.	Sep.	Oct.	Nov.	Dec.
Water temperature (°C) (Dec. 2005-Dec. 2007)												
Monthly mean	17.2	-	19.4	20.1	20.1	19.8	19.6	19.6	19.6	19.9	19.2	18.2
Instant. max.	20.2	20.2	20.4	20.7	20.6	20.4	20.1	19.9	20	20.4	20.4	20.3
Instant. min.	15.3	17	18.3	19.4	19.4	19.2	19.2	19.3	19.2	19.3	17.5	16.8
Conductivity (µS/cm) (Dec. 2005-Dec. 2007)												
Monthly mean	5.9	-	5.4	6.0	5.5	6.0	6.4	5.5	5.0	5.3	5.1	6.3
Daily max.	13.1	30.2	11.4	11.1	10.7	7.3	9.0	7.5	6.3	6.8	10.1	11.5
Daily min.	3.7	5.0	3.5	4.5	5.1	5.0	5.3	4.1	4.0	4.4	4.7	4.9
pH (Dec. 2005-Dec. 2007)												
Monthly mean	6.3	-	6.0	6.0	6.5	6.2	6.3	6.2	6.2	6.4	6.2	6.6
Daily max.	7.9	6.6	7.7	7.7	6.8	6.7	6.7	6.8	7.0	6.9	6.9	7.4
Daily min.	5.9	6.0	5.9	5.9	5.7	5.7	5.9	5.9	5.9	5.8	5.9	5.9
Dissolved oxygen (% saturation) (Dec. 2005-Dec. 2007)												
Monthly mean	84.1	-	77.0	81.3	86.0	83.5	88.2	87.8	87.7	87.1	88.6	82.3
Daily max.	92.3	95.6	99.9	86.7	89.4	90.6	96.5	94.7	93.5	93.3	94.5	89
Daily min.	73.5	70.2	62.8	75.4	82.6	78.9	80.1	74.4	74.5	80.3	77.3	72.3
Dissolved oxygen (mg/l) (Dec. 2005-Dec. 2007)												
Monthly mean	7.1	-	6.3	6.4	6.7	6.6	7.0	7.0	6.9	6.9	7.1	6.7
Daily max.	8.0	7.8	8.3	8.8	7.1	7.2	7.7	7.5	7.4	7.3	7.6	7.4
Daily min.	6.1	5.5	4.9	5.9	6.5	6.2	6.3	5.9	5.9	6.3	6.0	6.0
Turbidity (NTU) (Dec. 2005-Dec. 2007)												
Monthly mean	266	-	33	297	3,093	1,439	3,035	1,510	118	336	84	607
Daily max.	3,208	41	79	2,825	1,981	3,271	211	5,833	1,163	3,000	282	5,543
Daily min.	3	4	1	2	23	2	8	3	4	3	3	40

Source: Water Management Consultants 2009b

During the period of monitoring, the data collected indicated only a slight seasonal variation in the mean water temperature. Mean water temperatures are lower during the dry season in comparison to the wet season. Once the wet season starts in March, water temperatures increases in contrast to air temperatures that decrease.

Mean electrical conductivity is 6 to 7 µS/cm throughout the year, with minor variation associated to storm events. WMC (2009b) assumed that salt deposits that have accumulated in the watershed during evaporation between flow events are flushed down the stream network following new rainfall events. Maximum conductivities measured during storm events reached about 15-20 µS/cm, which is still very low.

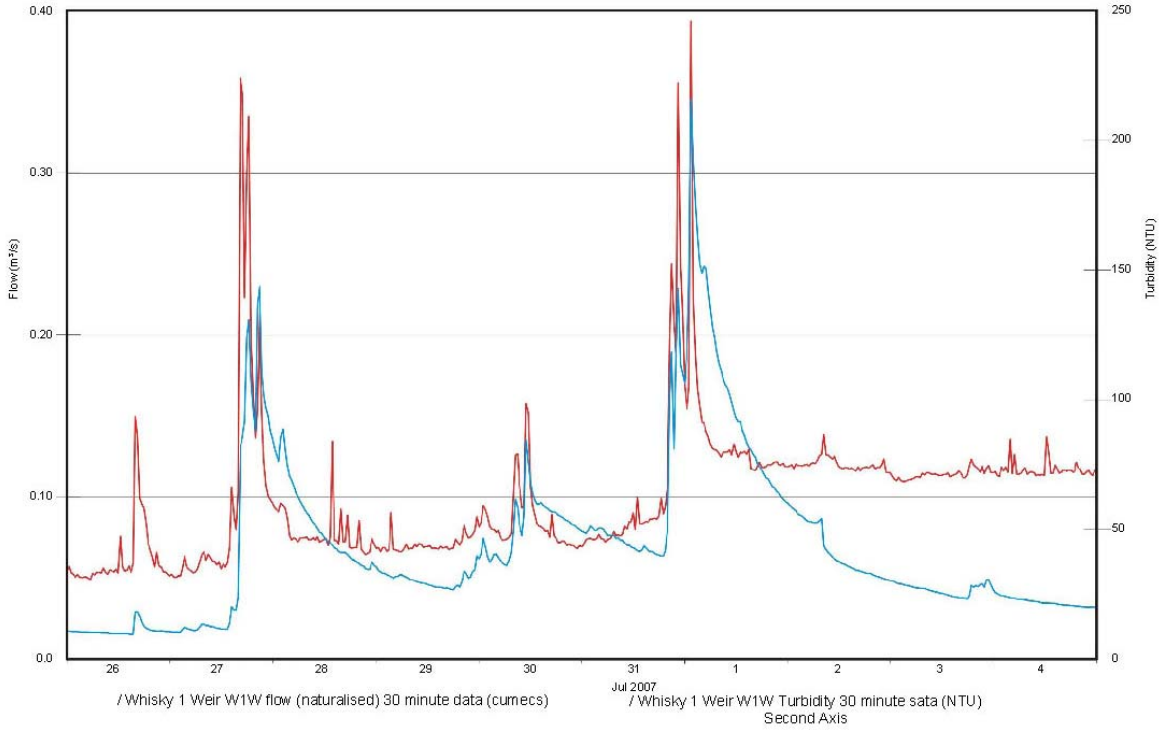
Limited seasonal variations are observed in monthly mean pH values. Typically, mean pH values range from 5.8 to 6.6. A larger variability is measured at the Whisky 1 weir than at Whisky 2.

The dissolved oxygen content displays more variability; values measured ranged between 6.3 and 8.3 mg/l. More variability is observed at Whisky 1 compared to Whisky 2. Lowest values were measured during summer months.

Turbidity data presents the most variability among the parameters monitored continuously in surface waters. Variability in turbidity reflects changes in a stream's capacity to transport sediment. The principal agents of erosion are rainfall drops and runoff. In the dry season, natural turbidity levels are low, typically below 100 NTU. In the early wet season, daily mean turbidity varies between 100 NTU and 200 NTU, with higher values up to 500 NTU related to storm events.

Figure 11.1 presents as an example the variations in turbidity at Whisky 1 during storm events. As observed, periods of high turbidity are clearly associated with increased flow.

Figure 11.1 Turbidity and flow during storm flow events measured at Whisky 1 weir



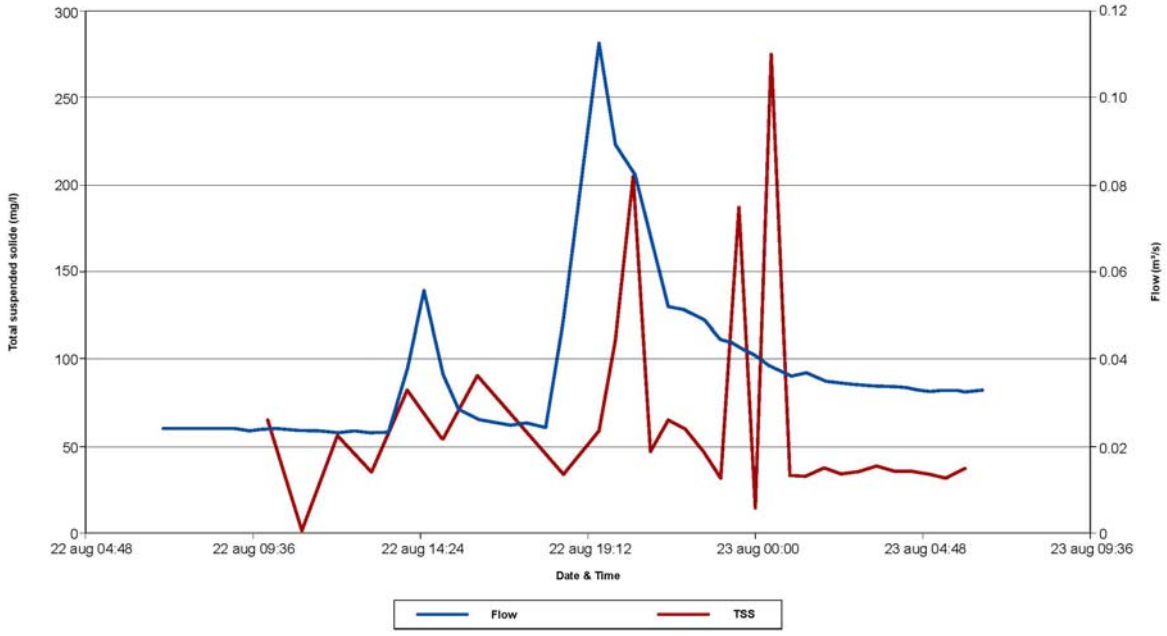
Source: Water Management Consultants 2009b

Natural variability in the same parameters, as discussed previously and observed in mean daily values, typically occurs over the course of single relatively small storm events. Temperature, conductivity and dissolved oxygen all display responses to the variation in flow, but there is clear significant short-term variability in turbidity and Total

Suspended Solids (TSS). Although turbidity and TSS can not directly be correlated using the data collected, both are closely related to rainfall and continuous variations in flow.

Figure 11.2 presents an example of the variations of TSS in comparison with a storm flow hydrograph over a two-day period in August 2008 at the Whisky 5 weir. As observed in the figure, from a base TSS level of 40 mg/l, the peak in TSS (275 mg/l) follows shortly the peak in storm flow. The daily rainfall giving rise to the hydrograph was 62 mm.

Figure 11.2 Total suspended solids and flow measured at Whisky 5 weir



Source: Water Management Consultants 2009b

At all the monitoring stations, water colour varied mostly between clear and light brown during storm flow events. The colour changes to dark brown or red as a function of the increased turbidity during periods of higher flow. These results suggest that spatial variations within the study area can be encountered in some parameters, such as turbidity and TSS, which require further discussion.

11.3.1.4 Spatial Variations in Surface Water Chemistry

Spatial variations of some physico-chemical parameters in surface water have been observed in the results of the various surface water sampling campaigns. These variations demonstrate the natural and/or human-related evolution of the surface water along the stream paths.

For instance, a general increase in dissolved content is observed with an increase in distance from the stream source. The sampling locations closer to the source of the streams, such as the six weirs monitored in the current study, display electrical

conductivity values closer to those measured at the spring locations. The highest bicarbonate concentrations are encountered in downstream samples, and total organic carbon values are generally higher in the downstream road crossing sampling sites. The small increase observed in pH from spring samples to stream samples is expected, as a result of the small increase in buffer capacity likely occurring through dissolution of base components and the degassing of dissolved atmospheric CO_2 (WMC 2009c).

Upstream/downstream differences in turbidity have been observed in a few villages, suggesting an influence from the villagers. Records for the upstream sampling sites are representative of the flow as it arrives at the point of use and the records for the downstream sampling points are representative of the water as it leaves the point of use. Any difference should be the result of the impact of the users themselves. The influence of the villagers on water colour is observed in 60% of the sampling sites, where upstream clear water, for example, turns to light brown downstream.

Turbidity provides a similar but less clear indicator of baseline conditions to colour, the values observed are mostly (95% and more) in the lowest turbidity range of 0-100 NTU. Upstream/downstream differences in turbidity are noted in a few villages, indicating an influence from the villagers. The upstream sample sites with the lowest range in turbidity are the Boe at Foma, the Worongbe at Lamadou, the Woron at Mamouridou, and the Pulowaye at Banko, the Dianiworo at Tourela, the Siankounfin and the Siankoungbe at Banankoro. These may be considered to be the least disturbed watersheds. Interestingly, the Soumourou at Kakano also exhibits a narrow range of turbidity indicating that range in turbidity may not be a good indicator of level of disturbance. Nevertheless, regardless of the level of disturbance, the turbidity data serve as a 2008 baseline against which data collected during the project may be compared.

11.3.2 Groundwater Quality

The summary statistics of the chemical results of the six groundwater sampling campaigns completed between November 2006 and August 2008 are presented in Table 11.6. Since groundwater may be used in the area as drinking water, the *WHO Guidelines for Drinking Water Quality* (2006) are included in the table as a general reference.

As in surface water, groundwater samples also exhibit the characteristics of very low mineralised waters. The results display very low dissolved solids concentrations in the groundwater samples. Due in part to the low concentrations of major ions and the absence of a dominant major cation, the water does not clearly fall into a specific water type (hydro-geochemical facies). The low ionic concentrations suggest that groundwater has a relatively short residence time following infiltration (WMC 2009c).

Table 11.6 Summary statistics for groundwater chemistry

Parameter	Unit	Method detection limit	Maximum	Minimum	Median	WHO guideline
Temp	C	-	32.8	19.7	25.4	-
pH	pH unit	-	6.6	3.8	5.35	-
ORP	mV	-	206	-170	76	-
DO	mg/l	-	7.1	3	4.65	-
EC	µS/m	-	43	7	11	-
Turbidity	NTU	0.1	10,000	0.2	15.85	-
Ca	mg/l	0.7	9.3	**0.35**	0.8	-
Na	mg/l	0.1	64.4	0.162	0.425	-
K	mg/l	0.03	15.9	0.16	0.545	-
Mg	mg/l	0.001	11	0.067	0.179	-
Cl	mg/l	0.03	2.99	0.04	0.285	-
SO_4	mg/l	0.03	26.3	**0.015**	0.27	-
CO_3	mg/l	-	0	0	0	-
HCO_3	mg/l	-	19.4	2.3	10.85	-
NO_3 (as N)	mg/l	0.01	0.29	**0.005**	0.05	50
NO_2 (as N)	mg/l	0.01	0.04	**0.005**	**0.005**	0.2
PO_4 (as P)	mg/l	0.02	0.09	**0.01**	**0.01**	-
Ammonia	mg/l	0.02	0.82	**0.01**	0.03	-
TOC	mg/l	0.01	19.7	0.12	1.9	-
F	mg/l	0.01	0.16	**0.005**	**0.005**	-
Ag	µg/l	0.2	0.1	**0.1**	**0.1**	1,500
Al	µg/l	2	143	**1**	6.5	-
As	µg/l	0.03	4.46	**0.015**	**0.015**	-
Ba	µg/l	0.1	98.9	1.5	5.6	20
Be	µg/l	0.1	**0.05**	**0.05**	**0.05**	-
Br	µg/l	3	392	**1.5**	6	10
Cd	µg/l	0.01	0.06	**0.005**	0.01	1
Co	µg/l	0.005	2.23	**0.002**	0.264	700
Cr	µg/l	0.5	12	**0.25**	**0.25**	-
Cu	µg/l	0.2	10.3	0.3	1.6	2,000
Fe	µg/l	10	3,330	**5**	7.5	15
Hg	µg/l	0.2	**0.1**	**0.1**	**0.1**	-
Li	µg/l	1	10	**0.5**	**0.5**	-
Mn	µg/l	0.1	1010	1.4	14.6	400
Mo	µg/l	0.1	2	**0.05**	**0.05**	70
Nb	µg/l	0.005	0.011	**0.0025**	**0.0025**	-
Ni	µg/l	0.3	12.8	**0.15**	0.85	20
Pb	µg/l	0.01	170	**0.005**	1.76	10
Se	µg/l	0.2	1.5	**0.1**	**0.1**	10
Si	µg/l	200	24,600	500	1,000	-
Sn	µg/l	0.1	1.1	**0.05**	**0.05**	-
Sr	µg/l	0.04	99.7	2.2	4.54	-
U	µg/l	0.001	0.098	**0.0005**	0.005	9
Zn	µg/l	0.5	250	2.4	14	-

Note: Values in bold are values less than the detection limit that have been reset to half of the detection limit for purposes of calculating summary statistics.

Source: Water Management Consultants 2009c

Measurements of electrical conductivity are in the range of 7 to 43 µS/cm with a median value of 11 µS/cm. Electrical conductivity results have been used to estimate total dissolved solids, applying a factor of 0.71 to electrical conductivity data. Total dissolved solids values in piezometers are therefore estimated in a range from 5 to 30 mg/l with a median concentration of 7.8 mg/l. The estimated total dissolved solids content in groundwater samples suggests a chemical evolution from rainwater due to dissolution of rock material.

Sample pH is typically low in groundwater indicating acidic water. Median pH value is 5.4, as measured in piezometers. These results are consistent with the pH effect of carbonic acid generation, which can decrease the pH of water to 5.5-6. This pH range could also be obtained when more acidic water is buffered by $FeOH_3$ or FeOOH. The low ionic strength of the water favours carbonic acid generation; however several pH values measured are lower, with a minimum pH of 3.8, assumed to be unrepresentative, and likely due to instrument error in measuring pH in low conductivity waters.

The major cations (calcium, sodium, potassium and magnesium) are measured in the samples at similar concentrations, i.e. typically less than 1 mg/l. The most abundant anion is bicarbonate (median of 10.85 mg/l), with much smaller concentrations of chloride (median of 0.28 mg/l), and sulphate (median of 0.27 mg/l). Silicon (from dissolved silica) with a median concentration of 1.0 mg/l is the only other chemical parameter present at concentrations comparable to those of the major ion constituents.

Iron and manganese concentrations are generally low with median concentrations of 7.5 µg/l and 14.6 µg/l, respectively. Iron is not detected in 50% of the samples. Iron and manganese concentrations are however slightly elevated in some piezometers, which is not surprising in an iron ore geological environment. Manganese and lead are above the WHO reference concentration in a few samples.

Several chemical parameters detected in the piezometer water samples are close to, or below the method detection limit in spring samples, e.g. copper, lead, zinc and nickel. The same situation occurs for bromine and iodine present at relatively high concentrations in some Pic de Fon groundwater samples. Currently, limited data cannot explain these concentrations. However, they can probably be considered as background values of the natural groundwater geochemistry.

11.3.3 Village Wells and Boreholes Water Quality

Village wells and boreholes can display signs of groundwater pollution. This pollution can originate from latrines, surface spills and other effects of human activity in the surroundings of the infrastructure. Thus, the construction of the infrastructure has a large bearing on the extent to which sources of contamination can influence the water quality. Among the village wells included in the current sampling campaign, there are boreholes with hand pumps; while the remainder is dug wells presenting various quality of construction. Open dug wells are highly susceptible to direct contamination, whereas hand pump wells, which are typically sealed at the surface, provide much

better protection from potential surface contamination. Photo 11.2 presents a typical village dug well and a recent borehole.

Table 11.7 presents the summary statistics of the water quality data for the village wells and boreholes. The data are presented for comparison in the table against the WHO *Guidelines for Drinking Water Quality* (2006) since wells are used as a drinking water source.

The water sampled in the village wells generally displays a larger dissolved content than the piezometer samples. The median electrical conductivity of the village well samples is 117 µS/cm, significantly exceeding the electrical conductivity values for other sample groups (springs, streams, piezometers). Some samples exhibit the highest dissolved content with mean electrical conductivity values ranging from 260 to 494 µS/cm. Despite these higher mean conductivity values, the maximum conductivity measured in well water samples is 521 µS/cm, which reflects an estimated total dissolved solids of 370 mg/l (applying a conversion factor of 0.71). Consequently, the dissolved content measured in the water still indicates fresh water.

Nitrate is present in much larger concentrations in the village well water than in the piezometer water. In the piezometer water samples, the maximum concentration of nitrate is 0.29 mg/l, whilst nitrate is present in village well water samples in a median concentration of 48.5 mg/l. The elevated nitrate concentrations are assumed to be related to surface contamination from livestock and pit latrines, typically found in the vicinity of the wells. Nitrate is measured in 19 samples at concentrations exceeding the 11.3 mg/l WHO guideline value. Large concentrations of trace metals in village wells also exceed the WHO guideline values for barium, manganese, nickel, lead, selenium and uranium.

Photo 11.2 Typical dug well and hand pump borehole in the local study area



Source: SNC-Lavalin Environment 2008

During the hydrocensus, well water was tested for the presence of faecal coliforms. There is a strong correlation between well construction and the number of faecal coliforms. Samples showing high levels of faecal coliforms are those collected in open dug wells; whereas samples from boreholes equipped with hand pumps showed little

or no faecal coliforms. This situation may be partly due to the fact that boreholes have a deeper penetration than dug wells, thus limiting contamination which is generally found in the shallow horizons, and boreholes and well heads are properly protected. The use of a hand pump, as opposed to a bucket, also reduces the risk of groundwater contamination through handling of the bucket at the surface. The maximum number of coliforms found in boreholes with hand pumps is 8 coliforms/100 ml, as opposed to a maximum of 300 coliforms/100 ml in dug wells.

Surface water and groundwater in the LSA*-* are generally of good quality, with a few exceptions (some metals). However, the results from the sampling campaigns suggest that quality is already affected by human activities near some villages and in the vicinity of roads (large total dissolved solids values). The quality of water is also naturally affected during storm events. These conclusions should be considered in the elaboration of a water quality monitoring network for mining operations and the interpretation of future data collected.

Table 11.7 Summary statistics for village well and borehole water chemistry

Parameter	Unit	Method detection limit	Maximum	Minimum	Median	WHO guideline
Temperature	°C	-	203	20.2	25.2	-
pH	pH unit	-	9.8	4.7	5.6	-
ORP	mV	-	198	-244	47	-
DO	mg/l	-	5.1	0.6	4.8	-
EC	µS/m	-	521	21	117	-
Turbidity	NTU	0.1	445	0.2	1.2	-
Ca	mg/l	0.7	63	1.2	10.7	-
Na	mg/l	0.1	46.3	0.9	7.8	200
K	mg/l	0.1	65.1	0.31	5.1	-
Mg	mg/l	0.001	17.7	0.19	2.92	-
Cl	mg/l	0.03	97	0.09	6.5	-
SO_4	mg/l	0.03	38	**0.02**	0.8	500
CO_3	mg/l	-	0	0	0	-
HCO_3	mg/l	-	25.8	2.5	12.5	-
NO_3 (as N)	mg/l	0.01	48.5	**0.005**	4.6	11.3
NO_2 (as N)	mg/l	0.01	0.18	**0.005**	0.01	0.9
PO_4 (as P)	mg/l	0.02	2.51	**0.01**	**0.01**	-
Ammonia	mg/l	0.02	0.94	**0.01**	0.03	-
TOC	mg/l	0.01	35.3	0.48	1.9	-
F	mg/l	0.01	0.49	**0.005**	0.008	1.5
Ag	µg/l	0.2	0.3	**0.1**	**0.1**	-
Al	µg/l	2	1470	**1**	6	-
As	µg/l	0.03	4.39	**0.02**	0.11	10
Ba	µg/l	20	3340	6	204	700

Parameter	Unit	Method detection limit	Maximum	Minimum	Median	WHO guideline
Be	µg/l	0.1	4.3	**0.05**	**0.05**	-
Br	µg/l	3	60	**1.5**	17	-
Cd	µg/l	0.01	0.25	**0.005**	0.02	3
Co	µg/l	0.005	48.5	**0.0025**	0.137	-
Cr	µg/l	0.5	20.8	**0.25**	**0.25**	50
Cu	µg/l	0.2	67	**0.1**	0.5	2000
Fe	µg/l	10	660	**5**	**5**	-
Hg	µg/l	0.2	**0.1**	**0.1**	**0.1**	-
Li	µg/l	1	12	**0.5**	2	-
Mn	µg/l	0.1	1670	**0.05**	21.2	400
Mo	µg/l	0.1	2.2	**0.05**	**0.05**	70
Ni	µg/l	0.3	36	**0.15**	1.2	20
Pb	µg/l	0.01	26.9	**0.005**	0.11	10
Se	µg/l	0.2	20.5	**0.1**	**0.1**	10
Si	µg/l	200	43400	900	12200	-
Sn	µg/l	0.1	0.1	**0.05**	**0.05**	-
Sr	µg/l	10	660	13.1	143	-
U	µg/l	0.001	26.8	**0.0005**	0.108	9
Zn	µg/l	5	872	0.8	13.3	-

Note: Values in bold are values less than the detection limit that have been reset to half of the detection limit for purposes of calculating summary statistics.

Source: Water Management Consultants 2009b

CHAPTER 12

Natural Hazards

12. NATURAL HAZARDS

12.1 INTRODUCTION

A preliminary review of potential natural terrain hazards was performed for the baseline study. These include landslide hazards, potential seismic events and floodable areas. Knowledge of natural hazards at regional and local scales can be useful in order to identify potential risks on mine infrastructure integrity, mining operations, local transportation; or potential risks that can affect the environment in general.

12.2 METHODS

The approach used for the baseline is a desktop study, using existing information for interpretation. More specifically, three studies prepared for Rio Tinto have been examined in detail (Baynes 2008; LGS 2008; WMC 2009b) for the assessment of the main typical natural hazards: landslide, seismicity, and flooding.

12.3 RESULTS

12.3.1 Terrain Hazards

The combination of steep natural slopes on the flanks of the Simandou Range, weak geological conditions and seasonal tropical rainfall creates favourable conditions for landslide hazards. The erosional history with debris outflows, which formed the canga deposits, and the still relatively immature landform, provides indications of unstable ground and poor foundation conditions. This is evidenced by unstable slopes in numerous access road cuttings and beneath drilling pads, particularly during the wet season. Photo 12.1 presents examples of landslides resulting from natural causes.

Photo 12.1 Examples of landslides resulting from natural causes on Pic de Fon





Source: Rio Tinto 2010

The engineering characteristics of the natural terrain result entirely from the geological history of the Simandou Range, which indicates that faulting, weathering and erosion created the landform. Baynes Geologic (Baynes 2008) conducted a terrain hazard assessment and their key findings are as follows:

- There is very little evidence of current, natural, active landslide instability.
- Landslides that may have developed in the past have largely been stabilised, at least at the surface. Observations in the area suggest that a period of landslide development that occurred in the late Tertiary or early Quaternary geological eras was followed by some form of climate change and a period of cementation which stabilised the landscape. Disturbance of this cemented layer can result in future instability and the risk is enhanced by the steep slopes and heavy rainfall.
- Large palaeo-landslides have been observed on the Simandou ridge as follows:
  - Deep seated rotational or translational failures at the northwest, northeast and southwest of the Ouéléba deposit, which appear to be associated with weathered phyllites, where they are refolded and faulted along structural corridors.
  - Possibly structurally controlled rock slides on the west side of Ouéléba, near an apparent graben, i.e. an elongated depression, associated with wetlands.
  - Some landslides in the basement have been observed, suggesting that locally there are adversely oriented weak zones, possible schistose or phyllitic zones, which are gently dipping and can daylight on the slopes.

These paleo features represent a hazard to pit planning and operations where such features remain in the pit walls and/or along the alignment of, or within the foundations of mine infrastructure.

The adverse landforms and potential hazard areas will be taken into account by Rio Tinto, particularly in defining dump and stockpile locations and selecting mine infrastructure routes and systems and defining drainage control measures.

12.3.2 Regional Seismicity

Guinean territory lies on very ancient rocks of the West African Craton, which are typically relatively stable. These geological formations have not been affected by recent tectonic phenomenons. However, regional landscape features, such as the presence of numerous modifications to the hydrographic system along the coast, suggest some reactivation of geological constraints after the Paleozoic. The last episodes of important tectonism would date from the opening of the North Atlantic at the Mesozoic (Marten 2000 and 2004; Wright et al*.* 1985).

The review of the United States Geological Survey (USGS) database on earthquakes indicates that seismicity is low in Guinea. Historically, earthquakes have been reported in Guinea. The most important earthquakes that occurred recently in Guinea were in the area of Koumbia in 1983 and Boffa 1986.

Lahontan GeoSciences (LGS 2008) reviewed the seismic hazards for the mine site area and their main findings are:

- Seismicity is indicated to be low, though the seismicity of the southeast Guinea region is not well known.
- The largest earthquakes recorded in the southeast of Guinea were of magnitude between 4.5 and 5.0 on the Richter scale, which typically produces limited damages. These earthquakes occurred in two areas west of the Simandou Range, near Kérouané in the north, and Macenta in the south indicating seismically active structures in the area.
- Northwest and northeast trending fractures of significant length are evident in satellite imagery and air photographs. Reactivation of these structures could possibly result in earthquakes of magnitude greater than 5. The lack of information on the tectonic stress field in southeastern Guinea currently precludes which structural orientations may be active, the maximum size of earthquake and where an event may occur in relation to the Simandou Project.

12.3.3 Floodable Areas

The zones that are sensitive to flooding during periods of heavy rainfall are primarily the so-called *bas-fonds* (lowlands)*.* As discussed earlier, these flat-bottomed alluvial valleys, often encountered at the base of the Simandou Range, are sometimes used by local people for agricultural purposes. However, all villages are located outside these potential flooding areas (WMC 2009b). These *bas-fonds* areas are found on

hydromorphic soil on both sides of the Simandou Range; mainly along the Diani River on the west side of the ridge and along the Dion River at the northeast limit of the LSA (see Map 8.1).

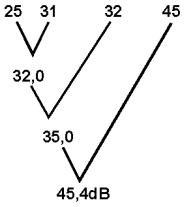
Floods typically occur as short-lived events of a few hours duration. During such events, it is expected that valley floors may become inundated, although this is not well-documented.

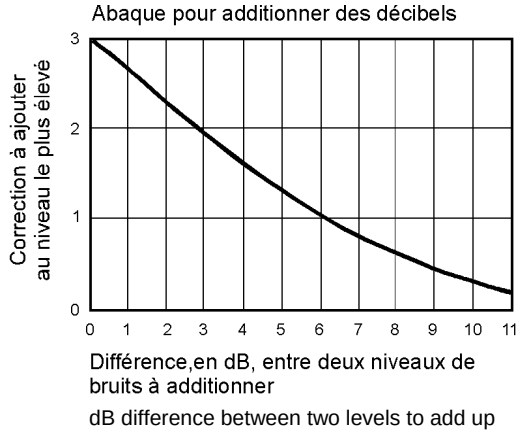
Some traces of floods have been observed at road crossings. For example, damages to riparian vegetation up to 3 m above the stream bed were reported in June 2007 at one road crossing the Tamanko River on the Canga East road. This has been reported to be the result of an exceptionally intense rainfall event that occurred over that specific watershed. Signs of flash floods have not been reported in neighbouring watersheds (WMC 2009b).

GLOSSARY

Acid Rock Drainage Refers to the outflow of acidic water from metal or coal mines, as a consequence of the oxidation of iron-sulphur minerals (pyrite and pyrrhotite) catalysed by a bacteria (Thiobacillus ferrooxidans).

Addition of noise levels The addition of noise levels can not be directly done. Noise levels sum on a logarithmic basis. The following chart can be used to add up dB or dBA levels: for example the sum of 25, 31, 32 and 45 equals to 45,5 dB.





Ambient noise Total noise existing in a given situation at a given time, typically composed of sounds emitted by several sources, close or far.

Antiformal structure Arch-shaped rock structure which, by definition, closes (i.e. arches) upward, but in which it may not be possible to determine the oldest rocks. It is frequently observed in complex orogenic regions.

Aquiclude A hydrogeologic unit which, although porous and capable of storing water, does not transmit it at rates sufficient to furnish an appreciable supply for a well or spring.

Assessment level Measured or predicted noise level to which a corrective factor has been added.

Background noise Ambient noise prior to any modification of a current or initial or baseline noise situation.

Base flow index Specific characteristic to a watershed that describes as a percentage the proportion of base flow on total stream flow.

Base flow Component of stream flow primarily composed of groundwater flow and interflow.

Basement	Define the rocks below a sedimentary platform or cover, or more generally any rock below sedimentary rocks or sedimentary basins that are metamorphic or igneous in origin.
Canga	Debris flow consisting of poorly-sorted detrital iron-rich fragments cemented by limonite.
Cleavage	Breaking of certain minerals along specific planes, which produces smooth surfaces. The latter are parallel to the faces of the molecular crystals that make up the mineral.
Convection	Vertical transport of heat and moisture, especially by updrafts and downdrafts in an unstable atmosphere.
Corrective factor	A correction, positive or negative, constant or variable, that is added to a measured or predicted sound level to take into account certain noise characteristics, the type of source or the time of the day.
Dorsal	Boundary, which form a typical mountainous relief, between diverging tectonic plates where molten rock is brought up from deep depths beneath the Earth's crust. Oceanic dorsals are currently forming at the bottom of many oceans, but older ones, such as the Guinea Dorsal, are inactive.
Evapotranspiration	Evaporation occurring from water intercepted by vegetation and from plant stomata
Easterly waves	Easterly waves are atmospheric pressure troughs moving westwards in the generally easterly airflow overlying the surface monsoon layer. Easterly waves cross locations in West Africa every 3-5 days at a speed of 8 m/s (6-7 degrees of longitude per day) and with a separation distance of about 2,500 km. As the wave passes, the overlying easterly wind reaches the ground sometimes causing a sudden burst of strong wind from the east.
Fluctuating noise	Continuous noise with a notable sound pressure variation by the ear, but not on an impulsive basis.
Fracture flow	Groundwater flow within the fracture network of rocks.
Frequency of a sound	This is the number of cycles per second. It is measured in Hz (Hertz). The human ear can perceive sound with a frequency between 20 Hz and 20 000 Hz. A low pitch sound will have a low frequency and a high pitched

	sound will have a high frequency. By comparison, the low pitch sound on a piano have a frequency around 30 Hz and the high pitch sound have a frequency around 4 000 Hz. To simplify the processing, the frequencies are grouped in bands corresponding in an octave or 1/3 octave. One octave is equivalent to eight keys on a piano, the frequency of the key 8 being twice the frequency of the key 1.
Gangue	Sand, rock, and other impurities of no commercial value surrounding the mineral of interest in an ore. Common gangue minerals are quartz, silica, calcite, and fluorite.
Geomorphological unit	Typical landform in an area presenting similar topographical, pedological and hydrological characteristics; and created by distinct natural or anthropogenic processes.
Geothitised	made richer in iron minerals (iron hydroxide) through washing of other cations as a result of the long action of a humid climate.
Harmattan	Dry wind blowing from the northeast and the Sahara, often loaded with suspended particulate matter
Hematite	Brown to reddish brown or red iron oxide mineral. Varieties include kidney ore, martite, iron rose and specularite. Goethite is another iron oxide-hydroxides mineral. Hematite is harder than pure iron, but much more brittle. Large deposits of hematite are encountered in banded iron formations. They are mined as the main ore of iron in Simandou.
Hydraulic conductivity	Property of a material (soil, rock) that describes the ease with which the soil or rock voids or fracture network permit water movement. It is typically expressed in m/s or cm/s.
Hydrostratigraphy	Geological units that have considerable extent and exhibiting similar water-bearing characteristics (aquifer/ aquitard) on the basis of their hydraulic properties.
Impulsive noise	Noise characterized by short duration increases of the sound pressure.
Intermittent noise	Noise observed only during certain periods and that occurs at regular or irregular intervals and for which occurrence duration is higher than 5 seconds.

Inter-Tropical Convergence Zone The complex dynamics of the global atmosphere result in there being a latitudinal belt of relatively low atmospheric pressure around the globe near the equator, towards which surface winds converge. This zone is termed the 'Inter-tropical convergence zone'.

Itabirite Rock type that consists in a laminated, metamorphosed, oxide-facies iron formation in which the original chert mineral or jasper bands have been recrystallised into large distinguished grains of quartz. Iron is present as thin layers of hematite, magnetite, goethite, or martite. The name was originally applied in Itabira, Brazil, to a high-grade, massive specular-hematite ore (66% iron).

L_{A95} The noise level exceeded for 95% of the sample period. This noise level is described as the average minimum background sound level or simply the background level.

L_{Aeq} The A-weighted equivalent noise level (basically the average noise level). It is defined as the steady sound level that contains the same amount of acoustical energy as the corresponding time-varying sound.

$L_{Aeq\ T}$ Level of sound pressure equivalent, for a duration T, expressed in dBA. It represents the average value of the sound pressure on a logarithmic basis. At the present state of knowledge, this level seems to be the most appropriate way to assess the disturbance associated with a long-term noise exposure.

L_{dn} Daily level (day/nigth), for a duration of 24 hours, expressed in dBA. This level represents the level of continuous equivalent sound pressure $L_{Aeq\ 24h}$ to which are added corrective factors, such as +10 dBA for the night time period between 22h00 and 7h00.

Laterite Surface formation (soil), typical to hot and wet tropical areas, rich in iron and aluminium. It develops by intensive and long lasting weathering of the underlying parent rock. Laterite consists mainly of the minerals kaolinite, goethite, hematite and gibbsite, which are formed in the course of weathering. Many laterites contain quartz as relatively stable relic mineral from the parent rock. The iron oxides goethite and hematite give the typical red-brown color to laterite.

Matrix flow Groundwater flow through the voids of a porous rocks or soils.

Metamorphism	The natural process by which rocks experience changes in composition, texture, or structure by extreme heat and pressure.
Mineralisation	In the course of the formation of ore bodies in rocks, deposition of economically important metals, resulting in a valuable or potentially valuable deposit.
Noise	All the sounds perceptible by the ear. Noise is a subjective notion generally related to annoyance. Weighted decibel A (dBA) is used as a measurement unit. More the noise is high, more its level in dBA is high. The scale of sound is generally between 0 dB, the threshold of audition, and 140 dB, the threshold of pain.
Orographic precipitation	Forced ascent of monsoon air over the Simandou ridge from the west, particularly in mid-wet season when the monsoon air mass is relatively deep and covers the ridge.
Permeability	Property of a material or a rock that describes the ease to transmit a fluid (air, water, oil, etc.). It is controlled by the packing, shape, and sorting of the granular materials of the soil, sediment or rock. Typically expressed in m^2 or cm^2.
Porosity	Ratio of the volume of openings (voids) to the total volume of material. It represents the storage capacity of the geologic material. Although a rock may be highly porous, if the voids are not interconnected, then fluids within the closed, isolated pores cannot move. The degree to which pores within the rock are interconnected is known as the effective porosity.
Precambrian	Period of geologic time included between 3.8 billion to 540 million years ago. The Precambrian Eon is divided into Achaean and Proterozoic geological periods.
Schistosity	Characteristic of some metamorphic rocks that split according to parallel or almost parallel layers due to the constant action of pressures during metamorphism. The prominent foliation in schist produced by parallel orientation of platy materials.
Shear zone	Tabular to sheetlike, planar or curviplanar zone composed of rocks that are more highly strained than rocks adjacent to the zone. Typically, it may form zones of much more intense foliation, deformation, and folding.

	It is often considered as the deep-level equivalents to faults. Many shear zones host ore deposits as they are a focus for hydrothermal flow through orogenic belts.
Sound	Ear sensation caused by a propagating air fluctuation (vibration). This fluctuation is detected as pressure variation by the ear. These variations are very small compared to the atmospheric air pressure.
Specific noise	Ambient noise component that can be specifically identified and that is associated with a specific source (example : construction noise, noise from a facility).
Squall lines	Squall lines are atmospheric disturbances produced when several convective storm cells merge together in a line, forming a particularly violent line of rainfall.
Standpipe piezometer	Borehole equipped to monitor piezometric water levels. Typically, it consists of a filter tip joined to a riser pipe. Water level readings are usually obtained with a water level indicator (manual or automatic).
Storm flow	Lateral movement of water through the upper layers until it enters a stream channel. Storm flow usually takes longer time to reach stream channels in comparison to runoff. Also known as interflow.
Supergene overprint	A mineral deposit or enrichment formed near the surface as a result of surficial weathering.
Phyllite	Type of foliated metamorphic rock primarily composed of quartz, sericite mica, and chlorite. Typically green, gray, or red. Similar to slate, but often with a wavy surface and a distinctive micaceous lustre. It represents a gradation in the degree of low metamorphism between slate and mica schist
Richter Scale	A logarithmic scale of 1 to 10+ for measuring the magnitude (intensity) of earthquakes on the basis of the size of seismograph oscillations. Introduced in 1935 by Charles F. Richter.
Synformal fold	A concave-upward fold in which the relative ages of the folded rocks is unknown.
Vibrating Wire Piezometer	Piezometer used primarily to monitor pore-water pressure. They can also be used to monitor water levels. They convert water pressure to a frequency signal via a diaphragm, a tensioned steel wire, and an

	electromagnetic coil. The VWP is designed so that a change in pressure on the diaphragm causes a change in tension of the wire. An electro-magnetic coil is used to excite the wire, which then vibrates at its natural frequency. The vibration of the wire in the proximity of the coil generates a frequency signal that is transmitted to the readout device. The readout or data logger stores the reading in Hz.
Watershed	Drainage basin that includes both the streams and rivers that convey the water as well as the land surfaces from which water drains into those channels. It is separated from adjacent basins by a drainage divide. Also known as catchment or basin.
Weighting A	The human ear is not equally sensitive to sounds of different frequencies. To better represent the noise impression by the ear, the levels of noise are adjusted against a weighting normalized curve «A».

ACRONYMS AND ABBREVIATIONS

ACRONYMS

ABA	Acid Base Accounting (test)
AQG	Air Quality Guidelines
AP	Acid Generation Potential
ARD	Acid Rock Drainage
BFI	Base Flow Index
BIF	Banded Iron Formation
CAP	Weathered carapace
DNH	Direction Nationale de l'Hydraulique (National Directorate of Hydraulic)
DNM	Direction Nationale de la Météorologie (National Directorate of Meteorology)
DO	Dissolved Oxygen
DTM	Digital Terrain Model
EC	Electrical Conductivity
FS	Faisability Study
GPS	Global Positioning System
HCT	Humidity Cell Test
HEC	Compact Hematite
HEF	Friable Hematite
HGF or HGC	Martite-Goethite mineralization
IEC	International Electrotechnical Commission
IFC	International Finance Corporation
IHC	Itabirite compact
IHF	Itabirite friable
IRC or IRF	Enriched Itabirite
IRD	Institut de Recherche en Développement
IT	Interim Target
ITCZ	Inter-Tropical Convergence Zone
LGS	Lahontan GeoScience Inc.
LSA	Local Study Area
MDL	Method Detection Limit
NAG	Net Acid Generation (test)
NNP	Net Neutralization Potential
NP	Neutralising Potential
NTU	Nephelometric Turbidity Units
ORP	Oxidation-Reduction Potential

PdF CF	Pic de Fon Classified Forest
PFS	Pre-Feasibility Study
pH	Potential of Hydrogen
PHC	Compact Phyllite
PHS	Soil Strength Phyllite
PHV	Very Weak Phyllite
PHW	Weak Phyllite
PM	Particulate Matter
PM_1	Particulate Matter under 1 micrometers
$PM_{2.5}$	Particulate Matter under 2.5 micrometers
PM_{10}	Particulate Matter under 10 micrometers
PHY	Phyllite
RSA	Regional Study Area
SEBS	Social and Environmental Baseline Studies
SEIA	Social and Environmental Impact Assessment
SIMFER	Simandou Iron Ore Project
SPLP	Synthetic Precipitation Leaching Protocol
SWS	Schlumberger Water Services
TDS	Total Dissolved Solids
TOC	Total Organic Carbon
TOPAS	Turnkey Optical Particle Analysis System
TSP	Total Suspended Particulates (in ambient air)
TSS	Total Suspended Solids (in water)
UK	United Kingdom
UKMO	United Kingdom Met Office
USGS	United States Geological Survey
UTM	Universal Transverse Mercator
VOC	Volatile Organic Compound
VWP	Vibrating Wire Piezometre
WEA	Weathered Mineralisation
WEG	Weathered Martite-Geothite mineralisation
WGS	World Geodetic System
WHO	World Health Organization
WMC	Water Management Consultants

ABBREVIATIONS

alt.	altitude
ann.	annually
°C	degree Celsius
c.	*circa:* about
cm	centimetre
dBA	a-weighted decibels
e.g.	for example
Eo	evaporation from an open water surface
ETa	estimated actual evapotranspiration
ETo	reference crop evapotranspiration
et al.	*et alii*: and others
g	gram
h or hr	hour
ha	gectare
i.e.	that is
id.	identification
inst.	instantaneous
kg	kilogram
km	kilometre
l	litre
L/s	litre per second
L_{A95}	noise level exceeded for 95% of the sample period
L_{Aeq}	average equivalent noise level
L_{AeqT}	average equivalent noise level over time T
L_{dn}	day-night average noise level
m	metre
M	Million
mASL	meters above sea level
max.	maximum
mbar	millibar
mBGL	meters below ground level
MCM	million cubic metres
mg	milligram
min.	minimum

MJ	Megajoules
mm	millimetre
mRL	metres Relative Level
MV	Millivolts
n.a.	not applicable or not available
nb. or n	number
NTU	nephelometric turbidity units
ppm	parts per million
s or sec.	second
t	tonne
µg	micrograms
µm	micrometres
µS	microSiemens (conductivity unit)
wt	weight
yr	year

REFERENCES

REFERENCES

ALLEN, R.G., L.S. PEREIRA, D. RAES AND M. SMITH, (1998). *Crop evapotranspiration. Guidelines for computing crop water requirements.* Irrigation and Drainage Paper 56, Food and Agriculture of the United Nations, Rome.

BALME, M., T. LEBEL AND A. AMANI., 2006. *Années sèches et années humides au Sahel: quo vadimus ?* Hydrological Sciences Journal, 51(2), 254-271.

BAYNES, F., 2008. *Simandou Project Terrain Hazard Assessment*, August 2008, Report Number 080815-188-2-1, Baynes Geologic, Perth, Australia.

BAYNES, F., 2007. *Simandou Project Provisional Engineering Geology Overview*. Baynes Geologic (Rio Tinto Internal Report).

BILLA, M., J.-L. FEYBESSE, G. BRONNER, C. LEROUGE, J.-P. MILESI, S. TRAORE AND S. DIABY, 1999. *Les formations à quartzites rubanés ferrugineux des Monts Nimba et du Simandou : des unités empilées tectoniquement, sur un soubassement plutonique Archéen (craton de Kénéman-Man), lors de l'orogène Éburnéen*. C.R. Acad. Sci. Paris, Sciences de la terre et des planètes, 329, p.287-294.

BOULVERT, Y., 2003. *Carte morphopédologique de la République de Guinée : Notice*. Edition IRD, 181 p.

GAUTHIER, F. et al., 1998. *Variabilité du regime pluviometrique de l'Afrique de l'Ouest non sahelienne entre 1959 et 1989.* Hydrological Sciences Journal, 43(6).

HVORSLEV, M.J., 1951. *Time lag and soil permeability in groundwater observations*. U.S. Army Corps of Engineers, Waterway Experimentation Station. Vickburg, Mississipi. Bulletin 36.

INTERNATIONAL ELECTROTECHNICAL COMMISSION, 1979. Publication 651, *Sound level meters*.

IRAG (INSTITUT DE RECHERCHE AGRONOMIQUE DE GUINÉE), 2009. *Notice explicative sur le zonage de la Guinée Forestière*. 11 pp. Downloaded from http://guinee-hcr.cirad.fr/media/bibliographie/aboubacar.pdf on 02-02-2009.

LAHONTAN GEOSCIENCE INC. (LGS), 2008. *Preliminary Seismic Hazard Assessment of Project Simandou*, Guinea. Prepared for Scott Wilson Group, UK.

MARTEN, B.E., 2004. *Simandou Iron Ore Project, Guinea*, Report on Structural Mapping. Internal Report, Rio Tinto.

MARTEN, B.E., 2000. *Simandou Iron Ore Project, Guinea*, Report on Structural Mapping. Internal Report, Rio Tinto.

RANKIN L. R., 2004. *Structural Geology of the Simandou belt, Guinea: Analysis from Airborne Magnetic and Remotely Sensed Data*, GeoInterp, Rio Tinto Internal Report.

RIO TINTO, October 2008. *Simandou Interim Pre Feasibility Study.* Simandou Project. Multitple pagination.

THIEBLEMONT, D., 1999. *Notice explicative de la carte géologique de la Guinée. Feuille n°31-32 : Beyla – Touba*. Conakry, GIN, Ministère des Mines de la Géologie et de l'Evironnement, 21p.

THIEBLEMONT, D., C. DELOR, A. COCHERIE, J.-M. LAFON, J. C. GOUJOU, A. BALDE, M. BAH, H. SANE AND C. M. FANNING, 2001. *A 3.5 Ga granite-gneiss basement in Guinea; further evidence for early Archean accretion within the West African Craton*. Precambrian Research 108 (3-4): pp: 179-194.

TURNKEY INSTRUMENT LTD., December 2004. *TOPAS & Osíris Environmental Monitor Training manual*, 33 p.

UK MET OFFICE, Janvier 2008a. *Climatological Study of the Simandou Hills Area of Guinea West Africa – Climate Predictions.* Prepared for WMC. 8 p.

UK MET OFFICE, March 2008b. *Potential Impacts of Mining in the Simandou Hills. PHASE 1: Current climate and mechanisms.* Final Report prepared for WMC. 60 p.

UK MET OFFICE, April 2008c. *Potential Impacts of Mining in the Simandou Hills. PHASE 2: Numerical Modelling.* Final Report prepared for WMC. 25 p.

UK MET OFFICE, December 2008d. *Climatological Study of the Simandou Hills area of Guinea. PHASE 3: Extended Numerical Modelling Study of Impacts of Mining.* Stage 2a: Short report, progress on 5 cases. Prepared for WMC. 14 p.

VAN OOSTERWIJK, K., 2004. *Geology and Haematite Mineralisation of the Pic de Fon Deposit, Guinea, West Africa*. Masters Thesis University of Tasmania (unpub).

WATER MANAGEMENT CONSULTANTS LTD., 2009e. *Report on sediment at Simandou*. Technical memorandum 1849-34 prepared for Rio Tinto (June 2009). 18 p. and appendices.

WATER MANAGEMENT CONSULTANTS LTD., 2009d. *Baseline Climate Report*. Report 1849/R4 prepared for Rio Tinto (January). 21 p. and appendices.

WATER MANAGEMENT CONSULTANTS LTD., 2009c. *Baseline Hydrogeology Report*. Report 1849/R6 prepared for Rio Tinto (March). 73 p. and appendices.

WATER MANAGEMENT CONSULTANTS LTD., 2009b. *Baseline Hydrology Report*. Report 1849/R5 prepared for Rio Tinto (February). 55 p. and appendices.

WATER MANAGEMENT CONSULTANTS LTD., 2009a. *Geochemical Testwork for Assesment of Acid Rock Drainage and Metal Leaching Potential, Simandou Iron Ore Project, Guinea.* Report 1849/R7 prepared for Rio Tinto (April). 40 p. and appendices.

WATER MANAGEMENT CONSULTANTS LTD., 2008. *Simandou Iron Ore Project Pre-Feasability Study, Mine Water Management System.* Report 1849/R3 prepared for Rio Tinto (July). 178 p.

WORLD HEALTH ORGANIZATION, 1999. *Guidelines for Community Noise.* Edited by Birgitta Berglund , Thomas Lindvall, Dietrich H Schwela. 159 p.

WORLD HEALTH ORGANIZATION, 2005. *Air Quality Guidelines, global update 2005.* Report on a Working Group meeting, Bonn, Germanty, 18-20 October 2005. 30 p.

WORLD HEALTH ORGANIZATION, 2006. *Guidelines for Drinking-water Quality*. Second Edition. World Health Organisation, Geneva.

WRIGHT, J. B., D.A. HASTINGS, W.B. JONES AND H.R. WILLIAMS, 1985. *Geology and Mineral Resources of West Africa*, George Allen & Unwin Ltd. Ed., London, UK, 187 p.

SNC·LAVALIN

www.snclavalin.com

SNC-Lavalin Environment
455 René-Lévesque Blvd. W.
Montréal, Québec
H2Z 1Z3 Canada
Telephone: (514) 393-1000
Fax: (514) 392-4758